SD2002-16-F

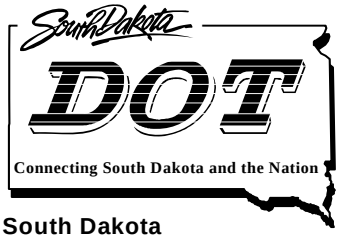

South Dakota
Department of Transportation
Office of Research

U.S. Department
of Transportation
Federal Highway
Administration

Evaluation of Metallized Stainless Steel Clad Reinforcement

Study SD2002-16
Final Report

Prepared by
University of Kansas Center for Research, Inc.
2385 Irving Hill Road
Lawrence, Kansas 66044-7552

July 2007

DISCLAIMER

The contents of this report reflect the views of the authors who are responsible for the facts and accuracy of the data presented herein. The contents do not necessarily reflect the official views or policies of the South Dakota Department of Transportation, the State Transportation Commission, or the Federal Highway Administration. This report does not constitute a standard, specification, or regulation.

ACKNOWLEDGEMENTS

This work was performed under the supervision of the SD2002-16 Technical Panel:

Mark Clausen ..... FHWA	Dan Johnston ..... Research
Tom Gilsrud ..... Bridge Design	Darin Larson ..... Operations Support
Todd Hertel ..... Aberdeen Region	Paul Nelson ..... Pierre Region
Darin Hodges ..... Materials & Surfacing	David Trejo ..... TexasA&M

The work was performed in cooperation with the United States Department of Transportation Federal Highway Administration and the Kansas Department of Transportation under Contracts 1131 and 1281. Lien Gong, Jianxin Ji, Guohui Guo, Sean Hughes, and Jason Draper made significant contributions to the research described in this report. Portions of this report were drawn from reports for which Drs. Gong and Ji served as first authors.

TECHNICAL REPORT STANDARD TITLE PAGE

1. Report No.	2. Government Accession No.	3. Recipient's Catalog No.
SD2002-16-F		

4. Title and Subtitle	5. Report Date
Evaluation of Metallized Stainless Steel Clad Reinforcement	July 25, 2007
	6. Performing Organization Code

7. Author(s)	8. Performing Organization Report No.
David Darwin, JoAnn Browning, Trung Van Nguyen, Carl Locke, Jr.	SM Report No. 90

9. Performing Organization Name and Address	10. Work Unit No.
University of Kansas Center for Research, Inc. 2385 Irving Hill Road Lawrence, Kansas 66044-7552	
	11. Contract or Grant No. 310805

12. Sponsoring Agency Name and Address	13. Type of Report and Period Covered
South Dakota Department of Transportation Office of Research 700 East Broadway Avenue Pierre, SD 57501-2586	Final Report October 2002 to July 2007
	14. Sponsoring Agency Code

15. Supplementary Notes
An executive summary is published separately as SD2002-16-X.

16. Abstract
SMI-316 SC™ stainless steel clad concrete reinforcement is evaluated for corrosion resistance, mechanical properties, life expectancy, and cost effectiveness and compared with conventional mild steel reinforcement and epoxy-coated reinforcement (ECR). Corrosion performance is evaluated using rapid macrocell, Southern Exposure, and cracked beam tests. MMFX Microcomposite reinforcement is evaluated for the chloride content required for corrosion initiation, which is used to supplement corrosion test results from earlier research. Life expectancy and cost effectiveness of bridge decks containing the different reinforcing systems are evaluated using laboratory results for the chloride content required for corrosion initiation and rate of corrosion along with field experience and costs in South Dakota.

The SMI-316 SC bars satisfy the mechanical properties specified by ASTM A 615 for Grade 60 reinforcing bars. The SMI-316 SC bars should be fabricated (bent) using protective equipment similar to that used for epoxy-coated bars to limit damage to the cladding. Cladding thickness is satisfactory for normal construction operations. The corrosion rates of both SMI-316 SC and ECR reinforcement are less than 0.4% or 1/250 of that for conventional reinforcement. Epoxy-coated reinforcement embedded in concrete can undergo a significant loss of bond between the epoxy and the reinforcing steel, although total corrosion losses are low compared to those observed for conventional reinforcement. Bridge decks containing SMI-316 SC reinforcing steel will not require repair due to corrosion-induced concrete cracking during a 75-year service life. In comparison, conventional bridge decks require repair 10 to 25 years after the construction, depending on exposure conditions. Bridge decks containing epoxy-coated reinforcement will not require repair due to corrosion-induced concrete cracking during a 75-year service life but are estimated to require repair approximately 40 years after construction due to corrosion near damaged areas where the bond between the epoxy and reinforcing steel has been lost. Bridge decks containing SMI-316 SC reinforcing steel are cost-effective compared to bridge decks containing epoxy-coated reinforcement. The critical chloride corrosion threshold for MMFX Microcomposite steel is three to four times the corrosion threshold for conventional reinforcement, and the corrosion rate is approximately one-half that of conventional steel. Bridge decks containing MMFX Microcomposite reinforcing steel will require repair due to corrosion-induced concrete cracking approximately 33 years after construction and do not appear to be cost-effective when compared to bridge decks containing epoxy-coated reinforcement.

17. Keywords	18. Distribution Statement
bridge decks, costs, corrosion, design life, reinforcing steel, stainless steel	No restrictions. This document is available to the public from the sponsoring agency.

19. Security Classification (of this report)	20. Security Classification (of this page)	21. No. of Pages	22. Price
Unclassified	Unclassified	156	

TABLE OF CONTENTS

LIST OF FIGURES

LIST OF TABLES

CHAPTER 1

EXECUTIVE SUMMARY

1.1 PROBLEM DESCRIPTION

The annual cost for maintenance and replacement of highway structures due to the corrosion of reinforcing steel is measured in billions of dollars in the United States. The principal cause of the corrosion is the diffusion of deicing chemicals into the concrete surrounding the steel. The average annual direct cost of corrosion of highway bridges is estimated at $8.3 billion, with indirect costs to users due to traffic delays and lost productivity estimated to be more than 10 times that value. As a result, techniques to significantly reduce or halt chloride-induced corrosion have been pursued aggressively for well over 30 years.

For most applications, especially bridge decks, the corrosion protection system of choice consists of a combination of epoxy-coated reinforcement (ECR) and increased concrete cover over the reinforcing bars. There are, however, some concerns about the combined system. The increased concrete cover increases the bridge self weight and the cost of construction. And, if poorly adhering epoxy coatings are used on the reinforcement, corrosion problems may be increased. These problems include imperfections in the coating that cause disbondment between the coating and the steel. Even if the coating has no local defects, water and, to a lesser extent, oxygen and chloride ions, may penetrate the epoxy, which may result in corrosion. This has happened for poorly applied coatings in substructures in Florida. Even properly applied coatings will lose adhesion over time, which means that coatings can deteriorate to an extent that prevents the epoxy from protecting the reinforcement once chlorides have reached the reinforcing steel.

As a result of these concerns, a number of other protective measures have been developed or are under development. These include the use of denser concretes, corrosion inhibitors, and corrosion-resistant steel alloys. Among the latter are 316LN stainless steel clad reinforcement (SMI-316 SC^{TM}), manufactured using a metallizing technique called the Osprey Process, and MMFX Microcomposite reinforcement.

To produce SMI-316 SC steel, stainless steel is sprayed on a mild steel billet. In the spraying and subsequent rolling process, the coating forms a metallic bond with the base metal. The surface of the steel is then blasted and pickled with acid to remove mill scale and other oxidation products. Based on earlier studies, the new steel should be less susceptible to corrosion than either conventional or epoxy-coated reinforcement (ECR) and should significantly limit corrosion caused by deicing salts throughout the life of the bridge deck.

MMFX Microcomposite steel is a high-strength, low carbon alloy with a chromium content of about 9% alloy (in practice, the range can be 8 to 10.9%) and a yield strength in excess of 100 ksi. The alloy was evaluated in an earlier study for the South Dakota Department of Transportation (SD2001-05) and found to be more corrosion resistant than conventional steel

but less corrosion resistant than epoxy-coated reinforcement. Some questions remained after that study, which are addressed in the current report.

This report describes work to compare the performance of stainless steel clad reinforcement and MMFX Microcomposite steel with that of conventional and epoxy-coated reinforcement. The goal of this research is to determine the ability of these systems to slow the initiation of corrosion and lengthen the corrosion period.

1.2 OBJECTIVES

The research program has four objectives. They are to:

1) Determine the corrosion resistance of SMI-316 SC^{TM} steel compared to ECR reinforcement.
2) Determine the mechanical properties, quality, and suitability of SMI-316 SC^{TM} steel for use in bridge decks.
3) Estimate life expectancy and cost effectiveness of SMI-316 SC^{TM}, ECR, and mild steel reinforcement in South Dakota.
4) Obtain additional data on the corrosion performance of MMFX Microcomposite steel and formulate changes in Conclusions and Recommendations to SDDOT as appropriate.

The selection of a new reinforcing material for concrete bridge decks should be based on its ability to improve the life expectancy and cost effectiveness of the structural system. To be selected, the new material must provide a significant improvement in corrosion resistance compared to the current material of choice, epoxy-coated reinforcement (ECR), and serve as a structural replacement for the conventional mild steel reinforcement used to manufacture ECR. To this end, SMI-316 SC steel is compared based on corrosion-resistance with conventional mild steel reinforcement and ECR using rapid macrocell, Southern Exposure, and cracked beam tests and based on mechanical properties with conventional mild steel reinforcement using the tests used to qualify reinforcing steel in U.S. practice.

The results of the corrosion evaluation are combined with construction and maintenance experience in South Dakota and other states to evaluate the impact of SMI-316 SC reinforcing steel on the life expectancy and cost effectiveness of reinforced concrete bridge decks.

MMFX Technologies Corporation objected to some of the conclusions reached in an earlier report, SD2001-05-F, with special attention to the chloride thresholds at corrosion initiation for conventional and MMFX Microcomposite steel. Additional tests are used to update the current understanding of the corrosion resistance, life expectancy, and cost effectiveness of MMFX steel.

1.3 FINDINGS

A series of tasks were completed to evaluate the performance of SMI-316 SC and MMFX Microcomposite steel. The principal results of that research are summarized in this section.

1.3.1 Literature Search

Tests of a prototype of SMI-316 SC reinforcement, consisting of conventional steel clad with 304 stainless steel, indicated that the prototype reinforcement exhibited superior corrosion resistance compared to conventional reinforcing steel but that it required adequate protection at cut ends, where the mild steel core is not covered by cladding. Bare stainless steel clad bars corroded at about 1/100 of the rate for conventional mild steel bars. Bars embedded in mortar corroded at 1/20 to 1/50 of the rate for conventional bars. The early tests were limited to rapid macrocell tests, and longer-term tests were recommended.

Structural Metals Inc. remains in the development stage for the SMI-316 SC reinforcement and has not yet begun regular production of the bars. As a result, SMI-316 SC reinforcement has not been used in practice, with the exception of a single bridge over a tidal inlet on Johns Island, South Carolina, which was completed on May 23, 2005. In addition to SMI-316 SC bars, the bridge includes solid stainless, MMFX, epoxy-coated, and conventional steel reinforcement. Due to its short time in service, no observations are available on any of the reinforcing systems used in the bridge.

1.3.2 Mechanical Tests and Cladding Uniformity

Samples of conventional and SMI-316 SC reinforcing steel were tested to determine tensile and bend properties, and SMI-316 SC bars were evaluated for cladding uniformity and thickness variation.

Stress-strain and bend tests were performed for conventional and SMI-316 SC No. 5 and No. 6 bars. All bars met the requirements of ASTM A 615 for yield strength, tensile strength, and elongation, and all bars satisfied the bend requirements. The tests demonstrate that No. 5 and No. 6 SMI bars satisfy the mechanical properties required by ASTM A 615 and can be used as replacements for conventional No. 5 and No. 6 bars.

SMI-316 SC bars were sectioned and evaluated for cladding uniformity and thickness variation using a scanning electron microscope (SEM). Micrographs obtained using the SEM demonstrate that a metallurgical bond is obtained between the 316LN stainless steel cladding and the mild steel core of the bars. No unclad regions or cracks through the cladding were observed. Average cladding thicknesses varied between 26 and 30 mils (1 mil = 0.001 in.), with standard deviations between 8 and 13 mils for the No. 5 bars, and between 24 to 45 mils, with standard deviations between 6 and 13 mils for the No. 6 bars. The minimum cladding thickness measured on any bar was 6 mils, which is adequate to physically protect the core during normal construction operations.

1.3.3 Corrosion Tests of SMI-316 SC Reinforcement

The corrosion performance of SMI-316 SC, conventional, and epoxy-coated reinforcement was compared using No. 5 bars in rapid macrocell and longer-term bench-scale tests.

In the rapid macrocell test, either a bare or mortar-covered (wrapped) reinforcing bar is placed in a container containing simulated concrete pore solution and a preselected concentration of sodium chloride. Two similar specimens are placed in a second container containing simulated pore solution. The specimens are electrically connected across a 10-ohm resistor and the solutions are connected with a salt bridge. The specimen subjected to chlorides (the anode) represents the top layer of a bridge deck, while the specimens in the other container (cathode) represent the bars in the bottom layer of a bridge deck. Air is supplied to the liquid surrounding the cathode to ensure an adequate supply of oxygen. The corrosion rate, measured in micrometers per year (μm/yr), is determined based on the current in the system, which can be determined based on the voltage drop across the resistor, and the total corrosion loss, measured in μm, can be calculated by numerically integrating the corrosion rate over time. Corrosion losses for bare and mortar-wrapped bars are shown in Figures 1.1 and 1.2, respectively. The bare bar tests include conventional steel (Conv.), epoxy-coated steel with four $^1/_8$-in. diameter holes drilled through the epoxy (ECR), SMI-316 SC bars with no holes in the cladding and with ends of the bars protected by a cap filled with epoxy (SMI), SMI bars with four $^1/_8$-in. diameter holes drilled through the cladding with ends of the bars protected by a cap filled with epoxy (SMI-d), SMI bars with no holes in the cladding but *without* the ends of the bars protected by a cap filled with epoxy (SMI-nc), and SMI bars with a 180° bend, without holes and with end caps (SMI-b), all tested using a 1.6 m ion concentration of NaCl at the anode. The mortar-wrapped tests include the same series with the exception of the bent bars.

The figures show that ECR and SMI bars corrode at just a fraction of the rate of conventional steel, even if the epoxy or stainless steel cladding is damaged. For the bare bar tests shown in Figure 1.1, at 15 weeks, the ECR bars have losses under 6% of that for conventional reinforcement. The SMI and SMI-b bars have losses well below 0.1% of that for conventional steel, while the corresponding values for the SMI-d and SMI-nc bars are 1.0 and 0.2%, respectively. For the mortar-wrapped bar tests shown in Figure 1.2, the losses for ECR and SMI are less than 0.05% of that for conventional steel, with the SMI-d and SMI-nc bars showing losses equal to 0.5 and 0.25%, respectively, of that for conventional steel. In mortar, the ECR bars exhibit lower losses than the SMI-d bars, even though both have four $^1/_8$-in. diameter holes through the coating or cladding, because of the high resistivity of the epoxy coating, which limits the bar area that can serve as a cathode (limiting the rate of the overall reaction), while the full area of the SMI bars is conductive and can, thus, serve as a cathode.

The longer-term corrosion performance of reinforcing steel is measured using Southern Exposure and cracked beam tests. The specimens used in these tests are 7-in. deep slabs with two layers of steel that represent portions of bridge decks. The Southern Exposure specimen represents deck regions with intact concrete, and the cracked beam specimen represents regions

in which the top layer of steel is exposed due to settlement and drying-induced shrinkage cracks. A 15% sodium chloride solution is ponded on the surface of the slabs, and the specimens are subjected to cycles of wetting and drying, which raises the chloride concentration within the concrete. In addition to evaluating corrosion performance, the results of the tests are used in the economic analysis.

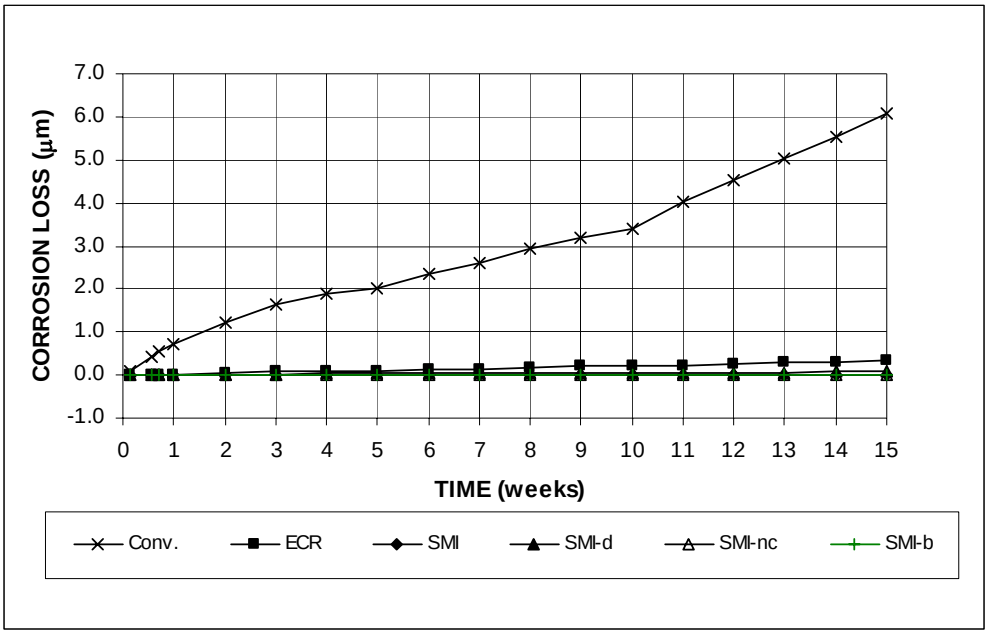

Figure 1.1 – Macrocell Test. Average corrosion loss versus time. Bare bars in NaCl and simulated concrete pore solutions.

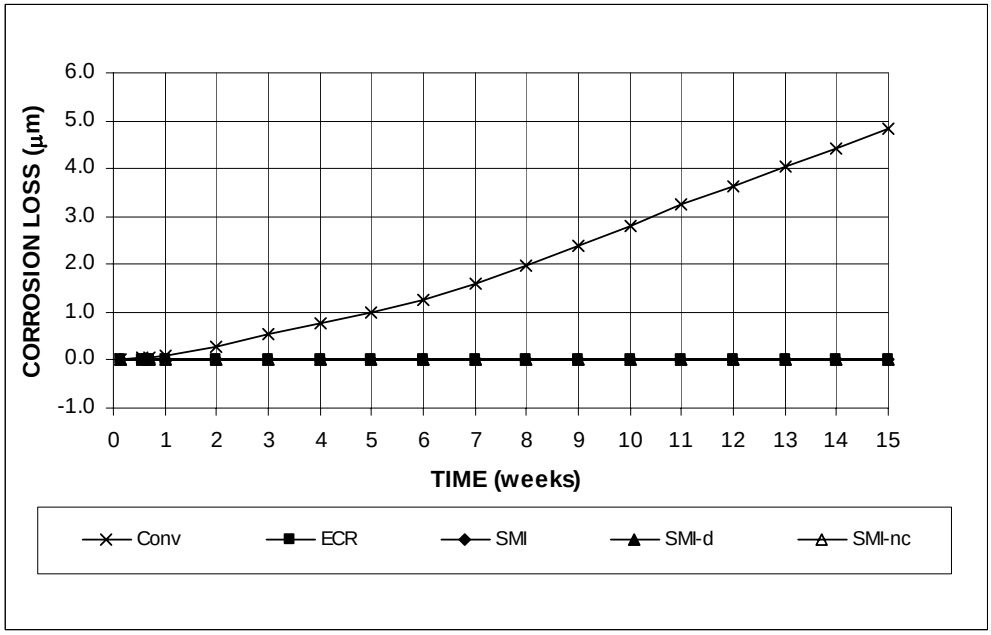

Figure 1.2 – Macrocell Test. Average corrosion loss versus time. Mortar-wrapped bars in NaCl and simulated concrete pore solutions.

The key results for the Southern Exposure and cracked beam tests are summarized in terms of total corrosion loss, in micrometers, in Figures 1.3 and 1.4, respectively. The Southern Exposure tests are used to evaluate straight conventional (Conv.), epoxy-coated (coating breached by four $^{1}/_{8}$-inch diameter holes) (ECR), SMI-316 SC reinforcing steel with no damage to the cladding (SMI), and SMI bars with four $^{1}/_{8}$-inch diameter holes drilled through the cladding (SMI-d). Additional Southern Exposure tests are used for two sets of specimens combining SMI and conventional steel to evaluate galvanic effects. One set is configured with SMI bars in the top mat and conventional steel in the bottom mat (SMI/ Conv.), while in the other set, the position of the steels is reversed (Conv./SMI). One more set of specimens is used to evaluate bent SMI bars (SMI-b). The bending equipment used did not have a protective coating, which resulted in damage to the cladding. Cracked beam tests are used to evaluate Conv., ECR, SMI, and SMI-d bars.

A comparison of Figures 1.3 and 1.4 illustrates the effect of concrete cracking on corrosion rate, with the conventional steel Southern Exposure specimens exhibiting six times the corrosion loss of the corresponding cracked beam specimens. Figure 1.3 also shows that combining SMI-316 SC with conventional reinforcement has little apparent effect on the corrosion rate of either material. As observed for the rapid macrocell tests, Figures 1.3 and 1.4 illustrate that ECR and SMI steel, damaged or not, corrode at a fraction of the rate of conventional steel, with the ECR and SMI bar specimens exhibiting losses equal to less than 0.4% (1/250) of that for conventional steel specimens in either test. The losses for the SMI-d and damaged SMI-b specimens equal 4.5% and 2%, respectively, of the losses observed for conventional steel. The damage that occurred during the bending operation emphasizes the importance of using fabrication equipment of the type now used for epoxy-coated bars that will not damage the cladding when the bars are bent.

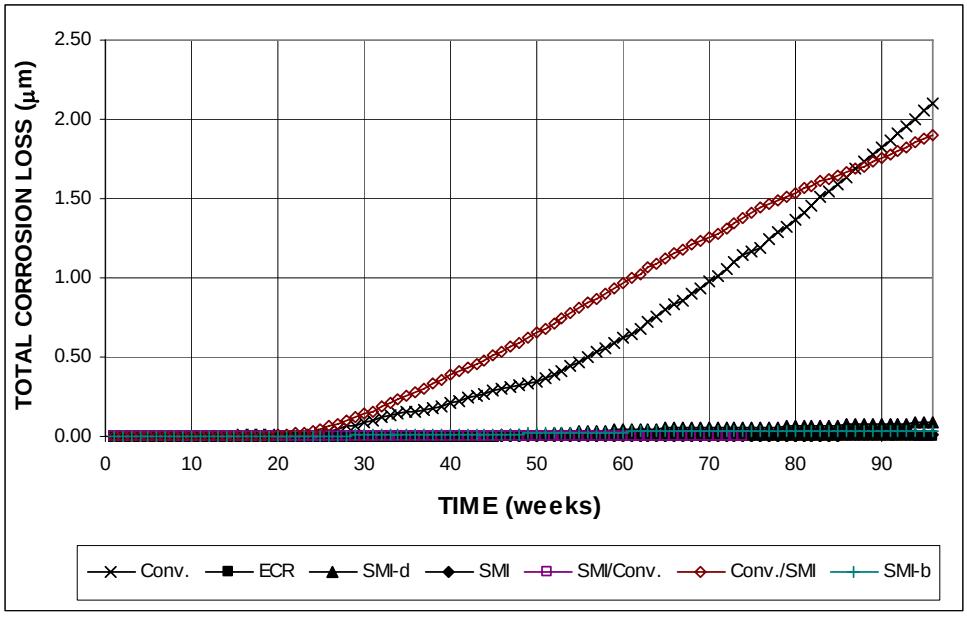

Figure 1.3 – Southern Exposure Test. Average total corrosion loss versus time.

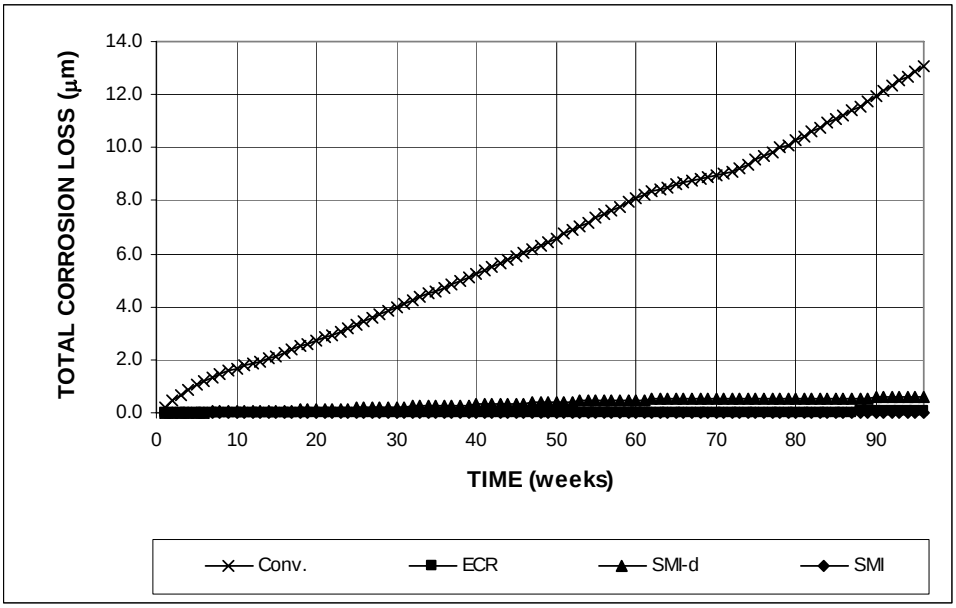

Figure 1.4 – Cracked Beam Test. Average total corrosion loss versus time.

1.3.4 Corrosion Tests of MMFX Microcomposite Reinforcement

For MMFX reinforcement, the key task was to establish the critical chloride corrosion threshold, that is the chloride concentration in concrete that causes the reinforcement to begin to corrode. Earlier studies had established the value to be between 1 and 2 lb/yd^3 for conventional steel and between 3 and 8 lb/yd^3 for MMFX Microcomposite steel.

The current study found the critical chloride threshold for conventional steel to be between 0.90 to 2.21 lb/yd^3, with an average of 1.75 lb/yd^3, based on water-soluble chlorides. The critical chloride threshold for MMFX Microcomposite steel ranged from 4.5 to 9.2 lb/yd^3, with an average of 6.5 lb/yd^3. These values are combined with corrosion rates measured in this and earlier studies to determine the life expectancy of bridges containing these reinforcing materials.

These values are well below the threshold (concentrations in excess of 25 lb/yd^3) for 316LN stainless steel, which is used to clad SMI-316 SC reinforcement.

1.3.5 Life Expectancy and Economic Analysis

The life expectancy and cost effectiveness of bridges containing SMI-316 SC, MMFX Microcomposite, ECR, and conventional reinforcement are determined based on an analysis of laboratory results and the experience of the South Dakota Department of Transportation. Laboratory results in the current and earlier studies indicate that conventional reinforcement or exposed epoxy-coated reinforcement will begin corroding at an average chloride concentration of 1.75 lb/yd^3. The corresponding values for the stainless steel used as the cladding for SMI-316 SC steel and MMFX Microcomposite steel are more than 25 lb/yd^3 and 6.5 lb/yd^3, respectively. These values are used to estimate time-to-corrosion-initiation based on observed chloride contents in cracked bridge decks. One-half of the average of the corrosion rates after corrosion

initiation in the Southern Exposure and cracked beam tests is used to estimate the time required to reach a total thickness loss of 25 μm (0.001 in.), the expected value that will result in concrete cracking due to the deposition of corrosion products adjacent to the bar.

Based on laboratory results, times to first repair of 12 and 33 years are calculated for conventional and MMFX steel, respectively. Stainless steel clad reinforcement will not require repair during the 75-year service life used to evaluate the cost-effectiveness of the reinforcing systems. Based on experience, SDDOT estimates of times to first repair for conventional reinforcement are 10 years under harsh conditions and 25 years under arid conditions. Time to first repair for epoxy-coated reinforcement is estimated to be 40 years based on the observation that no bridges built with epoxy-coated reinforcement in South Dakota have required repair due to corrosion of the reinforcing steel.

Using the time to first repair and a standard 25-year period for subsequent repairs, the cost effectiveness of conventional, epoxy-coated, SMI-316 SC, and MMFX reinforcement was evaluated using a typical 8.5-in bridge deck over a service life of 75 years at discount rates of 2, 4, and 6%. The analysis indicates that, at a discount rate of 2%, SMI-316 SC has the lowest present value cost, $\$250/yd^2$, which is equal to the initial cost alone, since no repairs are required. Next is epoxy-coated reinforcement, with either a 35 or a 40-year time to first repair, \$421 or $\$399/yd^2$, compared to \$441 for MMFX steel with a time to first repair of 33 years, and $\$461/yd^2$ for conventional steel for a time to first repair of 25 years and a cost of $\$649/yd^2$ for time to first repair of 10 years.

1.4 CONCLUSIONS

The following conclusions are based on the test results and analyses presented in this report.

1. The No. 5 and No. 6 SMI-316 SC bars tested in this study satisfy the mechanical properties specified by ASTM A 615 and can be used as replacements for conventional No. 5 and No. 6 Grade 60 reinforcing bars. The steel, however, is not currently in production.

2. A metallurgical bond is obtained between the 316LN stainless steel cladding and the mild steel core of the SMI-316 SC bars. The average cladding thickness varied between 26 and 45 mils (0.026 and 0.045 in.). The minimum thickness measured at any location was 6 mils.

3. SMI-316 SC bars should be fabricated (bent) using protective equipment similar to that used for epoxy-coated bars. Without protection, there is significant potential for damage to the cladding. The minimum measured thickness of the cladding, however, is adequate for normal handling during construction.

4. The corrosion rate of SMI-316 SC reinforcement is less than 0.4% or 1/250 of that for conventional reinforcement. Total corrosion losses for SMI-316 SC bars were insignificant in the tests.

5. Corrosion losses for damaged epoxy-coated reinforcement were below those for damaged SMI-316 SC reinforcement. The difference results from the high resistivity of the epoxy coating, which limits the bar area that can serve as a cathode, while the full area of the SMI-316 SC bars can serve as a cathode.

6. Epoxy-filled plastic caps protect the cut ends of SMI-316 SC reinforcement from corrosion.

7. Epoxy-coated reinforcement embedded in concrete can undergo a significant loss of bond between the epoxy and the reinforcing steel when subjected to high moisture and high chloride concentrations. Corrosion products form under the coating, although total corrosion losses are low compared to those observed for conventional reinforcement.

8. Similar corrosion products are deposited on conventional reinforcing steel and on the mild steel core at damaged regions of SMI-316 SC steel.

9. Bridge decks containing SMI-316 SC reinforcing steel will not require repair due to corrosion-induced concrete cracking during a 75-year service life. In comparison, conventional bridge decks require repair 10 to 25 years after the construction, depending on exposure conditions. Bridge decks containing epoxy-coated reinforcement will not require repair due to corrosion-induced concrete cracking during a 75-year service life but are estimated to require repair approximately 40 years after construction due to corrosion near damaged areas where the bond between the epoxy and reinforcing steel has been lost.

10. Bridge decks containing SMI-316 SC reinforcing steel are cost-effective compared to bridge decks containing epoxy-coated reinforcement.

11. The critical chloride corrosion threshold for MMFX Microcomposite steel is three to four times the corrosion threshold for conventional reinforcement. The corrosion rate for MMFX steel is approximately one-half that of conventional steel.

12. Bridge decks containing MMFX Microcomposite reinforcing steel will require repair due to corrosion-induced concrete cracking approximately 33 years after construction.

13. Bridge decks containing MMFX Microcomposite steel do not appear to be cost-effective when compared to bridge decks containing epoxy-coated reinforcement.

1.5 IMPLEMENTATION RECOMMENDATIONS

The evaluation and test results presented in this report lead to the following implementation recommendations.

1. SMI-316 SC stainless steel clad reinforcement is recommended as a cost-effective direct replacement for epoxy-coated reinforcement. Cut ends of the bars should be protected with a system such as plastic caps filled with epoxy and the bars should be protected from damage to the cladding during bending operations.

This recommendation is based on observations that SMI-316 SC stainless steel clad reinforcement corrodes at a negligible rate when subjected to high moisture and chloride conditions. Based on field test results for chlorides in bridge decks, it is highly unlikely that the critical chloride corrosion threshold of the stainless steel cladding will be reached in less than 100 years in bridge decks. The corrosion performance of SMI-316 SC steel will equal or exceed that of epoxy-coated reinforcement as long as the ends of the bars are protected, such as with plastic caps filled with epoxy, and steps are taken, as they are for epoxy-coated reinforcement, to protect the bars from damage to the cladding during fabrication (bending). Normal handling will not result in damage to the cladding. Acid pickling to remove mill scale and other oxidation products will be needed to achieve the corrosion resistance obtained in this study by the SMI-316 SC stainless steel clad bars. The initial cost for construction with SMI-316 SC reinforcement is higher than that for epoxy-coated or conventional reinforcement, but because it requires no repair, the lifetime cost is significantly less.

2. MMFX Microcomposite reinforcing steel should not be used as a direct replacement for epoxy-coated reinforcement without the use of a supplementary corrosion protection system. Use of the material in its current form is not recommended for reinforced concrete bridge decks in South Dakota.

This recommendation matches that reported in SD 2001-5 and is based on observations that, while MMFX reinforcing steel has a higher corrosion threshold and corrodes at a lower rate than conventional reinforcement, (1) its corrosion-resistance properties are not superior to that of epoxy-coated reinforcement, and (2) bridge decks constructed with MMFX reinforcing steel will have a higher initial cost, a shorter life expectancy, and a higher lifetime cost than bridge decks constructed with epoxy-coated reinforcement.

CHAPTER 2

PROBLEM DESCRIPTION

The annual cost for maintenance and replacement of highway structures due to the corrosion of reinforcing steel is measured in billions of dollars in the United States. The principal cause of the corrosion is the diffusion of deicing chemicals into the concrete surrounding the steel. The average annual direct cost of corrosion of highway bridges is estimated at $8.3 billion, with indirect costs to users due to traffic delays and lost productivity estimated to be more than 10 times that value (Yunovich el at. 2002). As a result, techniques to significantly reduce or halt chloride-induced corrosion have been pursued aggressively for well over 30 years.

Methods to reduce the corrosion of reinforcing steel fall into two categories. The first includes methods that slow the initiation of corrosion, that is, the time it takes the chlorides to reach a threshold value at the reinforcing steel in the concrete. This category involves methods such as the use of corrosion inhibitors, low permeability concrete, and increased concrete cover over the reinforcing steel. The second category includes methods that lengthen the corrosion period, that is, the time from the initiation of corrosion to the end of the service life. Methods such as the use of corrosion-resistant steel, epoxy-coated steel, corrosion inhibitors, and cathodic protection belong in the second category.

For most applications, especially bridge decks, the corrosion protection system of choice consists of a combination of epoxy-coated reinforcement (ECR) and increased concrete cover over the reinforcing bars. There are, however, some concerns about the combined system. The increased concrete cover increases the bridge self weight and the cost of construction. And, if poorly adhering epoxy coatings are used on the reinforcement, corrosion problems may be increased. These problems include imperfections in the coating that cause disbondment between the coating and the steel. Even if the coating has no local defects, water and, to a lesser extent, oxygen and chloride ions, may penetrate the epoxy, which may result in corrosion (Manning 1996). This has happened for poorly applied coatings in substructures in Florida (Sagues el al. 1994). Even properly applied coatings will lose adhesion over time (Manning 1996, Smith and Virmani 1996), which means that coatings can deteriorate to an extent that prevents the epoxy from protecting the reinforcement once chlorides have reached the reinforcing steel.

As a result of these concerns, a number of other protective measures have been developed or are under development. These include the use of denser concretes, corrosion inhibitors, and corrosion-resistant steel alloys. Among the latter are 316LN stainless steel clad reinforcement (SMI-316 SC^{TM}) that is manufactured using a metallizing technique called the Osprey Process and MMFX Microcomposite reinforcement.

To produce SMI-316 SC^{TM} steel, stainless steel is sprayed on a mild steel billet. In the spraying and subsequent rolling process, the coating forms a metallic bond with the base metal. The surface of the steel is then blasted and pickled in acid to remove mill scale and other

oxidation products. Based on earlier studies (McDonald et al. 1998, Darwin et al. 1999, Balma et al 2005), the new steel should be less susceptible to corrosion than either conventional or epoxy-coated reinforcement (ECR) and should significantly limit corrosion caused by deicing salts throughout the life of the bridge deck. As demonstrated by Balma et al. (2005), acid pickling to remove mill scale and other oxidation products will be needed to achieve the full benefits provided by the stainless steel cladding.

MMFX Microcomposite steel is a high-strength, low carbon alloy with a chromium content of about 9% alloy (in practice, the range can be 8 to 10.9%) and a yield strength in excess of 100 ksi. The alloy was evaluated in an earlier study for the South Dakota Department of Transportation (Darwin et al. 2002) and found to be more corrosion resistant than conventional steel but less corrosion resistant than epoxy-coated reinforcement. Some questions remained after that study, which are addressed in the current report.

This report describes work to compare the performance of stainless steel clad reinforcement and MMFX Microcomposite steel with conventional and epoxy-coated reinforcement. The goal of this research is to determine the ability of these systems to slow the initiation of corrosion and lengthen the corrosion period.

CHAPTER 3

OBJECTIVES

This research program has four objectives. They are to (1) determine if SMI-316 SC™ (SMI) steel has superior corrosion-resistance compared to epoxy-coated reinforcement, (2) determine if SMI steel will serve as a suitable reinforcement for concrete, (3) compare the life expectancy and cost effectiveness of the new material with epoxy-coated reinforcement and conventional mild steel reinforcement, and (4) obtain additional data on the corrosion performance of MMFX Microcomposite steel and formulate changes in earlier conclusions and recommendations, as appropriate.

OBJECTIVE ONE

Determine the corrosion resistance of SMI-316 SC™ steel compared to ECR reinforcement.

As described in SD2001-05 (Darwin et al. 2002), the principal reason for selecting a new reinforcing material for concrete bridge decks is to improve the life expectancy and cost effectiveness of the structural system. A prerequisite for such a selection is the requirement that the material, which presumably is more expensive than the current system, provides a significant improvement in corrosion resistance compared to the current material of choice, epoxy-coated reinforcement (ECR) meeting the requirements of ASTM A 775. The corrosion-resistance of SMI-316 SC steel, conventional mild steel reinforcement, and ECR are evaluated using rapid macrocell, Southern Exposure, and cracked beam tests. Rapid macrocell tests in which both bare and mortar-clad reinforcing bars are subjected to elevated chloride levels provide insight into the corrosion resistance of the systems when subjected to high chloride concentrations. Longer-term bench-scale tests with fully intact concrete (Southern Exposure tests) and precracked concrete (cracked beam tests) provide the principal tools for comparing the systems. These tests demonstrate that SMI-316 SC steel provides superior corrosion protection. The nature of the corrosion products on the steels is also evaluated using a scanning electron microscope.

OBJECTIVE 2

Determine the mechanical properties, quality, and suitability of SMI-316 SC™ steel for use in bridge decks.

SMI-316 SC reinforcing bars consist of a mild steel core enclosed in a thin stainless steel cladding. As a result, the mechanical properties including yield strength, tensile strength, and elongation are similar to those observed for conventional reinforcing steel. Tensile and bend tests demonstrate that, not only does SMI steel meet the requirements for conventional steel under ASTM A 615, but that the cladding is bonded to the core metal. Further, evaluations using a scanning electron microscope indicate that a metallic bond exists between the cladding and the

core metal and that the cladding thickness is reasonably consistent and uniform for the bars evaluated.

OBJECTIVE 3

Estimate life expectancy and cost effectiveness of SMI-316 SC™, ECR, and mild steel reinforcement in South Dakota.

Prior to the adoption of reinforcement with superior corrosion resistance, such as SMI-316 SC steel, it is necessary to establish that the steel will not only increase life expectancy, but will also improve the cost effectiveness of reinforced concrete bridge decks. In this light, the corrosion test results are used in an economic analysis (Kepler et al. 2000, Darwin et al. 2002) to compare the cost effectiveness of the new system with those of conventional reinforcing steel and ECR. The comparisons include an estimate of the costs of construction and repair for each type of reinforcing material and the time periods from initial construction to first repair and between subsequent repairs. The present value of the construction and maintenance costs for bridge decks containing each form of reinforcement are compared at selected discount rates using a 75-year economic life.

OBJECTIVE 4

Obtain additional data on the corrosion performance of MMFX Microcomposite steel and formulate changes in Conclusions and Recommendations to SDDOT as appropriate.

The MMFX Technologies Corporation has objected to some of the conclusions reached in an earlier report, SD2001-05-F (Darwin et al. 2002), with special attention to the chloride thresholds at corrosion initiation for conventional and MMFX Microcomposite steel. The thrust of the additional effort has been to perform new tests to help establish the corrosion performance of MMFX Microcomposite steel. The new test results are used to update the current understanding of the corrosion resistance, life expectancy, and cost effectiveness of MMFX steel.

The following chapters cover the specific tasks, findings, conclusions, and implementation recommendations on the use and desirability of incorporating SMI-316 SC and MMFX Microcomposite steel in reinforced concrete bridge decks.

CHAPTER 4
TASK DESCRIPTION

4.1 LITERATURE SEARCH

Perform a literature search on SMI-316 SC™ steel and its use as reinforcement, including a survey of any identified users.

SMI-316 SC™ steel is a proprietary material that was manufactured for the first time in 2002, shortly before the initiation of this project. Manufacture of the material was preceded by the evaluation of a prototype reinforcement clad with 304 stainless steel (Darwin et al. 1999, Kahrs et al. 2001). Research on the prototype material demonstrated that stainless steel clad reinforcement provides superior corrosion performance when compared to conventional reinforcing steel. On the basis of the earlier study, including a recommendation to use 316 stainless steel as the cladding, Structural Metals, Inc. pursued the development of SMI-316 SC reinforcement.

Early in the production of the reinforcement, SMI discovered that there were some significant difficulties in producing a uniform product. As a result, they chose not to go into full production and are in the process of reevaluating the potential of the new product. As of this date, the product is not in production. Early production runs were used to produce the material that is described in this report and for one experiential bridge in South Carolina that is described in Section 5.1.

4.2 MECHANICAL TESTS

Conduct a series of laboratory tests consisting at a minimum of elongation, yield strength, tensile strength, ASTM bend properties, composition, and corrosion rate on #4, #5, and #6 SMI-316 SC™ steel and mild steel including end treatment effectiveness and provide recommendation for end treatment.

Three bar sizes, No. 4, No. 5, and No. 6, were initially planned for testing. The No. 5 bars were delivered in December 2003, and the No. 6 bars were delivered in April 2004. Structural Metals Inc. has not able to produce No. 4 bars during the course of this study.

Tests include tensile tests, to obtain full stress-strain curves, and bend tests, both performed in accordance with ASTM A 615. The stress-stain curves are obtained using an Instron servo-hydraulic testing machine under stroke control. Strain is measured using an extensometer from Epsilon Technology Corp. with a 4-in. gage length. Dual loading speeds are used to meet requirements in ASTM E 8. A stress rate between 10,000 psi/min and 100,000 psi/min is used before the steel yields, and a strain rate between 5%/min and 50%/min is used after the steel yields. The tensile tests are used to determined yield strength, tensile strength, and

elongation. Bond strength between the cladding and base metal is evaluated by observing the nature of the damage that occurs during mechanical testing.

The results of the mechanical tests are presented in Section 5.2. The procedures for evaluating corrosion rate and end treatment effectiveness are described in Section 4.4 and the results are presented in Section 5.4.

4.3 CLADDING UNIFORMITY

Provide evaluation of cladding uniformity, thickness variability, effects due to deformation profile and bond with the base metal on #4, #5, and #6 reinforcement.

Cladding thickness and bond to the underlying metal is evaluated using a Philips 515 Scanning Electron Microscope (SEM). Three longitudinal specimens and three transverse specimens are evaluated for each of three No. 5 and three No. 6 bars.

The methods used for the evaluation follow the procedures used by Darwin et al. (1999) and Kahrs et al. (2001). The bars are cut using a band saw and cleaned with acetone to remove grease, dust, and oil. The specimens are then polished by hand using progressively finer grades of silicon carbide (SiC) paper, starting with 150 grade SiC paper and proceeding to 300, 600, 1000, and 2000 grades. The specimens are cleaned using soap and water before moving to the next polishing step. Finally, the specimens are mounted on aluminum stubs using conductive double-sided carbon-coated tape.

The specimens are observed using backscattered electron imaging. Images are recorded using an ELMDAS digital image acquisition system at an acceleration voltage of 20 kV with a spot size of 100 nm, at a pixel density of 512 in both the vertical and horizontal directions. Four micrographs are taken for each longitudinal specimen. Six micrographs are taken for the No. 5 transverse specimens, and seven micrographs are taken for the No. 6 bar transverse specimens. On each micrograph, the maximum and minimum cladding thickness, along with the thickness at three other representative points, are measured in millimeters. The bars are also inspected for cracks and disbondment between the cladding and the core metal.

4.4 CORROSION TESTS

Conduct a series of statistically valid comparative tests of corrosion resistance of SMI-316 SC^{TM} steel, ECR, and mild steel reinforcement to determine general corrosion properties both inside and outside concrete, stress and pitting corrosion properties.

The corrosion resistance of SMI-316 SC steel is compared to that of epoxy-coated reinforcement, and conventional mild steel reinforcement using rapid macrocell and bench-scale tests. The tests have been shown to provide valid comparisons using realistic exposure conditions. Corrosion performance is evaluated based on relative corrosion rates, changes in

corrosion potential, and chloride concentrations needed for corrosion initiation. Much of the description of the test methods in this section has been drawn from SD2001-05-F (Darwin et al. 2002).

4.4.1 Rapid Macrocell Tests

Comparisons of corrosion response are made using the *rapid macrocell* test, a test originally developed at the University of Kansas under the SHRP program (Martinez et al. 1990, Chappelow et al. 1992) and updated under the NCHRP-IDEA program (Smith et al. 1995, Darwin 1995, Senecal et al. 1995, Darwin et al. 1996) and in subsequent studies (Darwin 2002). The goal of the technique is to obtain a realistic measure of the performance of corrosion protection systems in a short period of time. The basic test specimen consists of either a bare reinforcing bar or a mortar-wrapped specimen, illustrated in Figure 4.1. The contact surface between the mortar and bar simulates contact obtained between concrete and reinforcing bars in actual structures. When SMI and epoxy-coated bars are tested, the ends of the bars are protected with a plastic cap filled with epoxy, except in specific cases for SMI bars, as will be subsequentially described.

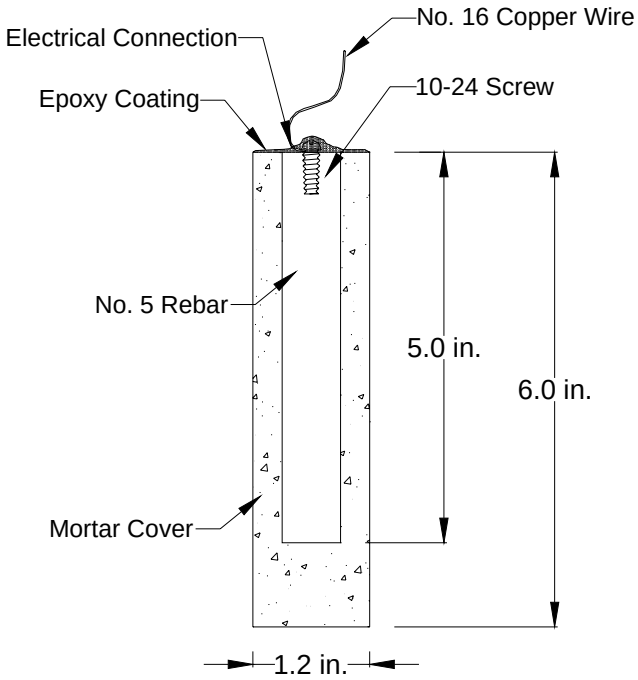

Figure 4.1 – Cross-Section of Mortar-wrapped Test Specimen Used for Rapid Corrosion Macrocell Test

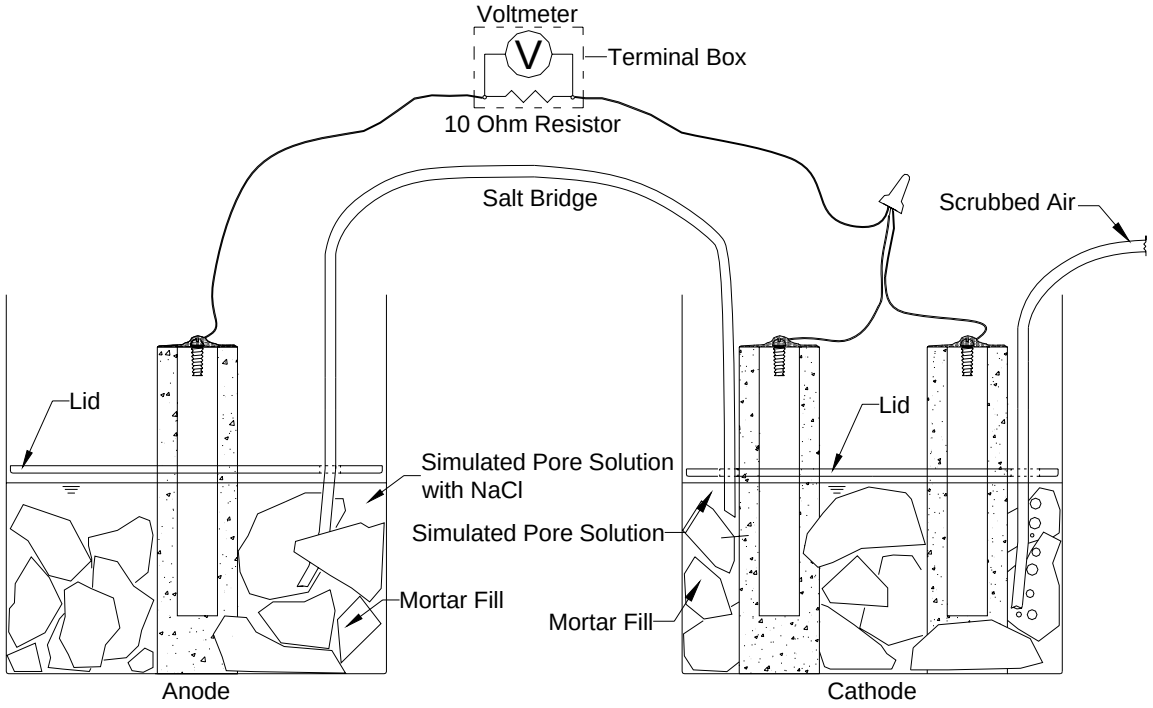

Figure 4.2 – Schematic of Macrocell Test

The macrocell test (Figure 4.2) requires two containers. The test specimen, either a bare bar or a mortar-wrapped specimen, is placed in a four-quart container, along with simulated pore solution containing a preselected concentration of sodium chloride. Two specimens are placed in a second container and immersed in simulated pore solution (with no chlorides added). Crushed mortar fill is added to containers with mortar-wrapped specimens to more closely simulate the concrete environment. The solution depth places 3 in. of the bar below the surface of the liquid. The solutions in the two containers are connected by a salt bridge and the test specimen in the pore solution containing sodium chloride (anode) is electrically connected through a single 10-ohm (± 0.3 ohms) resistor to the two specimens in the simulated pore solution (cathode). The resistors are mounted in a terminal box to consolidate the specimen wires.

Air (scrubbed to remove CO_2) is bubbled into the liquid surrounding the cathode to ensure an adequate supply of oxygen. The air causes some evaporation, which is countered by adding deionized water to the container to maintain a constant volume of the solution. The solutions in both containers are changed every five weeks to maintain the pH of the solution above 13.3 (Ji et al. 2005). The corrosion current and the rate of corrosion can be determined by measuring the voltage drop across the resistor. The corrosion rate is calculated by first determining the corrosion current, which is equal to the voltage divided by the resistance. The actual resistance of each 10-ohm resistor is measured separately. Once the current is measured, the corrosion rate, in terms of metal loss, is calculated using Faraday's law [Eq. (4.1)].

$$r = \frac{ia}{nFD} \tag{4.1}$$

where r = corrosion rate (thickness loss per unit time), i = current density (amperes/cm^2 or coulombs/cm^2 · sec), a = atomic weight (weight of a gram-mole; = 55.84 g for iron), n = number of equivalents exchanged (number of electrons transferred; for Fe^{++} = 2), F = Faraday's Constant = 96500 coulombs/equivalent, and D = density of metal (7.87 g/cm^3 for steel).

In terms of current density (i) in μmA/cm^2, r in μm/yr for iron is

$$r = 11.59i \tag{4.2}$$

The open circuit corrosion potential of the cathode and anode are also measured, using a saturated calomel electrode (SCE). The open circuit is maintained for two hours prior to taking potential readings. Corrosion potentials more negative than approximately –0.275 V indicate that the metal is corroding.

The simulated pore solution, consisting of sodium hydroxide and potassium hydroxide is based on pore solution analysis (Farzammehr 1985, Farzammehr et al. 1987). One quart of the solution contains 0.034 lb of potassium hydroxide (KOH) and 0.037 lb of sodium hydroxide (NaOH). The initial pH of the solution is 13.4. Tests are performed using 1.6 molal (m) ion and 6.04 m ion NaCl solutions at the anode for bare bars and a 1.6 m ion solution NaCl solution for the mortar-wrapped bars. The 1.6 and 6.04 m ion solutions are made, respectively, using 0.095 and 0.359 lb of NaCl in one quart of simulated concrete pore solution. Epoxy-coated steel and some of the SMI-316 SC steel is evaluated using specimens in which the coating is breeched by four $^1/_8$-inch diameter holes to simulate defects in the epoxy coating or damage to the cladding.

Specimen Fabrication – No. 5 reinforcing bars are cut with a band saw to a length of five inches. One end of the bar is then drilled and tapped to a depth of ½ in. to accommodate a No. 10-24 machine screw and the edges of both ends of the bar are belt sanded to grind off sharp edges. Acetone is used to remove grease, dirt, and oil from the surface of the conventional steel and stainless steel clad bars; soap and water is used to clean the epoxy-coated bars. The ends of the epoxy-coated bars and some of the SMI-316 SC bars that will be submerged in the macrocell are protected using a plastic cap filled with Herberts O'Brien Rebar Patch Kit epoxy. This technique serves as the prototype for end treatment to protect cut ends of the SMI-316 SC bars.

Some tests are performed on bare SMI bars to determine the effects of bending on the corrosion performance of the clad steel. For these tests, the reinforcing bar is cut to a length of 12 in., and the sharp edges on the ends of the bar are smoothed with a grinder. One end of the bar is drilled and tapped for a 10-24 threaded bolt to a depth of ½ in. The bar is then bent cold through 180° around a cylindrical steel mandrel with a diameter of 50 mm (2 in.). Bending causes some small indentations in the bar surface where contact is made with the pin that confines the bar from moving during bending. The bar is then cleaned with acetone. The end and

edges around the end of the bar that is not drilled and tapped are covered with Herberts O'Brien Rebar Patch Kit epoxy.

Mortar-wrapped bars are cast in a mold consisting of PVC pipe. The bars are centered using rubber stoppers. As shown in Figure 4.1, the mortar sheathing covers the exterior surface of the bar and projects 1 in. past one end of the bar. The mortar has a water-cement ratio of 0.5 and sand-cement ratio of 2.0, and is fabricated using Type I portland cement, distilled water, and ASTM C 778 graded Ottawa sand. The mix proportions represent the mortar constituent of concrete. The mortar is mixed following the procedures outlined in ASTM C 305. Mortar is placed in the cylindrical mold in four layers. Each layer is rodded 25 times using a $^1/_8$-in. diameter rod, followed by external vibration for 30 seconds using a vibration table with an amplitude of 0.006 in. and a frequency of 60 Hz.

Specimens are cured in the molds for 24 hours. Specimens are then removed from the molds and cured in lime [$Ca(OH)_2$] saturated water (pH = 12.5) for 13 days. After 14 days of curing, the specimens are vacuum dried for one day. For both bare and mortar-wrapped bars, a 16-gage copper electrical wire is secured to the tapped end of each specimen with a 10-24 steel screw. The top of the screw wire and mortar are then coated with two layers of Herberts O'Brien epoxy for bare bars and two layers of Sewer Guard HBS 100 Epoxy Liner, from Degussa Admixtures (now BASF Admixtures).

Mortar fill, made with the same mixture proportions as used for the mortar wrapping, is added to containers holding mortar-wrapped specimens, but not bare specimens.

Test Program – The rapid macrocell test program, summarized in Table 4.1, consists of a total of 90 individual tests in 16 series. The tests evaluate both bare and mortar-wrapped specimens. The bare specimen tests consist of conventional steel (Conv.), epoxy-coated steel with four $^1/_8$-in. diameter holes drilled through the epoxy (ECR), SMI-316 SC bars with no holes in the cladding and with ends of the bars protected by a cap filled with epoxy (SMI), SMI-316 SC bars with four $^1/_8$-in. diameter holes drilled through the cladding with ends of the bars protected by a cap filled with epoxy (SMI-d), and SMI-316 SC bars with no holes in the cladding but *without* the ends of the bars protected by a cap filled with epoxy (SMI-nc), all tested using a 1.6 m ion concentration of NaCl at the anode. The three SMI bar configurations are also tested using the 6.04 m ion concentration NaCl solution. These tests are identified as SMIh, SMIh-d, and SMIh-nc. The SMI tests also include bars with a 180° bend and tests in which SMI bars without holes and with end caps are combined with conventional steel in which one type of steel is used as the anode and the other is used as the cathode.

Mortar-wrapped bar tests are used to evaluate conventional, epoxy-coated, and SMI 316 SC reinforcing steel, with latter tested in the SMI, SMI-d, and SMI-nc configurations, using a 1.6 m ion NaCl concentration at the anode.

Macrocell tests continue for 15 weeks, with readings obtained daily for the first week and weekly thereafter. The results of the tests are presented in Section 5.4.1.

Table 4.1 – Rapid macrocell test program

Bare Bar Specimens			
Steel	**NaCl**	**Number**	
Designation[a]	**Concentration**	**of Specimens**	**Notes**
Conv.	1.6 m	6	
ECR	1.6 m	6	w/ 4 drilled holes
SMI	1.6 m	6	w/ end cap, w/o holes
SMI-d	1.6 m	6	w/ end cap and holes
SMI-nc	1.6 m	6	w/o end cap, w/o holes
SMIh	6.04 m	6	w/ end cap, w/o holes
SMIh-d	6.04 m	6	w/ end cap and holes
SMIh-nc	6.04 m	6	w/o end cap, w/o holes
SMI-b	1.6 m	6	SMI bent 180 degree as anode
SMI/Conv.	1.6 m	3	SMI w/o holes as anode, Conv. as cathode
Conv./SMI	1.6 m	3	Conv. as anode, SMI w/o holes as cathode
Mortar-Wrapped Specimens			
Conv.	1.6 m	6	
ECR	1.6 m	6	w/ 4 drilled holes
SMI	1.6 m	6	w/ end cap, w/o holes
SMI-d	1.6 m	6	w/ end cap and holes
SMI-nc	1.6 m	6	w/o end cap, w/o holes

[a] Conv. = conventional steel. ECR= normal epoxy-coated reinforcement.
SMI = Stainless steel clad reinforcement SMI-316 SC^{TM} reinforcing bars.

4.4.2 Bench-Scale Tests

Bench-scale tests, such as the Southern Exposure, ASTM G 109, and cracked beam tests, have been used for over 25 years to evaluate the corrosion performance of reinforcing steel (Pfeifer and Scali 1981). Although these tests typically require one to two years for completion, they qualify as accelerated tests, considering that the service life of actual structures should be 30+ times as long. Of these tests, the Southern Exposure and cracked beam tests have proven to give the most useful data and are used in this study.

Southern Exposure Test – The specimen used for the Southern Exposure, or SE, test (Pfeifer and Scali 1981) consists of a small slab containing two mats of reinforcing steel (Figure 4.3). A dam is cast integrally with the slab to retain liquid on the upper surface. The top mat of reinforcement consists of two bars; the bottom mat consists of four bars. The mats are connected electrically across a 10-ohm resistor and the sides of the concrete are sealed with epoxy (Sewer Guard HBS). A 15% sodium chloride solution is placed inside the dam, allowing chlorides to penetrate into the concrete. The slabs are subjected to a seven day alternate ponding and drying regime, with ponding at 68-78°F for four days and drying at 100°F for three days. The ponding and drying regime continues for 12 weeks. The specimens are then subjected to continuous ponding for 12 weeks, at which time the alternating ponding and drying regime begins again.

The two regimes are continued for 96 weeks. Corrosion current and the corresponding corrosion rates are determined by measuring the voltage drop across the resistor. The corrosion potential for top and bottom mats and mat-to-mat resistance are also measured. The test provides a very severe corrosion environment that is believed to simulate 30 to 40 years of exposure for bridges within a 48-week period (Perenchio 1992). To obtain an estimate of the chloride concentration required for corrosion initiation, chloride samples are taken at the level of the top reinforcing bars (1 in. below the top surface) at the initiation of corrosion.

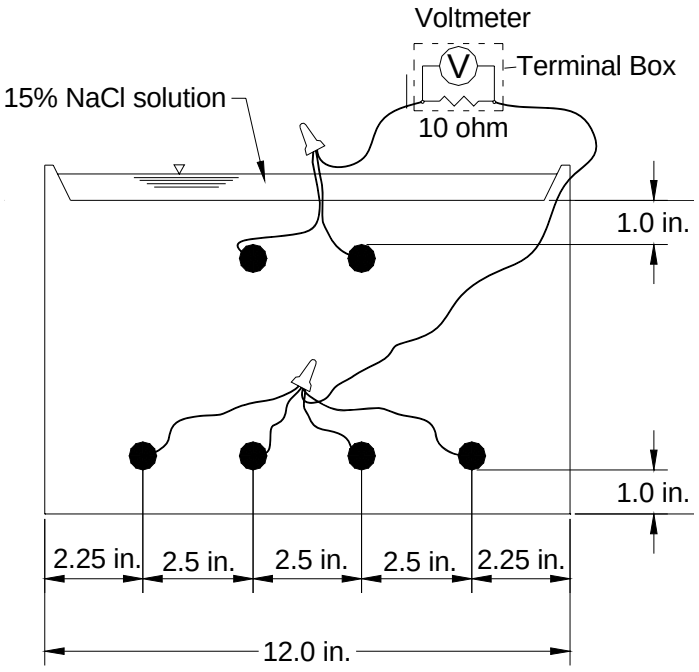

Figure 4.3 – Test Specimen for Southern Exposure Test

The Southern Exposure specimens are fabricated in an inverted position. The concrete is consolidated in two layers. Each layer is vibrated for 30 seconds on a vibrating table with an amplitude of 0.006 in. and a frequency of 60 Hz. The concrete mix proportions (Table 4.2) are selected to provide an objective comparison between the different systems. The concrete has a water-cement ratio of 0.45 and an air content of 6%. The specimens are wet cured for three days (one day in the form and two days in a plastic bag with deionized water) and then air cured until the test begins at 28 days. The top surface of the concrete is sanded lightly prior to initiation of the tests.

Table 4.2 – Concrete properties and mix proportions

Material or Test	Quantity or Property
Cement	598 lb/yd^3
Water	270 lb/yd^3
Fine aggregate [1]	1436 lb/yd^3
Coarse aggregate [2]	1473 lb/yd^3
Air-entraining agent	0.02 gal/yd^3
Slump	3.0 in.
Air content	6.0 %
Unit weight	139.9 lb/ft^3 (3777 lb/yd^3)

[1] S.G.(SSD) = 2.60, absorption = 0.78%, fineness modulus = 2.51
[2] S.G.(SSD) = 2.58, absorption = 2.27%, unit weight = 95.9 lb/ft^3, 3/4 in. nominal maximum size

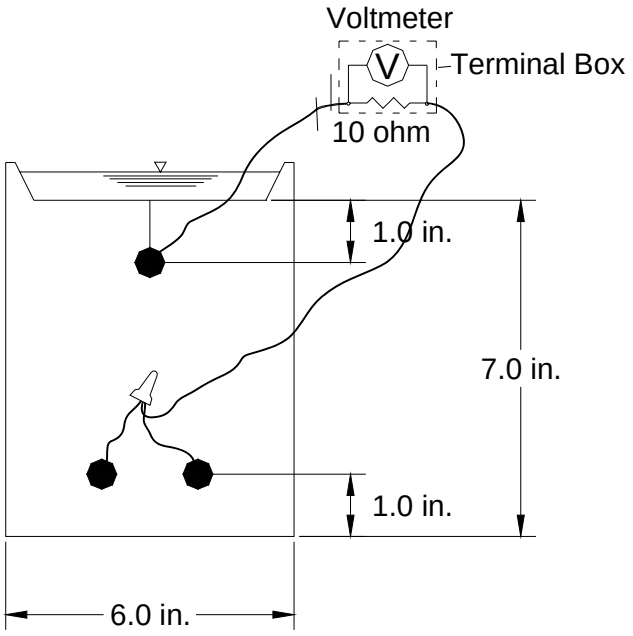

Figure 4.4 – Test specimen for cracked beam test

Cracked Beam Test – The cracked beam specimen (Figure 4.4) is used to model the corrosion of reinforcing steel in concrete where cracks directly expose the steel to deicing chemicals. The specimen is half the width of the SE specimen, with one bar on top and two bars on the bottom. A crack is simulated parallel to and above the top reinforcing bar through the insertion of a 0.012-in. thick stainless steel shim when the specimen is fabricated. The shim is removed within 24 hours of placement, leaving a direct path for chlorides to the reinforcing steel and simulating the effects of a settlement crack over the bar. Like the SE specimen, the cracked beam specimen is subjected to cycles of wetting and drying with a 15% sodium chloride

solution, continuing up to 96 weeks. For conventional steel, the cracked beam specimens typically exhibit corrosion initiation within the first two weeks.

Test Program – The bench-scale test program, summarized in Table 4.3, consists of 33 Southern Exposure and 24 cracked beam tests. Six each Southern Exposure and cracked beam tests are used to evaluate straight conventional, epoxy-coated, and SMI-316 SC reinforcing steel, the latter both without and with four $^{1}/_{8}$-inch diameter holes drilled through the cladding. Three additional Southern Exposure tests are used for each of two configurations combining SMI-316 SC steel and conventional steel to evaluate galvanic effects. For three of the specimens, SMI-316 SC bars are used as the top mat, with conventional steel as the bottom mat; in the other three specimens, the position of the steels is reversed. Three additional Southern Exposure tests are used to evaluate bent SMI bars (pin diameter = 2 in.). As will be discussed in Chapter 5, the cladding was damaged on these bars during the bending process by the bending equipment, which did not have a protective coating.

For tests of epoxy-coated steel, the coating is breached by four $^{1}/_{8}$-inch diameter holes on each bar, to simulate defects in the epoxy coating.

The results of the bench-scale tests are presented in Section 5.4.2.

Table 4.3 – Bench-scale test program

Steel Designation[a]	**Number of Specimens**	**Notes**
Southern Exposure Tests		
Conv.	6	
ECR	6	w/ 4 drilled holes
SMI-d	6	w/ 4 drilled holes
SMI	6	w/o drilled holes
SMI/Conv.	3	SMI w/o holes at top, Conv. at bottom
Conv./SMI	3	Conv. at top, SMI w/o holes at bottom
SMIb	3	SMI bent 180 degree at top
Cracked Beam Tests		
Conv.	6	
ECR	6	w/ 4 drilled holes
SMI-d	6	w/ 4 drilled holes
SMI	6	w/o drilled holes

[a] Conv. = conventional steel. ECR = epoxy-coated reinforcement.
SMI = Stainless steel clad SMI-316 SC^{TM} reinforcing bars.

4.5 CORROSION EFFECTS

Analyze corrosion effects on the SMI-316 SC™ steel using scanning electron microscopy.

The nature of the steel surface on both bare and mortar-wrapped bars after completion of the macrocell tests is evaluated using a Phillips 515 scanning electron microscope (SEM). The technique used follows that developed by Axelsson, Darwin, and Locke (1999) and reported in SD2001-05-F (Darwin et al. 2002).

As the macrocell tests are discontinued, specimens are tagged for identification purposes. A visual inspection is made of the steel surface, epoxy coating, and the mortar cover. Mortar is removed following an evaluation of the intact specimen and mortar pieces are examined for voids. The nature of surface damage and corrosion products are evaluated. The bar surface is examined with a light microscope, providing information for the selection of areas on the specimen to be examined further using the SEM. A hacksaw is used to obtain reinforcing bar slices of the proper size for SEM imaging.

Prior to SEM analysis, cut pieces of steel are mounted with conductive double-sided sticky carbon tabs on aluminum stubs. Conductive carbon paint is used to provide a good conductive path from the top of the specimen to the stub. An Anatech Hummer X sputter coater is used to coat the specimens with a 10-20 nm thick layer of gold palladium to prevent charging.

Specimens are examined using secondary electron imaging to record surface morphology. Images were recorded using an ELMDAS digital image acquisition system at an accelerating voltage of 20 kV with a spot size of 20 nm at a pixel density of 512 in both the vertical and horizontal directions.

The results of the analysis are presented in Section 5.5.

4.6 LIFE EXPECTANCY AND COST EFFECTIVENESS

Estimate the life expectancy and cost effectiveness of SMI-316 SC™ steel, epoxy-coated reinforcement, and mild steel reinforcement in South Dakota.

The life expectancy and cost effectiveness of bridges containing metallized stainless steel clad reinforcement, ECR, and conventional steel reinforcement are determined based on the experience of the Department of Transportation in South Dakota (Gilsrud 2007) and other states (Kepler, Darwin, and Locke 2000) in conjunction with the laboratory results obtained in this study.

4.6.1. Life Expectancy

The life expectancy of bridges constructed with different steel reinforcing systems is estimated based on both experience and analysis. In South Dakota and Kansas, bridges containing epoxy-coated reinforcement, dating to the late 1970s, have never required repair due

to corrosion-induced damage (Gilsrud 2002 and Kepler et al. 2000). Engineers in the two states estimate time to first repair for epoxy-coated reinforcement as 40 and 35 years, respectively. Both figures are used in the current study for comparison. An analytical estimate of life expectancy is obtained based on estimates of the time required for corrosion initiation and subsequent period required to cause delamination cracking due to corrosion. The time to corrosion initiation is estimated using chloride concentrations measured at crack locations on bridge decks (Miller and Darwin 2000, Lindquist et al. 2005) and chloride concentrations at corrosion initiation, as measured in the current study. Prior research has demonstrated that chloride concentrations between 1.0 and 2.0 lb/yd^3 will result in corrosion initiation for conventional uncoated reinforcement and epoxy-coated reinforcement for which the coating has been damaged. In contrast, stainless steel exhibits values on the order of 18 to 30 lb/yd^3 (McDonald, Pfeifer, and Sherman 1998, Ji et al. 2005). The time required to reach a particular threshold value is estimated using results from field studies of bridge deck cracking and chloride contents at various layers of actual bridge decks (Miller and Darwin 2000, Lindquist et al. 2005) and laboratory specimens. Time to delamination cracking for uncoated steel with relatively uniform corrosion losses along the length of the reinforcing bar is estimated based on the rate of corrosion measured in the current study and an estimate that a thickness loss of 0.025 mm (0.00098 in.) will result in a volume of corrosion products that will crack concrete (Pfeifer 2000). For coated steel, estimates of required corrosion loss products to crack concrete at areas of limited damage in the protective epoxy coating are calculated using equations developed by Torres-Acosta and Sagues (2005).

4.6.2 Cost Effectiveness

Life Cycle Cost Analysis – A 75-year economic life is used to compare the current costs associated with using conventional, epoxy-coated, and stainless steel clad reinforcement in South Dakota bridge decks. An 8.5-in. bridge deck is used in the analysis including the costs associated with a new bridge deck and repair costs over the 75-year life of the bridge.

Repair Costs – Repair costs for a "typical" 8.5-in. bridge deck were obtained from SDDOT (Gilsrud 2007). Current data includes repair of bridge decks with conventional reinforcement only because the bridge decks constructed since the late 1970s have been constructed using epoxy-coated reinforcement and have not needed repair as of the date of this report. It is estimated that repair costs of bridge decks with epoxy-coated reinforcement will be similar to those for decks with conventional reinforcement.

The repair costs are based on an average of costs for previous bridge deck repair projects through the end of the year 2006 (Gilsrud 2007). A "typical" repair project includes costs for removing deleterious concrete and replacing with a low-slump dense concrete overlay, bridge rail modifications, approach guard rail replacement, approach pavement work, mobilization, traffic control and other miscellaneous costs. Costs were determined per square yard considering a typical bridge deck as described by SDDOT (Gilsrud 2007) with a width of 36 ft and a total length of 150 ft. A summary of the repair costs and conversion to \$/yd^2 are shown in Table 4.4

and described in Eqs. (4.3)-(4.8). User costs are difficult to quantify and are not included in this analysis.

Table 4.4 – Repair costs for bridge decks in South Dakota (Gilsrud 2007)

Item	Unit	Cost	Cost/yd^2
Low Slump Dense Concrete Overlay	Per yd^2	$130.00	$130
Bridge Rail Modification	Per linear ft	$62.00	$31
Approach Guard Rail	Lump sum	$16,500.00	$28
Approach Pavement Work	Lump sum	$17,000.00	$28
Mobilization	Lump sum	$25,000.00	$42
Traffic Control and Misc.	Lump sum	$20,000.00	$33
Total Repair Costs			$292

Bridge Rail Modification

$$\frac{\$62}{\text{ft}} \times \frac{2\text{ sides}}{\text{bridge}} \times \frac{1}{36 - \text{ft deck width}} \times \frac{9\text{ ft}^2}{\text{yd}^2} = \$31/\text{yd}^2 \tag{4.3}$$

Approach Guard Rail

$$\frac{\$16{,}500}{\text{project}} \times \frac{\text{typical bridge}}{5{,}400\text{ ft}^2} \times \frac{9\text{ ft}^2}{\text{yd}^2} = \$28/\text{yd}^2 \tag{4.4}$$

Approach Pavement Work

$$\frac{\$17{,}000}{\text{project}} \times \frac{\text{typical bridge}}{5{,}400\text{ ft}^2} \times \frac{9\text{ ft}^2}{\text{yd}^2} = \$28/\text{yd}^2 \tag{4.5}$$

Mobilization

$$\frac{\$25{,}000}{\text{project}} \times \frac{\text{typical bridge}}{5{,}400\text{ ft}^2} \times \frac{9\text{ ft}^2}{\text{yd}^2} = \$42/\text{yd}^2 \tag{4.6}$$

Traffic Control and Misc.

$$\frac{\$20{,}000}{\text{project}} \times \frac{\text{typical bridge}}{5{,}400\text{ ft}^2} \times \frac{9\text{ ft}^2}{\text{yd}^2} = \$33/\text{yd}^2 \tag{4.7}$$

Total repair costs = Total overlay deck + bridge rail modification + approach guard rail + mobilization + traffic control and misc.

$$= \$130/yd^2 + \$31/yd^2 + \$28/yd^2 + \$28/yd^2 + \$42/yd^2 + \$33/yd^2 \quad (4.8)$$
$$= \$292/yd^2$$

New Bridge Deck Costs – Current costs for new bridge decks are calculated considering the in-place costs of concrete and the various types of reinforcing steel. The costs were calculated for a "typical" 8.5-in. bridge deck using conventional, epoxy-coated, and stainless steel clad reinforcement. The in-place costs for the concrete is obtained from SDDOT (Gilsrud 2007). The in-place cost for stainless steel clad reinforcement is estimated considering a base cost of $1.80/lb, placement costs of $0.65/lb (based on the fabrication, shipping, and placement costs of epoxy-coated steel), and an assumed cost of $0.02/lb for end protection [updated from Gong et al. (2006) based on increases in costs of other types of reinforcing bars]. The total in-place cost of stainless steel clad reinforcement is, thus, $2.47/lb. The corresponding costs for conventional steel are $0.36/lb (base cost) and $0.59/lb (fabrication, etc.) for a total cost of $0.95/lb and for epoxy-coated steel are $0.53/lb and $0.65/lb for a total of $1.18/lb [based on 20-city average of spot prices in June 2007 (*Engineering News Record* 2007) and checked with an industry source (Marquart 2007)]. The costs for conventional and epoxy-coated steel are higher than for recent construction in South Dakota (Gilsrud 2007), but are used to provide values that are consistent with the estimated base cost of the stainless steel clad bars.

The in-place costs considered in the analysis are listed in Table 4.5. The calculations for cost/yd^2 are shown in Eqs. (4.9)-(4.13). The reinforcement costs were calculated considering an average amount of reinforcement of 210 lb/yd^3 (Gilsrud 2007).

Table 4.5 – Bridge deck construction costs in South Dakota

Item	In-place Cost	Cost/yd^2
Concrete	$540/yd^3	$127.5
Conventional steel	$0.95/lb	$47.1
Epoxy-coated steel	$1.18/lb	$58.5
Stainless steel clad	$2.47 /lb	$ 122.5

Concrete

$$\frac{\$540}{yd^3} \times \frac{8.5\,\text{in.}}{\text{typical deck}} \times \frac{yd}{36\,\text{in.}} = \$127.5/yd^2 \quad (4.9)$$

Typical Amount of Reinforcement

$$\frac{210\,\text{lb}}{yd^3} \times \frac{8.5\,\text{in.}}{\text{typical deck}} \times \frac{yd}{36\,\text{in.}} = 49.6\ \text{lb/yd}^2 \quad (4.10)$$

Conventional Steel

$$\frac{\$0.95}{\text{lb}} \times \frac{49.6\,\text{lb}}{\text{yd}^2} = \$47.1/\text{yd}^2 \tag{4.11}$$

Epoxy-Coated Steel

$$\frac{\$1.18}{\text{lb}} \times \frac{49.6\,\text{lb}}{\text{yd}^2} = \$58.5/\text{yd}^2 \tag{4.12}$$

Stainless Steel Clad

$$\frac{\$2.47}{\text{lb}} \times \frac{49.6\,\text{lb}}{\text{yd}^2} = \$122.5/\text{yd}^2 \tag{4.13}$$

Calculations for current costs for a new deck using the various options of reinforcement are shown in Eqs. (4.14)-(4.16).

Conventional Steel
8.5-in. Concrete Deck + Conventional Steel = $\$127.5/\text{yd}^2 + \$47.1/\text{yd}^2 = \$174.6/\text{yd}^2$ (4.14)

Epoxy-Coated Steel
8.5-in. Concrete Deck + Epoxy-Coated Steel = $\$127.5/\text{yd}^2 + \$58.5/\text{yd}^2 = \$186.0/\text{yd}^2$ (4.15)

Stainless Steel Clad
8.5-in. Concrete Deck + Stainless Steel Clad = $\$127.5/\text{yd}^2 + \$122.5/\text{yd}^2 = \$250.0/\text{yd}^2$ (4.16)

4.7 MMFX CORROSION POTENTIAL TESTS

Compare the corrosion potential of conventional and MMFX Microcomposite steel in simulated concrete pore solution at NaCl molal ion concentrations ranging from 0.4 to 6.04.

The corrosion potential test provides a relative measure of the chloride concentrations at which corrosion will be initiated. The test configuration is similar to that described for the rapid macrocell test in Section 4.4.1, but with a single bare bar in a single container for each test. The corrosion potentials of the two steels are compared in simulated pore solution at NaCl molal ion concentrations of 0.2, 0.4, 0.5, 0.6, 0.7, 1.0, 1.6, and 6.04. Three bars are tested for each concentration. The solution is changed every five weeks to maintain the pH. The corrosion potentials are taken with respect to a saturated calomel electrode (SCE), which is electrically connected to the test bar and submerged in the solution surrounding the test bar. A difference in

voltage between the bar and the electrode, the corrosion potential, more negative than – 0.275 V indicates that the steel is corroding.

4.8 MMFX CRITICAL CHLORIDE CORROSION THRESHOLD

Determine the chloride content at the corrosion threshold for conventional and MMFX Microcomposite steel.

The purpose of this task is to determine the chloride contents in the concrete that correspond with the initiation of corrosion for conventional and MMFX reinforcement. This is accomplished using a direct analysis of the chloride content of the concrete adjacent to the reinforcing steel when corrosion starts in Southern Exposure or beam specimens (CB specimens without the crack). The methods of sampling and testing for chloride ion concentration in concrete and the test program are discussed next. The test is described in greater detail by Ji et al. (2005).

Pulverized concrete samples are obtained by drilling 0.25 in. diameter holes using a rotary impact drill into the side of bench scale specimens. The first ½ in. of material is discarded and drilling is continued for a total depth of 3.5 in. Each hole produces a sample yield of about six grams (four grams if the depth of the hole is 64 mm (2.5 in.) for beam specimens).

The water-soluble chloride content in the concrete sample is determined using Procedure A in AASHTO T260-97 with boiled distilled water to digest the powdered concrete sample and titration of the chlorides with a silver nitrate solution. Millivolt readings are taken for the sample solution using an ion selective electrode and a voltmeter during the titration. The endpoint of the titration is indicated by the largest difference in two consecutive voltmeter readings. An Orion Model 94-17B chloride selective electrode, an Orion Model 90-02 double junction reference electrode, and a Fluke 83 digital multimeter are used.

In this study, the chloride content, in percent of weight of concrete, is converted to lb/yd^3 of concrete by multiplying by the unit weight of concrete, taken as 3780 lb/yd^3.

To determine the chloride content at corrosion initiation (often referred to as the chloride threshold or critical chloride threshold), concrete samples are taken at the level of the top reinforcing steel in the SE and beam specimens immediately after the reinforcing steel begins to corrode. For each sample, holes are centered so that the top of the holes and the top surface of the bar are in the same plane. Since the concrete cover for each bar is not exactly 25.4 mm (1 in.), the actual value is measured to determine the depth of the sample.

Corrosion initiation for these specimens is considered to have occurred when either the corrosion rate based on the corrosion current through the resistor connecting the top and bottom mats of steel first reaches a value greater than or equal to 0.3 μm/year or the corrosion potential of the top mat of steel first shifts to a value more negative than –0.350 V with respect to a copper-copper sulfate electrode (CSE).

Samples to determine the critical chloride threshold are obtained in two ways: First, chloride samples are taken from modified SE specimens where each top mat bar is connected to two bottom mat bars across a 10-ohm resistor. When corrosion begins for the top bar, ten powdered samples are obtained by drilling ten holes perpendicular to the bar into the side of the SE specimen. The holes are at the side closest to the corroding bar. The sampling locations are shown in the Figures 4.5a and 4.5b. The holes are then filled with modeling clay to allow the tests to continue until the other top bar corrodes.

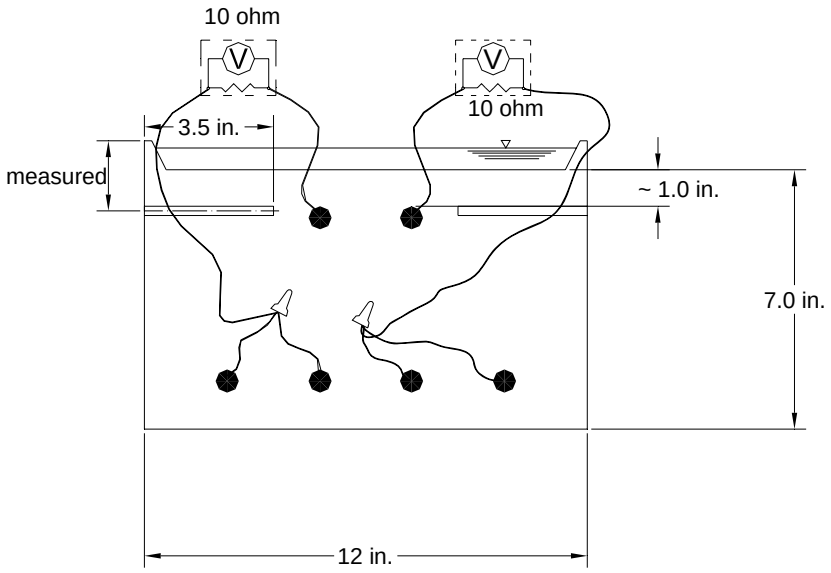

Figure 4.5a – Sampling locations in modified SE specimens (front view)

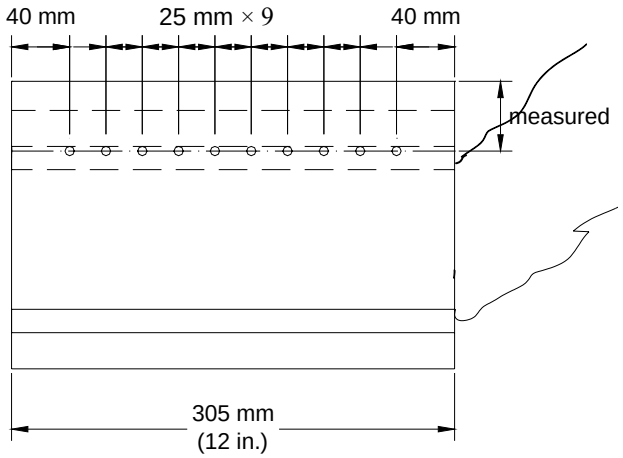

Figure 4.5b – Sampling locations in modified SE specimens (side view)

Second, chloride samples are taken from beam specimens that are fabricated using the mold for the cracked beam specimen with the slot to form the crack sealed with a layer of

masking tape. The purpose of the beam test is to obtain a high number of chloride samples for a single bar. The sampling method is the same as that used for the modified SE specimens, except that sampling is performed from both sides of the specimen, as illustrated in Figure 4.6, producing 20 samples for each specimen.

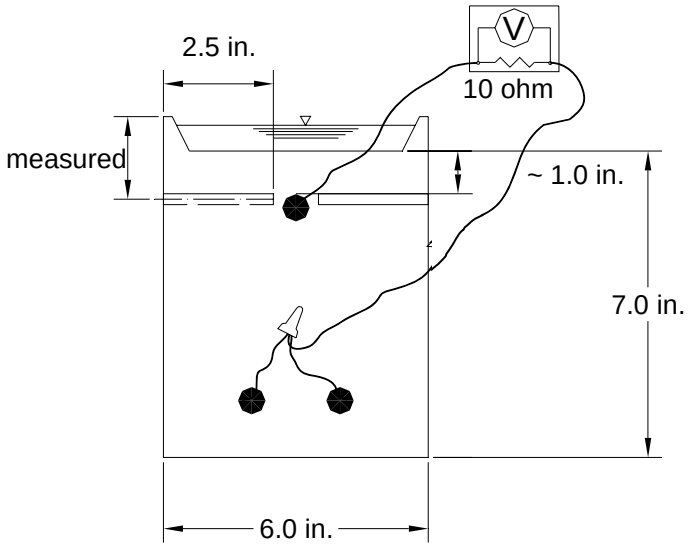

Figure 4.6 – Sampling locations in beam specimens (front view)

Six modified SE specimens and three beam specimens are fabricated to determine the chloride threshold of conventional and MMFX reinforcing steel. The test program is summarized in the Table 4.6. Results of the critical chloride threshold tests are presented in Section 5.8.

Table 4.6 – Test programs for determining chloride thresholds directly

Test specimens*	Type of steel	Number of specimens	Samples of each specimen
MSE-N2	N2	6	10
MSE-MMFX	MMFX	6	10
B-N2	N2	3	20
B-MMFX	MMFX	3	20

*Test method, MSE =modified Southern Exposure test; B = beam test.
Steel type, N2 = conventional N2 steel; MMFX = MMFX Microcomposite steel.

4.9 MMFX LIFE EXPECTANCY AND COST EFFECTIVENESS

Use the new data to modify life expectancy and cost effectiveness calculations for bridge decks containing MMFX Microcomposite steel.

The life expectancy and cost effectiveness of bridges containing MMFX Microcomposite steel reinforcement are determined based on the experience of the Department of Transportation in South Dakota (Gilsrud 2007) and other states (Kepler, Darwin, and Locke 2000) in conjunction with laboratory results. These results are compared with the analysis described in Section 4.6.

4.9.1 Life Expectancy

The life expectancy, as described in Section 4.6, is based on the expected time to corrosion initiation and the additional time required to form enough corrosion products to crack the concrete. The initial life of bridge decks containing MMFX reinforcement are necessarily derived from laboratory studies of chloride contents at corrosion initiation and measured corrosion rates because bridges constructed with MMFX steel have been in service for much less than the expected service life of bridges containing conventional steel reinforcement. As will be described in Section 5.8, the critical chloride threshold for MMFX reinforcement is approximately 6.5 lb/yd^3. The time to delamination cracking is determined based on corrosion rates measured in laboratory specimens, an assumed relatively uniform distribution of corrosion losses over the length of the reinforcement, and a thickness loss of 0.025 mm (0.00098 in.) (Pfeifer 2000).

4.9.2 Cost Effectiveness

Life Cycle Cost Analysis – As described in Section 4.6.2, an economic life of 75 years is used to compare the costs associated with using MMFX reinforcement in South Dakota bridge decks with the costs associated with using other reinforcement systems. The representative bridge deck (8.5-in. thickness with 2.5-in. cover on the reinforcement, 36-ft width, and 150-ft length) and initial costs and repair costs discussed in Section 4.6 are used for this evaluation.

Repair Costs – It is estimated that repair costs of bridge decks containing MMFX reinforcement will be similar to those for decks containing conventional reinforcement. Repair costs are calculated as described in Section 4.6 and are based on an average of costs for previous bridge deck repair projects through the end of the year 2003. User costs are not included in this analysis.

New Bridge Deck Costs – As described in Section 4.6 for bridge decks with conventional, epoxy-coated, and stainless steel clad reinforcement, current costs for new bridge decks are calculated considering the in-place costs of concrete and the various types of reinforcing steel. The costs in this section were calculated for a "typical" 8.5-in. bridge deck using MMFX reinforcement. In-place costs for MMFX reinforcement are estimated considering two base costs at the mill ($0.82/lb and $1.00/lb) and the cost of fabrication, delivery, and

placement ($0.59/lb) to provide in-place costs of $1.41/lb and $1.59/lb for use in the economic analysis.

The in-place costs for MMFX steel are calculated as shown in Eqs. (4.24) and (4.25) and found to be $69.9/yd^2 and $78.9/yd^2. The reinforcement costs are calculated considering an average amount of reinforcement of 210 lb/yd^3 (Gilsrud 2007).

In-place costs of using MMFX steel based on the two base prices at the mill are

$$\frac{\$1.41}{\text{lb}} \times \frac{49.6 \text{ lb}}{\text{yd}^2} = \$69.9/\text{yd}^2 \tag{4.24}$$

$$\frac{\$1.59}{\text{lb}} \times \frac{49.6 \text{ lb}}{\text{yd}^2} = \$78.9/\text{yd}^2 \tag{4.25}$$

Calculations for the current costs based on the two mill costs for a new deck using MMFX reinforcement are shown in Eqs. (4.26) and (4.27).

Current costs for a new deck using MMFX steel are

8.5-in. Concrete Deck + MMFX Steel = $127.5/yd^2 + $69.9/yd^2 = $197.4/yd^2 (4.26)

8.5-in. Concrete Deck + MMFX Steel = $127.5/yd^2 + $78.9/yd^2 = $206.4/yd^2 (4.27)

The costs of a new deck using MMFX steel are calculated to range between $197.4/yd^2 and $206.4/yd^2, which exceeds the costs calculated for using conventional ($174.6/yd^2) and epoxy-coated reinforcement ($186.0/yd^2), but is less than the cost of using stainless steel clad reinforcement ($250.0/yd^2).

CHAPTER 5

FINDINGS AND CONCLUSIONS

5.1 LITERATURE SEARCH

Prototype reinforcement, consisting of conventional steel clad with 304 stainless steel, was evaluated prior to the manufacture of the material described in this report (Darwin et al. 1999, Kahrs, Darwin, and Locke 2001). The results of the earlier study indicated that the prototype 304 stainless steel clad reinforcement exhibited superior corrosion resistance compared to conventional reinforcing steel but that it required adequate protection at cut ends, where the mild steel core is not covered by cladding. For their tests, that protection consisted of plastic caps filled with epoxy. The use of epoxy repair material alone, as used for epoxy-coated reinforcement, did not provide adequate protection. For bare stainless steel clad bars, the macrocell corrosion rate was observed to vary between 0.0 and 0.3 μm/yr, equal to about 1/100 of the value observed for conventional bars. The stainless steel clad bars embedded in mortar exhibited corrosion rates between 0.0 and 0.2 μm/yr, equal to 1/20 to 1/50 of the value exhibited by conventional bars. The early tests were limited to rapid macrocell tests, described in Section 4.3, and longer-term tests were recommended.

Structural Metals Inc. remains in the development stage for the SMI-316 SC bars and has not yet begun regular production of the bars. As a result, the bars have not been used in practice, with the exception of a single bridge over a tidal inlet on Johns Island, South Carolina. Construction on the Chisolm Road Bridge began on January 5, 2004 and was completed on May 23, 2005. The bridge is 150 ft long and 31 feet wide and constructed on 3-ft bent caps and 24-in. prestressed concrete piling. The bridge deck is 16 in. thick (Bodiford 2006).

The bridge was built in five 30 ft. sections, each section insulated from the next and constructed with a different corrosion protection system. In addition to SMI-316 SC bars, the bridge includes solid stainless, MMFX, epoxy-coated, and conventional steel reinforcement (two spans for the latter). The bridge was constructed using IBRC funding and used a total of 6 tons of SMI-316 SC reinforcement (Rajabi 2006). Due to the short time in service, no observations are available on any of the five corrosion protection systems used in the bridge.

5.2 MECHANICAL TESTS

The stainless steel clad reinforcement and conventional steel were tested for mechanical properties. Stress-strain curves for No. 5 and No. 6 SMI-316 SC bars are shown respectively in Figures 5.1a and 5.1b. The yield strength, tensile strength, elongation, and bending results for both types of steel are summarized in Table 5.1.

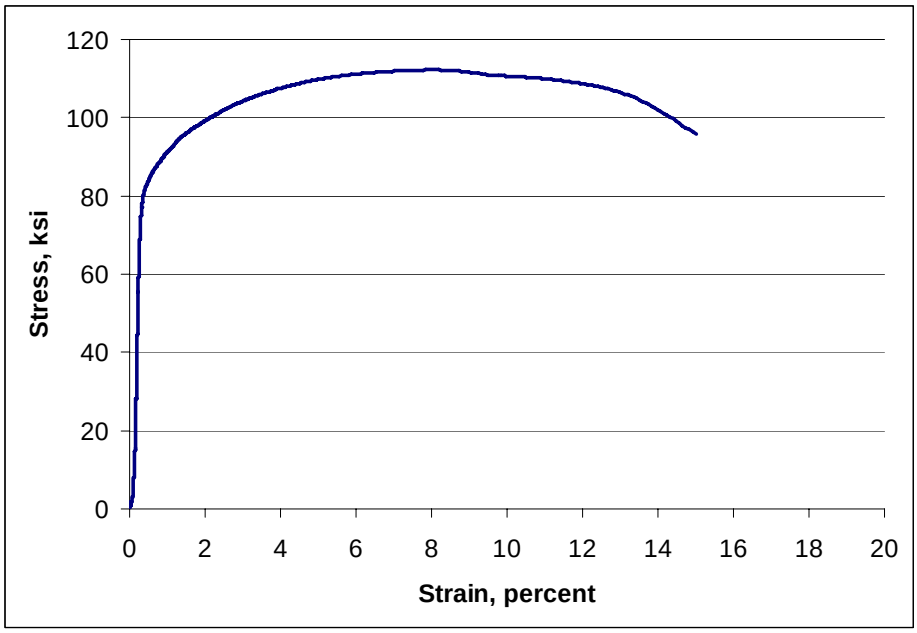

Figure 5.1a – Stress-stain curve for No. 5 SMI-316 SC bar

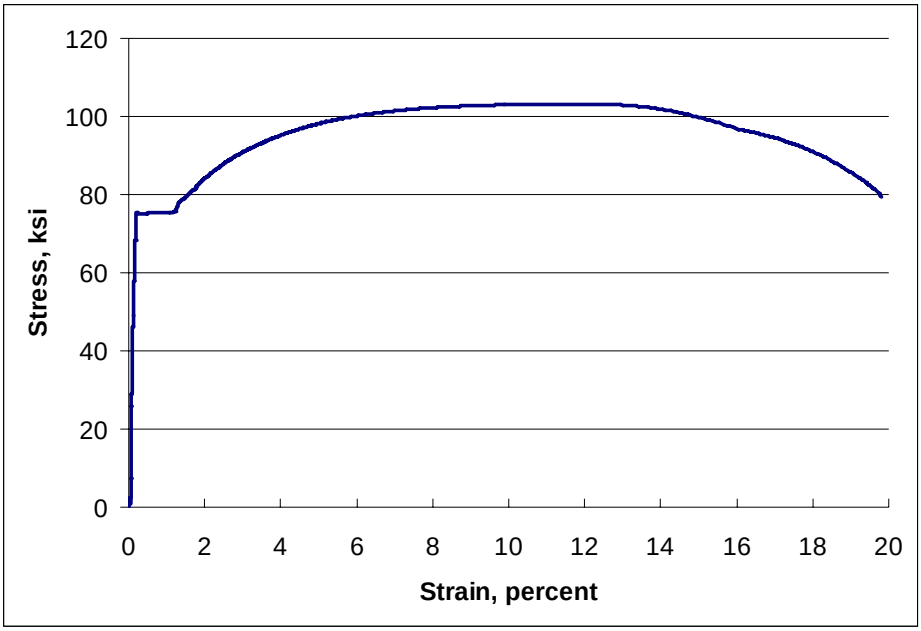

Figure 5.1b – Stress-stain curve for No. 6 SMI-316 SC bar

The yield strengths for *conventional steel* are obtained based on well-defined yield points. As shown in Table 5.1, the average yield strengths ranged from a low of 67.3 ksi for a heat of No. 5 bars to a high of 74.1 ksi for a heat of No. 6 bars. Average tensile strengths were between 109.1 ksi and 118.4 ksi. Average elongations ranged from 13.6 to 16.8%, with a low value of 12.5% for an individual test.

Table 5.1 – Mechanical test results for conventional and SMI-316 SC reinforcing steel

Steel	Heat No.	Size	Sample Number	Yield Strength ksi	Tensile Strength ksi	Elongation % in 8 in.	Bending
Conv.	S44407	No. 5	1	68.2	110.5	16.4	Pass
			2	67.0	108.5	15.6	
			3	66.8	108.3	14.8	
			Average	67.3	109.1	15.6	
Conv.	S44420	No. 5	1	68.1	113.1	12.5	Pass
			2	68.2	110.9	15.6	
			3	69.8	114.7	14.1	
			Average	68.7	112.9	14.1	
Conv.	S47695	No. 6	1	74.2	118.8	14.1	Pass
			2	74.7	119.2	12.5	
			3	73.2	117.2	14.1	
			Average	74.0	118.4	13.6	
Conv.	S47790	No. 6	1	73.7	115.6	12.9	Pass
			2	74.9	117.6	14.1	
			3	73.9	115.8	18.8	
			Average	74.1	116.3	15.3	
Conv.	S47814	No. 6	1	68.6	110.1	18.4	Pass
			2	69.5	111.1	16.4	
			3	68.9	110.2	15.6	
			Average	69.0	110.5	16.8	
SMI-316 SC		No. 5	1	79.2*	112.5	12.5	Pass
			2	78.2*	113.5	13.8	
			3	79.8*	109.8	14.3	
			4	77.1*	112.1	13.8	
			5	80.0*	113.0	14.3	
			Average	78.9*	112.2	13.7	
SMI-316 SC		No. 6	1	75.3	103.3	18.8	Pass
			2	75.1	103.6	23.4	
			3	76.9	105.1	17.2	
			4	77.0	105.2	18.8	
			5	77.7	104.6	17.2	
			Average	76.4	104.4	19.1	

* The yield strength based on the stress corresponding to a strain of 0.35% from the stress-strain diagram

The No. 5 *stainless steel clad reinforcement* does not have an obvious yield plateau, as shown in Figure 5.1a, while the No. 6 stainless steel clad reinforcement does (Figure 5.1b). Thus, the yield strengths of the No. 5 SMI-316 SC bars are based on 0.35% total strain, rather than the value on a yield plateau, as they are for the other bars in this study. The yield strengths for the No. 5 bars ranged from 77.1 to 80.0 ksi, with an average of 78.9 ksi. The yield strengths for the No. 6 bars ranged from 75.1 to 77.7 ksi, with an average of 76.4 ksi. The tensile strengths

averaged 112.2 ksi for the No. 5 bars and 104.4 ksi for the No. 6 bars. Average elongations for an 8 in. gage length were 13.7% and 19.1%, respectively.

All conventional and stainless steel clad bars passed the bend test.

The tests demonstrate that the No. 5 and No. 6 SMI bars satisfy the mechanical properties required by ASTM A 615 and can be used as replacements for conventional No. 5 and No. 6 bars.

5.3 CLADDING UNIFORMITY

Three longitudinal specimens and three transverse specimens for each of three No. 5 and three No. 6 stainless steel clad bars were evaluated for cladding uniformity and thickness variation. The micrographs obtained using the scanning electron microscope demonstrated that a metallurgical bond had been obtained between the 316LN stainless steel cladding and the mild steel core of the bars (Figure 5.2). No unclad regions or cracks through the cladding were observed.

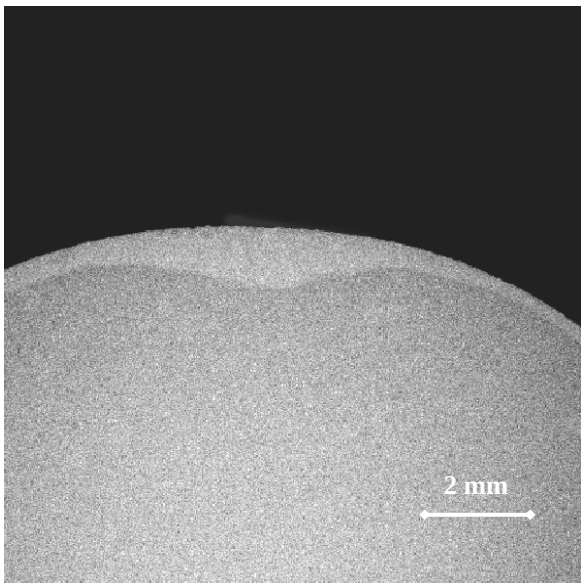

Figure 5.2 – Scanning electron image of cladding (transverse surface)

The measured thickness values in mm (the units of measure) are presented in Tables 5.2a through 5.2f. For the No. 5 bars, the average cladding thicknesses varied between 26 and 30 mils (0.65 and 0.75 mm), with standard deviations between 8 and 13 mils (0.20 and 0.34 mm). For the No. 6 bars, the average cladding thicknesses ranged from 24 to 45 mils (0.62 to 1.13 mm), with standard deviations between 6 and 13 mils (0.15 and 0.34 mm). The minimum thickness measured on any bar was 6 mils (0.15 mm), which is adequate to physically protect the core.

Table 5.2a – Cladding thickness for SMI-316 SC No. 5 bar, sample 1

Sample and Number		Measured Thickness(mm)					Max. Thickness (mm)		Min. Thickness (mm)		Average Thickness (mm)		Standard Deviation	
Longitudinal	1	0.75	0.52	0.65	0.65	0.41	0.91	1.05	0.41	0.23	0.72	0.66	0.13	0.20
		0.8	0.77	0.78	0.66	0.61								
		0.91	0.84	0.86	0.79	0.79								
		0.88	0.81	0.63	0.76	0.58								
	2	0.84	0.71	0.77	0.76	0.73	0.97		0.44		0.68		0.14	
		0.97	0.81	0.83	0.84	0.78								
		0.65	0.61	0.58	0.54	0.5								
		0.67	0.6	0.46	0.52	0.44								
	3	1.05	0.95	0.69	0.81	0.54	1.05		0.23		0.56		0.26	
		0.83	0.76	0.82	0.81	0.77								
		0.38	0.38	0.32	0.35	0.31								
		0.47	0.31	0.24	0.24	0.23								
Transverse	1	1.23	1.21	0.88	1.08	0.81	1.23	1.31	0.18	0.18	0.71	0.71	0.29	0.30
		0.94	0.26	0.44	0.68	0.18								
		0.82	0.79	0.5	0.66	0.4								
		1.16	1.05	0.91	0.84	0.81								
		0.96	0.47	0.26	0.4	0.25								
		0.84	0.78	0.66	0.5	0.49								
	2	1.15	0.94	0.86	0.95	0.74	1.31		0.22		0.68		0.32	
		0.91	0.63	0.29	0.35	0.26								
		0.65	0.39	0.26	0.4	0.22								
		1.31	1.04	0.94	1.15	0.89								
		0.9	0.55	0.8	0.52	0.47								
		1.24	0.44	0.5	0.32	0.32								
	3	1.11	0.92	0.76	0.94	0.69	1.19		0.21		0.74		0.27	
		0.92	0.41	0.5	0.82	0.86								
		0.9	0.57	0.77	0.8	0.54								
		1.19	1.13	0.86	0.99	0.86								
		0.97	0.76	0.41	0.34	0.21								
		1.02	0.95	0.49	0.36	0.26								

Table 5.2b – Cladding thickness for SMI-316 SC No. 5 bar, sample 2

Sample and Number		Measured Thickness(mm)					Max. Thickness (mm)		Min. Thickness (mm)		Average Thickness (mm)		Standard Deviation	
Longitudinal	1	1.12	0.78	1.07	1	0.73	1.12	1.15	0.56	0.16	0.83	0.75	0.16	0.25
		1.09	1.06	0.91	0.68	0.67								
		0.96	0.73	0.8	0.73	0.71								
		0.82	0.73	0.67	0.75	0.56								
	2	1.07	0.9	0.94	0.81	0.72	1.07		0.16		0.54		0.27	
		0.83	0.75	0.54	0.71	0.53								
		0.39	0.39	0.29	0.27	0.27								
		0.41	0.39	0.2	0.27	0.16								
	3	1.15	0.91	0.82	1.06	0.69	1.15		0.61		0.87		0.14	
		1.1	1.02	0.88	0.83	0.81								
		0.98	0.86	0.91	0.86	0.83								
		0.92	0.68	0.67	0.86	0.61								
Transverse	1	1.12	1.04	0.86	0.81	0.76	1.23	1.36	0.26	0.25	0.72	0.71	0.26	0.29
		0.93	0.86	0.5	0.61	0.43								
		0.64	0.37	0.43	0.59	0.34								
		1.05	0.33	0.69	0.44	0.26								
		1.23	1.13	1.05	0.9	0.76								
		0.8	0.71	0.69	0.8	0.52								
	2	1.13	1.05	0.85	0.9	0.74	1.21		0.28		0.67		0.27	
		0.69	0.63	0.55	0.64	0.43								
		0.84	0.43	0.54	0.81	0.42								
		1.21	1.02	0.93	0.83	0.73								
		0.58	0.37	0.34	0.29	0.28								
		1.09	0.46	0.55	0.35	0.31								
	3	1.27	1.17	1.22	0.95	0.92	1.36		0.25		0.74		0.34	
		0.94	0.83	0.47	0.34	0.33								
		1.36	0.64	0.51	0.83	0.49								
		1.27	0.88	0.86	1.07	0.75								
		0.79	0.43	0.39	0.26	0.25								
		1.02	0.95	0.49	0.36	0.26								

Table 5.2c – Cladding thickness for SMI-316 SC No. 5 bar, sample 3

Sample and Number		Measured Thickness(mm)					Max. Thickness (mm)		Min. Thickness (mm)		Average Thickness (mm)		Standard Deviation	
Longitudinal	1	0.58	0.56	0.52	0.35	0.33	1.42	1.42	0.33	0.15	0.82	0.65	0.37	0.34
		0.58	0.52	0.53	0.43	0.37								
		1.42	1.13	1.28	1.11	0.95								
		1.37	1.21	1.18	1.05	0.93								
	2	0.65	0.57	0.49	0.6	0.39	1.22		0.38		0.76		0.28	
		0.66	0.53	0.6	0.51	0.38								
		1.22	0.98	1.21	1.13	0.78								
		1.2	1.05	0.96	0.71	0.62								
	3	0.31	0.3	0.29	0.29	0.24	0.6		0.15		0.38		0.14	
		0.28	0.23	0.2	0.2	0.15								
		0.57	0.53	0.48	0.56	0.37								
		0.6	0.53	0.55	0.49	0.47								
Transverse	1	0.75	0.52	0.43	0.47	0.33	1.6	1.6	0.21	0.21	0.66	0.67	0.34	0.31
		0.75	0.58	0.72	0.49	0.34								
		1.6	1.07	1.14	0.81	0.55								
		1.6	0.73	0.83	0.49	0.21								
		0.59	0.4	0.34	0.44	0.25								
		1	0.56	0.77	0.61	0.44								
	2	1.04	0.8	0.82	0.68	0.57	1.52		0.24		0.71		0.32	
		1.17	0.62	0.82	0.88	0.46								
		0.61	0.5	0.43	0.43	0.41								
		1.44	0.96	1.02	0.86	0.47								
		1.52	0.65	1.03	0.61	0.24								
		0.66	0.61	0.33	0.37	0.29								
	3	1.36	0.76	0.61	0.73	0.24	1.36		0.24		0.65		0.26	
		0.78	0.52	0.33	0.43	0.26								
		0.89	0.47	0.88	0.47	0.34								
		1.23	0.63	1.17	0.75	0.53								
		0.85	0.74	0.58	0.57	0.5								
		0.72	0.62	0.48	0.63	0.42								

Table 5.2d – Cladding thickness for SMI-316 SC No. 6 bar, sample 1

Sample and Number		Measured Thickness(mm)					Max. Thickness (mm)		Min Thickness (mm)		Average Thickness (mm)		Standard Deviation	
Longitudinal	1	1.45	1.21	1.25	1.20	1.18	1.71	1.71	0.75	0.69	1.30	1.13	0.20	0.23
		1.24	1.13	1.15	1.03	0.75								
		1.71	1.33	1.59	1.46	1.29								
		1.47	1.44	1.34	1.41	1.31								
	2	1.13	1.10	0.88	0.81	0.73	1.63		0.73		1.08		0.21	
		0.88	0.93	0.91	0.97	0.91								
		1.34	1.18	1.25	1.19	0.96								
		1.63	1.24	1.09	1.29	1.09								
	3	1.13	0.96	1.07	0.91	0.79	1.36		0.69		1.02		0.19	
		0.94	0.93	0.91	0.81	0.77								
		1.36	1.22	1.17	1.22	1.17								
		1.26	0.82	1.17	1.03	0.69								
Transverse	1	1.04	0.71	0.76	0.81	0.42	1.80	1.80	0.36	0.22	0.80	0.82	0.30	0.34
		1.30	1.04	0.96	1.04	0.81								
		0.96	0.53	0.60	0.62	0.41								
		1.03	0.50	0.54	0.78	0.46								
		0.88	0.80	0.80	0.78	0.67								
		1.80	0.90	1.47	1.05	0.73								
		0.90	0.48	0.55	0.64	0.36								
	2	1.21	0.77	0.80	0.57	0.51	1.60		0.22		0.74		0.33	
		1.06	0.81	0.54	0.40	0.40								
		0.81	0.59	0.81	0.74	0.58								
		1.60	1.40	1.18	1.09	0.92								
		1.29	0.58	0.68	0.74	0.57								
		0.78	0.57	0.40	0.30	0.22								
		1.05	0.74	0.43	0.37	0.29								
	3	1.36	0.73	0.87	0.69	0.61	1.73		0.30		0.91		0.37	
		0.79	0.31	0.72	0.78	0.30								
		1.02	0.94	0.81	0.95	0.62								
		0.90	0.64	0.64	0.51	0.38								
		0.97	0.86	0.64	0.75	0.59								
		1.73	1.44	1.71	1.17	1.15								
		1.57	1.57	1.08	1.19	0.84								

Table 5.2e – Cladding thickness for SMI-316 SC No. 6 bar, sample 2

Sample and Number		Measured Thickness(mm)					Max. Thickness (mm)		Min Thickness (mm)		Average Thickness (mm)		Standard Deviation	
Longitudinal	1	1.48	1.23	1.29	1.44	1.21	1.48	1.78	0.60	0.44	1.18	1.08	0.24	0.34
		1.45	1.34	1.40	0.86	0.64								
		1.43	1.11	1.15	1.38	1.04								
		1.20	1.14	1.18	1.11	0.60								
	2	1.15	1.07	1.15	1.10	0.58	1.42		0.50		0.99		0.24	
		1.42	1.18	1.29	1.21	0.75								
		1.05	0.99	0.71	1.05	0.50								
		1.11	1.08	0.84	0.76	0.71								
	3	1.78	1.66	1.59	1.55	1.44	1.78		0.44		1.08		0.45	
		1.70	1.66	1.52	1.01	0.81								
		0.83	0.77	0.64	0.64	0.64								
		0.83	0.71	0.70	0.73	0.44								
Transverse	1	0.80	0.77	0.54	0.39	0.38	1.34	1.57	0.38	0.33	0.82	0.79	0.26	0.27
		1.15	1.01	0.73	0.81	0.73								
		1.34	1.34	1.19	0.93	0.71								
		1.06	0.57	0.65	0.80	0.53								
		0.68	0.65	0.67	0.65	0.63								
		1.22	1.07	1.03	0.74	0.68								
		1.30	0.61	1.03	0.79	0.49								
	2	0.76	0.61	0.56	0.59	0.54	1.57		0.37		0.79		0.26	
		1.01	0.92	0.77	0.83	0.67								
		0.94	0.90	0.70	0.73	0.69								
		1.07	0.55	0.63	0.85	0.39								
		0.96	0.81	0.77	0.37	0.37								
		1.57	1.25	1.07	0.86	0.73								
		1.34	0.58	0.80	1.03	0.47								
	3	0.66	0.48	0.57	0.44	0.36	1.36		0.33		0.75		0.27	
		1.36	1.05	0.67	0.68	0.57								
		1.26	1.03	1.01	1.06	1.00								
		1.22	0.78	0.84	0.96	0.74								
		0.75	0.63	0.61	0.65	0.56								
		0.81	0.48	0.49	0.65	0.33								
		1.11	0.80	0.85	0.56	0.34								

Table 5.2f – Cladding thickness for SMI-316 SC No. 6 bar, sample 3

Sample and Number		Measured Thickness(mm)					Max. Thickness (mm)		Min Thickness (mm)		Average Thickness (mm)		Standard Deviation	
Longitudinal	1	0.97	0.84	0.80	0.77	0.67	1.19	1.19	0.57	0.53	0.87	0.81	0.18	0.15
		1.06	0.89	0.75	1.05	0.57								
		1.00	0.90	0.92	0.97	0.61								
		1.19	0.69	1.17	0.94	0.64								
	2	0.84	0.64	0.81	0.63	0.60	1.00		0.60		0.79		0.13	
		0.75	0.71	0.70	0.67	0.63								
		1.00	0.78	0.97	0.84	0.75								
		0.99	0.86	0.98	0.92	0.78								
	3	0.84	0.68	0.80	0.68	0.65	1.00		0.53		0.75		0.12	
		0.70	0.59	0.69	0.69	0.59								
		1.00	0.85	0.94	0.85	0.78								
		0.90	0.73	0.86	0.70	0.53								
Transverse	1	0.80	0.76	0.71	0.63	0.50	1.15	1.15	0.25	0.25	0.61	0.62	0.21	0.20
		0.78	0.59	0.59	0.56	0.51								
		0.71	0.39	0.52	0.58	0.39								
		0.55	0.50	0.45	0.47	0.43								
		1.14	1.06	0.86	0.81	0.79								
		1.15	0.47	0.55	0.52	0.44								
		0.58	0.50	0.43	0.44	0.25								
	2	0.68	0.44	0.50	0.56	0.41	1.10		0.39		0.65		0.20	
		0.60	0.58	0.49	0.49	0.46								
		1.03	0.58	0.73	0.79	0.56								
		1.10	0.72	0.71	0.93	0.48								
		0.59	0.48	0.45	0.47	0.39								
		1.02	0.54	0.83	0.56	0.52								
		1.09	0.76	0.72	0.86	0.60								
	3	0.54	0.37	0.45	0.50	0.36	1.09		0.34		0.60		0.21	
		0.57	0.56	0.47	0.50	0.42								
		1.07	0.84	1.07	0.91	0.66								
		1.09	0.75	0.88	0.82	0.58								
		0.64	0.37	0.51	0.56	0.34								
		0.72	0.50	0.50	0.49	0.46								
		0.71	0.45	0.43	0.65	0.42								

Note: 1 in. = 1000 mils = 25.4 mm.

5.4 CORROSION TESTS

The corrosion tests demonstrate that SMI-316 SC (SMI) steel is significantly more corrosion resistant than conventional reinforcement and is superior to epoxy-coated reinforcement under severe corrosion conditions. SMI steel has a very high critical chloride corrosion threshold and exhibits very low corrosion losses. The results of the rapid macrocell and bench scale tests are described next. The results for individual specimens are presented in Appendix A.

5.4.1 Rapid Macrocell Tests

Macrocell tests were performed with both bare and mortar wrapped bars. The corrosion rates of the bare bar specimens are presented as a function of time in Figures 5.3a through 5.3c based on the total area of the bar exposed to the solution and in Figure 5.3d based on the exposed area at the penetrations through either the epoxy or the cladding.

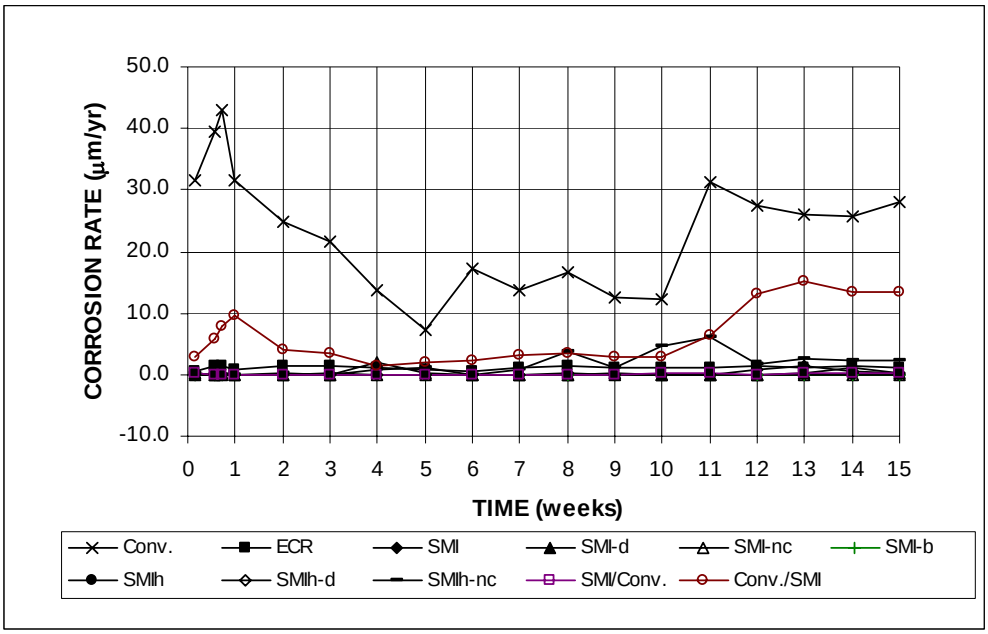

Figure 5.3a – Macrocell Test. Average corrosion rate (based on total area). Bare bars in 1.6 and 6.04 m ion NaCl and simulated concrete pore solutions.

Bare Bar Tests – As shown in Figure 5.3a, conventional steel (Conv.) exposed to the 1.6 m ion NaCl solution corroded more rapidly than any of the other steels in the study, with corrosion rates ranging between 7 and 43 µm/yr. Second in corrosion rate was conventional steel used as an anode coupled with SMI steel at the cathode (Conv./SMI). Figures 5.3b and 5.3c provide additional information by extending the vertical scale of the plots. These results indicate that epoxy-coated steel reinforcement with four $^{1}/_{8}$-in. diameter holes through the epoxy (ECR) exposed to the 1.6 m ion NaCl solution corroded at an average rate of about 1 µm/yr throughout the tests. The other specimens, including SMI specimens exposed to 1.6 and 6.04 m ion NaCl

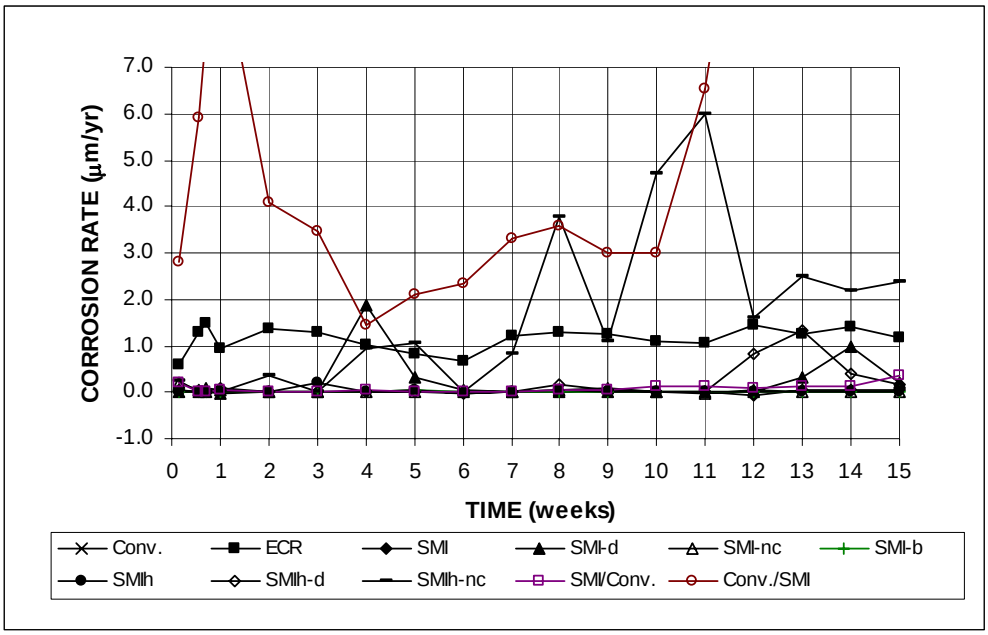

Figure 5.3b – Macrocell Test. Average corrosion rate (based on total area). Bare bars in 1.6 and 6.04 m ion NaCl and simulated concrete pore solutions. (different scale)

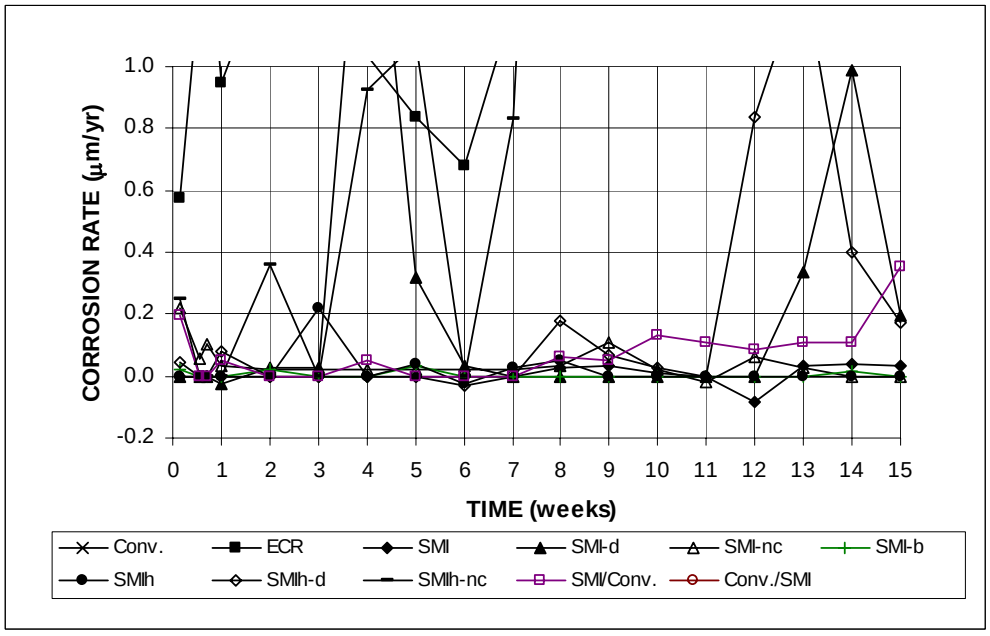

Figure 5.3c – Macrocell Test. Average corrosion rate (based on total area). Bare bars in 1.6 and 6.04 m ion NaCl and simulated concrete pore solutions. (different scale)

solutions (SMI and SMIh, respectively), corroded at a rate below 1 µm/yr throughout most of the test period with the exception of the SMI bars without caps in the 6.04 m ion NaCl solution (SMIh-nc); corrosion in this case was dominated by corrosion of the exposed steel core. As shown in Figure 5.3c, the SMI bars with the ends protected by caps (SMI) exhibited essentially no corrosion loss in either NaCl concentration. Drilled specimens, SMI-d and SMIh-d, exhibited

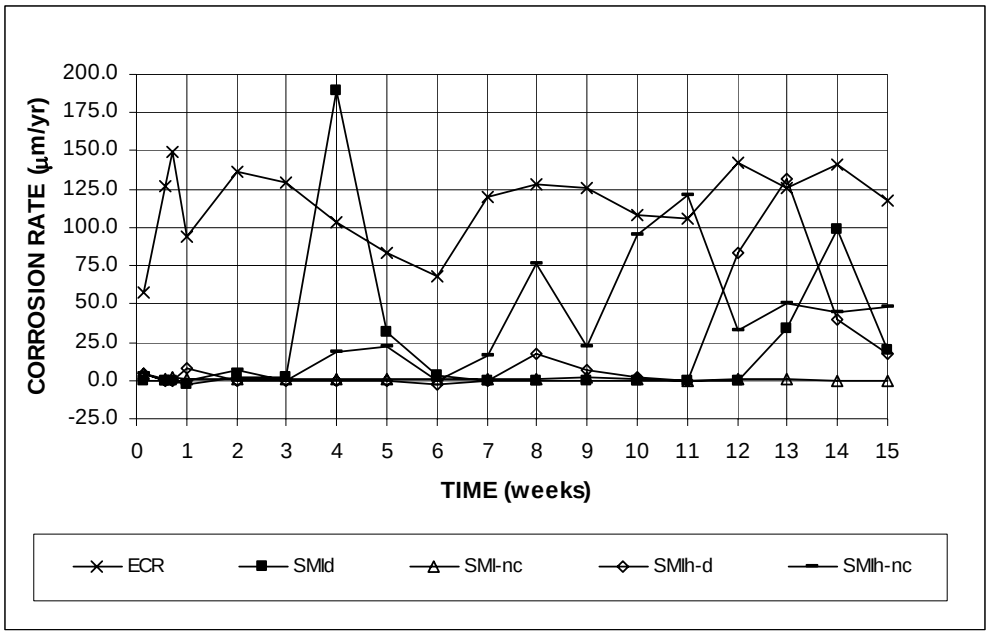

Figure 5.3d – Macrocell Test. Average corrosion rate (based on exposed area). Bare bars in 1.6 and 6.04 m ion NaCl and simulated concrete pore solutions.

small but measurable corrosion, while the SMI bars without a cap in the 1.6 m ion NaCl solution (SMI-nc) exhibited little measurable corrosion throughout the test period. The bent SMI bars (SMI-b) also exhibited no measurable corrosion. Specimens combining SMI bars at the anode with conventional bars at the cathode (SMI/Conv.) exhibited a small increase in corrosion rate during the final six weeks of the test.

Based on the area exposed by penetrations in the epoxy or the cladding (Figure 5.3d), all specimens exhibited significant corrosion rates during the 15-week test period, with the exception of the SMI-nc bars, the bars without caps and exposed to the 1.6 m ion NaCl solution. For the epoxy-coated steel, corrosion rates on the exposed area ranged to values as high as 150 μm/yr, while the SMI-d, SMIh-d, and SMIh-nc bars exhibited average corrosion rates on the four $^{1}/_{8}$-in. diameter penetrations with peak values of 180, 122, and 100 μm/yr, respectively.

Total corrosion losses based on the total area in contact with the test solutions are shown in Figures 5.4a and 5.4b and based on the exposed area at the penetrations in Figure 5.4c. The total losses ranged from high values of 6.1 and 1.8 μm at 15 weeks for the Conv. and Conv./SMI specimens to values of less than 0.01 μm for the SMI, SMI-b, SMI-nc, and SMIh specimens, with the other specimens exhibiting values between 0.53 and 0.02 μm.

Average corrosion potentials with respect to a saturated calomel electrode for the anode and cathode bars are shown, respectively, in Figures 5.5a and 5.5b. Corrosion potentials more negative than –0.275V indicate that the bar is undergoing active corrosion. As shown in Figure 5.5a, the Conv., Conv./SMI, ECR, SMIh-d, and SMIh-nc specimens were undergoing active corrosion at some time during the period based on this criterion. As shown in Figure 5.5b, none of the cathode bars exhibited active corrosion based on corrosion potential, except in some cases on the initial day of the tests.

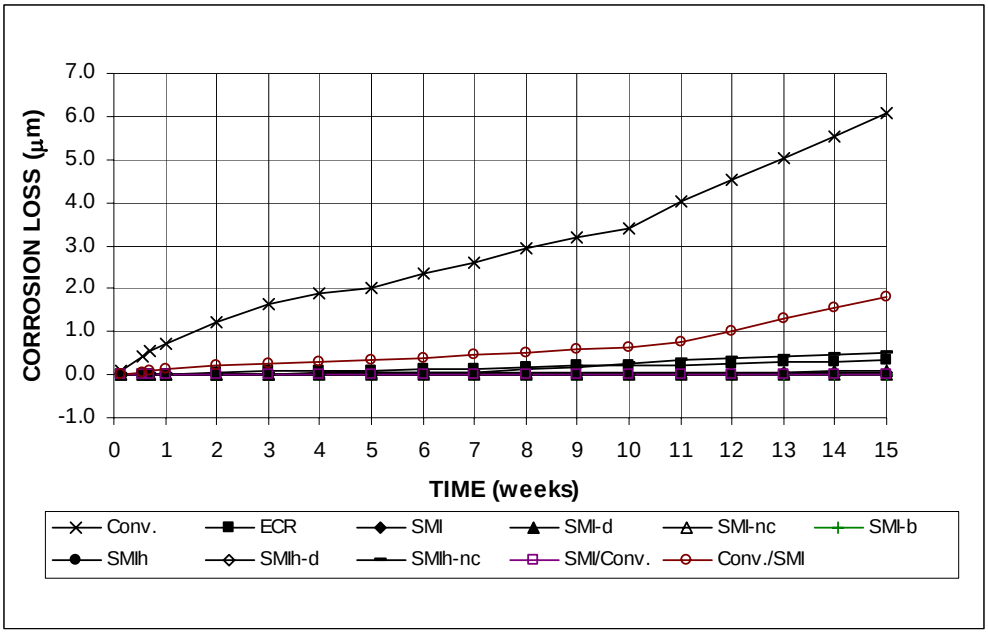

Figure 5.4a – Macrocell Test. Average corrosion loss (based on total area). Bare bars in 1.6 and 6.04 m ion NaCl and simulated concrete pore solutions.

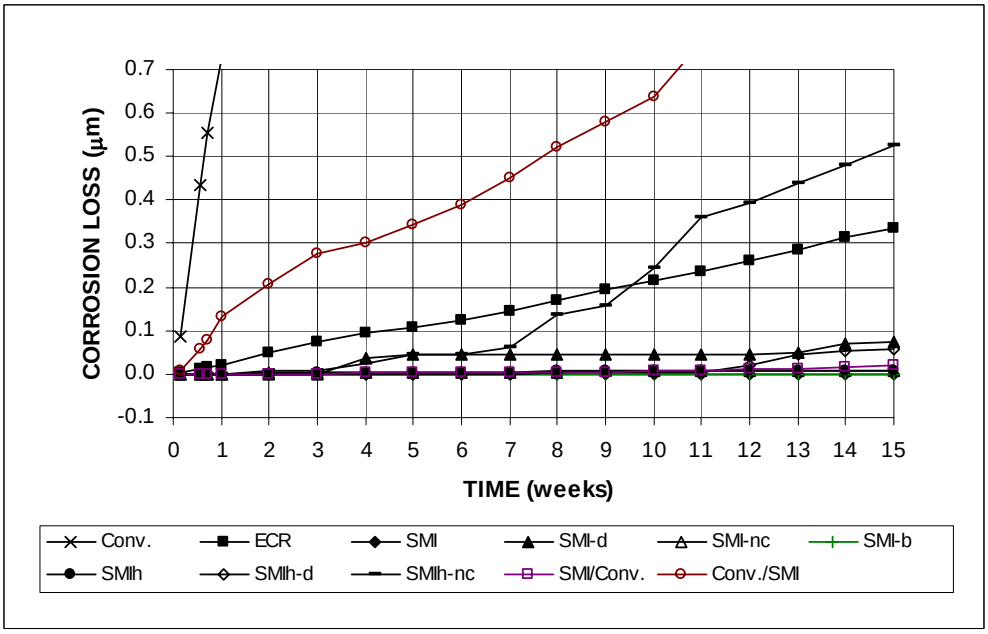

Figure 5.4b – Macrocell Test. Average corrosion loss (based on total area). Bare bars in 1.6 and 6.04 m ion NaCl and simulated concrete pore solutions. (different scale)

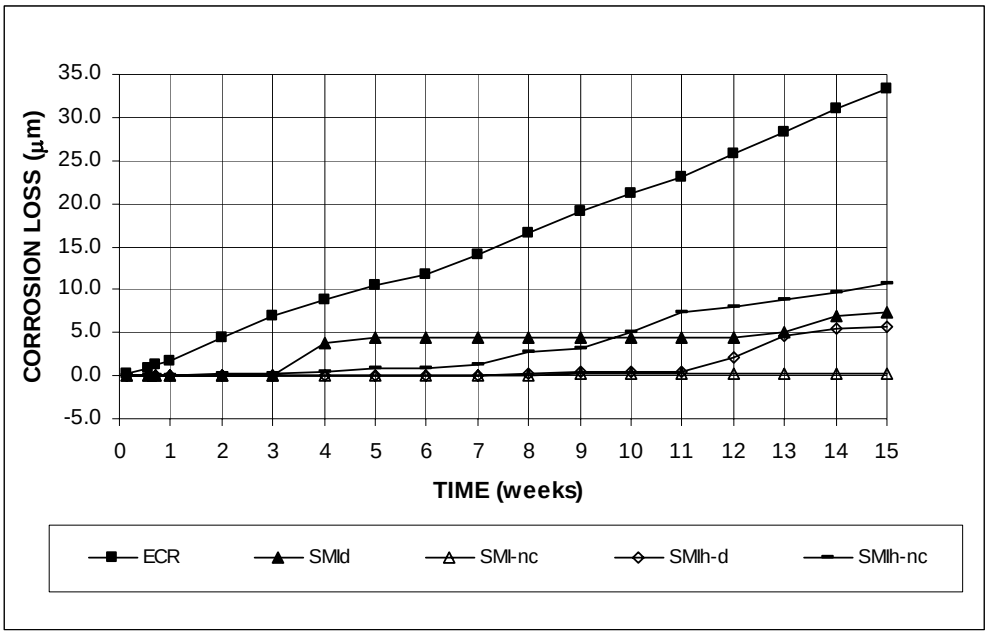

Figure 5.4c – Macrocell Test. Average corrosion loss (based on exposed area). Bare bars in 1.6 and 6.04 m ion NaCl and simulated concrete pore solutions.

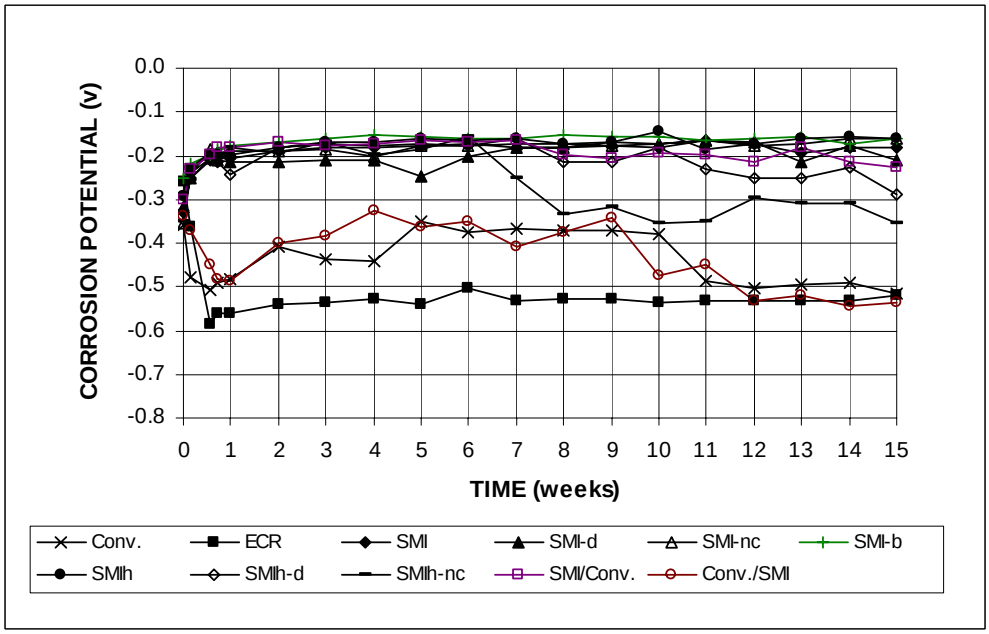

Figure 5.5a – Macrocell Test. Average corrosion potentials. Anode, bare bars in 1.6 and 6.04 m ion NaCl and simulated concrete pore solutions.

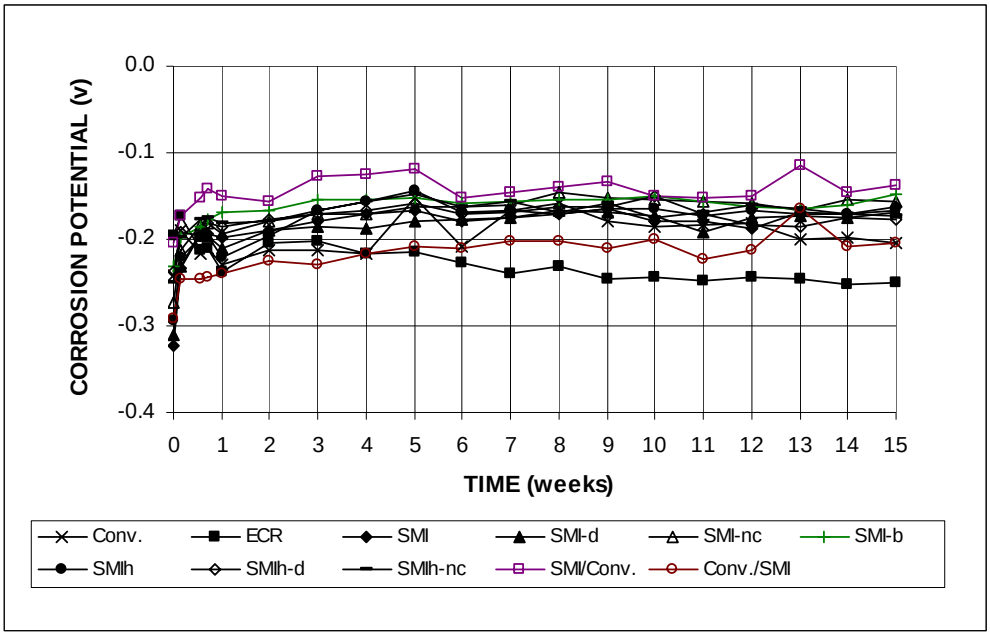

Figure 5.5b – Macrocell Test. Average corrosion potentials. Cathode, bare bars in 1.6 and 6.04 m ion NaCl and simulated concrete pore solutions.

Mortar-Wrapped Bar Tests – The corrosion rates for the mortar wrapped bars are shown in Figures 5.6a and 5.6b based on the total area of the bars in contact with the solution and in Figure 5.6c based on the exposed area at the penetrations. As shown in Figure 5.6a, only conventional steel exhibited significant corrosion, with average rates between 18 and 23 μm/yr during the final 8 weeks of the test period. Figure 5.6b indicates that the SMI-d and SMI-nc bars exhibited corrosion at various points throughout the test period, while the intact SMI bars exhibited no measurable corrosion. Based on the exposed areas at the penetrations (Figure 5.6c), local corrosion rates reached as high as 28 μm/yr for SMI-d and 5 μm/yr for SMI-nc bars. The total corrosion losses as a function of time are shown in Figures 5.7a and 5.7b based on total area and 5.7c based on the exposed area at penetrations. In concert with the corrosion rate plots in Figures 5.6a and 5.6b, only the conventional reinforcement exhibited significant corrosion losses, with a value of 4.8 μm at the end of the 15-week test period. All other losses based on total area were below 0.025 μm, with no measurable loss for either the intact SMI or the ECR bars. The corrosion losses based on exposed area (Figure 5.7c) are 2.3 μm for the drilled bars (SMI-d) and 0.3 μm for the SMI bars without caps (SMI-nc). The epoxy-coated reinforcement actually exhibits a slightly negative value for the total losses at the end of 15 weeks. This is, in fact, not a negative loss but rather the result of the integration of corrosion rates that are based on currents that are sometimes positive and sometimes negative.

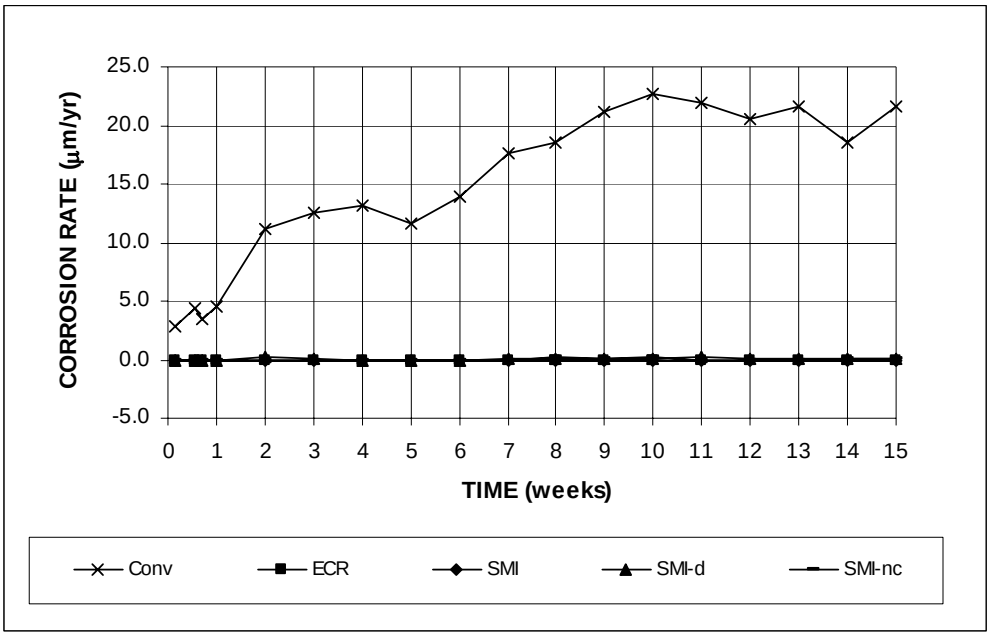

Figure 5.6a – Macrocell Test. Average corrosion rate (based on total area). Mortar-wrapped bars in 1.6 m ion NaCl and simulated concrete pore solution.

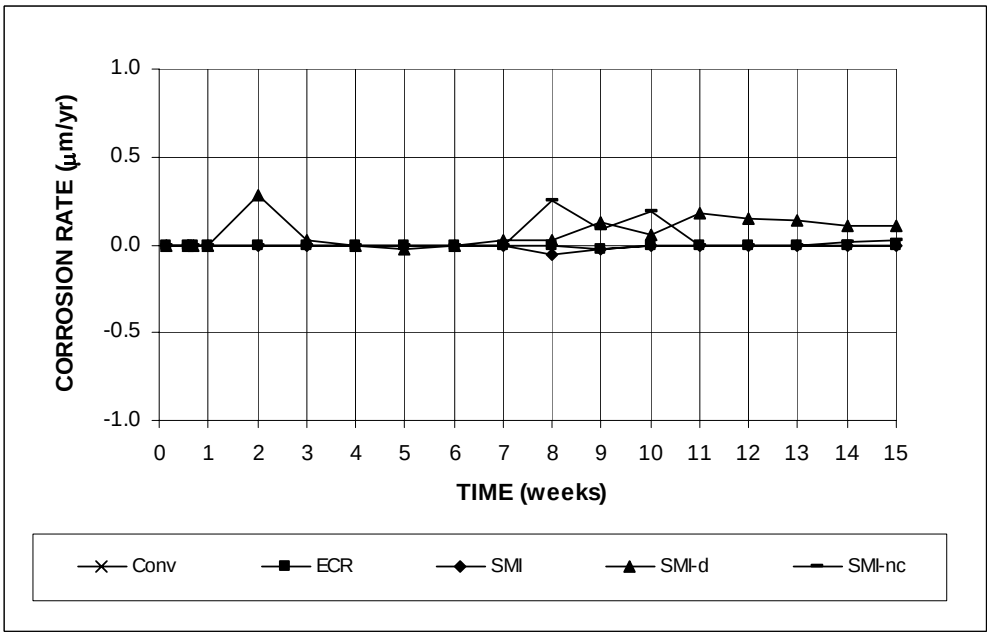

Figure 5.6b – Macrocell Test. Average corrosion rate (based on total area). Mortar-wrapped bars in 1.6 m ion NaCl and simulated concrete pore solution. (different scale)

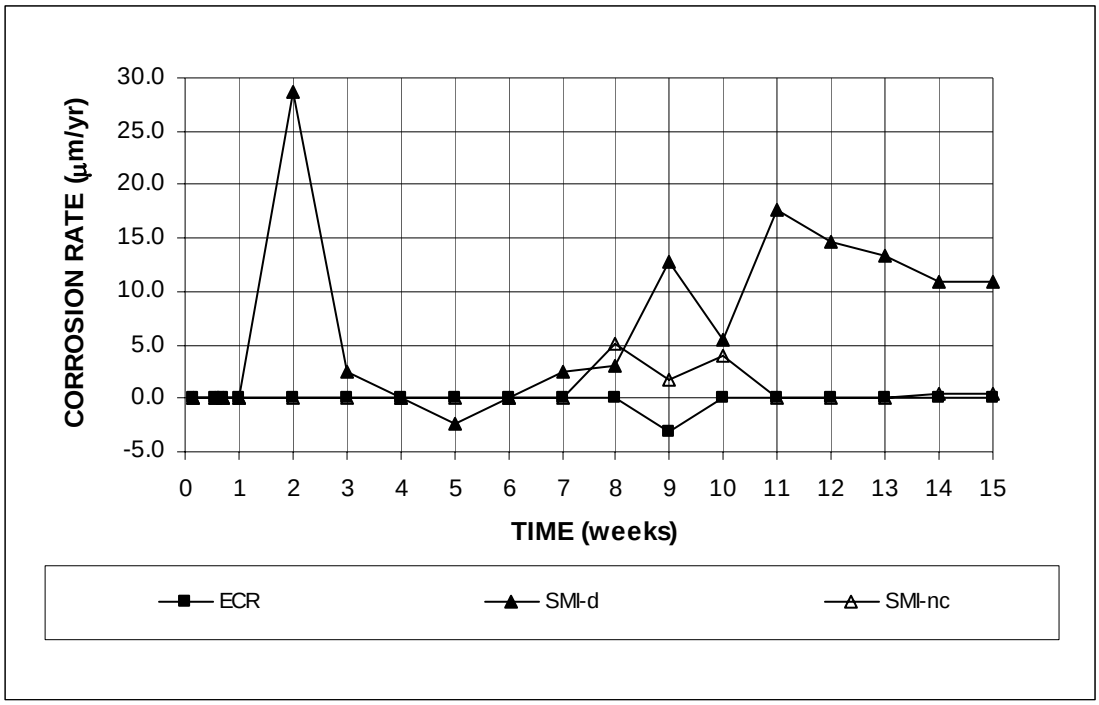

Figure 5.6c – Macrocell Test. Average corrosion rate (based on exposed area). Mortar-wrapped bars in 1.6 m ion NaCl and simulated concrete pore solution.

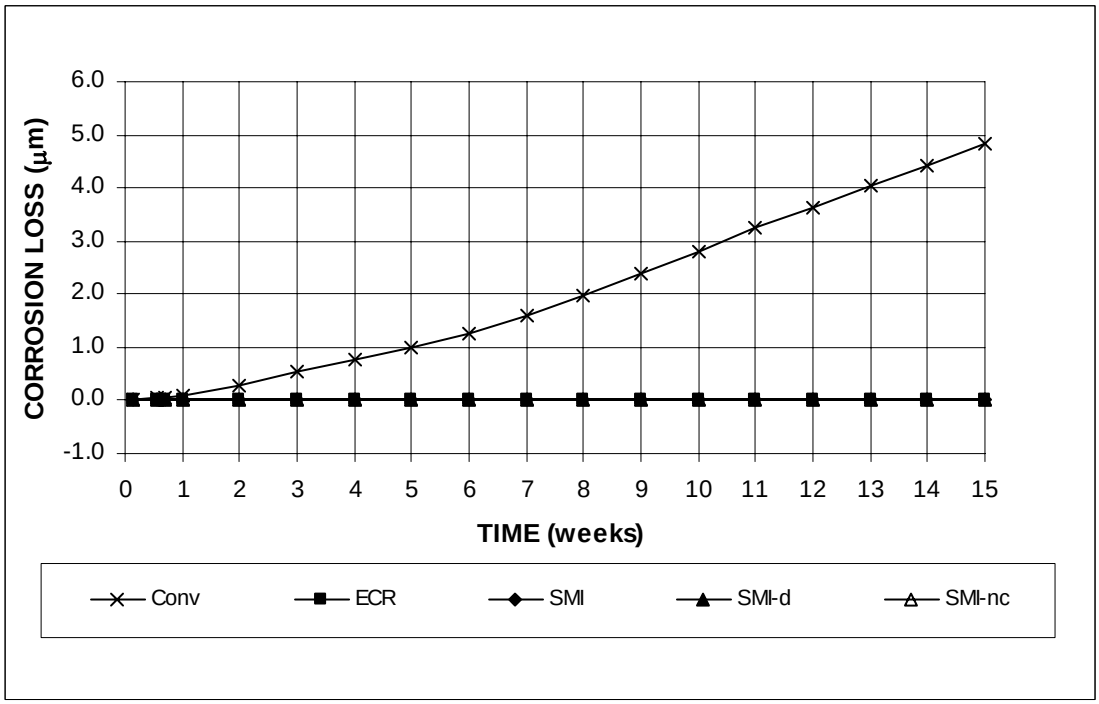

Figure 5.7a – Macrocell Test. Average corrosion loss (based on total area). Mortar-wrapped bars in 1.6 m ion NaCl and simulated concrete pore solution.

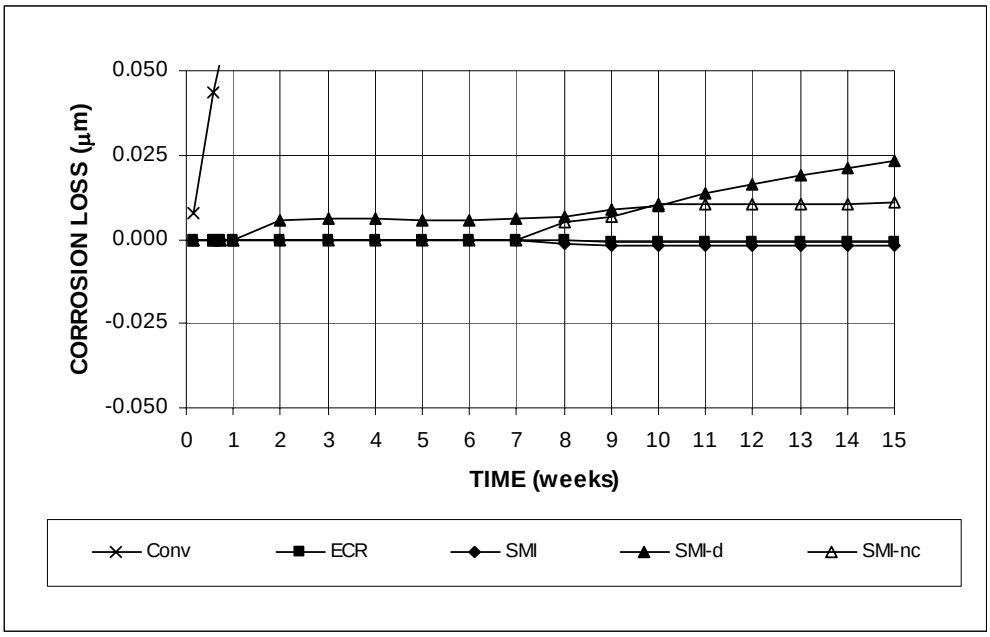

Figure 5.7b – Macrocell Test. Average corrosion loss (based on total area). Mortar-wrapped bars in 1.6 m ion NaCl and simulated concrete pore solution. (different scale)

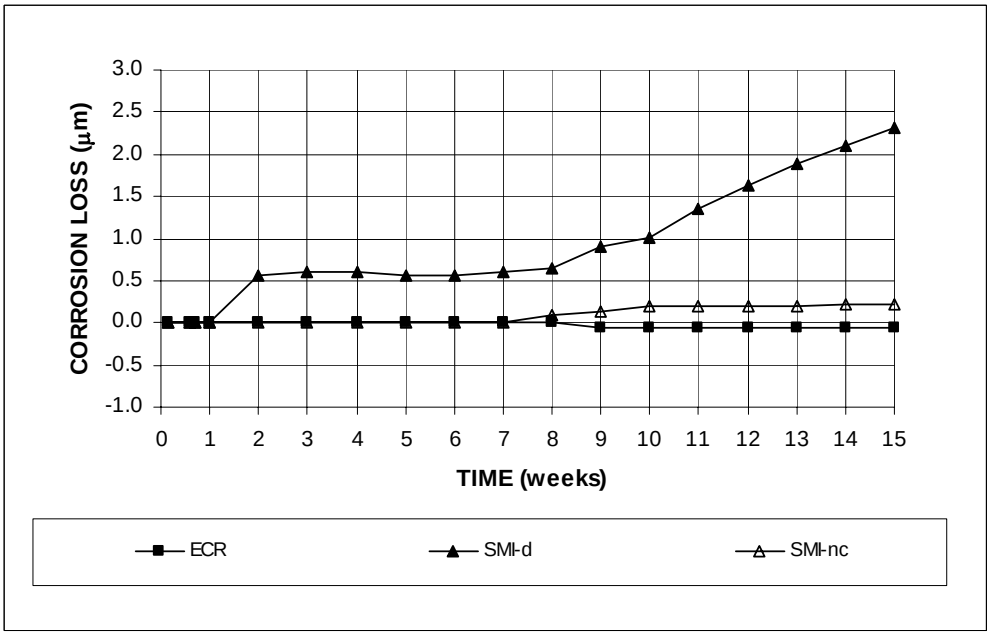

Figure 5.7c – Macrocell Test. Average corrosion loss (based on exposed area). Mortar-wrapped bars in 1.6 m ion NaCl and simulated concrete pore solution.

As shown in Figures 5.8a and 5.8b, only the conventional steel reached a corrosion potential more negative than –0.275 V during the 15-week test, with the exception of the SMI-d specimens, which exhibited an average value of about –0.280 V at the ninth week.

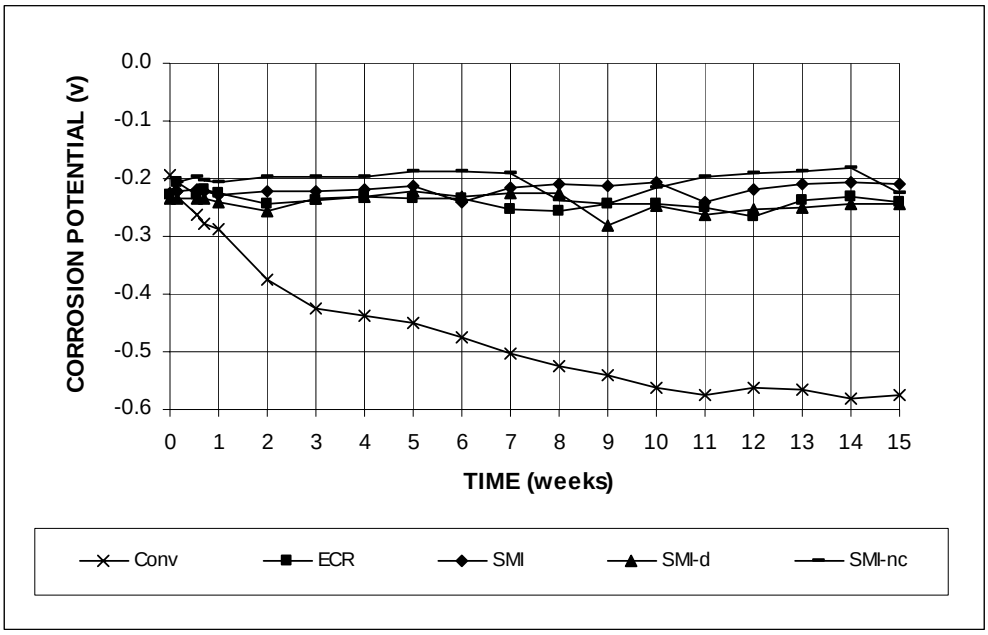

Figure 5.8a – Macrocell Test. Average corrosion potentials. Anode, mortar-wrapped bars in 1.6 m ion NaCl and simulated concrete pore solution.

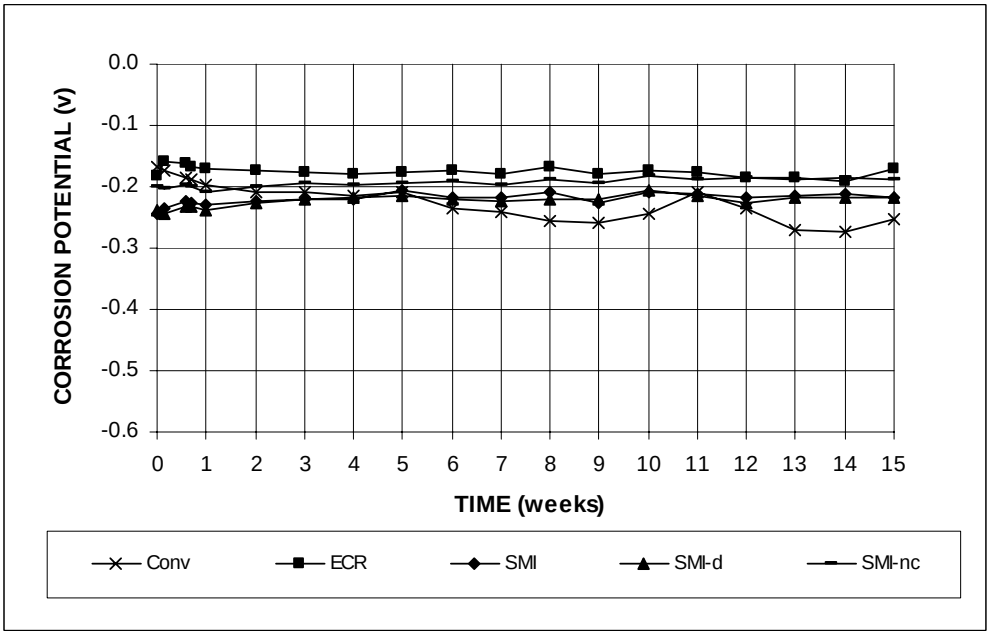

Figure 5.8b – Macrocell Test. Average corrosion potentials. Cathode, mortar-wrapped bars in 1.6 m ion NaCl and simulated concrete pore solution.

The total corrosion losses over the 15-week period for the individual specimens, along with the average values and standard deviations for each specimen type, are shown in Tables 5.3a and 5.3b for bare and mortar wrapped bars based on total and exposed area, respectively.

Table 5.3a – Corrosion loss (in μm) for rapid macrocell specimens based on total area

Steel Designation	Specimen 1	2	3	4	5	6	Average	Standard Deviation	Notes*
Bare Bar									
Conv.	7.05	5.26	4.86	7.59	6.50	5.24	6.08	1.12	Conventional steel
ECR	0.256	0.649	0.218	0.384	0.494	0.018	0.337	0.222	Epoxy-coated steel
SMI	-0.007	-0.004	-0.003	0.025	-0.003	0.000	0.002	0.012	SMI steel with intact cladding
SMI-d	0.241	-0.001	0.003	0.198	-0.003	0.000	0.073	0.114	SMI steel with four drilled holes
SMI-nc	0.003	-0.002	0.000	0.000	0.000	0.051	0.009	0.021	SMI steel, no end cap
SMI-b	0.005	0.000	-0.001	0.000	0.001	0.004	0.001	0.002	SMI with 180 degree bend
SMIh	0.000	0.030	0.000	0.000	0.000	0.006	0.006	0.012	SMI in 6.04 m ion NaCl
SMIh-d	0.000	0.275	0.001	0.039	0.027	0.003	0.057	0.108	SMI, 6.04 m ion NaCl, 4 drilled holes
SMIh-nc	0.537	0.486	0.140	0.202	0.978	0.825	0.528	0.332	SMI, 6.04 m ion NaCl, no cap
SMI/Conv.	0.041	0.014	0.008	-	-	-	0.021	0.018	SMI anode, conventional cathode
Conv./SMI	1.854	1.743	1.869	-	-	-	1.822	0.069	Conventional anode, SMI cathode
Mortar-Wrapped Bar									
Conv.	5.81	6.63	3.51	3.80	3.76	5.40	4.82	1.30	Conventional steel
ECR	0.000	0.000	0.000	0.000	-0.003	0.000	-0.001	0.001	Epoxy-coated steel
SMI	0.000	0.000	-0.007	0.000	-0.003	0.000	-0.002	0.003	SMI steel, intact cladding
SMI-d	0.000	0.000	0.094	0.033	0.008	0.003	0.023	0.037	SMI steel, 4 drilled holes
SMI-nc	0.000	0.000	0.027	0.037	0.000	0.002	0.011	0.017	SMI steel, no end cap

Table 5.3b – Corrosion loss (in μm) for rapid macrocell specimens based on exposed area

Steel Designation	Specimen 1	2	3	4	5	6	Average	Standard Deviation	Notes*
Bare Bar									
ECR	25.62	64.89	20.76	37.13	49.41	1.82	33.3	22.3	Epoxy-coated steel
SMI-d	24.14	-0.08	0.28	19.78	-0.28	0.00	7.31	11.44	SMI steel with drilled holes
SMI-nc	0.068	-0.045	0.000	0.000	0.000	1.030	0.175	0.420	SMI steel, no end cap
SMIh-d	0.00	27.45	0.07	3.94	2.75	0.26	5.74	10.76	SMI, 6.04 m ion NaCl, four drilled holes
SMIh-nc	10.83	9.81	2.83	4.08	19.75	16.67	10.7	6.70	SMI, 6.04 m ion NaCl, no cap
Mortar-Wrapped Bar									
ECR	0.000	0.000	0.000	0.000	-0.352	0.000	-0.059	0.144	Epoxy-coated steel
SMI-d	0.00	0.00	9.43	3.31	0.84	0.28	2.31	3.71	SMI steel with 4 drilled holes
SMI-nc	0.000	0.000	0.552	0.743	0.000	0.045	0.223	0.335	SMI steel, no end cap

*****All ECR and SMI-d bars have four $^{1}/_{8}$-in. diameter penetrations to the underlying mild steel.

Visual Observations – As the tests were discontinued, the specimens were inspected visually. For conventional steel, corrosion products were observed on the bar surface within the solution. In some cases, corrosion products appeared on the bar at contact points with the plastic

lid, presumably due to crevice corrosion. Figure 5.9 shows a conventional steel bare anode bar at 15 weeks with corrosion products that formed on the bar below the surface of the solution, while Figure 5.10 shows corrosion products at the contact points between the conventional steel anode and plastic lid. Figure 5.11 shows a bare epoxy-coated bar with the corrosion products that formed at the drilled holes.

For the mortar-wrapped specimens, the mortar was removed following the tests and some corrosion products were found under the mortar. Figure 5.12 shows a conventional bar with the corrosion products that formed on the bar surface. For mortar-wrapped epoxy-coated bars, no corrosion products were found on the specimens.

Figure 5.9 – Bare conventional anode bar, at 15 weeks, showing corrosion products that formed below the surface of the solution.

Figure 5.10 – Bare conventional anode bar, at 15 weeks, showing corrosion products that formed at contact points between the bar and plastic lid.

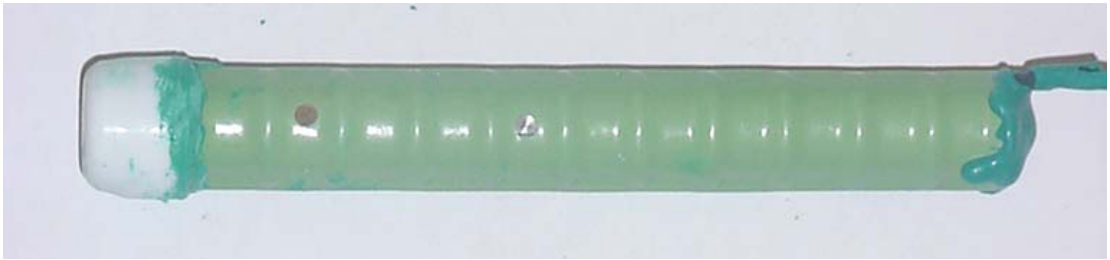

Figure 5.11 – Bare ECR anode bar, at 15 weeks, showing corrosion products that formed at drilled holes.

Figure 5.12 – Conventional anode bar after removal of mortar, at 15 weeks.

For bare bar SMI-nc and SMIh-nc specimens, corrosion products were found on the unprotected ends; for bare bar SMI-d and SMIh-d specimens, corrosion products were observed within the drilled holes. No corrosion products appeared on the bare SMI bars with protected ends and without drilled holes. Figure 5.13 shows the end of an SMI-nc anode bar at 15 weeks with the corrosion products that formed on the uncapped end. Figure 5.14 shows an SMI-d bar, with the corrosion products that formed at the drilled holes.

After the mortar was removed from the mortar-wrapped specimens, some corrosion products were found under the mortar on SMI-nc and SMI-d bars, as shown in Figures 5.15 and 5.16, while no corrosion products were found on the SMI bars.

Figure 5.13 – Bare SMI-nc anode bar from 1.6 m ion salt solution, at 15 weeks, showing corrosion products that formed at the unprotected end.

Figure 5.14 – Bare SMI-d anode bar from 1.6 m ion salt solution, at 15 weeks, showing corrosion products that formed at penetrations through the cladding.

Figure 5.15 – SMI-nc anode bar after removal of mortar, at 15 weeks, showing corrosion products that formed at the unprotected end.

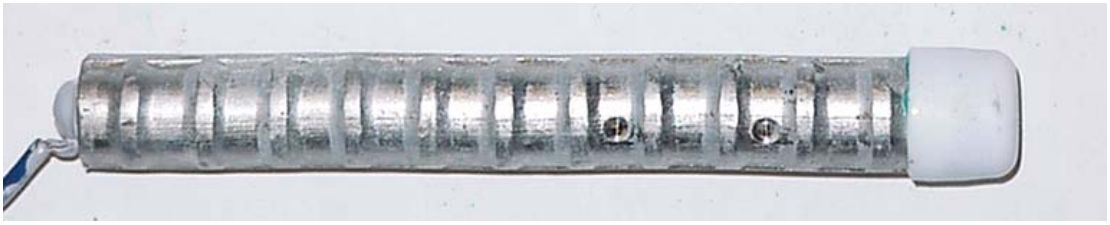

Figure 5.16 – SMI-d anode bar after removal of mortar, at 15 weeks, showing corrosion products that formed at penetrations through the cladding.

Summary **–** Overall, the results of the macrocell tests indicate that SMI bars, when exposed to even very high chloride concentrations, perform in a superior manner when the cladding is not penetrated. Exposing the conventional steel core at the ends of the bars reduces the corrosion performance, as does penetrating the cladding. With the penetrations, SMI steel exhibits less corrosion than ECR under the same conditions for bare bars, while the opposite is true for the mortar-wrapped bars. The effectiveness of the epoxy-filled caps in limiting corrosion indicates that such a system should work well as an end treatment in the field.

A comparison of the performance of the test specimens in which SMI steel was used as an anode and conventional steel was used as the cathode and in the specimens in which conventional steel used as the anode and SMI steel was used as the cathode indicates that corrosion performance appears to be principally governed by the type of steel used as the anode.

5.4.2 Bench-Scale Tests

The Southern Exposure and cracked beam tests provide realistic evaluations of the corrosion performance of concrete reinforcement systems, simulating several decades of chloride exposure during the 96-week test period. The results of the tests are used both to compare the performance of the systems and to estimate the life expectancy of reinforced concrete bridge decks containing the systems (Section 5.6).

Corrosion performance is compared based on corrosion rate and total corrosion loss. Figures 5.17a and 5.17b for Southern Exposure and cracked beam tests, respectively, show corrosion loss versus time for the individual test specimens containing conventional steel. The figures illustrate the variations that occur from specimen to specimen and the differences in behavior exhibited by specimens subjected to the two tests.

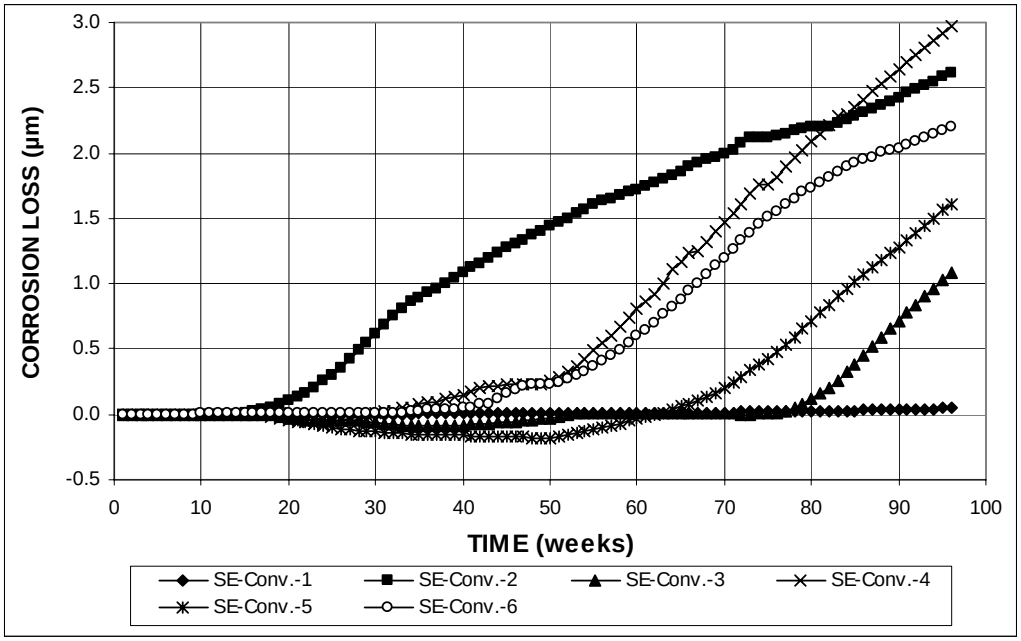

Figure 5.17a – Southern Exposure Test. Corrosion loss (based on total area) versus time of individual specimens containing conventional steel

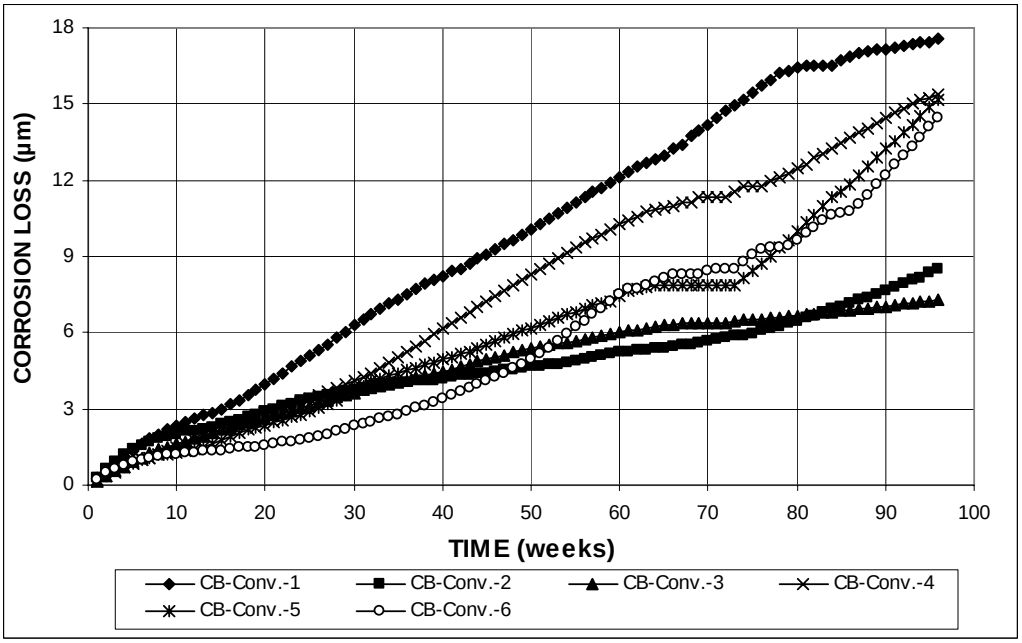

Figure 5.17b – Cracked Beam Test. Corrosion loss (based on total area) versus time of individual specimens containing conventional steel

As shown in Figure 5.17a, Southern Exposure specimens tend to exhibit corrosion initiation at different times. This results from differences in the time required for the chloride content to reach the critical chloride threshold (equal to 1.0 to 2.0 lb/yd^3) for conventional steel

at the level of the top bars. Until the corrosion threshold is attained, corrosion currents remain low and may vary slightly from positive to negative. When integrated, predominantly negative currents plot as negative corrosion losses, as shown for several specimens in Figure 5.17a.

During the course of the current study, a small number of specimens exhibited no corrosion activity during the 96-week tests, such as observed for specimen SE-Conv.-1. These specimens are not included in the evaluation.

In contrast to the Southern Exposure specimens, the cracked beam specimens can start corroding as early as the first week of the test. As illustrated in Figure 5.17b, the corrosion rate is generally more rapid during the first two weeks than during the balance of the test.

For use in this analysis, average corrosion rates for individual specimens are calculated as the average slope of the corrosion loss graph during a period in which the specimen is undergoing significant, steady-state or nearly steady-state corrosion. For Southern Exposure specimens, a corrosion loss corresponding to steady-state corrosion for all specimens in a test group is selected as the initial point for calculating the slope. For example, the conventional steel specimens exhibited a relatively steady corrosion rate after reaching a corrosion loss of 0.3 μm. Consequently, the initial point used for calculating the slope for Southern Exposure specimens containing conventional reinforcement is the point at which a specimen first reaches a corrosion loss of 0.3 μm. Because of their low corrosion rates, the corresponding values for ECR and SMI specimens is 0.001 μm, while the initial point for the SMI-d and SMI-b specimens is 0.01 μm. The final point used to calculate the average slope is the total loss at 96 weeks. For cracked beam specimens, steady-state corrosion begins by week 20. Therefore, the initial point for each specimen is the corrosion loss at week 20, while the final point is the corrosion loss at week 96.

The individual test results for the bench scale specimens follow those for the rapid macrocell tests in the Appendix A. Some tests were continued for as long as 120 weeks and those results are included in the appendix. Corrosion rates for individual specimens, along with the average corrosion rate and standard deviation for each system are presented in Table 5.4. The corresponding values for total corrosion loss are presented in Table 5.5. The systems under study are now compared based on corrosion performance for each of the two specimen types.

Southern Exposure Tests – The average corrosion rates after corrosion initiation for the Southern Exposure specimens, based on the total area of the top reinforcing bars, are summarized in Table 5.4. The specimens with conventional steel at the anode, Conv. and Conv./SMI, exhibit the highest average corrosion rates, with values of 2.66 and 1.43 μm/yr, respectively. These corrosion rates are significantly higher than observed for any of the other systems, which have no value exceeding 0.11 μm/yr. The similar corrosion rates observed for the Conv. and Conv./SMI specimens and the very low corrosion rates observed for the SMI and SMI/Conv. specimens indicate that there is no negative impact of combining SMI stainless steel clad reinforcement with conventional steel, as may happen in portions of a structure containing both forms of reinforcement. Corrosion rates based on the exposed area at the holes in the coating or cladding are summarized in Table 5.4b. The ECR and SMI-d specimens exhibit average corrosion rates based on exposed area of 0.625 and 52.3 μm/yr, respectively. The lower

Table 5.4a – Average corrosion rate (μm/yr) after corrosion initiation for bench-scale tests based on total area[a]

Steel Designation[a]	Specimen 1	2	3	4	5	6	Average[b]	Standard Deviation	Notes[a]
Southern Exposure (SE) Test									
Conv.	-[c]	1.69	3.28	3.13	2.89	2.32	2.66	0.655	Conventional steel
ECR	0.001	0.001	0.001	0.000	0.002	0.002	0.001	0.001	Epoxy-coated steel
SMI	0.004	0.003	0.002	0.010	0.002	0.002	0.004	0.003	with intact cladding
SMI-d	0.237	0.140	0.071	0.079	0.043	0.082	0.109	0.070	SMI steel with 4 drilled holes
SMI/Conv.	-[c]	-[c]	-[c]	-	-	-	-[c]	-	SMI at top, Conv. at bottom
Conv./SMI	1.58	1.50	1.20	-	-	-	1.43	0.199	Conv. at top, SMI at bottom
SMI-b	0.046	0.005	0.021	-	-	-	0.024	0.021	SMI bent 180 degree at top
Cracked Beam (CB) Test									
Conv.	9.30	3.85	3.18	8.61	8.76	8.83	7.09	2.79	Conventional steel
ECR	0.015	0.038	0.006	0.029	0.016	0.005	0.018	0.013	Epoxy-coated steel
SMI	0.002	0.008	0.002	0.001	-0.003	0.005	0.002	0.004	with intact cladding
SMI-d	0.859	0.382	-[c]	0.070	0.256	0.070	0.327	0.325	SMI steel with 4 drilled holes

Table 5.4b – Average corrosion rate (μm/yr) after corrosion initiation for bench-scale tests based on exposed area[a]

Steel Designation[a]	Specimen 1	2	3	4	5	6	Average[b]	Standard Deviation	Notes[a]
Southern Exposure (SE) Test									
ECR	0.715	0.33	0.439	0.192	0.892	1.19	0.625	0.376	Epoxy-coated steel
SMI-d	114	67.4	34.3	38.1	20.6	39.1	52.3	33.9	SMI steel with 4 drilled holes
Cracked Beam (CB) Test									
ECR	7.33	18.37	2.86	14.10	7.72	2.19	8.76	6.36	Epoxy-coated steel
SMI-d	412	183	-[c]	34	123	34	157	156	SMI steel with 4 drilled holes

[a] All ECR and SMI-d bars have four $^1/_8$-in. diameter penetrations to the underlying mild steel.

[b] SE corrosion rates are taken as the average slope of the corrosion loss graph between the corrosion initiation and the corrosion loss at 96 weeks.
CB corrosion losses are taken as the average slope of the corrosion loss graph between week 20 and week 96.

[c] No corrosion observed in these specimens.

corrosion rate exhibited by the ECR specimens results from the low conductivity (high resistivity) of the epoxy coating, especially at the cathode. The much higher conductivity of the SMI-d cathodes results in a corrosion rate approximately 100 times higher than that exhibited by the ECR specimens. This higher corrosion rate is consistent with that observed in earlier tests of ECR specimens in which the top layer consisted of epoxy-coated bars with four $^1/_8$-in. diameter holes, as used in this study, but the bottom layer of bars consisted of uncoated conventional steel,

Table 5.5a – Corrosion loss (in μm) at 96 weeks for bench scale tests based on total area[a]

Steel Designation[a]	Specimen						Average[b]	Standard Deviation	Notes[a]
	1	2	3	4	5	6			
Southern Exposure (SE) Test									
Conv.	-[b]	2.61	1.08	2.97	1.61	2.21	2.09	0.76	Conventional steel
ECR	0.003	0.002	0.003	0.002	0.004	0.005	0.003	0.001	Epoxy-coated steel
SMI	0.008	0.001	0.005	0.020	0.004	0.004	0.007	0.007	with intact cladding
SMI-d	0.098	0.137	0.084	0.071	0.043	0.089	0.087	0.031	SMI steel with 4 drilled holes
SMI/Conv.	-[b]	-[b]	-[b]	-	-	-	-[b]	-	SMI at top, Conv. at bottom
Conv./SMI	1.90	2.15	1.66	-	-	-	1.90	0.25	Conv. at top, SMI at bottom
SMI-b	0.061	0.016	0.037	-	-	-	0.038	0.023	SMI bent 180 degree at top
Cracked Beam (CB) Test									
Conv.	17.6	8.5	7.3	15.4	15.2	14.5	13.1	4.1	Conventional steel
ECR	0.035	0.071	0.017	0.069	0.042	0.015	0.041	0.024	Epoxy-coated steel
SMI	0.009	0.024	0.011	0.007	0.006	0.015	0.012	0.007	with intact cladding
SMI-d	1.347	0.726	-[b]	0.292	0.383	0.243	0.598	0.459	SMI steel with 4 drilled holes

Table 5.5b – Corrosion loss (in μm) at 96 weeks for bench scale tests based on exposed area[a]

Steel Designation[a]	Specimen						Average[b]	Standard Deviation	Notes[a]
	1	2	3	4	5	6			
Southern Exposure (SE) Test									
ECR	1.44	0.95	1.23	0.74	2.08	2.60	1.51	0.71	Epoxy-coated steel
SMI-d	47.1	66.0	40.5	34.1	20.6	42.7	41.8	15.0	SMI steel with 4 drilled holes
Cracked Beam (CB) Test									
ECR	17.0	34.1	8.0	33.1	20.3	7.0	19.9	11.8	Epoxy-coated steel
SMI-d	647	349	-[b]	140	184	117	287	221	SMI steel with 4 drilled holes

[a] All ECR and SMI-d bars have four $^{1}/_{8}$-in. diameter penetrations to the underlying mild steel.
[b] No corrosion observed in these specimens.

which provided a large area of steel that could serve as a cathode (Darwin et al. 2002, Balma et al. 2005).

Corrosion losses based on the total area of the top bars during the 96-week test period are shown in Figures 5.18a and 5.18b and summarized in Table 5.5a. Total losses reach values in excess of 1.9 μm for the Conv. and Conv./SMI specimens by the end of the 96-week test period and are below 0.09 μm for all other test specimens. Interestingly, the lowest total corrosion loss is exhibited by the Southern Exposure specimens containing ECR bars, with total average losses of 0.003 μm, compared to 0.007 μm for the SMI bars. Neither value, however, is significant. Corrosion losses based on exposed area are shown in Figure 5.18c and Table 5.5b, with average values at 96 weeks of 42 μm for the SMI-d specimens and 1.5 μm for the ECR specimens.

Again, the key aspect in the difference is the high resistivity of the epoxy coating, which limits the bar area that can serve as a cathode, while the full area of the SMI bars can serve as a cathode.

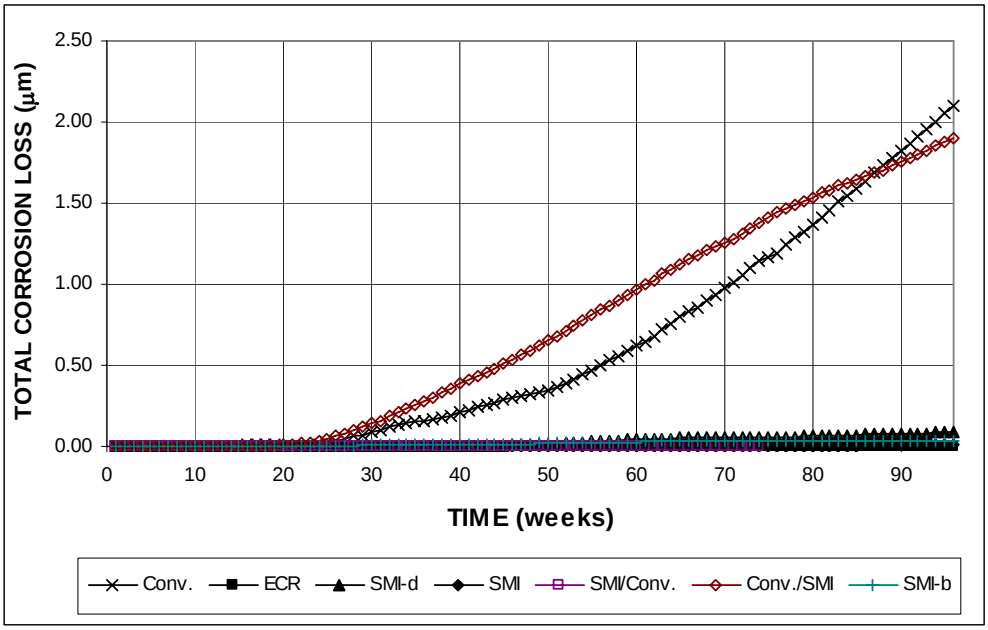

Figure 5.18a – Southern Exposure Test. Average total corrosion loss (based on total area).

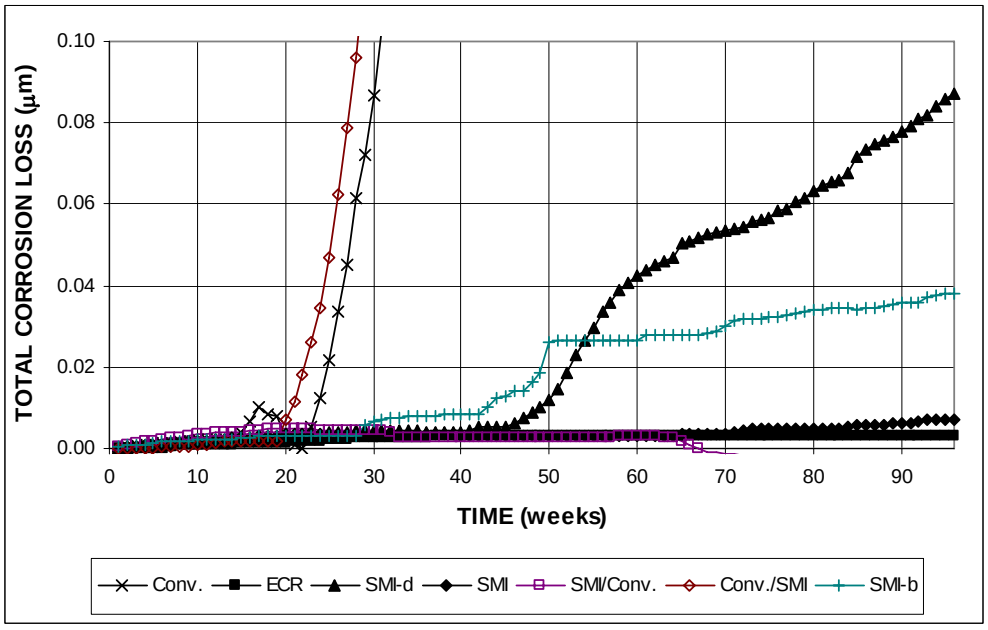

Figure 5.18b – Southern Exposure Test. Average total corrosion loss (based on total area). (different scale)

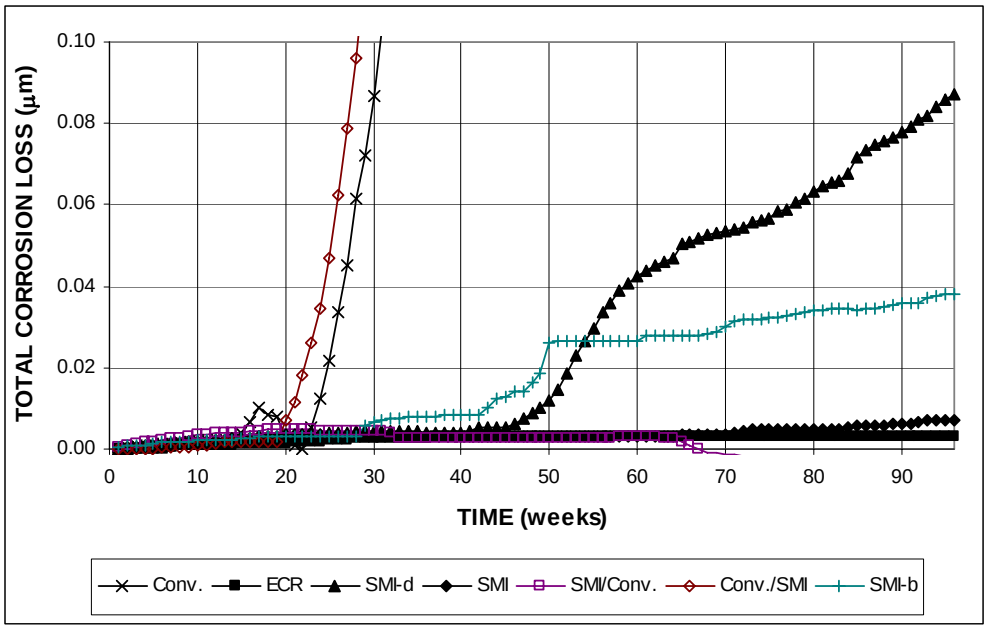

Figure 5.18c – Southern Exposure Test. Average corrosion loss (based on exposed area).

The corrosion potentials with respect to a copper-copper sulfate electrode for the top and bottom mats of steel are shown in Figures 5.19a and 5.19b, respectively. Values more negative than –0.350 V indicate active corrosion. As shown in Figure 5.19a, the Conv./SMI and Conv. specimens exhibited corrosion relatively early in the test, with the former reaching a value more negative than –0.350 V at week 24 and the latter reaching at a value more negative than –0.350 V at week 42. The SMI-d specimens exhibited active corrosion beginning at week 63. The ECR, SMI, and SMI/Conv. specimens did not attain a value more negative than –0.350 V during the test. As shown in Figure 5.19b, the SMI bottom bars in the Conv./SMI test briefly exhibited a corrosion potential below –0.350 V at week 46, while the Conv. bottom bars in the SMI/Conv. specimens exhibited corrosion potentials below –0.350 V during weeks 64 through 75 and weeks 93 through 96.

Cracked Beam Tests **–** The corrosion rates for the cracked beam specimens are summarized in Table 5.4a based on the total area of the top bar and in Table 5.4b based on the exposed area for the ECR and SMI-d specimens with $^{1}/_{8}$-in. diameter holes through the epoxy and stainless steel cladding, respectively. In this highly corrosive environment, the conventional steel (Conv.) specimens exhibit an average corrosion rate of approximately 7 µm/yr between week 20 and week 96 of the tests. The SMI-d specimens exhibit a corrosion rate based on the total area of the top bar of 0.3 µm/yr, while the ECR and SMI specimens exhibit corrosion rates of 0.018 and 0.002 µm/yr, respectively.

Based on exposed area, average corrosion rates of 9 and 157 µm/yr are measured for the ECR and SMI-d specimens (Table 5.4b). As observed for the Southern Exposure specimens, this difference results from the low conductivity provided by the epoxy coating.

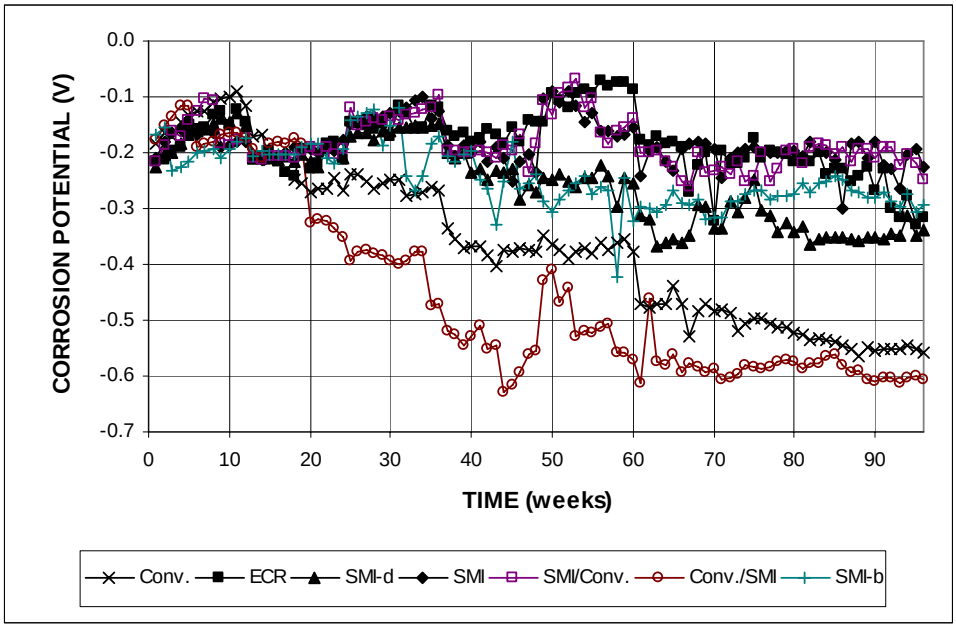

Figure 5.19a – Southern Exposure Test. Average corrosion potentials of top mat.

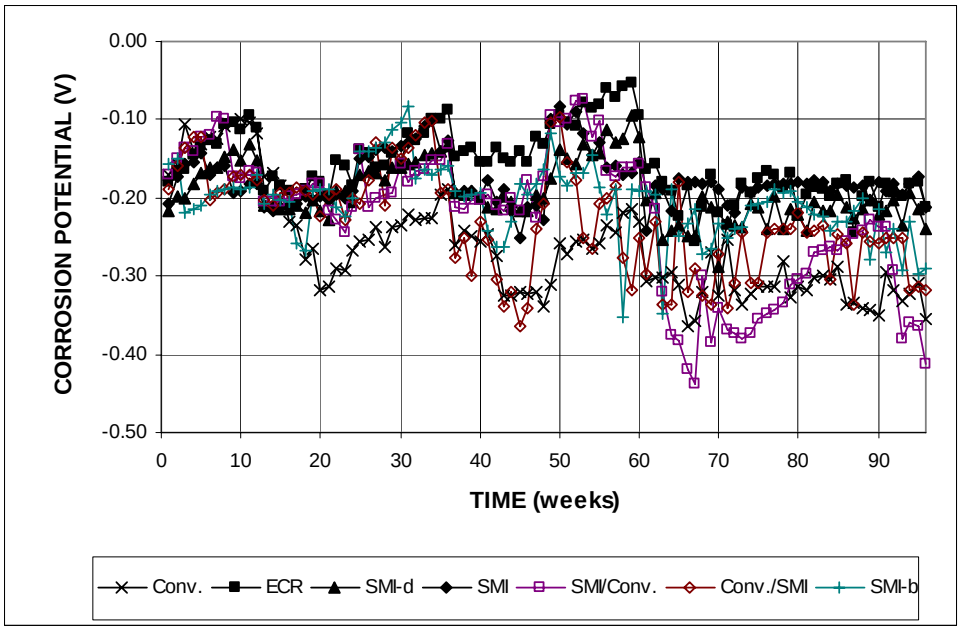

Figure 5.19b – Southern Exposure Test. Average corrosion potentials of bottom mat.

Corrosion losses based on the total area of the top bars are shown in Figures 5.20a and 5.20b and summarized in Table 5.5a, with values at 96 weeks of 13 µm for the conventional steel (Conv.) specimens, 0.6 µm for the SMI-d specimens, 0.04 µm for the ECR specimens, and 0.01 µm for the SMI specimens. The latter two values bode well for the long-term performance of both ECR and SMI bars. As shown in Figure 5.20c, corrosion losses are significantly higher

based on exposed area at the $^{1}/_{8}$-in. diameter holes through the cladding for the SMI-d specimens, with an average loss of 287 μm compared to a value of 20 μm at the damaged area for the ECR specimens.

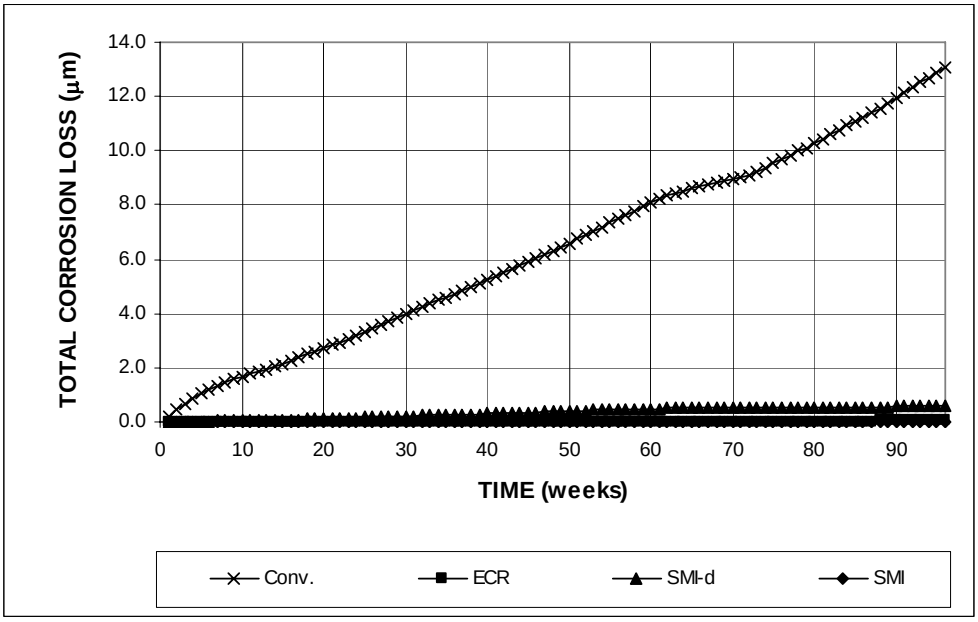

Figure 5.20a – Cracked Beam Test. Average total corrosion loss (based on total area).

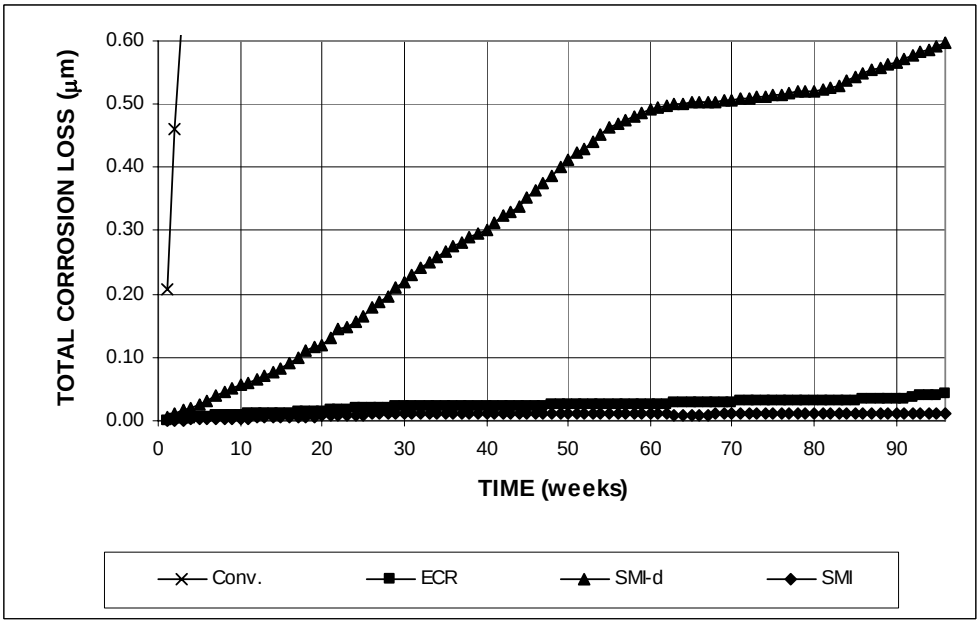

Figure 5.20b – Cracked Beam Test. Average total corrosion loss (based on total area). (different scale)

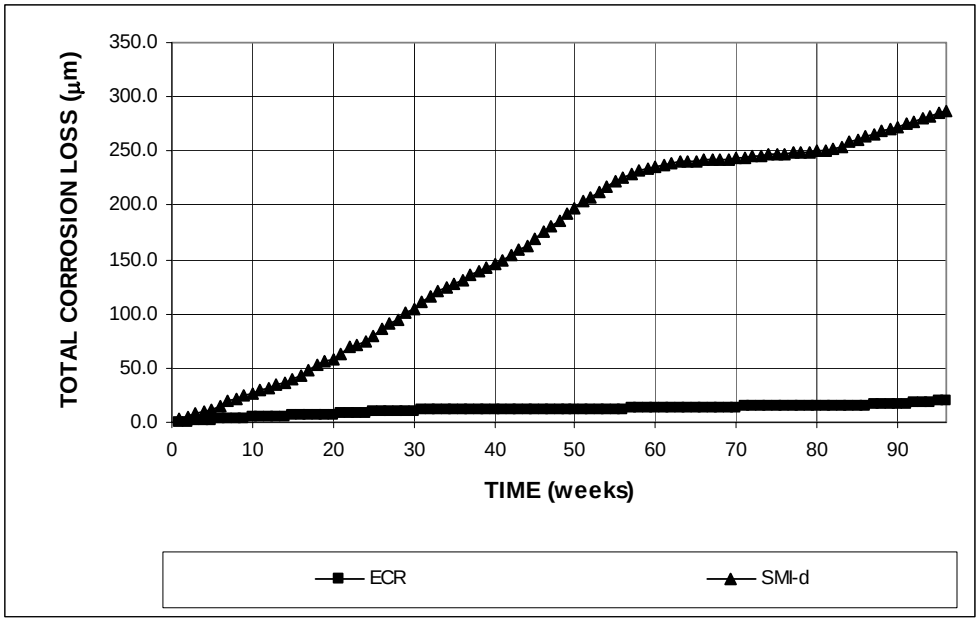

Figure 5.20c – Cracked Beam Test. Average corrosion loss (based on exposed area).

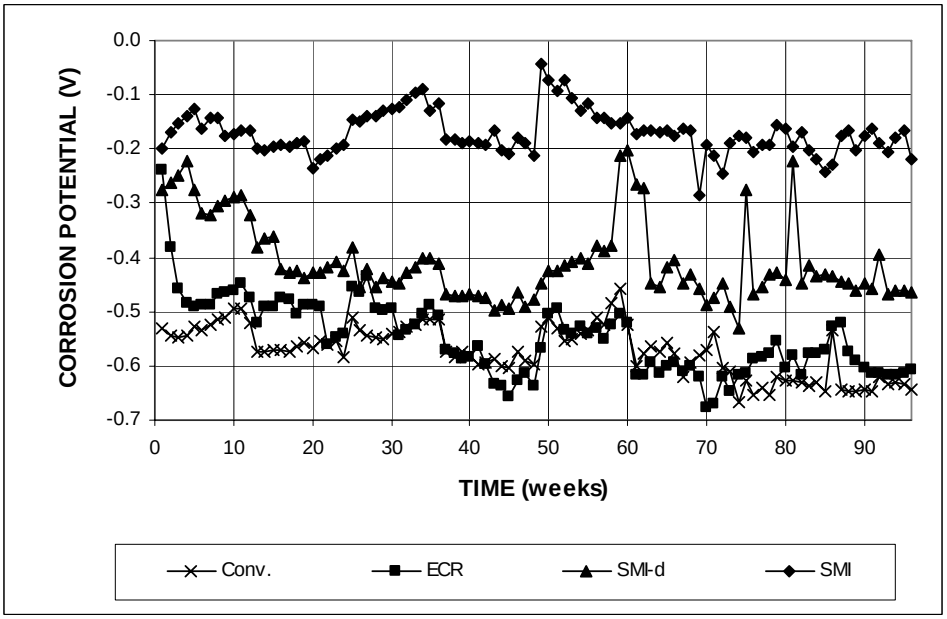

Figure 5.21a – Cracked Beam Test. Average corrosion potentials of top mat.

Corrosion potentials for the cracked beam tests are shown in Figures 5.21a and 5.21b for the top and bottom mats, respectively. As shown in Figure 5.21a, only the SMI bars remained passive, with values of approximately –0.200 V throughout the test. The other specimens initially dropped below –0.350 V with respect to a copper-copper sulfate electrode at weeks 1, 2, and 13 for the conventional, ECR, SMI-d specimens, respectively. It is interesting to note that, for most of the test period, the corrosion potential of the ECR specimens matched that of the conventional

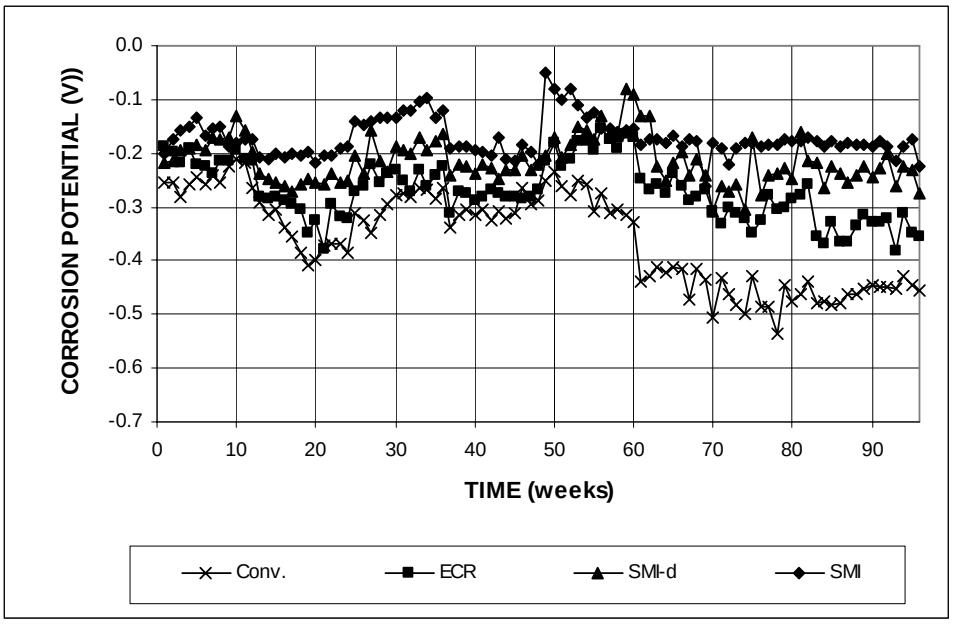

Figure 5.21b – Cracked Beam Test. Average corrosion potentials of bottom mat.

steel specimens, although the corrosion losses were very low for the ECR specimens. The low corrosion loss can be attributed to the high resistivity of the epoxy coating.

Visual Observations – Following the tests, the specimens were observed visually for cracking, staining, and the degree of corrosion on the reinforcing steel bars.

As shown in Figure 5.22a, the Southern Exposure specimens containing conventional steel showed clear evidence of corrosion, with staining visible on the outside of the unbroken specimens. Relatively large areas of the top bars (5.22b) were covered with a dark red-brown corrosion product. The top side of the bars showed more corrosion product than the bottom. Corrosion products, however, appeared on both sides. The top bars also had areas that appeared to be uncorroded. The bottom bars in some specimens also showed signs of corrosion, but to a much lower extent than the top bars, as expected.

At the conclusion of the tests, the cracked beam specimens containing conventional steel showed major signs of corrosion as shown in Figure 5.23a. In all tests, almost the entire surface of the top bar was covered with corrosion products. The volume of the corrosion products on the top bar (see Figure 5.23b) resulted in the formation of a vertical crack through the entire specimen for all but one specimen. The bottom bars exhibited some areas of corrosion while other areas remain uncorroded (Figure 5.23b).

(a) **(b)**

Figure 5.22 – Southern Exposure specimen Conv.-2. (a) Specimen and (b) top bars (left) and bottom bars (right) at conclusion of corrosion test

(a) **(b)**

Figure 5.23 – Cracked beam specimen Conv.-5. (a) Specimen exhibiting corrosion induced cracking and (b) top bar (top) showing heavy corrosion and bottom bars (bottom) exhibiting some corrosion at the conclusion of the test

Like the conventional steel Southern Exposure specimens, the Southern Exposure specimens with conventional steel in the top mat and stainless steel clad reinforcement in the bottom mat showed signs of corrosion on the top bars, as shown by the surface staining in Figure 5.24a. In addition to the staining, the volume of corrosion products was sufficient to cause slight cracking in two out of the three specimens. Corrosion products covered a majority of the surface area of the top bars, while the bottom bars showed no visible signs of corrosion, as shown in Figure 5.24b.

The exterior of the Southern Exposure specimens containing ECR generally showed little or no sign of corrosion. After removing the concrete, the epoxy on the bars showed no signs of damage on initial inspection. The bond of the epoxy to the underlying steel was measured for the epoxy-coated bars in bench-scale specimens at the conclusion of test using a procedure

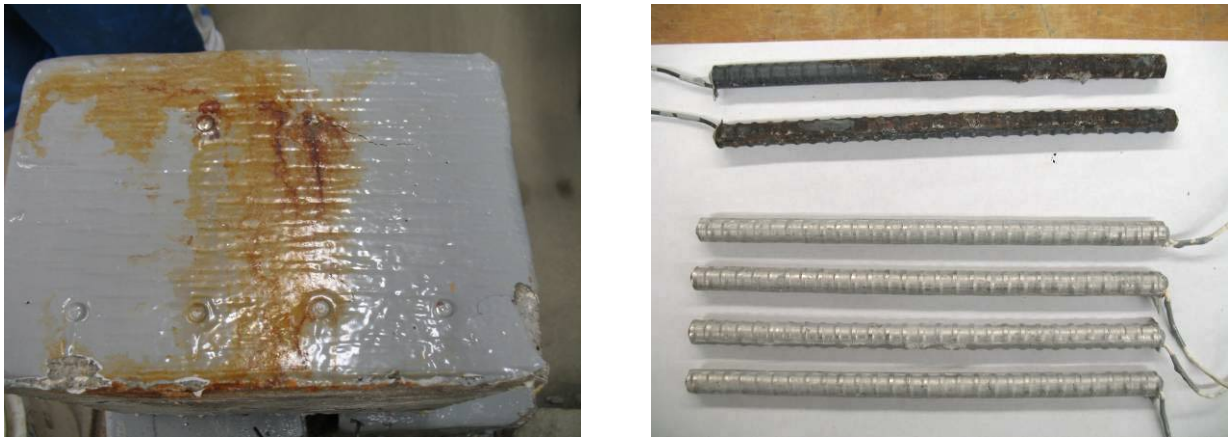

(a) **(b)**

Figure 5.24 – Southern Exposure specimen Conv./SMI-1. (a) Specimen and (b) conventional top bars (top) and stainless steel clad bottom bars (bottom) at conclusion of corrosion test

similar to the cathodic disbondment test specified in ASTM A 775. Using the procedure, two radial cuts (at 90° to each other, at a 45° with respect to longitudinal axis of the bar) are made through the coating, intersecting at the center of the $^{1}/_{8}$ in. drilled holes using a sharp, thin bladed knife. An attempt is then made to lift the coating. The result is illustrated in Figures 5.25a and b. The damaged areas in the figures are the result of the disbondment testing and were not apparent prior to the attempt to remove the epoxy. Three out of six of the ECR Southern Exposure specimens exhibited disbondment of the epoxy-coating in the area surrounding at least one drilled hole on a top bar; disbondment was observed on both the top and bottom sides of the reinforcement. The steel underneath the disbonded area had a thin layer of dark brown-black corrosion product on the surface, as shown in Figure 5.25b. The top bars on the other three specimens showed no signs of corrosion or disbondment.

(a) **(b)**

Figure 5.25 – Southern Exposure specimen ECR-6. (a) ECR top bars (top) and bottom bars (bottom) – damaged area it the result of disbondment testing and (b) area on top bar after disbondment testing at conclusion of corrosion test

At the conclusion of the tests, the exterior of the ECR cracked beam specimens showed no obvious indications of corrosion. As shown in Figure 5.26a, the epoxy coating remained intact on the bars, with the exception of small blisters on some bars (Figure 5.26b), but the bars in all six ECR cracked beam specimens showed signs of corrosion and disbondment of the epoxy coating. For the most part, the disbonded area after testing at drilled holes (Figures 5.26c and d) was larger than the disbonded area observed on the Southern Exposure specimens. Disbondment was observed on both sides of the bars in both top and bottom mats (Figure 5.26d). Orange and brown blistering in the epoxy coating (Figure 5.26b) was observed on four of the six top bars in the ECR cracked beam specimens. In each case, blistering was accompanied by disbondment of the surrounding epoxy.

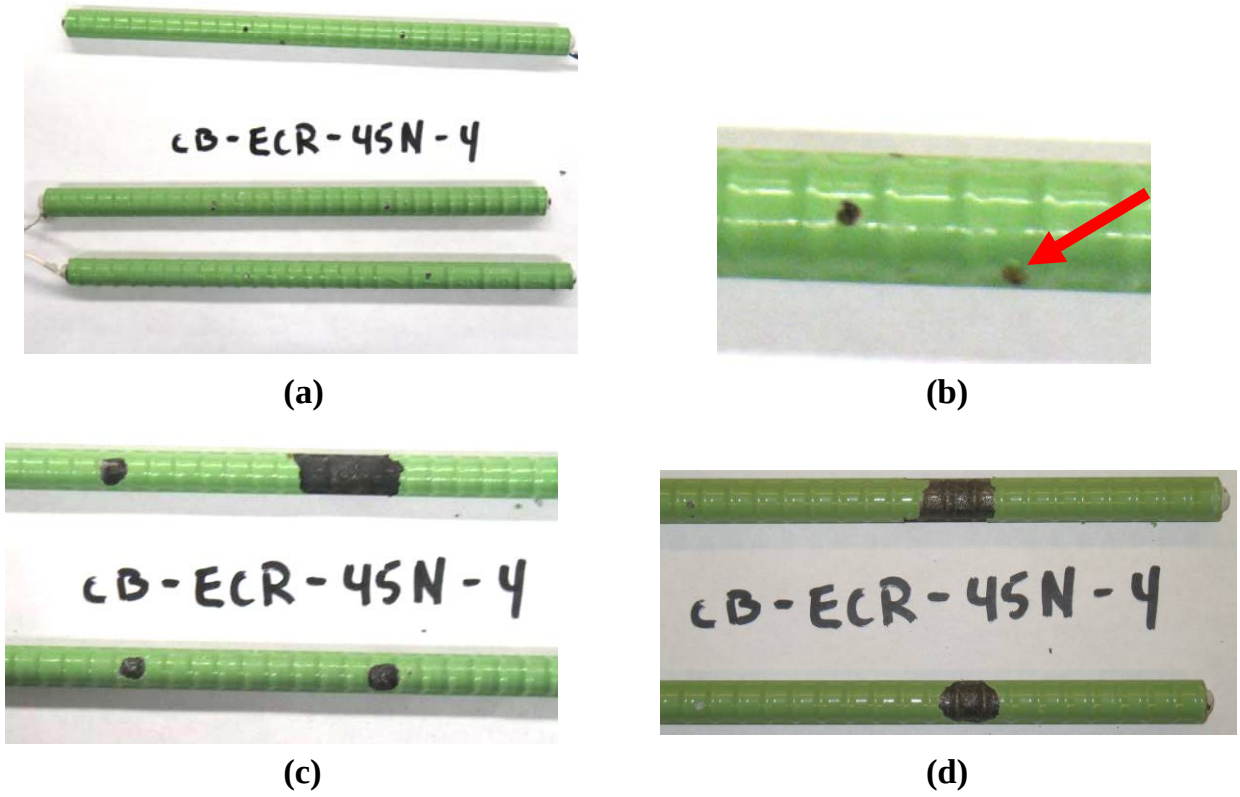

Figure 5.26 – Cracked beam specimen ECR-4. (a) ECR top bars (top of photograph) and bottom bars (bottom) before the disbondment test, (b) blister on top bar, (c) ECR top bar (top) and bottom bar (bottom) – damaged areas as the result of disbondment testing on the upper side of the bar, and (d) ECR top bar (top) and bottom bar (bottom) – damaged areas as the result of disbondment testing on the lower side of the bars

The stainless steel clad bars without drilled holes showed no visible signs of corrosion in either of Southern Exposure or cracked beam tests, as shown in Figures 5.27a and b. Both the upper and lower sides of top and bottom bars retained a shiny appearance at the conclusion of the test period.

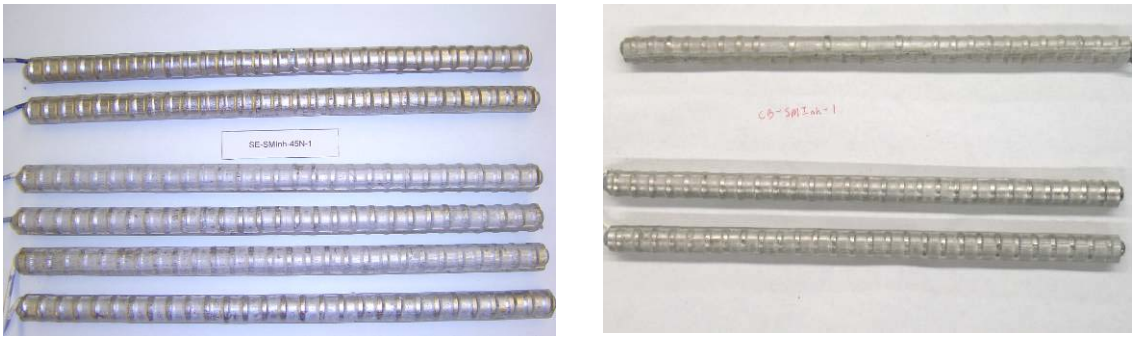

(a) **(b)**

Figure 5.27 – (a) Southern Exposure Specimen SMI-1, top bars (top) and bottom bars (bottom) and (b) cracked beam specimen SMI-1, top bar (top) and bottom bars (bottom). The bars exhibited no corrosion damage at the conclusion of the test

The Southern Exposure specimens with stainless steel clad top reinforcement and conventional steel bottom reinforcement showed signs of corrosion on the bottom bars but not in the top bars; as shown in 5.28a, slight orange staining could be seen on the exterior of the concrete in areas surrounding the ends of the bottom bars. Corrosion products generally formed on both the upper and lower sides, towards the ends of the bottom bars, as shown in Figure 5.28b.

(a) **(b)**

Figure 5.28 – Southern Exposure Specimen SMI/Conv.-1. (a) Specimen and (b) top bars (top) and bottom bars (bottom) at conclusion of corrosion test

Southern Exposure and cracked beam specimens containing stainless steel clad bars with drilled holes exhibited no signs of corrosion on the exterior of the concrete at the conclusion of the tests. The bars themselves also showed little or no sign of corrosion on the stainless steel cladding. On the top bars, a black corrosion product covered the exposed conventional steel core at the location of the drilled holes, as shown in Figures 5.29 and 5.30, and in some cases, an orange/brown stain was observed in the areas surrounding the holes, as shown in Figures 5.29b and 5.30b. Corrosion was observed on two of twelve bottom bars. For the top bars and, in the

two cases, the bottom bars, signs of corrosion are more pronounced on the upper than on the lower side of the bar.

(a) **(b)**

Figure 5.29 – Southern Exposure specimen SMI-d-5 (stainless steel clad bars with drilled holes) (a) top bars (top) and bottom bars (bottom) and (b) corrosion detail on upper side of top bars at conclusion of corrosion test

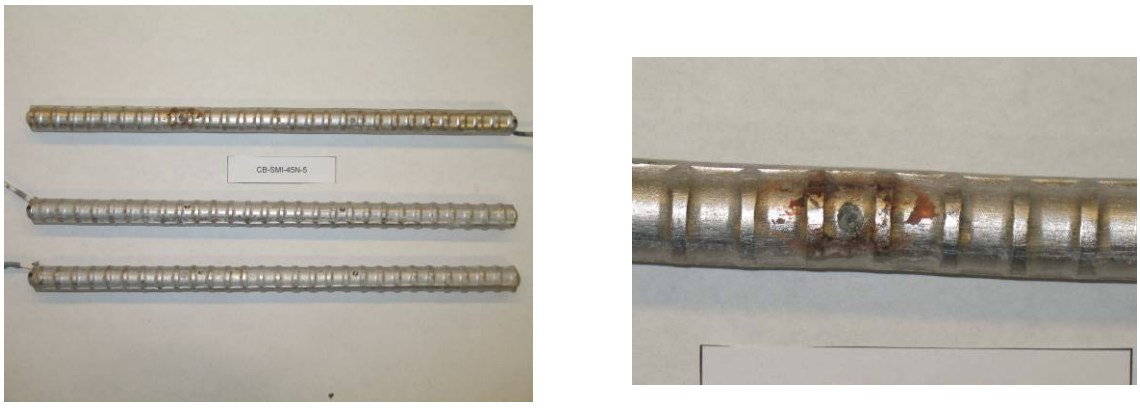

(a) **(b)**

Figure 5.30 – Cracked beam specimen SMI-d-5 (stainless steel clad bars with drilled holes) (a) top bar (top) and bottom bars (bottom) and (b) corrosion detail on upper side of top bar at conclusion of corrosion test

The Southern Exposure specimens containing a bent top bar showed no signs of corrosion on the exterior of the concrete at the conclusion of the tests. The same is true of the reinforcing bars with the exception of those areas where the cladding had been damaged during the bending operations, as shown in Figure 5.31. These observations emphasize the importance of using bending equipment that will not damage the cladding. In one case, shown in Figure 5.31c, the appearance of the corrosion product suggests the presence of a small penetration in the cladding.

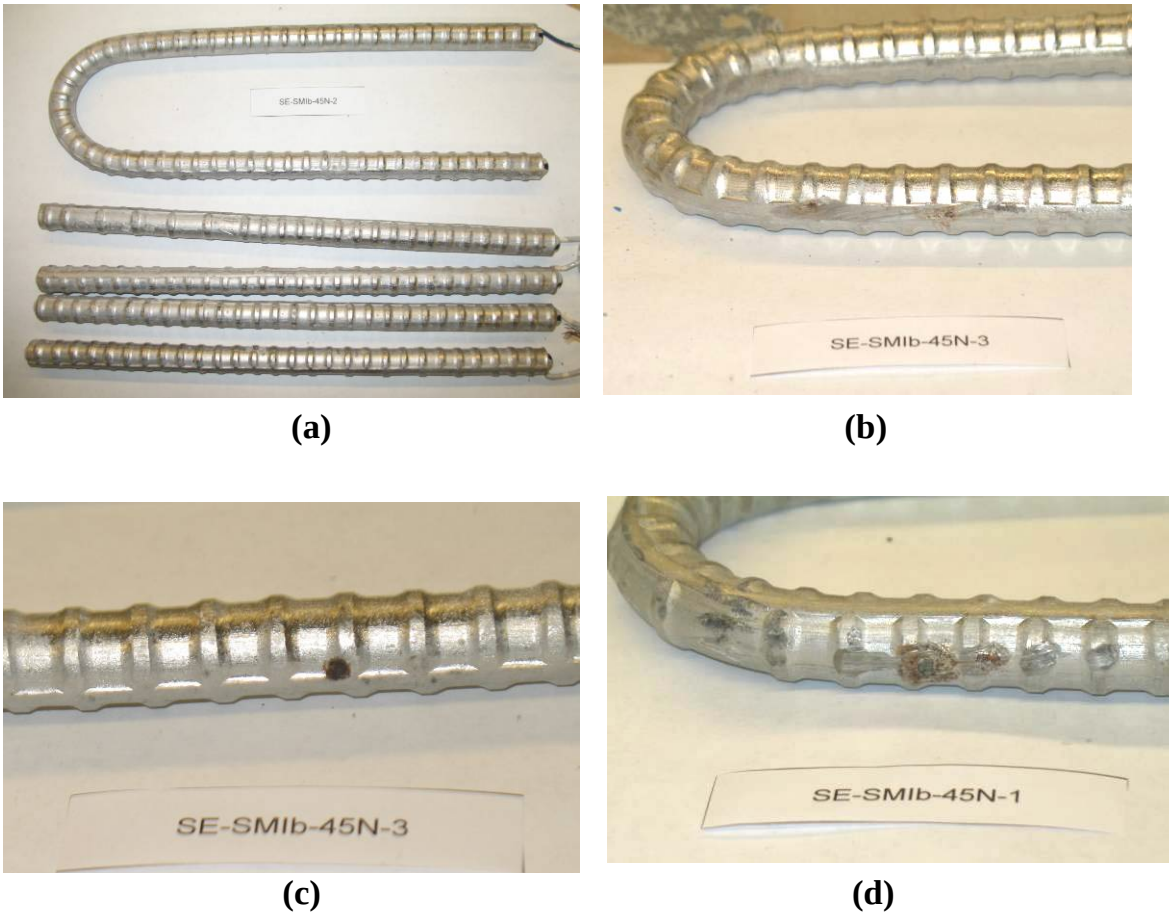

Figure 5.31 – Bars from Southern Exposure specimens containing bent top bar. (a) Bent top bar and straight bottom bars from specimen SMI-b-2. (b) Bent top bar from specimen SMI-b-3. (c) Detail of region with a deposit on top bar from specimen SMI-b-3. (d) Corrosion at region of damaged cladding on specimen SMI-b-3.

Summary **–** The bench scale tests demonstrate that epoxy-coated and SMI clad reinforcement provide superior corrosion protection compared to conventional steel. SMI steel with the cladding intact, exhibits no corrosion products, although one bar did appear to have a penetration in the cladding (Figure 5.31c). When cladding or epoxy-coating is damaged, total corrosion losses are very low, although the losses based on the exposed area at the holes through the cladding or epoxy are significantly lower on the epoxy-coated reinforcement than on the SMI steel because of the high resistivity of the epoxy coating, which limits the area of the cathode. The corrosion products observed on damaged regions of the bent SMI (SMI-b) specimens emphasizes the importance of using protective measures, such as are used for bending epoxy-coated reinforcement, when bending stainless steel clad reinforcement. The thickness of the cladding, however, should be more than adequate to withstand any damage during normal handling.

5.5 CORROSION EFFECTS

The scanning electron microscope was used to obtain images of corrosion products from both conventional and stainless steel clad bars. The selected images are shown in Figures 5.32 through 5.41. The images of corrosion products from conventional steel are shown on the left (a) and the images of corrosion products from the mild steel cores of the stainless steel clad bars are shown on the right (b). The figures show corrosion products on the anode bars from bare steel macrocell tests.

Figure 5.32 shows corrosion products with nodular structures for both conventional and SMI clad steel. The corrosion products are similar, but the product from the SMI steel shown in Figure 5.32b is not covered with short fibers as are those shown in Figure 5.32a. Figures 5.33 and 5.34 show corrosion products consisting of amorphous structures with angular crystal-like elements. Figure 5.35 shows a smoother amorphous structure, with fewer crystal-like elements compared to Figures 5.33 and 5.34. Figure 5.36 shows nodular structures similar to those seen in Figure 5.32, but the corrosion products from both steels are not covered with fibers. Figures 5.37 and 5.38 show an amorphous structure that is very similar for both materials. Figure 5.39 shows corrosion products with fibrous structure, while Figure 5.40 shows corrosion products with shorter fiber structure, for both convention and SMI steel. The corrosion products shown in Figure 5.41 are dissimilar, with the conventional steel [Figure 5.41a] showing obviously crystal-like particles.

The images shown here only cover a portion of the corrosion product structures. However, it can be concluded that 1) the structure of the corrosion products can vary widely and 2) products with similar morphology are observed on both types of reinforcement, indicating that the presence of the stainless steel cladding does not alter the nature of the corrosion products formed in an exposed region of the mild steel core.

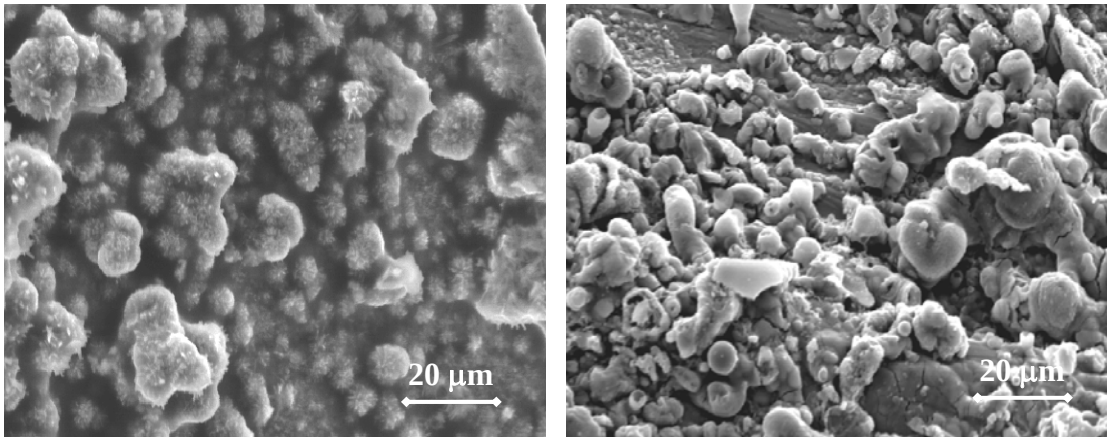

Figure 5.32 – Nodular corrosion products with fibers on bare bar anodes for (a) Conventional and (b) SMI steel at unprotected ends. 680X

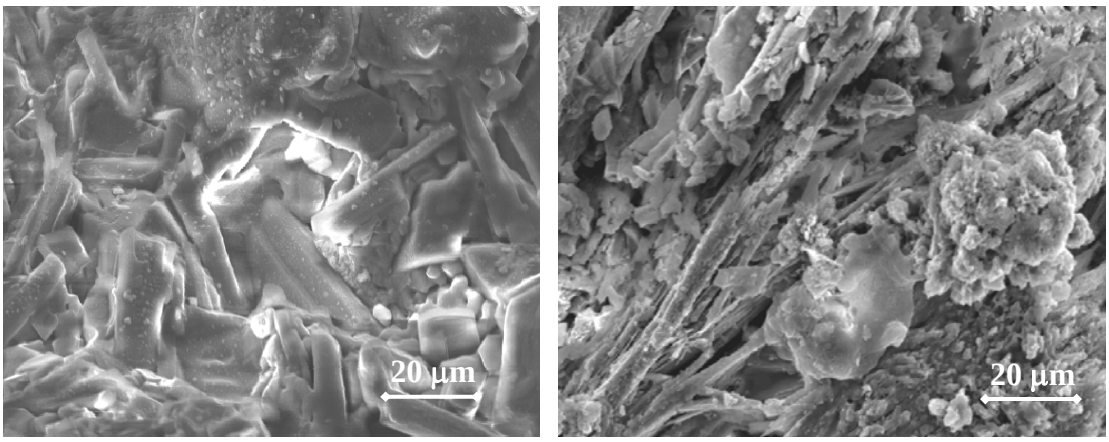

(a) **(b)**

Figure 5.33 – Amorphous corrosion products with crystal-like elements on bare bar anodes for (a) conventional and (b) SMI steel at penetrations through the cladding. 680X

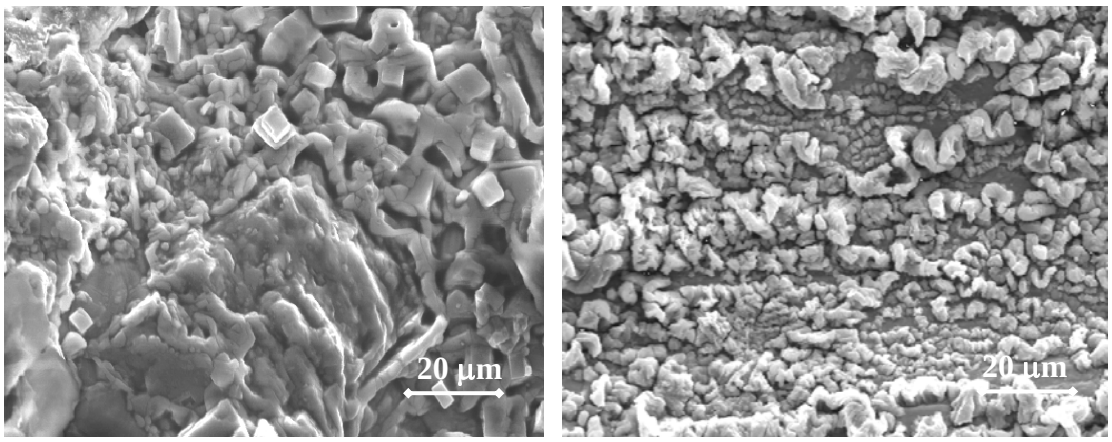

(a) **(b)**

Figure 5.34 – Amorphous corrosion products on bare bar anodes for (a) conventional and (b) SMI steel at unprotected ends. 680X

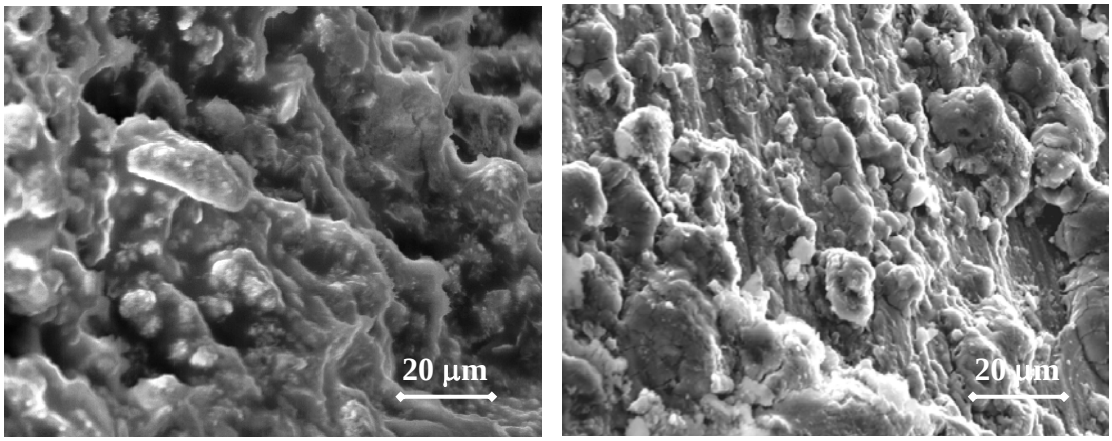

(a) **(b)**

Figure 5.35 – Amorphous corrosion products with small crystal-like elements on bare bar anodes for (a) MMFX and (b) conventional steel at unprotected ends. 680X

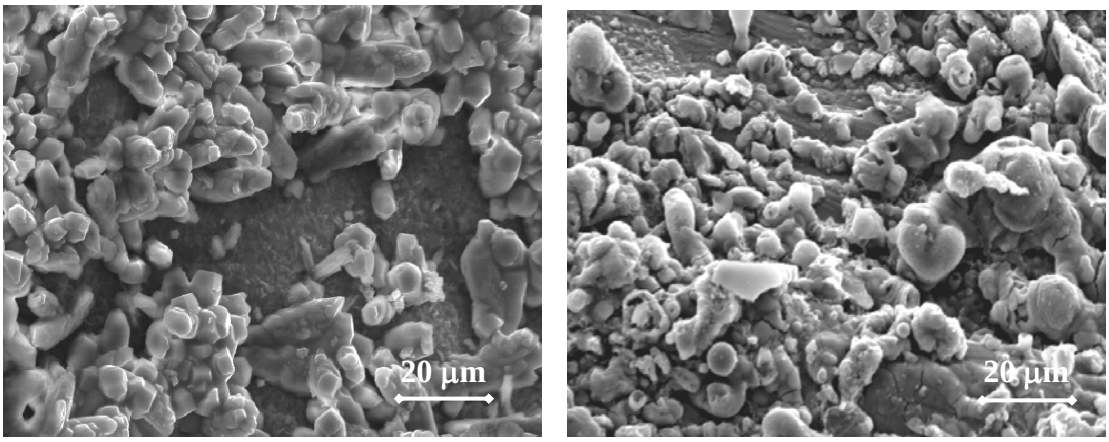

(a) **(b)**

Figure 5.36 – Nodular corrosion products on anode bars for (a) conventional and (b) SMI steel at unprotected ends**.** 680X

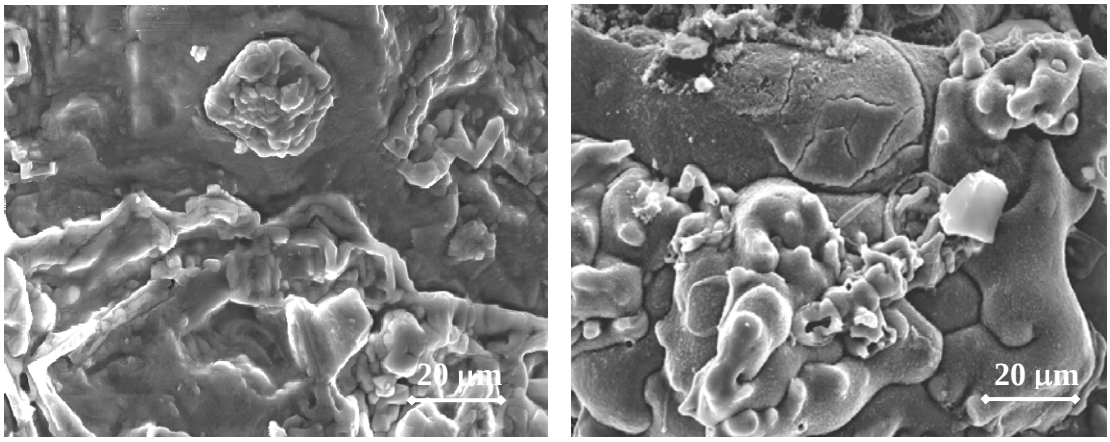

(a) **(b)**

Figure 5.37 – Smooth, amorphous corrosion products on anode bars for (a) conventional and (b) SMI steel at unprotected ends**.** 680X

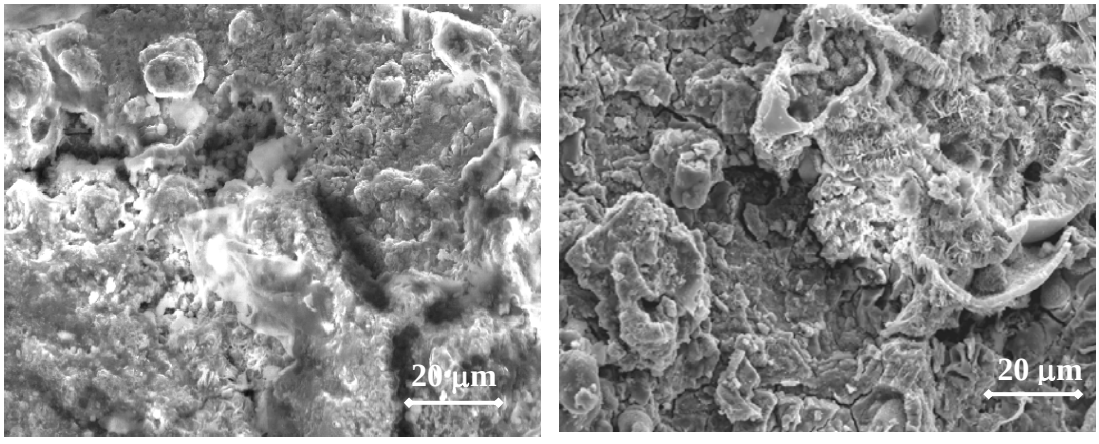

(a) **(b)**

Figure 5.38 – Amorphous corrosion products for anode bars for (a) conventional and (b) SMI steel at penetrations through the cladding**.** 680X

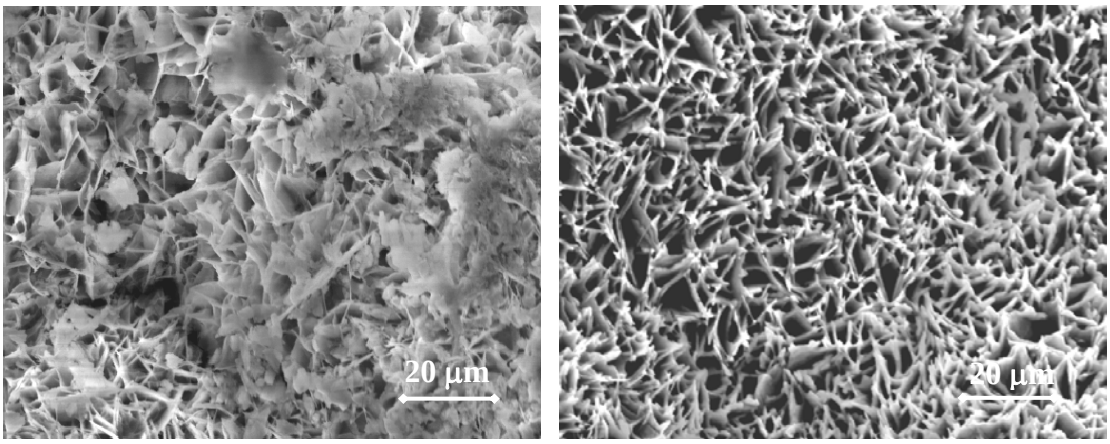

(a) **(b)**

Figure 5.39 – Corrosion products with long fiber structure for anode bars for (a) conventional and (b) SMI steel at unprotected ends**.** 680X

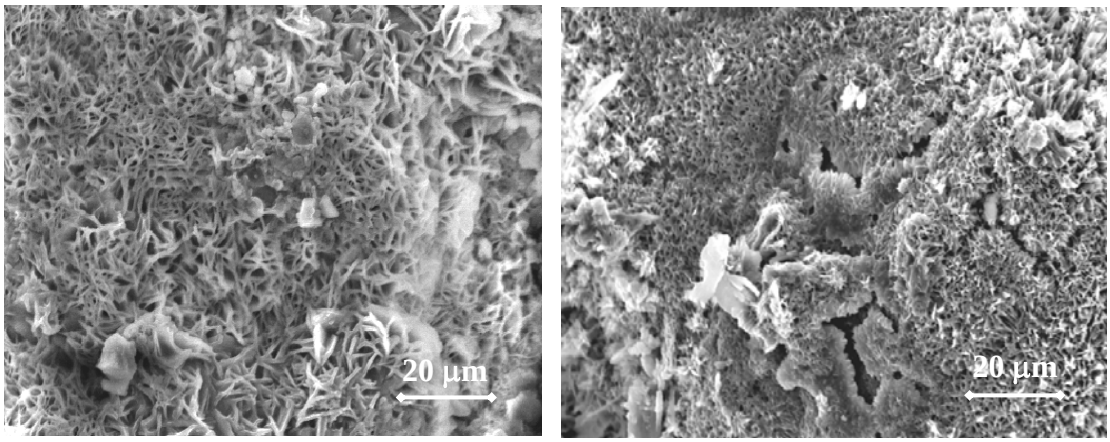

(a) **(b)**

Figure 5.40 – Corrosion products with short fiber structure for anode bars for (a) conventional and (b) SMI steel at penetrations through the cladding**.** 680X

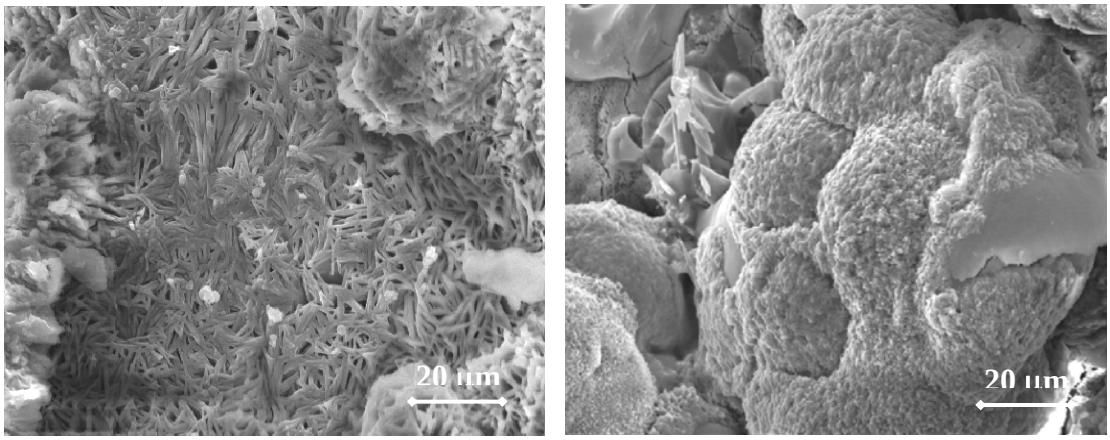

(a) **(b)**

Figure 5.41 – Corrosion products dissimilar structure for anode bars for (a) conventional and (b) SMI steel at penetrations through the cladding**.** 680X

5.6 LIFE EXPECTANCY AND COST EFFECTIVENESS

5.6.1 Life Expectancy

As described in Section 4.6.1, the life expectancy of bridge decks is estimated based on both experience and analysis. Estimates are provided for the time to initial repair, or "initial life," and the time between repairs. Based on experience by SDDOT (Gilsrud 2007), the initial life for bridge decks containing conventional uncoated reinforcement is estimated to be 10 years under harsh environmental conditions and 25 years in arid conditions. The 25-year period matches that estimated by KDOT (Kepler et al. 2000). For epoxy-coated reinforcement, the SDDOT estimate is 40 years, while the KDOT estimate is 35 years. The estimates for epoxy-coated steel are based on the experience that, over the past 30 years, no bridge decks with epoxy-coated reinforcement have required repair due to corrosion damage in either state.

Analysis is required to obtain an estimate for the time to first repair for bridges with stainless steel clad reinforcing steel and can also be used to estimate the time to first repair for decks with conventional and epoxy-coated reinforcement. The prototype design used for the estimate is a bridge deck with a total deck thickness of 8.5 in. and cover on the top layer of steel of 2.5 in. Time to first repair is estimated based on (1) the chloride content required for corrosion initiation, (2) the time required to reach that chloride concentration at the level of the steel, and (3) the time required for a thickness loss of 25 μm (0.001 in.) for uncoated steel, which will produce a volume of corrosion products that will crack the concrete (Pfeifer 2000), or the time required to produce corrosion products at localized areas of corrosion to crack concrete for systems with epoxy-coated steel.

Time to corrosion initiation – For any corrosion protection system, the time to corrosion initiation depends on (1) the chloride content in concrete corresponding to corrosion initiation (taken here as water-soluble chloride), referred to as the critical chloride corrosion threshold, and (2) the time required to reach that chloride content in the structure.

The chloride corrosion thresholds for bridge decks containing conventional and epoxy-coated steel are based on chloride threshold tests at the University of Kansas described by Ji et al. (2005) and summarized in Section 5.8. The chloride threshold for bridge decks with stainless steel clad reinforcement is based on values for stainless steel from a previous study in the University of Kansas (Balma et al. 2005).

Once the chloride threshold is determined, the time to reach that specific chloride content in a prototype bridge deck, which has cracks parallel to and on top of the top layer of reinforcement, can be determined using results from bridge surveys reported by Miller and Darwin (2000) and Lindquist et al. (2005). Cracked decks are selected for this model because the surveys demonstrate that reinforced concrete bridge decks exhibit significant cracking parallel to and immediately above the reinforcing bars. Based on the chloride data presented by Lindquist et al. (2005, 2006), which includes the results from both studies, the correlation between average chloride concentration (C, in lb/yd^3) and time (T, in months) at a depth of 2.5

in. at crack locations in bridges with an average annual daily traffic (AADT) greater than 7500 can be obtained using a linear trend line:

$$C = 0.0373T + 0.8328 \tag{5.1}$$

[Note: Equation (5.1), as shown in Figure 5.42, was developed after the publication of Lindquist et al. (2005) and does not appear in the report.]

The average time to reach the chloride corrosion threshold is

$$T_c = (C_c - 0.8328)/0.0373 \tag{5.2}$$

where C_c = chloride threshold, lb/yd^3 and T_c = time to reach chloride threshold, months.

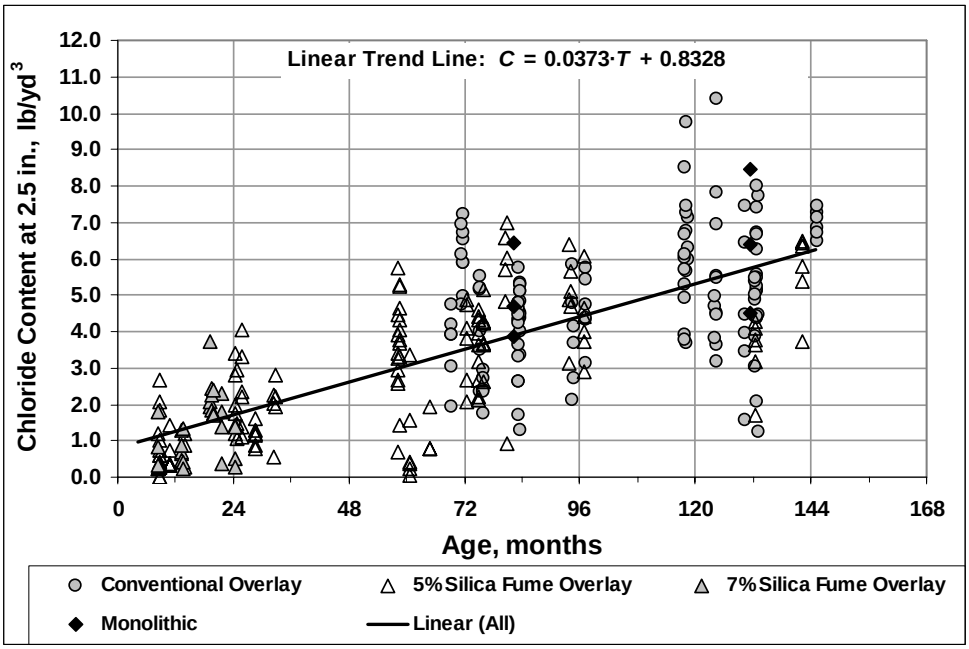

Figure 5.42 – Chloride content taken on cracks interpolated at a depth of 2.5 in. versus placement age for bridges with an AADT greater than 7500

For example, if the chloride content required for corrosion initiation is 2 lb/yd^3 for a bridge deck, the average time T_c to reach that chloride concentration is (2–0.8328)/0.0373 = 31.3 months (2.6 years), which is the time to corrosion initiation at cracks.

Estimates of chloride corrosion threshold and time to corrosion initiation for various types of reinforcement are listed in Table 5.6. The analysis used to determine these chloride corrosion threshold values is described in Section 5.8. The chloride threshold for conventional steel and epoxy-coated steel with a damaged coating is in the range of 1 to 2 lb/yd^3, which gives a range of corrosion initiation times between 4.5 and 31.3 months (0.4 and 2.6 years) at crack locations. A chloride threshold of 1.75 lb/yd^3, the average obtained in the tests described in Section 5.8, is used to estimate initiation of corrosion in this study, which corresponds to a time

to corrosion initiation of 24.6 months, rounded down to 2.0 years. As shown by Balma et al. (2005) and listed in Table 5.6, stainless steel of the type used as the cladding for SMI bars has a chloride threshold in excess of 25 lb/yd^3, which corresponds to a time to corrosion initiation in excess of 75 years. Although the life expectancy of decks containing MMFX reinforcement is discussed in Section 5.9, chloride threshold values are presented in Table 5.6 for comparison with other reinforcement systems. The chloride threshold for MMFX steel is found to be 6.50 lb/yd^3 with a time to corrosion initiation of 12.7 years. The life expectancy and cost effectiveness of bridge decks containing MMFX reinforcement are addressed in Section 5.9.

Table 5.6 – Corrosion initiation time for bridge decks containing different corrosion protection systems

Steel Designation	**Chloride corrosion threshold**	**Time to corrosion initiation***
	lb/yd^3	**years**
Conv.	1.75	2.0
ECR	1.75	2.0
SMI	>25	>75
MMFX	6.50	12.7

*Assumes reinforcement located under a crack

Time to Cracking – To calculate the time to cracking for a bridge deck after corrosion initiation, the corrosion loss that corresponds to the quantity of corrosion product that causes cracking and spalling of the concrete cover, along with the average corrosion rate of each corrosion protection system, is used to determine when a repair is needed.

A total corrosion loss of about 25 μm (0.001 in.) will cause concrete to crack when the loss is relatively uniform along the length of a reinforcing bar (Pfeifer 2000). For cases where only a fraction of the reinforcing bar is subject to corrosion, such as epoxy-coated bars with limited damage to the coating, the total corrosion loss needed to crack the concrete cover can be calculated using an empirical equation developed by Torres-Acosta and Sagues (2004).

Torres-Acosta and Sagues (2004) determined the value of metal loss needed to crack the concrete cover of a reinforced concrete element if only a portion of a steel bar is corroding. In their study, 16 cylindrical concrete specimens with various dimensions and 22 prismatic beam concrete specimens with dimensions of 5.5 × 5.5 × 16 in. were tested. Pipes cast in the center of the cylindrical specimens were mechanically continuous but had a center segment (anodic region) made of carbon steel pipe with a machined surface and two polyvinyl chloride (PVC) pipe sections for the remainder. The carbon steel pipe segment had a 0.83 in. external diameter, a 0.12 in. wall thickness, and a length ranging from 0.75 to 3.74 in. The concrete covers varied from 1.08 to 2.59 in., and the concrete had water-cement ratios of 0.47, 0.49, or 0.51. The concrete cylinders were used to measure the amount of steel corrosion penetration (x_{CRIT}) upon autopsy, as well as pressure at the steel/concrete interface and dimensional changes during corrosion of the embedded steel pipe segment using strain gauges. The prismatic beams contained one dual-material reinforcing bar placed lengthwise centered on one of the cross

section sides, with the carbon steel segment at the center and two Type 316 LN stainless steel segments at both ends. No. 2 (not a standard size) and No. 4 reinforcing bars were used in these specimens, with lengths ranging from 0.74 to 16 in. for the carbon steel segments. Concrete covers varied from 0.51 to 1.77 in. Water-cement ratios of 0.47, 0.49, and 0.51 were used in these tests. The beam specimens were used to estimate the value of x_{CRIT} only.

After the tests were completed, x_{CRIT} was obtained experimentally for the specimen. An empirical relationship between x_{CRIT} and the specimen dimensions was obtained.

$$x_{CRIT} = 0.000433(c/\phi)(c/L+1)^2 \quad \text{(in.-lb), or} \qquad (5.3)$$
$$x_{CRIT} = 0.011(c/\phi)(c/L+1)^2 \quad \text{(SI)}$$

where x_{CRIT} = critical amount of steel corrosion penetration, in. or mm, c = concrete cover, in. or mm, ϕ = reinforcing bar diameter, in. or mm, and L = length of a local corrosion region (anodic ring region) on the bar, in. or mm.

Gong (2006) verified the accuracy of Eq. (5.3) based on the corrosion losses of bench-scale specimens containing damaged epoxy-coated steel as the anode and conventional steel as cathode, tested by Balma et al. (2005) and McDonald et al. (1998).

Based on Eq. (5.3), a corrosion loss of 1426 μm would be needed at a $^1/_8$-in. long damaged region on a No. 5 epoxy-coated or stainless steel bar to crack the overlying concrete of a Southern Exposure or cracked beam specimen (1-in. cover). However, the tensile stress produced by the increased volume of the corrosion products from isolated damage at a $^1/_8$-in. diameter hole on *one side* of the epoxy-coated steel should be at most one-half of that caused by the rust over a ring-shaped region with length L. Using this reasoning, twice the corrosion loss given by Eq. (5.3), approximately 2850 μm, will be needed to crack the concrete cover for a specimen with 1-in. cover. Based on this analysis and considering the typical concrete cover used in bridge decks of 2.5 in., the corrosion loss required to crack the concrete in a bridge deck jumps to 1.5 in. (39,000 μm or 39 mm), or more than twice the diameter of a No. 5 reinforcing bar. Therefore, corrosion protection systems such as stainless steel clad reinforcement and epoxy-coated steel with small damaged areas, like the $^1/_8$-in. holes used in this study, will not form enough corrosion products to crack the concrete during the life of a bridge deck.

An estimate of the corrosion rate for each corrosion protection system is used in conjunction with the corrosion losses to cause cracking to calculate the time to cracking after corrosion initiation. A value equal to one-half of the average value of corrosion rates for the Southern Exposure and cracked beam tests described in this report is used as the corrosion rate for a bridge deck with the corresponding corrosion protection system. A value of one-half is used because the Southern Exposure and cracked beam specimens are subjected to higher salt concentrations and more aggressive exposure cycles than actual structures.

The corrosion rate for each system is estimated using the calculated corrosion losses divided by the period of time that is defined between corrosion initiation and the end of the test, as described in Section 5.4.2. Calculated corrosion losses are used to determine corrosion rate

for two reasons: 1) the calculated corrosion rate over time has great variability so that it is difficult to select an appropriate average rate that adequately represents the performance of the system over the length of the test, and 2) variability in the concrete materials in the tests causes a variation in the corrosion initiation date. For example, Fig. 5.17a shows the calculated corrosion losses for the conventional steel Southern Exposure specimens described in this report. Although corrosion initiation varies greatly (roughly between 20 and 80 weeks), the rates of corrosion, as indicated by the slopes of the individual plots, are similar. A summary of the corrosion rates calculated for the Southern Exposure and cracked beam tests is shown in Table 5.4a.

The final corrosion rate used for the analysis for conventional reinforcement is calculated as one-half the average values from Southern Exposure and cracked beam specimens, or [(2.66+7.09)/2]/2 = 2.43 μm/yr. Based on exposed area, the corrosion rates for epoxy-coated reinforcement and stainless steel clad reinforcement with drilled holes are calculated to be [(0.63 + 8.76)/2]/2 = 2.34 μm/yr and [(52 + 157)/2]/2 = 52.3 μm/yr, respectively. The large cathode provided by the bottom stainless steel clad bar contributes to the large corrosion rate for stainless steel clad reinforcement with drilled holes. The corrosion rate for solid stainless steel clad reinforcement is calculated as [(0.004+0.002)/2]/2 = 0.0015 μm/yr, which is effectively zero because corrosion did not initiate for the specimens.

The time to cracking can be calculated by considering the amount of corrosion products needed to crack concrete and the corrosion rate. For a total corrosion loss of 25 μm to cause concrete cracking, the time to first repair after corrosion initiation for conventional reinforcement is 25/2.43 = 10.3 years. For bridges containing conventional epoxy-coated steel or SMI stainless steel clad reinforcement with damage, the corrosion rates, 2.34 μm/year and 52.3 μm/year, respectively, are of little practical interest because the steel would be completely corroded at the damaged area before the concrete would crack. And even at a corrosion rate of 52 μm/year on an $^{1}/_{8}$-in. hole in the cladding, only 8% of the cross section of a No. 5 bar would be lost in 100 years. No repair would be needed for bridge decks containing intact stainless steel reinforcement because the corrosion rate is essentially zero below the corrosion threshold.

Time to First Repair – The time to first repair, or initial life, for the prototype bridge deck can be estimated by adding the time to corrosion initiation and the time to cracking after corrosion initiation. For a bridge deck containing conventional steel, the time to corrosion initiation is 2.0 years, and the time to cracking after corrosion initiation is 10.3 years. Therefore, the time to first repair is 2.0 + 10.3 = 12.3 years. For bridge decks containing stainless steel clad reinforcement or epoxy-coated steel, the time to first repair based on cracking the concrete cover is beyond the 75-year service life of the deck. The calculations for epoxy-coated steel do not, however, consider the potential effects of loss of adhesion between the epoxy and the steel, which are, as yet, difficult top address analytically.

For a bridge deck containing epoxy-coated steel, adhesion loss between the epoxy and the steel may reduce the time to first repair (Sagues et al. 1994, *Adhesion* 1995). To account for the potential effects of adhesion loss, times to first repair for bridges containing epoxy-coated steel

of 35 years and 40 years are included in the economic analyses that follow, as recommended by KDOT and SDDOT, respectively.

The times to first repair for bridge decks with different corrosion protection systems tested in this study, based on the corrosion initiation time and the time to cracking after corrosion initiation, are listed in Table 5.7. The recommended time to first repair for a bridge reinforced with epoxy-coated steel or conventional reinforcement, obtained from state maintenance engineers, is also shown in Table 5.7. The time to first repair for a bridge deck with conventional reinforcement based on an analysis of the laboratory results (12 years) is similar to estimates provided by bridge maintenance engineers (10 or 25 years). The time to cracking after corrosion initiation based on the corrosion rate of epoxy-coated and stainless steel clad reinforcement are omitted from the table for reasons just described.

Table 5.7 – Time to first repair for bridge decks containing different reinforcement

Steel designation	Average corrosion rate (μm/yr)	Total corrosion loss to crack concrete (μm)	Corrosion initiation time (yrs)	Time to cracking after corrosion initiation based on corrosion rate (yrs)	Time to first repair, based on corrosion rate or adhesion loss (yrs)
Conv.	2.3	25	2.0	10.3	10** 12* 25**
ECR	2.3	-	2.0	-	35** 40** >75*
SMI	0.0015	25	75+	-	>75*

*Time to first repair based on an analysis of lab results
**Time to first repair based on estimation by bridge management engineers

5.6.2 Cost Effectiveness

Cost effectiveness is evaluated using a typical 8.5 in. bridge deck containing conventional, epoxy-coated, or stainless steel clad reinforcement. The costs and design assumptions are described in Section 4.6.2.

Cost estimates for bridge decks containing conventional steel are based on the times to first repair calculated from the lab results, 12 years, as well as estimates provided by SDDOT (Gilsrud 2007), 10 and 25 years. Cost estimates for bridge decks containing epoxy-coated steel are obtained using values of 35, 40, and 75 years for the initial life. In all cases, additional repairs are based on 25-year cycles for the 75-year service life used in this analysis.

Cost effectiveness is estimated based on the present value of the costs for each of the bridge decks using discount rates of 2, 4, and 6%. The present value of repair and replacement costs is calculated using Eq. (5.4).

$$P = F \times (1+i)^{-n} \tag{5.4}$$

where P = present worth, F = cost of repair or replacement, i = discount rate (%/100), and n = time to repair or replacement (in years).

Table 5.8 summarizes the repair schedules and cost estimates for the reinforcement options evaluated. The lowest cost for all discount rates, $186/yd^2, is obtained for the bridge deck containing epoxy-coated reinforcement, based on the assumption that no repairs will be required during the 75-year service life. The cost for using conventional steel ranges from $461/yd^2 to $649/yd^2 based on a 2% discount rate. This is much more than the costs calculated for epoxy-coated reinforcement when the first repair is needed at 40 and 35 years, $399 and $421/yd^2, respectively. The present cost of using stainless steel clad reinforcement is $250/yd^2 at all discount rates, which exceeds only the $186/yd^2 "no repairs" cost for epoxy-coated reinforcement. The possibility of no repairs over 75-year service life, however, is generally discounted because of expected increased corrosion for epoxy-coated bars resulting from the loss of adhesion between the epoxy and the steel in concrete that is exposed to moisture (Sagues et al. 1994, Smith and Virmani 1996), and the best current estimate of the time to first repair for bridge decks containing epoxy-coated reinforcement is 40 years, which is based on the current performance of bridges in the region.

Table 5.8 – Cost estimates and repair schedules for bridge decks containing conventional, epoxy-coated, and stainless steel clad reinforcement

Reinforcement in deck	New cost ($/yd^2)	Repair 1 cost ($/yd^2)	Time to repair 1 (years)	Repair 2 cost ($/yd^2)	Time to repair 2 (years)	Repair 3 cost ($/yd^2)	Time to repair 3 (years)	Present value of costs at 2% ($/yd^2)	Present value of costs at 4% ($/yd^2)	Present value of costs at 6% ($/yd^2)
Conventional – Harsh environment	$175	$292	10	$292	35	$292	60	$649	$474	$384
Conventional- Low lab result	$175	$292	12	$292	37	$292	62	$631	$451	$361
Conventional – Arid environment	$175	$292	25	$292	50			$461	$325	$258
Epoxy-coated	$186	$292	35	$292	60			$421	$288	$233
	$186	$292	40	$292	65			$399	$270	$221
	$186							$186	$186	$186
Stainless steel clad	$250							$250	$250	$250

Thus, the bridge deck containing stainless steel clad reinforcement appears to be the most cost-effective option when compared with bridge decks containing conventional or epoxy-coated steel (time to first repair of 40 or less years or less) for a discount rate of 2%. At this rate, the present value of the savings when using stainless steel clad reinforcement is $149/yd^2 ($399/yd^2 – $250/yd^2) compared to the initial premium for using stainless steel clad reinforcement over epoxy-coated reinforcement of $64/yd^2 ($250/yd^2 – $186/yd^2). The most economical option, however, varies as different discount rates are considered. The same comparison at a discount rate of 4% shows that bridge decks containing stainless steel clad reinforcement (present value of $250/yd^2 at all discount rates) are most economical, followed by decks with epoxy-coated steel with 40 and 35 years to first repair (present value of $270/yd^2 and $288/yd^2, respectively).

Results using a discount rate of 6% show that decks with epoxy-coated reinforcement with a time to initial repair of 40 years are most economical (present value of $221/yd^2), followed by decks using epoxy-coated steel with 35 years to initial repair (present value of $233/yd^2), and then stainless steel clad reinforcement (present value of $250/yd^2).

As this analysis demonstrates, the reinforcing system of choice based on the present value of direct costs will be strongly influenced by the discount rate, which for most states is between 2 and 4%. In this range, stainless steel clad reinforcement is the most cost-effective system.

Direct costs, of course, do not present the whole picture. A primary benefit of using stainless steel clad reinforcement is the elimination of corrosion repair for a bridge deck over its life, which provides significant savings of time and money to the traveling public, typically considered to be indirect costs. In 2002, the Federal Highway Administration estimated that indirect user costs due to traffic delays and lost productivity caused by corrosion of highway bridges may be ten times as much as direct costs (Yunovich el at. 2002). These indirect user costs are not included in the current cost analysis. If they were considered, however, stainless steel clad reinforcement would be the system of choice and is, thus, recommended for use as a reinforcing system for reinforced concrete bridge decks.

5.7 MMFX CORROSION POTENTIAL TESTS

The corrosion potentials of conventional (Conv.) and MMFX reinforcement were compared in simulated pore solution at NaCl molal ion concentrations of 0.2, 0.4, 0.5, 0.6, 0.7, 1.0, 1.6, and 6.04. Three bare bars were tested for each concentration. The solution was changed every five weeks to maintain the pH. The corrosion potentials were taken with respect to a saturated calomel electrode (SCE). Potentials more negative than –0.275 V indicate that the steel is corroding. The average results are shown in Figures 5.43 through 5.50.

The tests show that the corrosion potentials for N2 and MMFX steels are similar, and based on corrosion potential, there appears to be no distinction between the two steels as a function of chloride concentration.

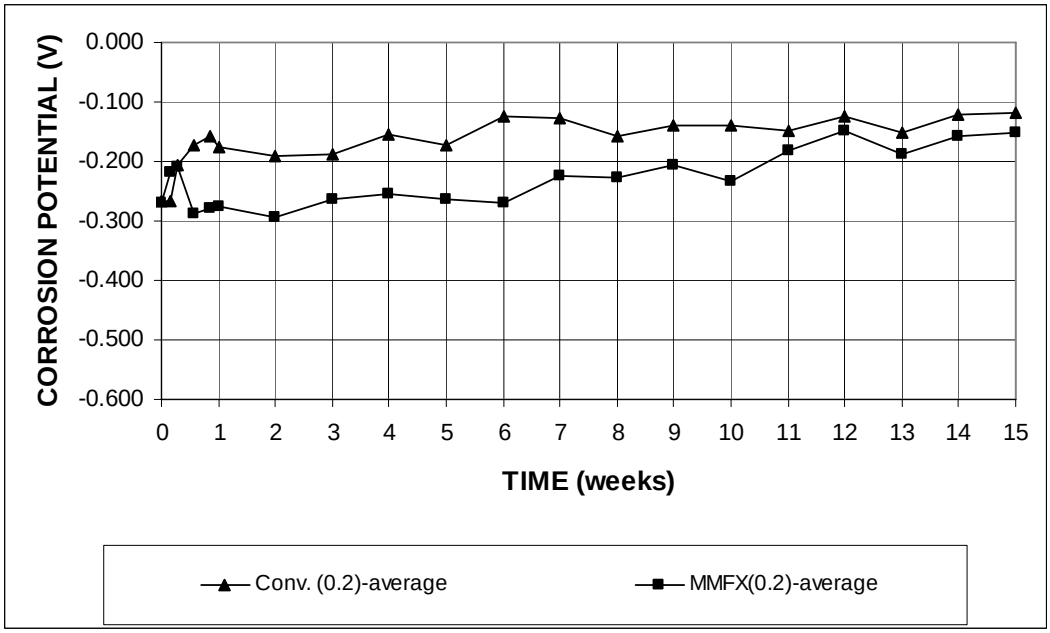

Figure 5.43 – Corrosion potential vs. saturated calomel electrode. Conventional and MMFX steel in simulated pore solution with 0.2 m ion NaCl.

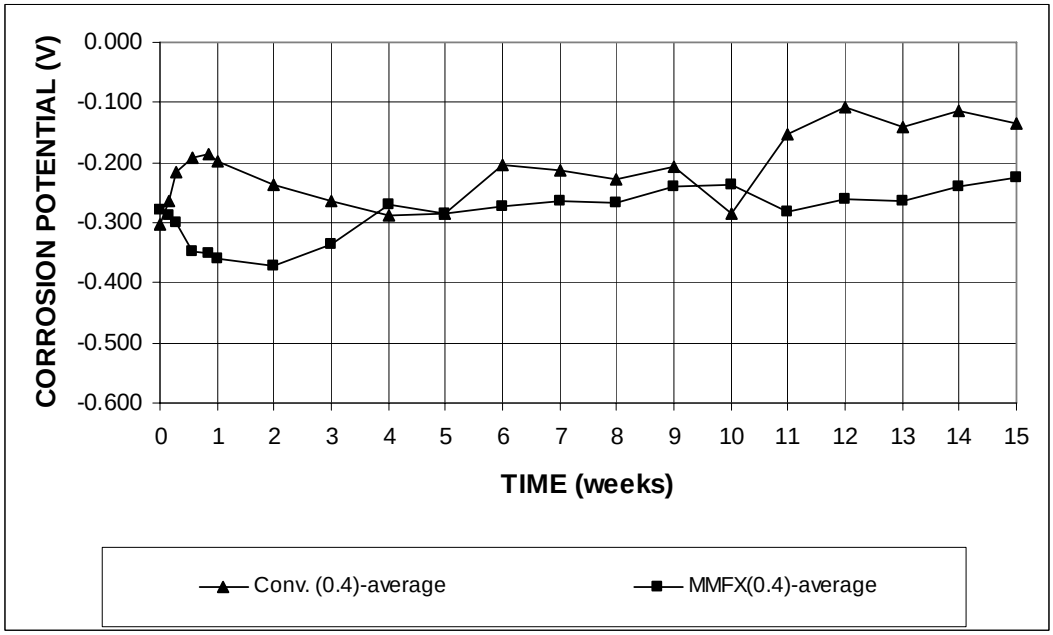

Figure 5.44 – Corrosion potential vs. saturated calomel electrode. Conventional and MMFX steel in simulated pore solution with 0.4 m ion NaCl.

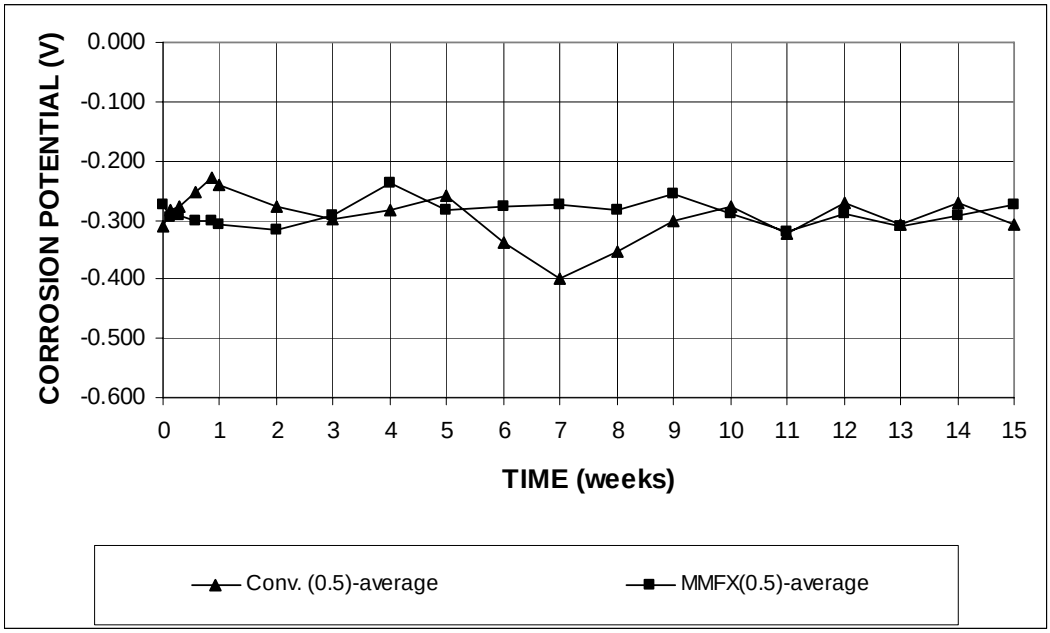

Figure 5.45 – Corrosion potential vs. saturated calomel electrode. Conventional and MMFX steel in simulated pore solution with 0.5 m ion NaCl.

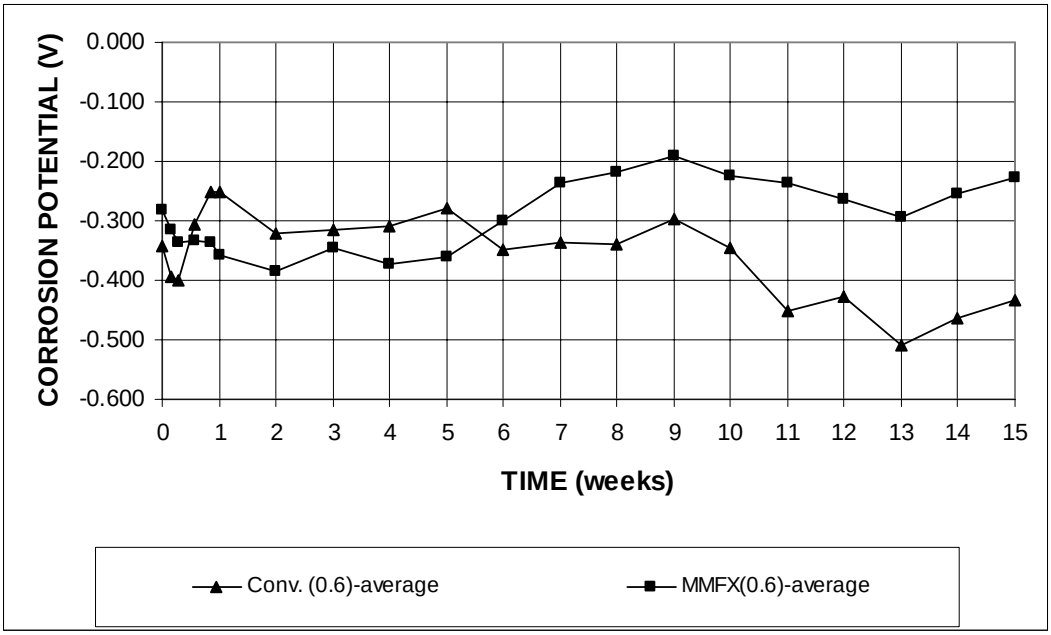

Figure 5.46 – Corrosion potential vs. saturated calomel electrode. Conventional and MMFX steel in simulated pore solution with 0.6 m ion NaCl.

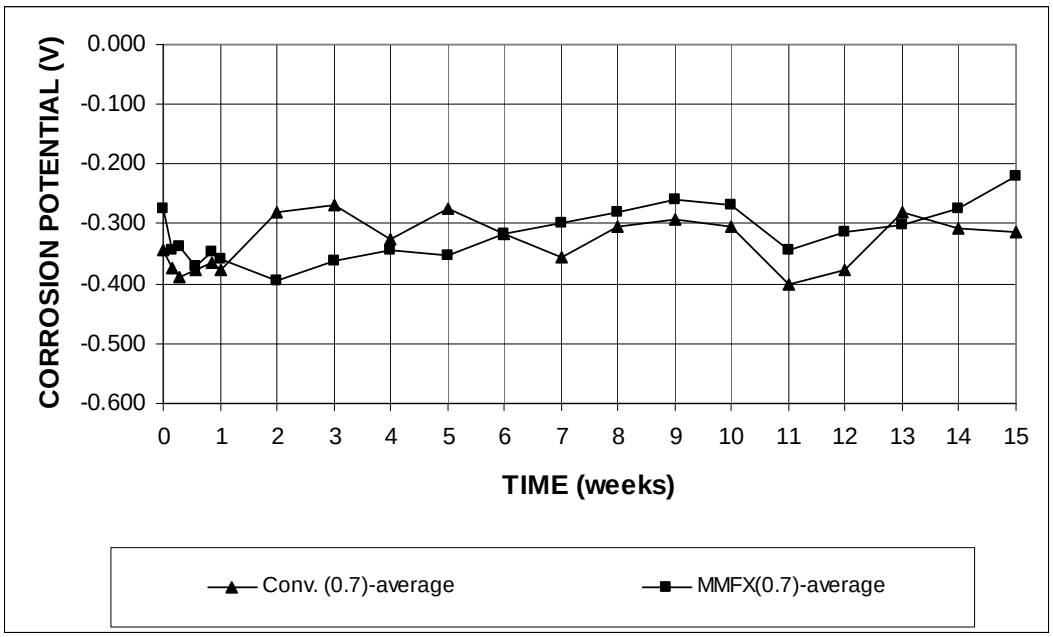

Figure 5.47 – Corrosion potential vs. saturated calomel electrode. Conventional and MMFX steel in simulated pore solution with 0.7 m ion NaCl.

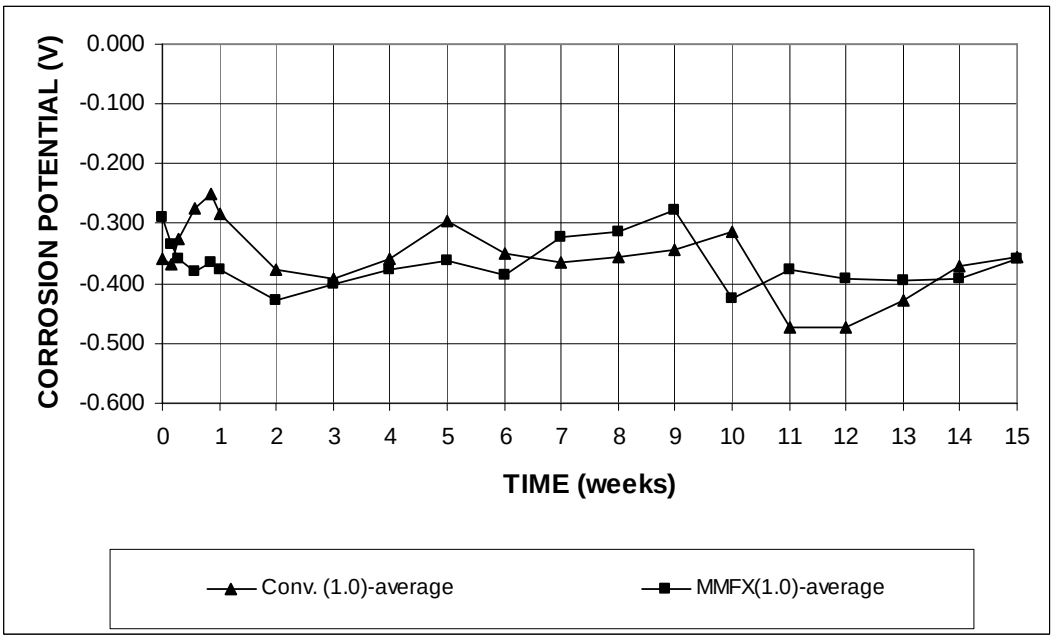

Figure 5.48 – Corrosion potential vs. saturated calomel electrode. Conventional and MMFX steel in simulated pore solution with 1.0 m ion NaCl.

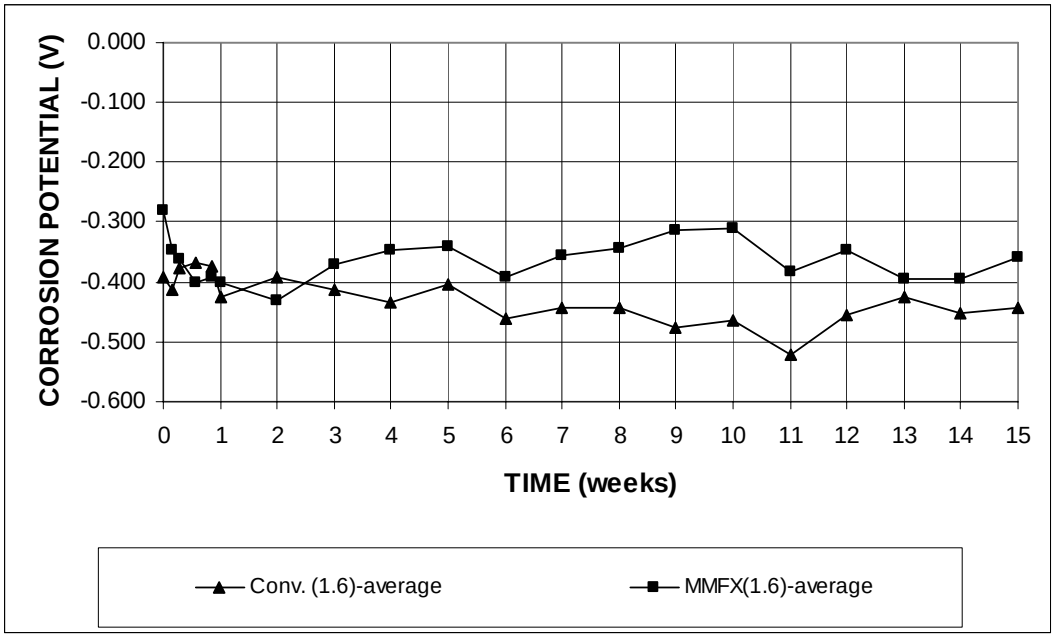

Figure 5.49 – Corrosion potential vs. saturated calomel electrode. Conventional and MMFX steel in simulated pore solution with 1.6 m ion NaCl.

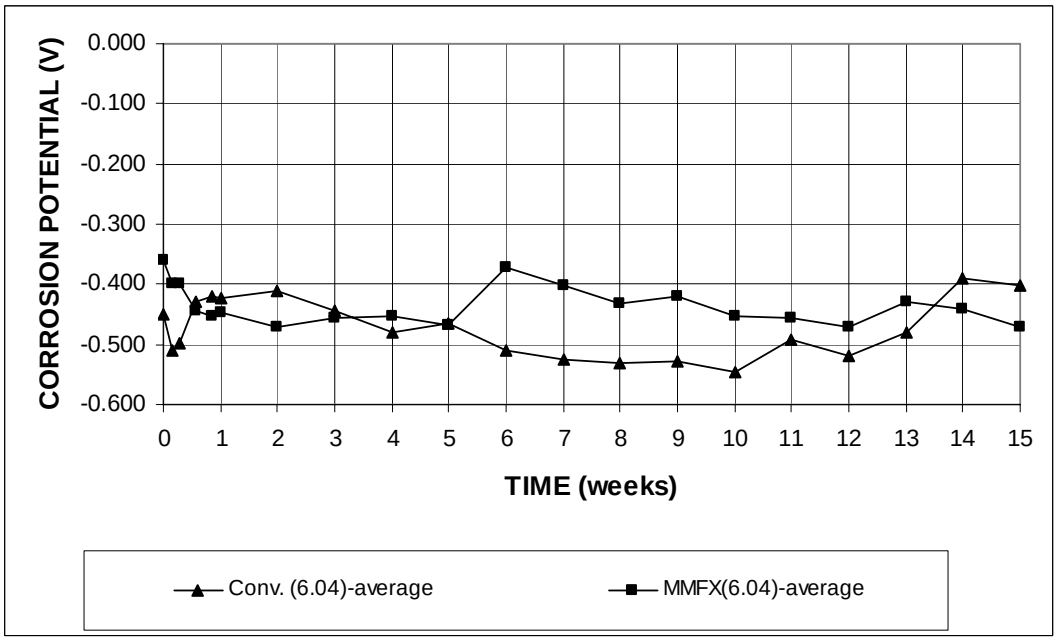

Figure 5.50 – Corrosion potential vs. saturated calomel electrode. Conventional and MMFX steel in simulated pore solution with 6.04 m ion NaCl.

5.8 MMFX CRITICAL CHLORIDE CORROSION THRESHOLD

The critical chloride thresholds for reinforcing steels in this study are determined based on direct analysis of the chloride contents adjacent to the steel in modified Southern Exposure

(MSE) and beam specimens (B). The modified Southern Exposure and beam specimens are used to obtain a high number chloride samples for a single bar. As described in Section 4.8, each top mat bar in the modified SE specimens is connected to two bottom mat bars across a 10-ohm resistor. Ten samples are taken for each of the top bars. The beam specimens have the same dimensions as the cracked beam specimens but without the simulated crack. Twenty samples are taken for the single top bar. The number of chloride samples taken for the modified SE and beam specimens has been statistically justified by Ji et al. (2005).

As stated in Section 4.8, corrosion initiation is considered to have occurred for the specimens when either the corrosion potential of the top mat of steel first shifts to a value more negative than –0.350 V with respect to a copper-copper sulfate electrode (CSE) or the corrosion rate first reaches a value greater than or equal to 0.3 μm/yr. The alternative requirement for the corrosion rate in this criterion increases the reliability of identifying corrosion initiation since active corrosion can occur when corrosion potentials are more positive than –0.350 V with respect to CSE, as will be described below.

The critical thresholds for the modified SE and the beam specimens are presented in Tables 5.9 and 5.11 for conventional steel (Conv.), and Tables 5.10 and 5.12 for MMFX steel, respectively.

Modified Southern Exposure specimens – Six modified Southern Exposure specimens were used to determine the chloride threshold of conventional steel and MMFX steel. In these specimens, the two top bars were monitored individually. Chloride samples (10 samples in most cases) were taken at the initiation of corrosion for each bar (except for one bar in Conv. specimens 1 and 2 and MMFX specimen 3, which were subjected to trial sampling using other methods, and the two bars in MMFX specimen 5 that were contaminated from the outside). The average value from the individual samples is regarded as the chloride threshold for the bar.

The times-to-initiation, corrosion rates, corrosion potentials, and individual and average critical chloride contents on a water-soluble basis for conventional steel (10 bars) are presented in Table 5.9.

The conventional steel bars had times-to-initiation ranging from 8 to 20 weeks, with corrosion rates ranging from 0.35 to 3.51 μm/yr (in the latter case, the corrosion rate was 0.05 μm/yr one week before reaching 3.51 μm/yr; the jump in the corrosion rate reflects the nature of the steel corrosion) and corresponding corrosion potentials ranging from –0.273 to –0.421 V with respect to CSE. The average critical chloride thresholds for the 10 bars are 1.56, 2.21, 1.20, 1.99, 0.91, 1.05, 1.54, 0.90, 2.07, and 1.97 lb/yd^3, with an average of 1.54 lb/yd^3.

For each of the 10 conventional bars, the individual chloride contents range from lows of 0.69, 0.94, 0.63, 1.01, 0.58, 0.60, 0.73, 0.65, 1.33, and 1.13 lb/yd^3 to highs of 2.71, 4.78, 2.58, 3.65, 1.37, 1.67, 2.39, 1.60, 3.21, and 3.02 lb/yd^3, respectively. The coefficients of variation for the individual bars range from 0.28 to 0.70. The scatter in the individual results is likely due to the non-homogeneity of concrete, which causes the uneven ingress of chlorides.

The times-to-initiation, corrosion rates, corrosion potentials, and individual and average critical chloride thresholds on a water-soluble basis for MMFX reinforcing steel (9 bars) are presented in Table 5.10.

The times-to-initiation for MMFX steel ranged from 17 to 39 weeks, with corrosion rates ranging from 0.01 to 2.00 μm/yr (the corrosion rate was 0.02 μm/yr one week before reaching 2.00 μm/yr) and corrosion potentials ranging from –0.333 to –0.460 V with respect to CSE. The average critical chloride thresholds for the MMFX bars were 9.01, 5.08, 8.08, 9.16, 5.45, 5.00, 4.48, 4.64, and 5.24 lb/yd^3, with an average of 6.24 lb/yd^3, four times the value for conventional steel.

Table 5.9 – Critical chloride thresholds for conventional steel based on the analysis of the chloride content in modified Southern Exposure (MSE) specimens

Specimens[a]	Bar No.	Initiation time (weeks)	Corrosion rate (μm/yr)	Corrosion potentials (V)	Water soluble Cl^- (lb/yd^3)			
					1	2	3	4
MSE-Conv.-1	1[b]	-	-	-	-	-	-	-
	2	8	0.84	-0.273	0.69	1.51	1.68	2.71
MSE-Conv.-2	1[b]	-	-	-	-	-	-	-
	2	12	2.89	-0.396	0.94	2.39	1.28	4.78
MSE-Conv.-3	1	15	1.96	-0.404	0.69	0.82	0.63	0.82
	2	14	1.79	-0.380	3.65	1.70	1.01	1.32
MSE-Conv.-4	1	9	1.76	-0.379	0.77	1.03	0.85	0.86
	2	9	3.51	-0.421	0.80	1.04	1.67	0.60
MSE-Conv.-5	1	14	0.82	-0.332	1.70	2.33	2.39	1.64
	2	9	0.35	-0.280	0.87	0.84	0.65	1.03
MSE-Conv.-6	1	20	1.52	-0.361	1.51	1.38	1.83	2.64
	2	17	1.84	-0.379	2.71	1.83	1.83	3.02

Specimens[a]	Bar No.	Water soluble Cl^- (lb/yd^3)						Average (lb/yd^3)	SD[c]	COV[c]
		5	6	7	8	9	10			
MSE-Conv.-1	1[b]	-	-	-	-	-	-	-	-	-
	2	1.20	-	-	-	-	-	1.56	0.74	0.48
MSE-Conv.-2	1[b]	-	-	-	-	-	-	-	-	-
	2	1.64	-	-	-	-	-	2.21	1.54	0.70
MSE-Conv.-3	1	0.94	1.83	1.26	2.58	-	-	1.20	0.68	0.57
	2	2.27	-	-	-	-	-	1.99	1.04	0.52
MSE-Conv.-4	1	0.77	0.77	0.58	1.29	0.77	1.37	0.91	0.25	0.28
	2	0.77	1.02	0.84	1.38	0.77	1.63	1.05	0.38	0.36
MSE-Conv.-5	1	1.83	1.13	1.51	0.92	0.73	1.20	1.54	0.56	0.36
	2	0.69	0.87	0.73	0.73	1.60	0.94	0.90	0.27	0.31
MSE-Conv.-6	1	3.21	1.33	3.02	1.45	2.27	2.08	2.07	0.70	0.34
	2	2.83	1.13	1.16	1.32	2.20	1.70	1.97	0.69	0.35
						Average		1.54		

[a] MSE = modified Southern Exposure specimen
[b] The samples for the bar were not available because the specimen was subjected to trial sampling using other methods
[c] SD = standard deviation; COV = coefficient of variation

Table 5.10 – Critical chloride thresholds for MMFX steel based on the analysis of the chloride content in modified Southern Exposure (MSE) specimens

Specimens[a]	Bar No.	Initiation time (weeks)	Corrosion rate (μm/yr)	Corrosion potentials (V)	Water soluble Cl^- (lb/yd^3)			
					1	2	3	4
MSE-MMFX-1	1	23	0.50	-0.390	5.41	5.98	5.70	7.93
	2	17	0.60	-0.362	2.64	2.96	3.90	3.71
MSE-MMFX-2	1	23	0.41	-0.333	5.85	4.85	10.07	8.99
	2	28	0.01	-0.363	7.43	8.75	9.38	9.13
MSE-MMFX-3	1[b]	-	-	-	-	-	-	-
	2	17	1.95	-0.460	2.52	4.09	4.31	5.04
MSE-MMFX-4	1	30	0.57	-0.348	3.15	5.10	5.29	6.30
	2	29	2.00	-0.367	4.91	3.97	3.46	6.67
MSE-MMFX-5[c]	-	-	-	-	-	-	-	-
MSE-MMFX-6	1	26	1.20	-0.359	5.04	2.71	3.53	4.28
	2	39	0.68	-0.368	4.23	4.91	5.59	5.36

Specimens[a]	Bar No.	Water soluble Cl^- (lb/yd^3)						Average (lb/yd^3)	SD[d]	COV[d]
		5	6	7	8	9	10			
MSE-MMFX-1	1	9.82	10.26	11.08	11.52	10.58	11.77	9.01	2.52	0.28
	2	4.66	7.37	6.17	6.55	7.24	5.60	5.08	1.74	0.34
MSE-MMFX-2	1	10.65	-	-	-	-	-	8.08	2.59	0.32
	2	10.07	8.75	13.09	8.37	8.25	8.37	9.16	1.56	0.17
MSE-MMFX-3	1[b]	-	-	-	-	-	-	-	-	-
	2	5.73	7.55	6.23	8.18	5.04	5.79	5.45	1.66	0.30
MSE-MMFX-4	1	5.67	5.67	3.84	-	-	-	5.00	1.11	0.22
	2	5.10	2.14	2.64	6.48	5.60	3.78	4.48	1.54	0.34
MSE-MMFX-5[c]	-	-	-	-	-	-	-	-	-	-
MSE-MMFX-6	1	4.28	7.21	3.78	4.60	6.11	4.85	4.64	1.29	0.28
	2	5.21	5.67	6.80	5.89	3.10	5.59	5.24	1.00	0.19
						Average		6.24		

[a] MSE = modified Southern Exposure specimen
[b] The samples for the bar were not available because the specimen was subjected to trial sampling using other methods
[c] The specimen was contaminated from outside
[d] SD = standard deviation; COV = coefficient of variation

For each of the 9 bars, the individual chloride contents range from lows of 5.41, 2.64, 4.85, 7.43, 2.52, 3.15, 2.14, 2.71, and 3.10 lb/yd^3 to highs of 11.77, 7.37, 10.65, 13.09, 8.18, 6.30, 6.67, 7.21, and 6.80 lb/yd^3, respectively. The coefficients of variation for the individual bars range from 0.17 to 0.34, lower than exhibited by the individual bars for conventional steel, indicating a more even distribution of chlorides at higher chloride contents.

Beam specimens – As described in Section 4.8, three beam specimens (one bar in each specimen) were fabricated to determine the chloride threshold of both conventional steel and MMFX steel. At the initiation of corrosion, 20 chloride samples were taken from each specimen.

The times-to-initiation, corrosion rates, corrosion potentials, and individual and average critical chloride contents on a water-soluble basis are presented in Table 5.11 for conventional steel and Table 5.12 for MMFX steel.

Conventional steel had times-to-initiation ranging from 14 to 23 weeks, with an average corrosion rate of 1.12 μm/yr and an average corrosion potential of –0.365 V with respect to CSE. The average chloride threshold for all three specimens was 2.05 lb/yd^3, about one-third higher than obtained in modified SE specimens, 1.54 lb/yd^3. The individual chloride contents ranged from 0.95 to 4.36 lb/yd^3, with an average of 2.01 lb/yd^3 and a coefficient of variation of 0.40, for specimen 1, from 0.85 to 4.81 lb/yd^3, with an average of 2.08 lb/yd^3 and a coefficient of variation of 0.44, for specimen 2, and from 0.82 to 3.97 lb/yd^3, with an average of 2.07 lb/yd^3 and a coefficient of variation of 0.38, for specimen 3.

Table 5.12 shows that the times-to-corrosion for MMFX steel ranged from 26 to 51 weeks. At initiation, the average corrosion rate and corrosion potential were 0.93 μm/yr and –0.343 V, respectively. The average chloride threshold for the three specimens was 6.86 lb/yd^3, about 3.3 times the value for conventional steel. The individual critical chloride contents ranged from 6.48 to 10.51 lb/yd^3, with an average of 9.04 lb/yd^3 and a coefficient of variation of 0.14, for specimen 1, from 2.14 to 9.38 lb/yd^3, with an average of 4.98 lb/yd^3 and a coefficient of variation of 0.38, for specimen 2, and from 2.91 to 10.89 lb/yd^3, with an average of 6.56 lb/yd^3 and a coefficient of variation of 0.26, for specimen 3.

Table 5.11 – Critical chloride thresholds for conventional steel based on the analysis of the chloride content in beam (B) specimens

Specimens[a]	Sides[b]	Initiation time (weeks)	Corrosion rates (μm/yr)	Corrosion potentials (V)	Water soluble Cl^- (lb/yd^3)			
					1	2	3	4
B-Conv.-1	1	21	1.17	-0.358	1.51	2.46	1.26	2.27
	2				4.36	2.29	1.95	2.31
B-Conv.-2	1	23	1.17	-0.392	2.27	0.85	1.82	1.67
	2				1.13	2.71	2.71	2.77
B-Conv.-3	1	14	1.02	-0.344	2.27	1.04	1.89	2.77
	2				2.14	3.08	1.57	2.90

Specimens[a]	Sides[b]	Water soluble Cl^- (lb/yd^3)						Average (lb/yd^3)	SD[c]	COV[c]
		5	6	7	8	9	10			
B-Conv.-1	1	1.38	3.08	1.89	1.64	1.95	1.57	2.01	0.80	0.40
	2	1.45	3.02	0.95	1.40	2.20	1.21			
B-Conv.-2	1	1.30	1.36	1.48	1.54	1.36	1.54	2.08	0.92	0.44
	2	2.58	2.84	2.33	1.55	2.96	4.81			
B-Conv.-3	1	3.97	2.51	1.13	1.89	2.52	1.51	2.07	0.78	0.38
	2	2.20	0.82	1.20	2.58	1.89	1.57			
						Average		2.05		

[a] Beam specimens
[b] 10 chloride samples were taken for each side of the bar in one specimen
[c] SD = standard deviation; COV = coefficient of variation

Table 5.12 – Critical chloride thresholds for MMFX steel based on the analysis of the chloride content in beam (B) specimens

Specimens[a]	Sides[b]	Initiation time (weeks)	Corrosion rates (μm/yr)	Corrosion potentials (V)	Water soluble Cl^- (lb/yd^3)			
					1	2	3	4
B-MMFX-1	1	51	1.02	-0.360	7.30	9.25	9.63	8.61
	2				9.95	9.90	10.51	10.12
B-MMFX-2	1	26	1.22	-0.341	2.14	2.46	3.15	3.12
	2				3.84	4.78	5.67	5.54
B-MMFX-3	1	36	0.56	-0.329	6.42	6.30	6.78	8.03
	2				8.37	6.17	4.60	5.92

Specimens[a]	Sides[b]	Water soluble Cl^- (lb/yd^3)						Average (lb/yd^3)	SD[c]	COV[c]
		5	6	7	8	9	10			
B-MMFX-1	1	9.32	10.39	10.39	7.22	7.30	8.12	9.04	1.26	0.14
	2	8.08	9.95	9.63	8.31	10.26	6.48			
B-MMFX-2	1	5.29	2.71	3.78	4.09	5.92	5.29	4.98	1.89	0.38
	2	5.16	5.73	7.62	9.38	7.49	6.56			
B-MMFX-3	1	7.35	5.23	5.23	7.81	10.89	4.97	6.56	1.74	0.26
	2	5.35	8.00	8.31	2.91	6.54	6.06			
						Average		6.86		

[a] Beam specimens
[b] 10 chloride samples were taken for each side of the bar in one specimen
[c] SD = standard deviation; COV = coefficient of variation

Summary – The critical chloride threshold on a water-soluble basis for conventional steel ranges from 0.90 to 2.21 lb/yd^3, with an average of 1.54 lb/yd^3 for the modified SE specimens, and from 2.01 to 2.08 lb/yd^3, with an average of 2.05 lb/yd^3 for the beam specimens.

The average chloride threshold for all 83 samples from the modified SE specimens and 60 samples from the beam specimens will be used as the chloride threshold for conventional steel in the service life prediction of bridge decks. The value, equal to $(1.54 \times 83 + 2.05 \times 60)/143 = 1.75$ lb/yd^3, is close to that obtained in earlier studies (1.0 to 2.0 lb/yd^3 on a total chloride basis).

The critical chloride threshold on a water-soluble basis for MMFX steel ranges from 4.48 to 9.16 lb/yd^3, with an average of 6.24 lb/yd^3 for the modified SE specimens, and from 4.98 to 9.04 lb/yd^3, with an average of 6.86 lb/yd^3 for the beam specimens.

The average chloride threshold for 82 samples from the modified SE specimens and 60 samples from the beam specimens will be used as the chloride threshold for MMFX steel in the service life prediction of bridge decks. The value, equal to $(6.24 \times 82 + 6.86 \times 60)/142 = 6.50$ lb/yd^3, matches values obtained in earlier studies [6.4 lb/yd^3 (Clemeña 2003) and 7.7 lb/yd^3 (Trejo and Pillai 2003) on a total chloride basis].

5.9 MMFX LIFE EXPECTANCY AND COST EFFECTIVENESS

5.9.1 Life Expectancy

Because no field experience is available on the time to first repair of bridge decks containing MMFX reinforcement, analyses from laboratory specimens (Ji, Darwin, and Browning 2005) and crack surveys (Miller and Darwin 2000, Lindquist et al. 2005) are used to estimate the time to first repair and life cycle costs. The estimates obtained for time to corrosion initiation and time to cracking are described in this section.

Time to Corrosion Initiation – The critical chloride threshold based on the average values from direct chloride analyses of Modified Southern Exposure and beam specimens is 6.50 lb/yd^3, as described in Section 5.8, giving a time to corrosion initiation of 12.7 years, as described in Section 5.6 (see Table 5.6).

Time to Cracking – The time to cracking for bridge decks containing MMFX reinforcement, corresponding to the time required to attain a total corrosion loss of about 25 μm, is determined using corrosion rates obtained from the Southern Exposure and cracked beam tests.

As described in Section 5.6 for conventional steel reinforcement, corrosion rates were determined for MMFX reinforcement based on corrosion losses calculated between the time of corrosion initiation (when the total corrosion losses reach 0.3 μm for Southern Exposure specimens and at 20 weeks for cracked beam specimens) to the end of the test. Figures 5.51a and 5.51b show the corrosion losses calculated for individual Southern Exposure and cracked beam specimens, respectively, containing MMFX steel (Ji et al. 2005). The average corrosion rates for these specimens are presented in Table 5.13. As described in Section 5.6, a corrosion rate equal to one-half of the average rate in the Southern Exposure and cracked beam tests is used to estimate service life. For MMFX steel, this value is [(2.54+2.44)/2]/2 = 1.25 μm/yr. Using this rate, the time required for a total corrosion loss of 25 μm, equal to the estimated time required for the corrosion products to crack the concrete after corrosion initiation, is estimated to be 20 years.

Table 5.13 – Average corrosion rate (μm/yr) after corrosion initiation for bench-scale tests based on total area for MMFX steel (Ji et al. 2005)

Steel Designation	Specimen						Average*	Standard Deviation
	1	2	3	4	5	6		
Southern Exposure (SE) Test								
MMFX	2.91	2.29	3.22	1.73	2.31	2.75	2.54	0.530
Cracked Beam (CB) Test								
MMFX	2.98	2.49	1.97	3.24	2.70	1.27	2.44	0.719

*SE corrosion rates are taken as the average slope of the corrosion loss graph between the corrosion initiation and the corrosion loss at 96 weeks (76 weeks for specimen 2).
CB corrosion losses are taken as the average slope of the corrosion loss graph between week 20 and week 96.

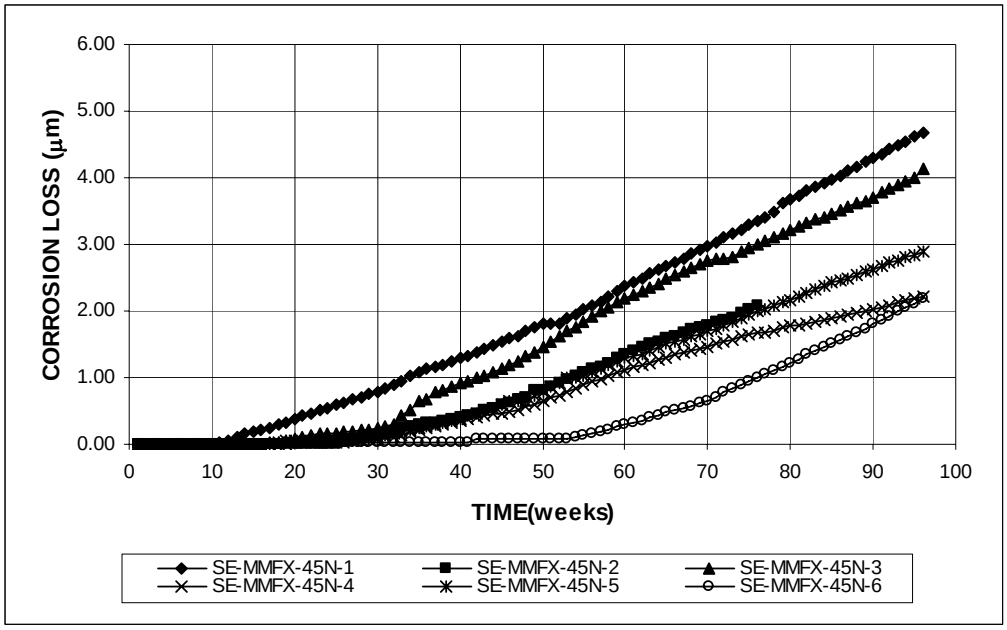

Figure 5.51a – Southern Exposure Test. Corrosion loss (based on total area) versus time of individual specimens containing MMFX steel (Ji et al. 2005)

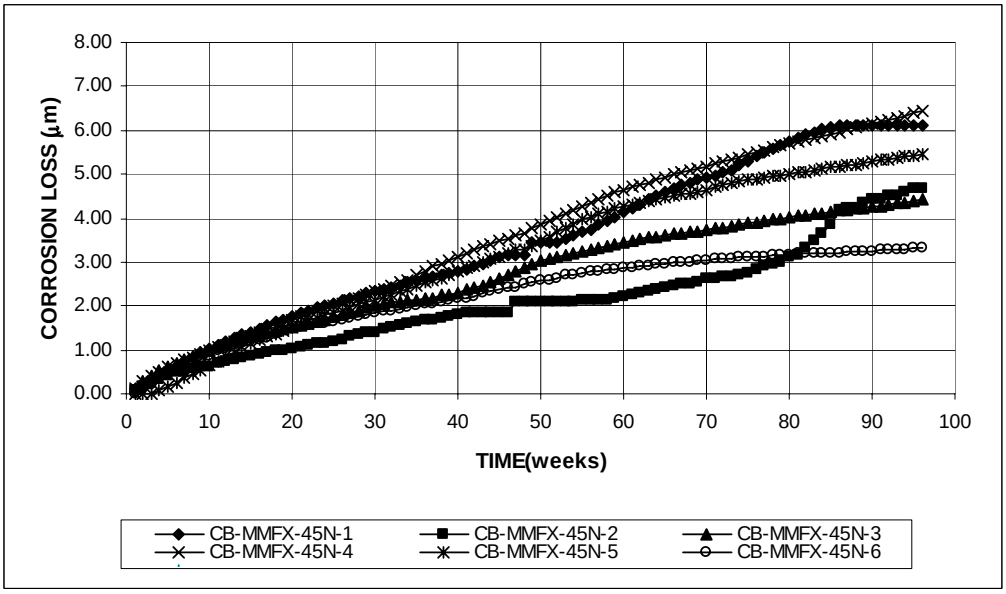

Figure 5.51b – Cracked Beam Test. Corrosion loss (based on total area) versus time of individual specimens containing MMFX steel (Ji et al. 2005)

Time to first repair – The time to first repair for the prototype bridge deck is estimated by adding the time to corrosion initiation to the time to cracking after corrosion initiates. For a bridge deck containing MMFX steel, the estimated time to corrosion initiation is 12.7 years, and the time to cracking after corrosion initiates is 20 years, giving a time to first repair of approximately 13 + 20 = 33 years, as shown in Table 5.14. This compares to a value of 30 years

Table 5.14 – Time to first repair for bridge decks containing MMFX reinforcement

Steel designation	Average corrosion rate (μm/yr)	Total corrosion loss to crack concrete (μm)	Corrosion initiation time (yrs)	Time to cracking after corrosion initiation based on corrosion rate (yrs)	Time to first repair, based on corrosion rate or adhesion loss (yrs)
MMFX	1.25	25	12.7	20	33

predicted earlier by Darwin et al. (2002) in SD 2201-5. Values for the other steels evaluated in this study are given in Table 5.7.

5.9.2 Cost Effectiveness

Cost effectiveness is evaluated using an 8.5-in. bridge deck containing MMFX reinforcement using the procedures described in Section 5.6.2. The costs and design assumptions are described in Section 4.9. Estimates of cost effectiveness are based on the present value of the costs for each of the bridge decks using discount rates of 2, 4, and 6%. The present value of repair and replacement costs is calculated using Eq. (5.4).

Table 5.15 includes the present worth values for bridge decks constructed using MMFX reinforcement. Two sets of values are shown based on the two possible costs of MMFX reinforcement used in the calculations described in Section 4.9.

Table 5.15 – Cost estimates and repair schedules for bridge decks containing MMFX reinforcement

Reinforcement in deck	New cost ($/yd^2)	Repair 1 cost ($/yd^2)	Time to repair 1 (years)	Repair 2 cost ($/yd^2)	Time to repair 2 (years)	Present value of costs at 2% ($/yd^2)	Present value of costs at 4% ($/yd^2)	Present value of costs at 6% ($/yd^2)
MMFX	$197	$292	33	$292	58	$441	$307	$250
	$206	$292	33	$292	58	$450	$316	$259

The present worth of costs for decks containing MMFX steel for a 2% discount range from $441/yd^2 to $450/yd^2 (Table 5.15). These values exceed the costs of all other systems except for conventional steel in a harsh or arid environment ($649/yd^2 or $461/yd^2) or conventional steel based on the results of laboratory specimens ($631/yd^2), as shown in Table 5.8. In comparison, the present value costs for bridges with stainless steel clad or epoxy-coated steel reinforcement range from $250/yd^2 to $421/yd^2 at a 2% discount rate. The order of cost effectiveness (the least effective being using conventional steel in a harsh environment, followed by conventional steel based on laboratory corrosion rates, conventional steel in an arid environment, and then MMFX reinforcement) is the same when using a discount rate of 4%, but using MMFX is approximately as cost effective as using conventional steel in an arid environment when using a discount rate of 6%. In addition, the time to first repair for a bridge deck reinforced with MMFX steel is estimated to be 33 years, which is shorter than the times estimated for a bridge deck reinforced with epoxy-coated or stainless-steel clad reinforcement.

A shorter time to first repair indicates that higher indirect user costs would also be incurred in the economic evaluation. Based on this analysis, it is not recommended that MMFX reinforcement be used as a replacement for epoxy-coated reinforcement as a corrosion-protection system.

5.10 CONCLUSIONS

The following conclusions are based on the test results and analyses presented in this report.

1. The No. 5 and No. 6 SMI-316 SC bars tested in this study satisfy the mechanical properties specified by ASTM A 615 and can be used as replacements for conventional No. 5 and No. 6 Grade 60 reinforcing bars. The steel, however, is not currently in production.

2. A metallurgical bond is obtained between the 316LN stainless steel cladding and the mild steel core of the SMI-316 SC bars. The average cladding thickness varied between 26 and 45 mils (0.026 and 0.045 in.). The minimum thickness measured at any location was 6 mils.

3. SMI-316 SC bars should be fabricated (bent) using protective equipment similar to that used for epoxy-coated bars. Without protection, there is significant potential for damage to the cladding. The minimum measured thickness of the cladding, however, is adequate for normal handling during construction.

4. The corrosion rate of SMI-316 SC reinforcement is less than 0.4% or 1/250 of that for conventional reinforcement. Total corrosion losses for SMI-316 SC bars were insignificant in the tests.

5. Corrosion losses for damaged epoxy-coated reinforcement were below those for damaged SMI-316 SC reinforcement. The difference results from the high resistivity of the epoxy coating, which limits the bar area that can serve as a cathode, while the full area of the SMI-316 SC bars can serve as a cathode.

6. Epoxy-filled plastic caps protect the cut ends of SMI-316 SC reinforcement from corrosion.

7. Epoxy-coated reinforcement embedded in concrete can undergo a significant loss of bond between the epoxy and the reinforcing steel when subjected to high moisture and high chloride concentrations. Corrosion products form under the coating, although total corrosion losses are low compared to those observed for conventional reinforcement.

8. Similar corrosion products are deposited on conventional reinforcing steel and on the mild steel core at damaged regions of SMI-316 SC steel.

9. Bridge decks containing SMI-316 SC reinforcing steel will not require repair due to corrosion-induced concrete cracking during a 75-year service life. In comparison, conventional bridge decks require repair 10 to 25 years after the construction, depending on exposure conditions. Bridge decks containing epoxy-coated reinforcement will not require repair due to corrosion-induced concrete cracking during a 75-year service life but are estimated to require

repair approximately 40 years after construction due to corrosion near damaged areas where the bond between the epoxy and reinforcing steel has been lost.

10. Bridge decks containing SMI-316 SC reinforcing steel are cost-effective compared to bridge decks containing epoxy-coated reinforcement.

11. The critical chloride corrosion threshold for MMFX Microcomposite steel is three to four times the corrosion threshold for conventional reinforcement. The corrosion rate for MMFX steel is approximately one-half that of conventional steel.

12. Bridge decks containing MMFX Microcomposite reinforcing steel will require repair due to corrosion-induced concrete cracking approximately 33 years after construction.

13. Bridge decks containing MMFX Microcomposite steel do not appear to be cost-effective when compared to bridge decks containing epoxy-coated reinforcement.

CHAPTER 6

IMPLEMENTATION RECOMMENDATIONS

The evaluation and test results presented in this report lead to the following implementation recommendations.

1. SMI-316 SC stainless steel clad reinforcement is recommended as a cost-effective direct replacement for epoxy-coated reinforcement. Cut ends of the bars should be protected with a system such as plastic caps filled with epoxy and the bars should be protected from damage to the cladding during bending operations.

This recommendation is based on observations that SMI-316 SC stainless steel clad reinforcement corrodes at a negligible rate when subjected to high moisture and chloride conditions (Section 5.4). Based on field test results for chlorides in bridge decks, it is highly unlikely that the critical chloride corrosion threshold of the stainless steel cladding will be reached in less than 100 years in bridge decks. The corrosion performance of SMI-316 SC steel will equal or exceed that of epoxy-coated reinforcement as long as the ends of the bars are protected, such as with plastic caps filled with epoxy, and steps are taken, as they are for epoxy-coated reinforcement, to protect the bars from damage to the cladding during fabrication (bending). Normal handling will not result in damage to the cladding. As discussed in Chapter 2, acid pickling to remove mill scale and other oxidation products will be needed to achieve the corrosion resistance obtained in this study by the SMI-316 SC stainless steel clad bars. The initial cost for construction with SMI-316 SC reinforcement is higher than that for epoxy-coated or conventional reinforcement, but because it requires no repair, the lifetime cost is significantly less (Section 5.6).

2. MMFX Microcomposite reinforcing steel should not be used as a direct replacement for epoxy-coated reinforcement without the use of a supplementary corrosion protection system. Use of the material in its current form is not recommended for reinforced concrete bridge decks in South Dakota.

This recommendation matches that reported in SD 2001-5 (Darwin et al. 2002) and is based on observations that, while MMFX reinforcing steel has a higher corrosion threshold and corrodes at a lower rate than conventional reinforcement, (1) its corrosion-resistance properties are not superior to that of epoxy-coated reinforcement (Sections 5.8 and 5.9), and (2) bridge decks constructed with MMFX reinforcing steel will have a higher first cost, a shorter life expectancy, and a higher lifetime cost than bridge decks constructed with epoxy-coated reinforcement (Section 5.9).

CHAPTER 7

ANALYSIS OF RESEARCH BENEFITS

The benefits achieved by the research described in this report are measured based on the estimated life expectancy and cost-effectiveness of bridges in South Dakota. As described in Chapter 5, bridge decks constructed using stainless steel clad reinforcement will not require repair during a 75-year service life, compared to multiple repairs required for bridge decks reinforced with conventional or epoxy-coated reinforcement. For an expected time to first repair of 40 years for a deck containing epoxy-coated reinforcement (the current standard in South Dakota), the present value cost for that deck is $\$399/yd^2$, compared to a present cost of $\$250/yd^2$ for the same bridge deck reinforced with stainless steel clad reinforcement. Of the $\$399/yd^2$ for a deck containing epoxy-coated reinforcement, $\$213/yd^2$ represents the present value of the repair costs at a 2% discount rate. A premium of $\$64/yd^2$ (the difference between the construction cost of a deck with stainless steel clad reinforcement and one with epoxy-coated reinforcement) will allow the full cost of repair to be saved. The payoff is 3.3 to 1. For a bridge deck inventory of 1.2 million yd^2, with new construction proceeding at a rate of 8500 yd^2/year (Gilsrud 2007), full implementation of stainless steel clad reinforcement, assuming that it can be produced, could produce annual savings of approximately $1.3 million.

If the cost to the traveling public is included, at the usual multiplier of 10 to 1, the annual savings would be nearly $14 million, including both the direct and indirect costs.

Based on initial construction cost and present value cost for the life of the bridge at a 2% discount rate, the use of MMFX reinforcement would result in cost increases of $\$11/yd^2$ and $\$42/yd^2$, respectively, for bridge decks constructed in South Dakota. Assuming that the steel is not implemented based on current research, this amounts to a savings in direct costs for new bridge construction of $93,500 per year and a total savings based on the present value of new construction and repair costs, of $357,000 per year.

REFERENCES

AASHTO T 260-97 (1997). "Standard Test Method for Sampling and Testing for Chloride Ion in Concrete and Concrete Raw Materials," Standard Specifications for Transportation Materials and Methods of Sampling and Testing, 19th Edition, Part II Tests, 1998, American Association of State Highway and Transportation Officials, pp. 925-931.

Adhesion Loss Mechanisms of Epoxy Coatings on Rebar Surfaces, (1995). Surface Science Western, Concrete Reinforcing Steel Institute, Schaumberg, IL.

ASTM A 615/A 615M-06a (2006). "Standard Specification for Deformed and Plain Billet-steel Bars for Concrete Reinforcement," American Society for Testing and Materials, West Conshohocken, PA.

ASTM A 775/A 775M-06 (2006). "Standard Specification for Epoxy-Coated Steel Reinforcing Bars," American Society for Testing and Materials, West Conshohocken, PA.

ASTM C 305-06 (2006). "Standard Practice for Mechanical Mixing of Hydraulic Cement Pastes and Mortars of plastic Consistency," American Society for Testing and Materials, West Conshohocken, PA.

ASTM C 778-06 (2006). "Standard Specification for Standard Sand," American Society for Testing and Materials, West Conshohocken, PA.

ASTM E 8-04 (2004). "Standard Test Methods for Tension Testing of Metallic Materials," American Society for Testing and Materials, West Conshohocken, PA.

ASTM G 109-99a (2005). "Standard Test Method for Determining the Effects of Chemical Admixtures on the Corrosion of Embedded Steel Reinforcement in Concrete Exposed to Chloride Environments," American Society for Testing and Materials, West Conshohocken, PA.

Axelsson, H., Darwin, D., and Locke, C. E, Jr. (1999). "Influence of Adhesion at Steel/Mortar Interface on Corrosion Characteristics of Reinforcing Steel," SL *Report* 99-4, University of Kansas Center for Research, Lawrence, Kansas, 55 pp.

Balma, J., Darwin, D., Browning, J., and Locke, C. E. (2005) "Evaluation of Corrosion Protection Systems and Corrosion Testing Methods for Reinforcing Steel in Concrete," *SM Report* No. 76, University of Kansas Center for Research, Inc., Lawrence, Kansas, January, 517 pp.

Bodiford, C. A. (2006). South Carolina Department of Transportation. Personal communication.

Chappelow, C. C., McElroy, A. D., Blackburn, R. R., Darwin, D., deNoyelles, F. G., and Locke, C. E. (1992). *Handbook of Test Methods for Evaluating Chemical Deicers*, Strategic Highway Research Program, Nat. Res. Council, Washington, D.C.

Clemeña, G. G. (2003). "Investigation of the resistance of Several New Metallic Reinforcing Bars to Chloride-induced Corrosion in Concrete," *Interim Report* VTRC 04-R7, Virginia Transportation Research Council, Charlottesville, Va., Dec., 24 pp.

Darwin, D. (1995). "Corrosion-Resistant Steel Reinforcing Bars, Summary Report," *SL Report* 95-2, University of Kansas Center for Research, Lawrence, KS, May, 22 pp.

Darwin, D., Locke, C. E, Jr., Balma, J., Kahrs, J. T. (1999). "Evaluation of Stainless Steel Clad Reinforcing Bars," *SL Report* 99-3, University of Kansas Center for Research, Inc., Lawrence, Kansas, 17 pp.

Darwin, D., Locke, C. E., Senecal, M. R., Schwensen, S. M., Smith, J. L. (1996). "Corrosion Resistant Steel Reinforcing Bars," *Materials for the New Millennium*, K. P. Chong, Ed., ASCE, Reston, VA, pp. 482-491.

Darwin, D., Browning, J. P., Nguyen, T. V., and Locke, C. E. (2002). "Mechanical and Corrosion Properties of a High-Strength, High Chromium Reinforcing Steel for Concrete," *South Dakota Department of Transportation Report*, SD2001-05-F, 142 pp. Also *SM Report* No. 66, University of Kansas Center for Research, Inc., Lawrence, KS.

Engineering News Record (2007). "Construction Economics: Structural Steel, Rebar, Building Sheet, Piling," June 25, p.88.

Farzammehr, H. (1985). "Pore Solution Analysis of Sodium Chloride and Calcium Chloride Containing Cement Pastes," *Master of Science Thesis,* University of Oklahoma, Norman, OK, 101 pp.

Farzammehr, H., Dehghanian, C., and Locke, C. E. (1987). "Study of the Effects of Cations on Chloride Caused Corrosion of Steel in Concrete, *Revista Técnica de la Facultad de Ingeniería*, Univ. Zulia, Venezuela, Vol. 10, No. 1, pp. 33-40.

Gilsrud, T. (2002). South Dakota Department of Transportation. Personal communication.

Gilsrud, T. (2004). South Dakota Department of Transportation. Personal communication.

Gilsrud, T. (2007). South Dakota Department of Transportation. Personal communication.

Gong, L., Darwin, D., Browning, J., and Locke, C. E. (2006) "Evaluation of Multiple Corrosion Protection Systems and Stainless Steel Clad Reinforcement for Reinforced Concrete," *SM Report* No. 82, University of Kansas Center for Research, Inc., Lawrence, Kansas, January, 540 pp.

Ji, J., Darwin, D., and Browning, J. (2005). "Corrosion Resistance of Duplex Stainless Steels and MMFX Microcomposite Steel for Reinforced Concrete Bridge Decks," *SM Report* No. 80, University of Kansas Center for Research, Inc., Lawrence, Kansas, 453 pp.

Kahrs, J. T., Darwin, D., and Locke, C. E. (2001). "Evaluation of Corrosion Resistance of Type 304 Stainless Steel Clad Reinforcing Bars," *SM Report* No. 65, University of Kansas Center for Research, Inc., Lawrence, Kansas, 76 pp.

Kepler, J. L., Darwin, D., and Locke, C. E. (2000). "Evaluation of Corrosion Protection Methods for Reinforced Concrete Highway Structures," *SM Report* No. 58, University of Kansas Center for Research, Lawrence, KS, 221 pp.

Lindquist, W. D., Darwin, D., and Browning, J. (2005). "Cracking and Chloride Contents in Reinforced Concrete Bridge Decks," *SM Report* No. 78, University of Kansas Center for Research, Inc., Lawrence, Kansas, February, 453 pp.

Lindquist, W. D., Darwin, D., Browning, J., and Miller, G. G. (2006). "Effect of Cracking on Chloride Content in Concrete Bridge Decks," *ACI Materials Journal*, Vol. 103, No. 6, Nov.-Dec., pp. 467-473.

Manning, D. G. (1996). "Corrosion Performance of Epoxy-Coated Reinforcing Steel: North American Experience," *Construction and Building Materials*, Vol. 10, No. 5, Jul. pp. 349-365.

Marquart, A. (2007). Gerdau AmeriSteel. Personal communication.

Martinez, S. L., Darwin, D., McCabe, S. L., and Locke, C. E. (1990). "Rapid Test for Corrosion Effects of Deicing Chemicals in Reinforced Concrete," *SL Report* 90-4, University of Kansas Center for Research, Lawrence, KS, Aug., 61 pp.

McDonald, D. B., Pfeifer, D. W., and Sherman, M. R. (1998). "Corrosion Evaluation of Epoxy-Coated, Metallic Clad and Solid Metallic Reinforcing Bars in Concrete," *Publication* No. FHWA-RD-98-153, Federal Highway Administration, Office of Engineering R&D, McLean, VA, 127 pp.

Miller, G. and Darwin, D. (2000). " Performance and Constructability of Silica Fume Bridge Deck Overlays," *SM Report* No. 57, The University of Kansas Center for Research, Inc., Lawrence, KS, 423 pp.

Perenchio, William F. (1992). "Corrosion of Reinforcing Bars in Concrete," Annual Seminar, Master Builders Technology, Cleveland, OH, Dec.

Pfeifer, D. W., and Scali, M. J. (1981). "Concrete Sealers for Protection of Bridge Structures," *NCHRP Report* No. 244, National Cooperative Highway Research Program, Transportation Research Board, Washington, DC, Dec.

Pfeifer, D. W. (2000). "High Performance Concrete and Reinforcing Steel with a 100-Year Service Life," *PCI Journal*, Vol. 45, No. 3, May-June, pp. 46-54.

Rajabi, J. (2006). South Carolina Department of Transportation. Personal communication.

Sagues, A. A., Powers, R. G., and Kessler, R. (1994). "Corrosion Processes and Field Performance of Epoxy-Coated Reinforcing Steel in Marine Structures," *Corrosion 94*, Paper No. 299, National Association of Corrosion Engineers, Houston, TX.

Senecal, M. R., Darwin, D., and Locke, C. E., Jr. (1995). "Evaluation of Corrosion-Resistant Steel Reinforcing Bars," *SM Report* No. 40, University of Kansas Center for Research, Lawrence, KS, July, 142 pp.

Smith, J. L., Darwin, D., and Locke, C. E., Jr. (1995). "Corrosion-Resistant Steel Reinforcing Bars Initial Tests," *SL Report* 95-1, University of Kansas Center for Research, Lawrence, KS, April, 43 pp

Smith, Jeffery L. and Virmani, Yash Paul (1996). "Performance of Epoxy-Coated Rebars in Bridge Decks," *Report* No. FHWA-RD-96-092, Federal Highway Administration, Washington, DC.

Torres-Acosta, A. A. and Sagues, A. A. (2004). "Concrete Cracking by Localized Steel Corrosion – Geometric Effects," *ACI Material Journal*, Vol. 101, No. 6, pp 501-507.

Trejo, D. and Pillai, R. G. (2003). "Accelerated Chloride Threshold Testing: Part I – ASTM A 615 and A 706 Reinforcement," *ACI Materials Journal*, Vol. 100, No. 6, Nov.-Dec., pp. 519-527.

Yunovich , M., Thompson, N. G., Balvanyos, T., and Lave, L. (2002). "Highway Bridges," Appendix D, *Corrosion Cost and Preventive Strategies in the United States*, By G. H. Koch, M. PO. H. Broongers, N. G. Thompson, Y. P. Virmani, and J. H. Payer, *Report* No. FHWA-RD-01-156, Federal Highway Administration, McLean, VA, Mar., 773 pp.

APPENDIX A CORROSION TEST RESULTS FOR INDIVIDUAL SPECIMENS

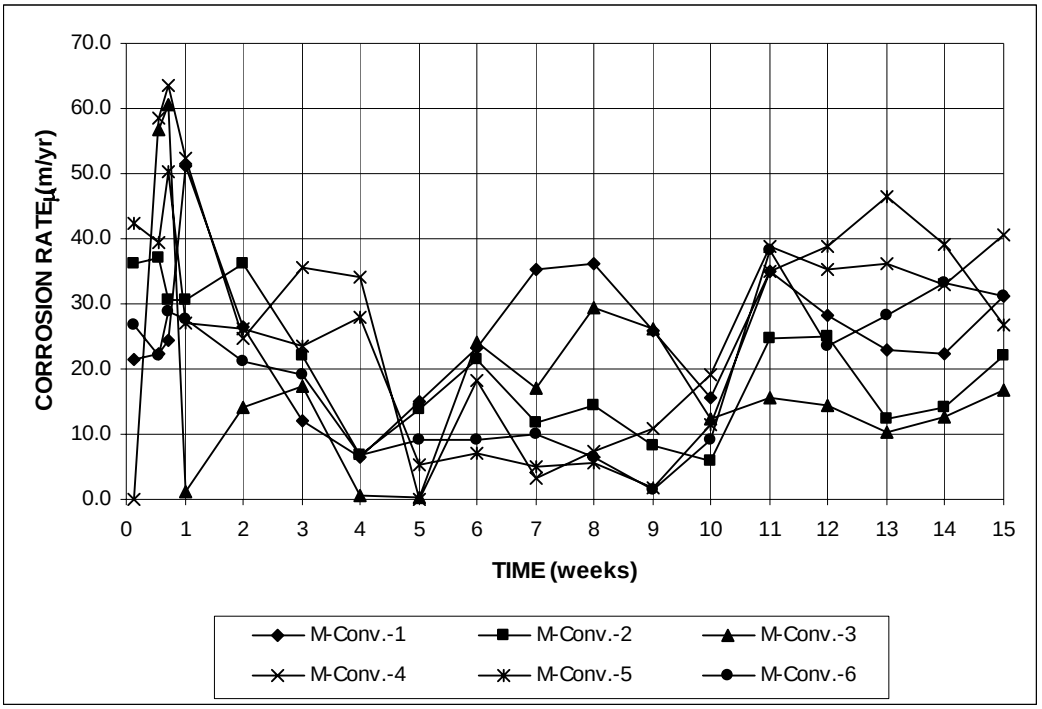

Figure A.1 – Macrocell Test. Corrosion rate (based on total area). Bare conventional steel in 1.6 m ion NaCl and simulated concrete pore solution

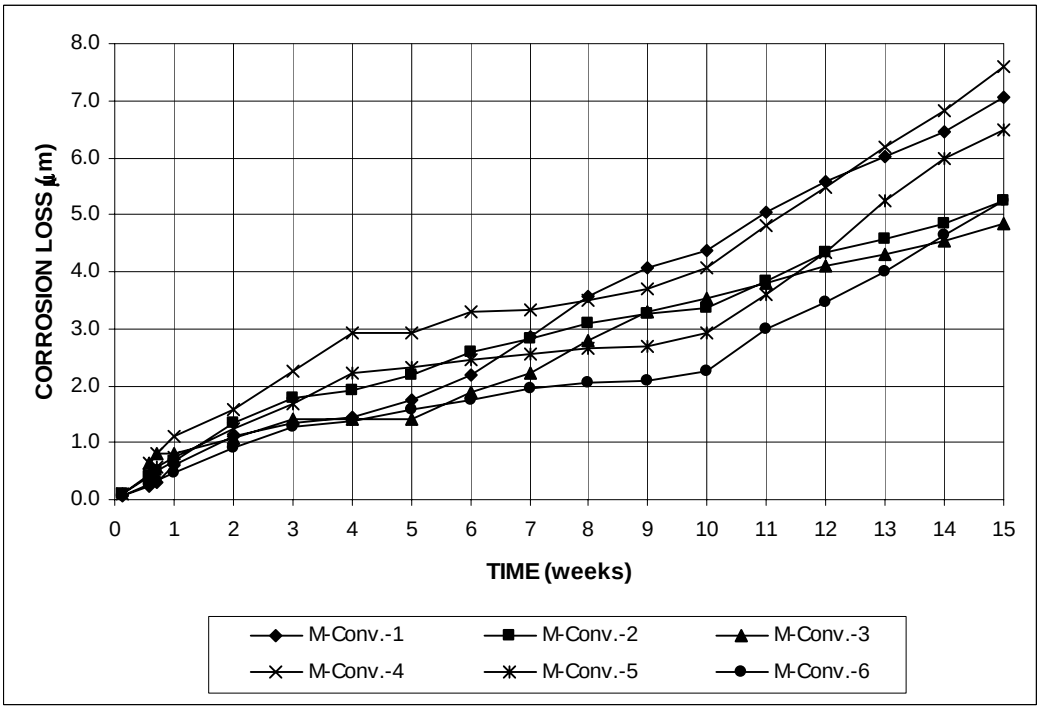

Figure A.2 – Macrocell Test. Corrosion loss (based on total area). Bare conventional steel in 1.6 m ion NaCl and simulated concrete pore solution

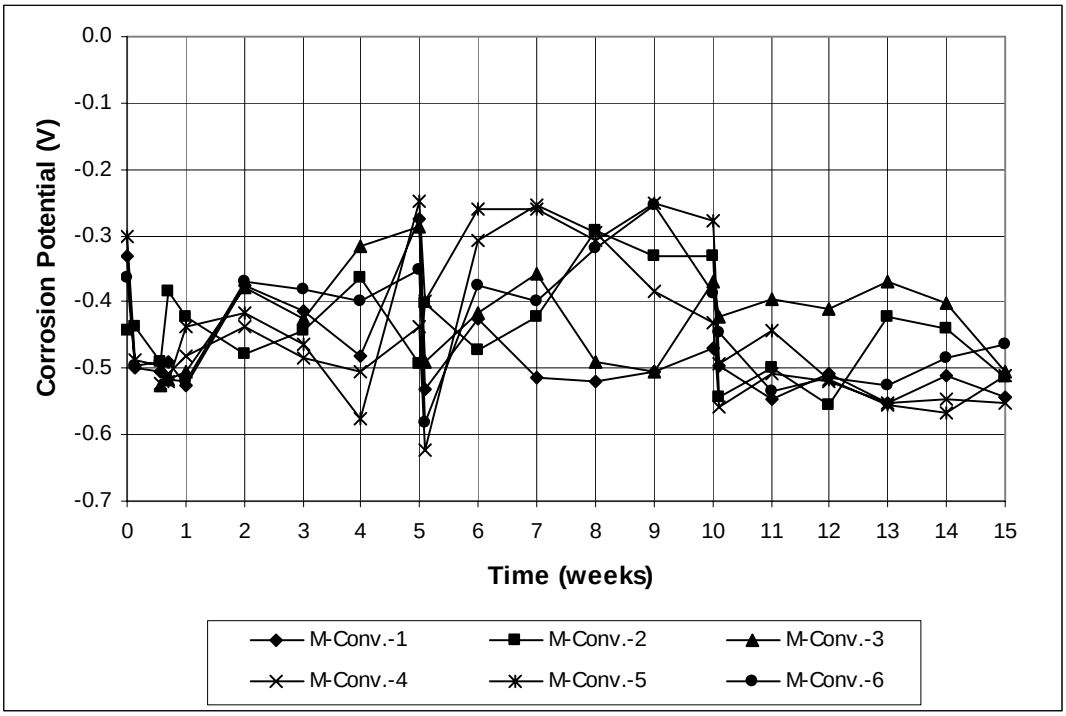

Figure A.3 – Macrocell Test. Anode corrosion potential vs. saturated calomel electrode. Bare conventional steel in 1.6 m ion NaCl and simulated concrete pore solution

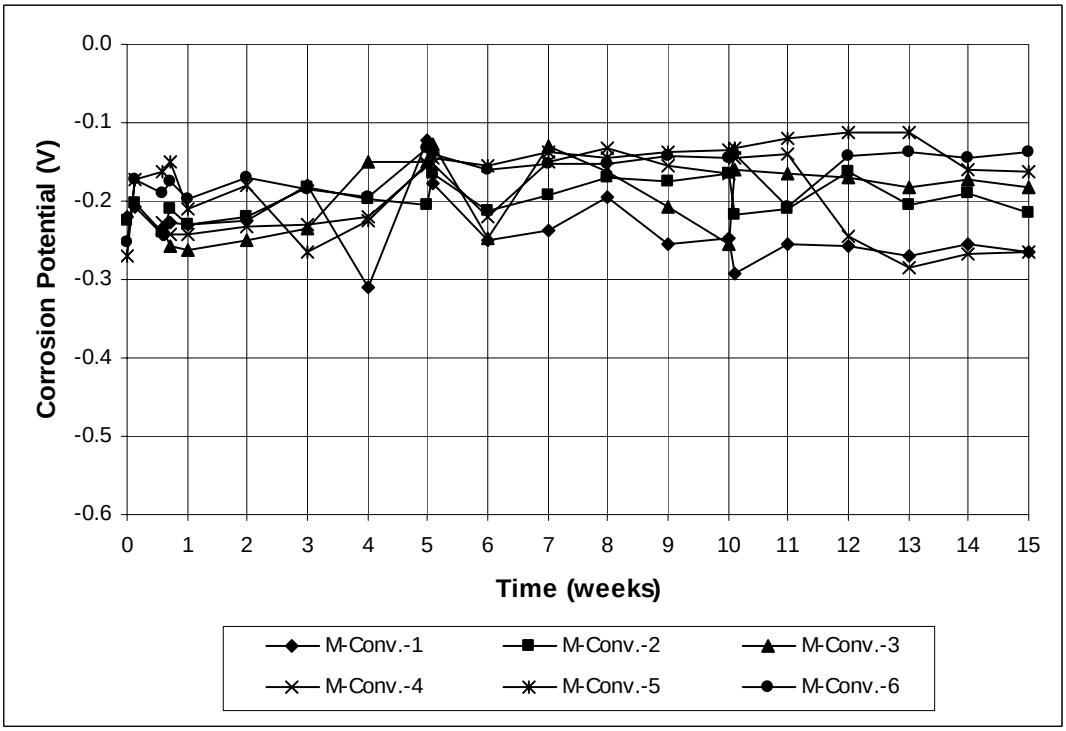

Figure A.4 – Macrocell Test. Cathode corrosion potential vs. saturated calomel electrode. Bare conventional steel in 1.6 m ion NaCl and simulated concrete pore solution

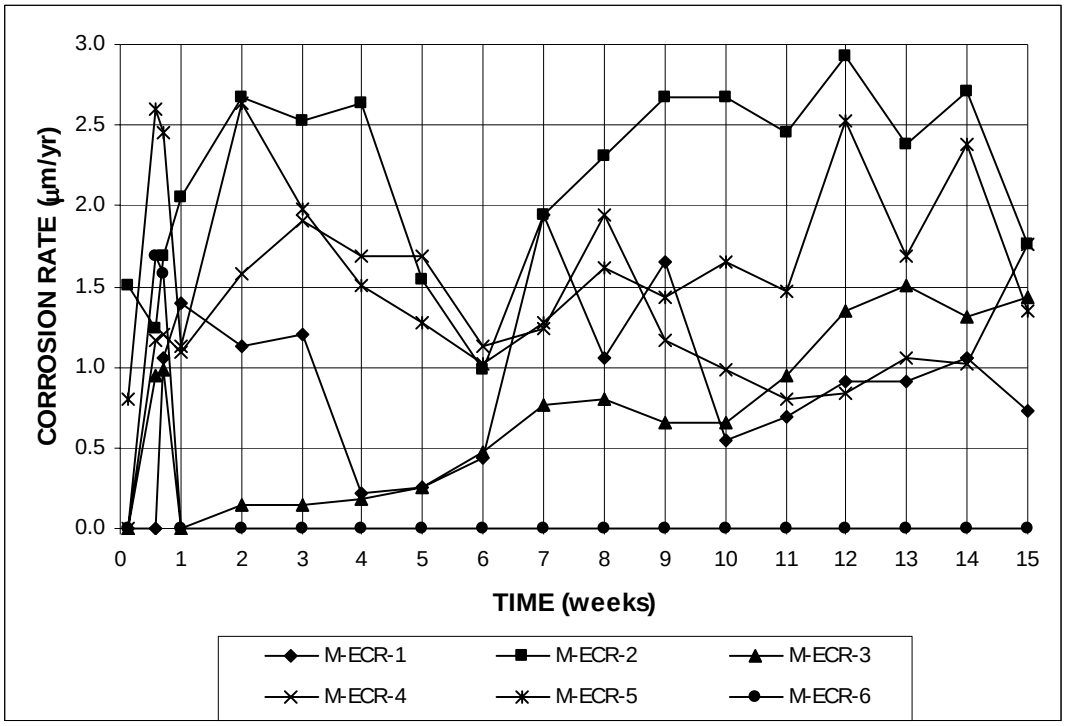

Figure A.5 – Macrocell Test. Corrosion rate (based on total area). Bare epoxy-coated steel with four drilled holes in 1.6 m ion NaCl and simulated concrete pore solution

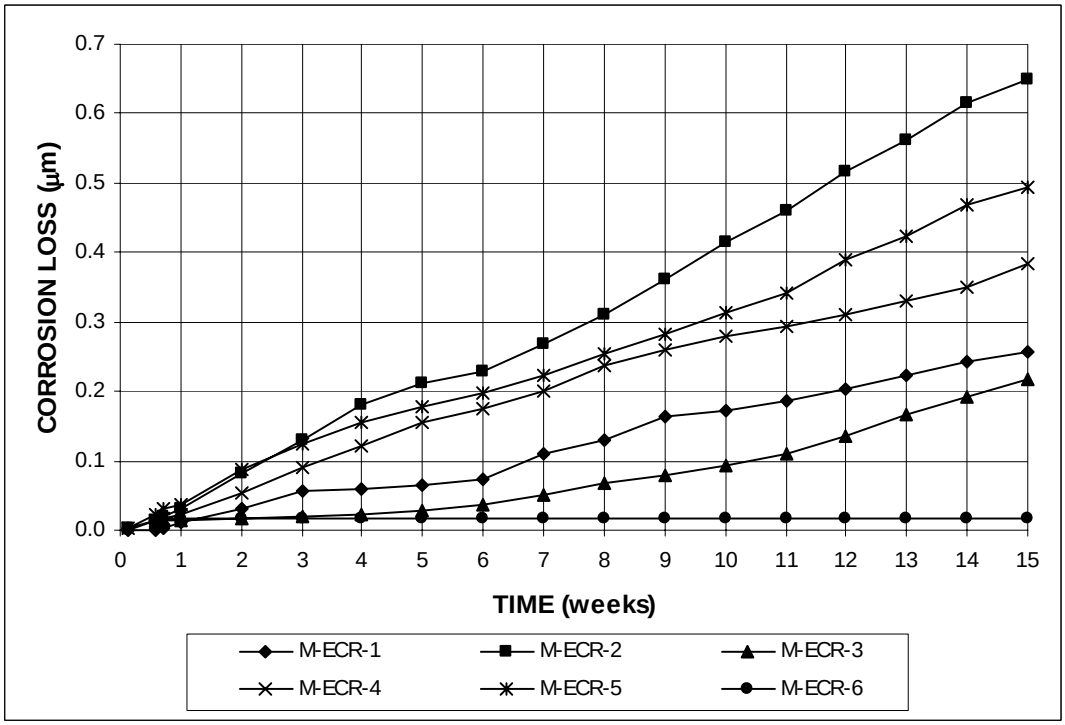

Figure A.6 – Macrocell Test. Corrosion loss (based on total area). Bare epoxy-coated steel with four drilled holes in 1.6 m ion NaCl and simulated concrete pore solution

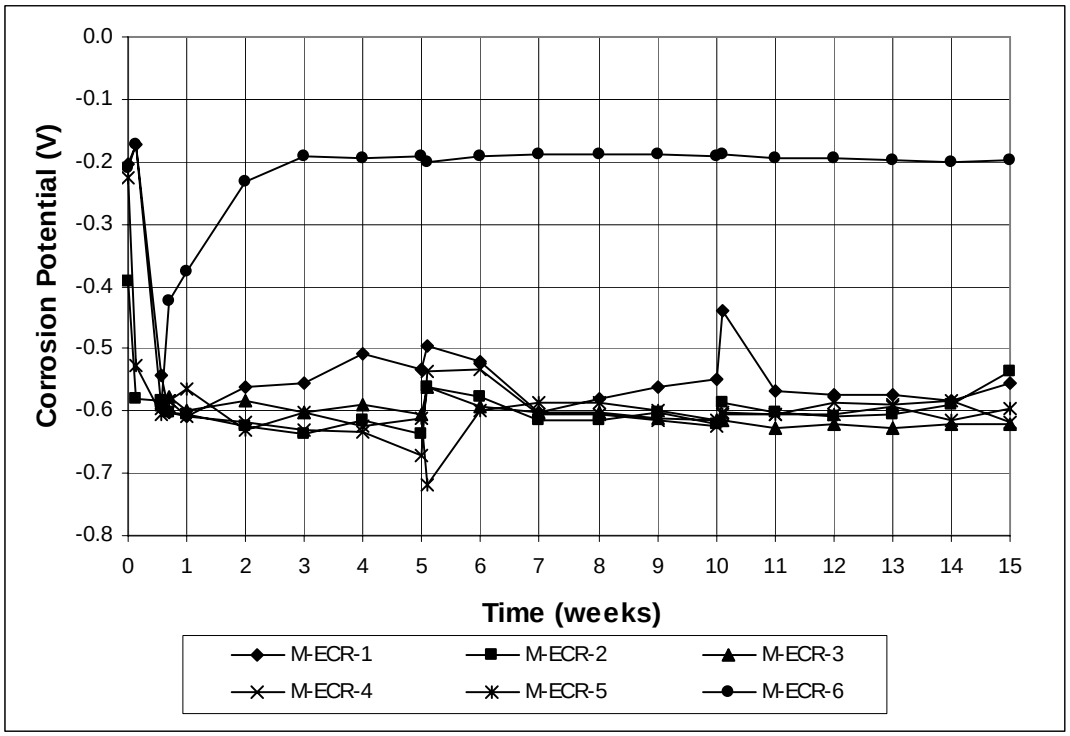

Figure A.7 – Macrocell Test. Anode corrosion potential vs. saturated calomel electrode. Bare epoxy-coated steel with four drilled holes in 1.6 m ion NaCl and simulated concrete pore solution

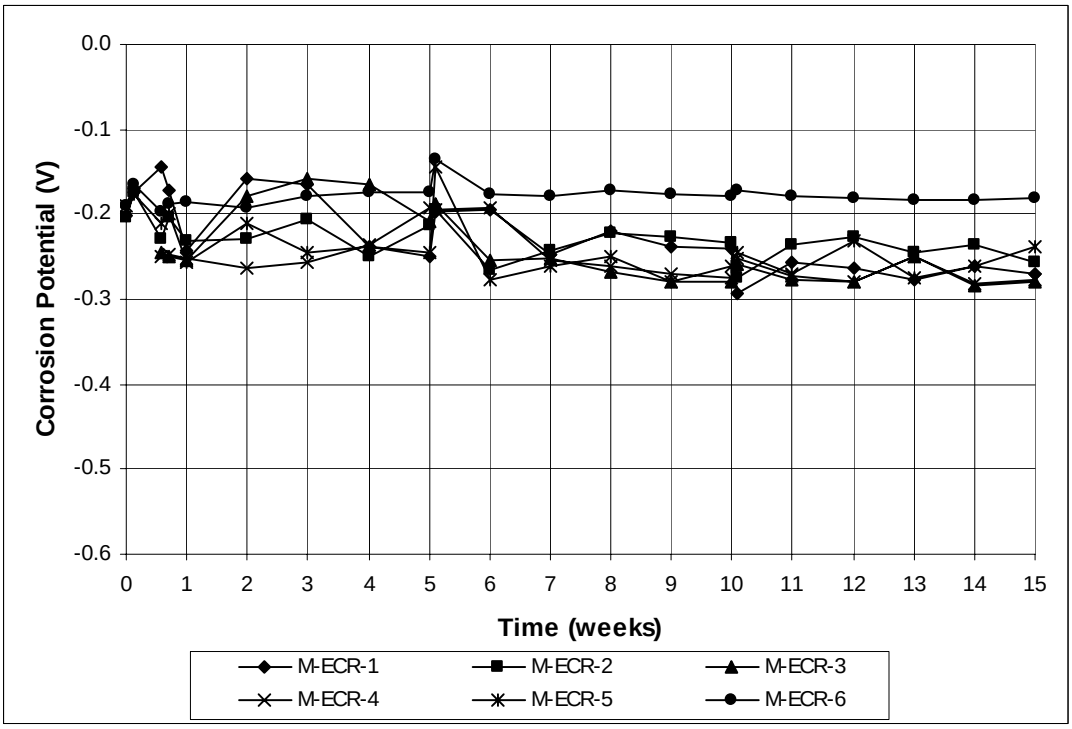

Figure A.8 – Macrocell Test. Cathode corrosion potential vs. saturated calomel electrode. Bare epoxy-coated steel with four drilled holes in 1.6 m ion NaCl and simulated concrete pore solution

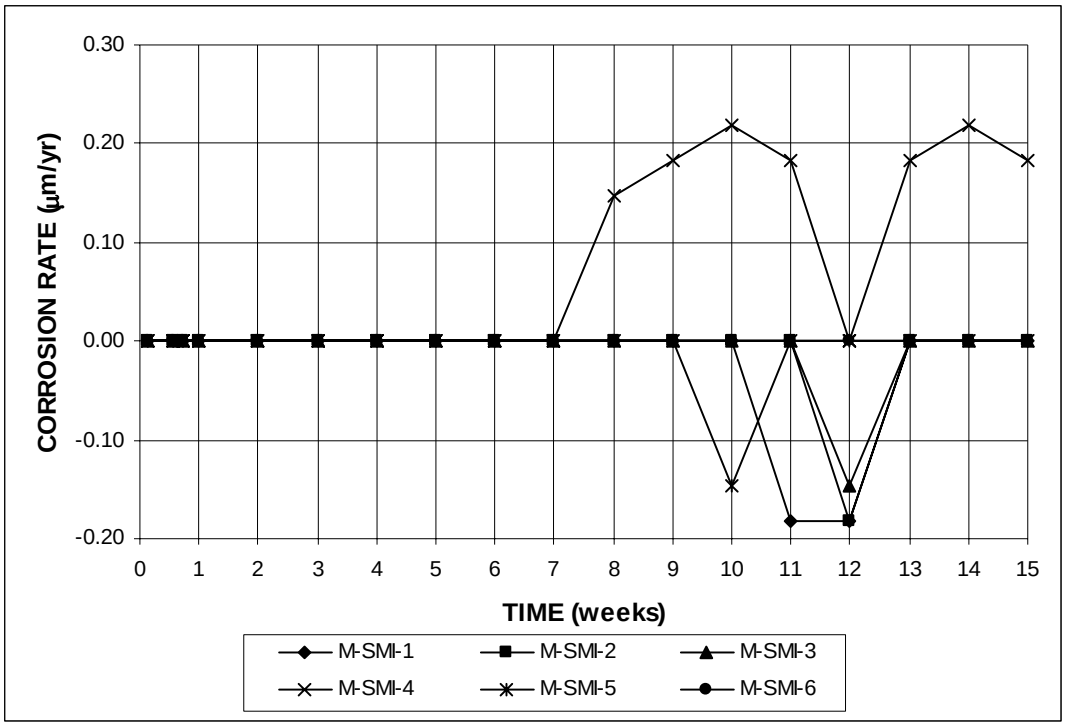

Figure A.9 – Macrocell Test. Corrosion rate (based on total area). Bare SMI steel with cap in 1.6 m ion NaCl and simulated concrete pore solution

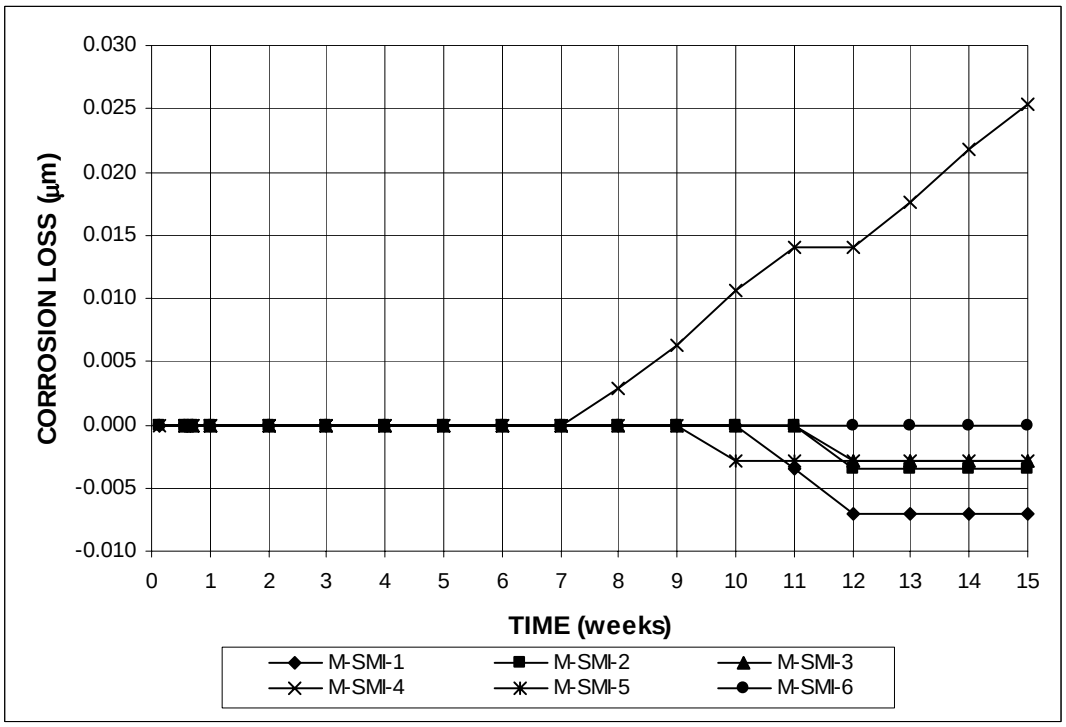

Figure A.10 – Macrocell Test. Corrosion loss (based on total area). Bare SMI steel with cap in 1.6 m ion NaCl and simulated concrete pore solution

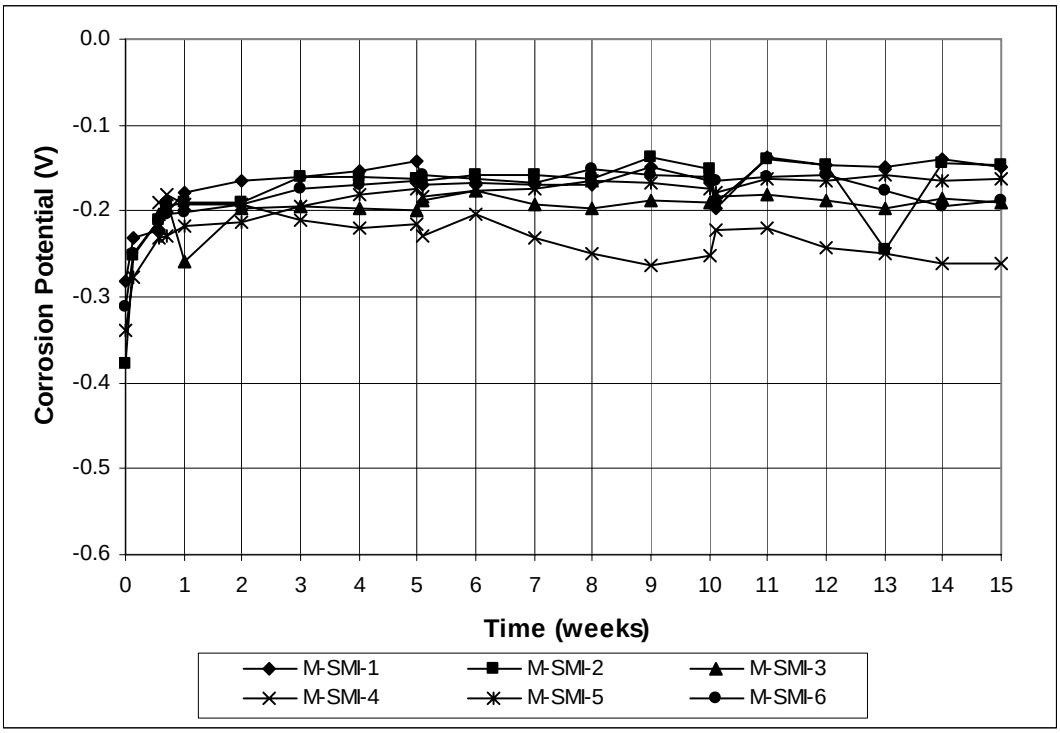

Figure A.11 – Macrocell Test. Anode corrosion potential vs. saturated calomel electrode. Bare SMI steel with cap in 1.6 m ion NaCl and simulated concrete pore solution

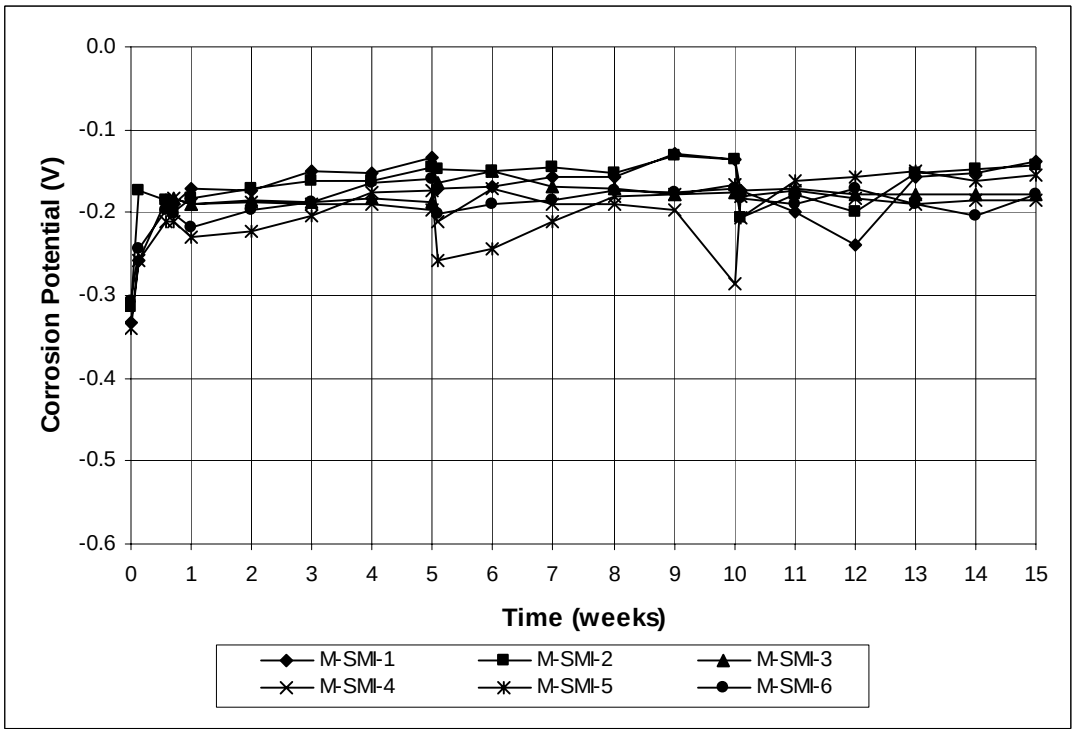

Figure A.12 – Macrocell Test. Cathode corrosion potential vs. saturated calomel electrode. Bare SMI steel with cap in 1.6 m ion NaCl and simulated concrete pore solution

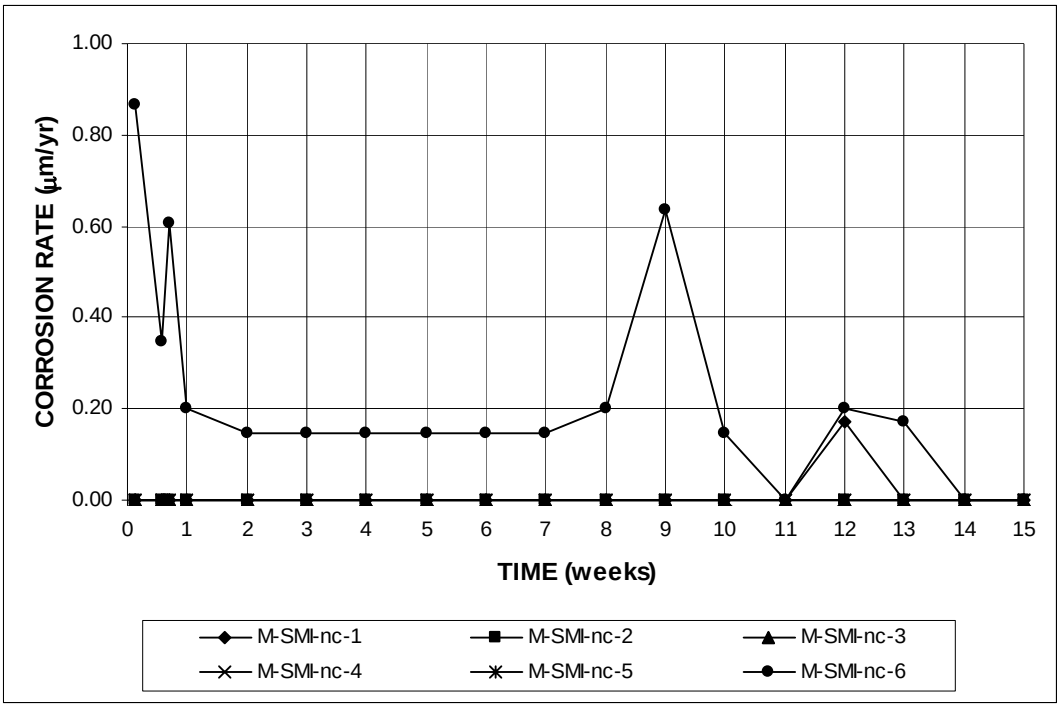

Figure A.13 – Macrocell Test. Corrosion rate (based on total area). Bare SMI steel without cap in 1.6 m ion NaCl and simulated concrete pore solution

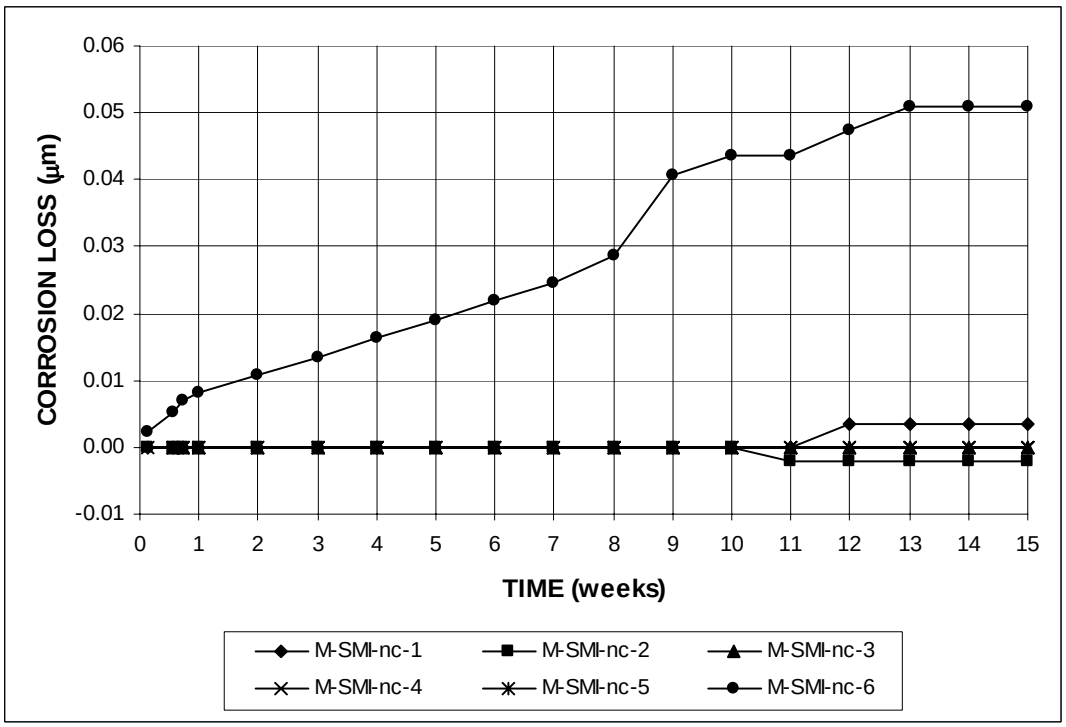

Figure A.14 – Macrocell Test. Corrosion loss (based on total area). Bare SMI steel without cap in 1.6 m ion NaCl and simulated concrete pore solution

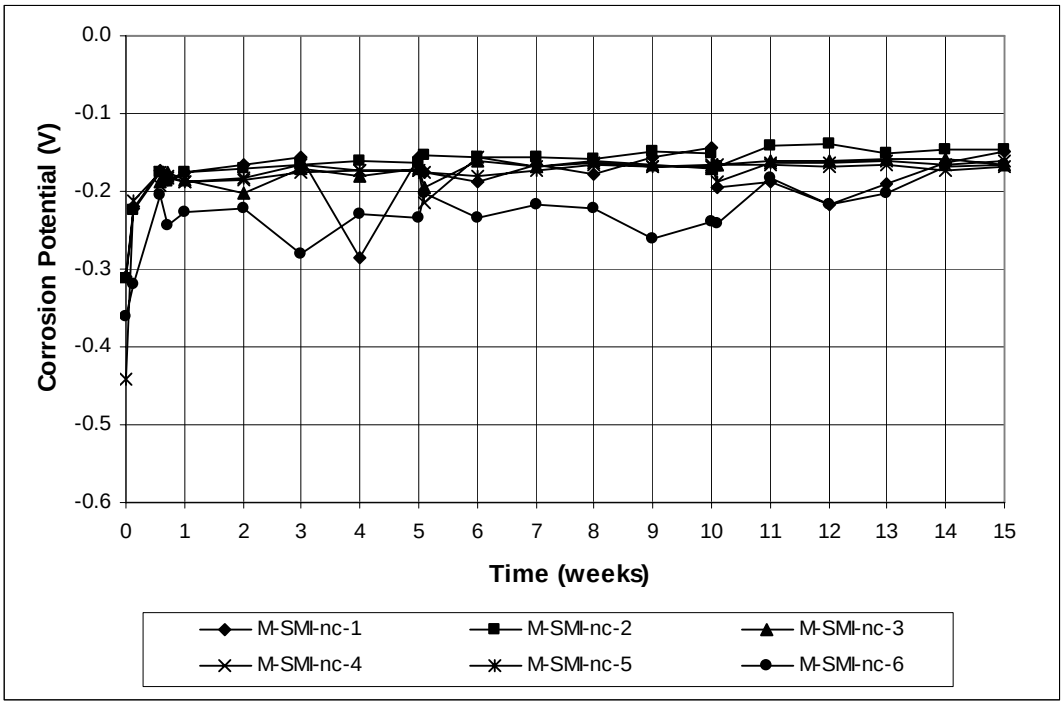

Figure A.15 – Macrocell Test. Anode corrosion potential vs. saturated calomel electrode. Bare SMI steel without cap in 1.6 m ion NaCl and simulated concrete pore solution

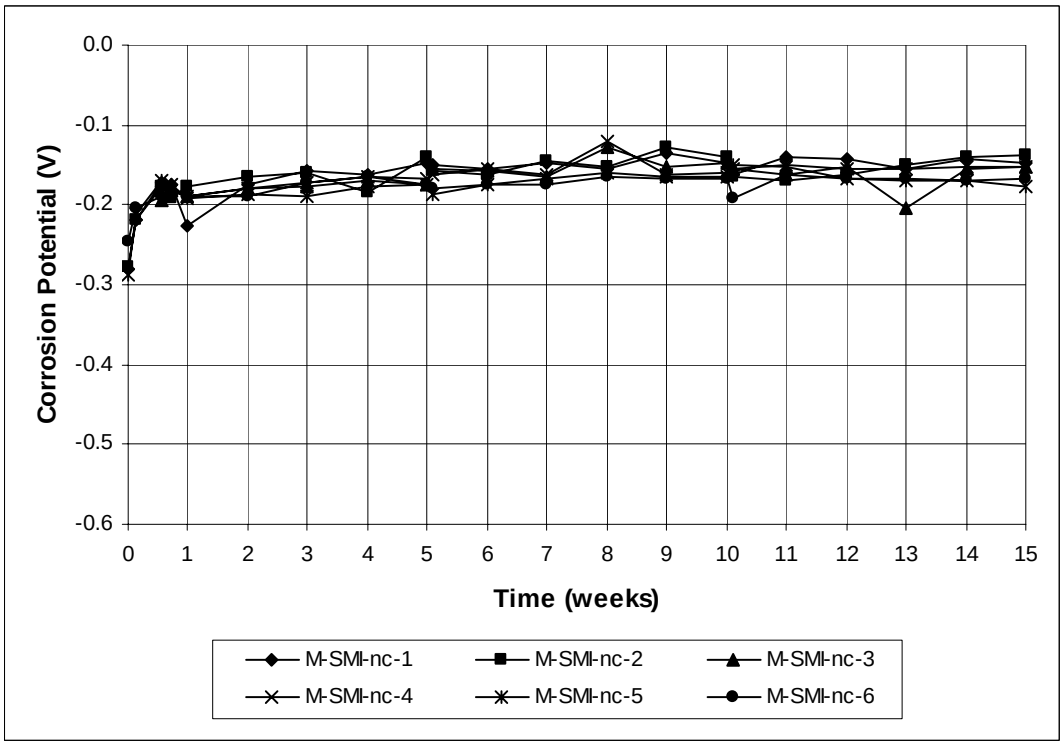

Figure A.16 – Macrocell Test. Cathode corrosion potential vs. saturated calomel electrode. Bare SMI steel without cap in 1.6 m ion NaCl and simulated concrete pore solution

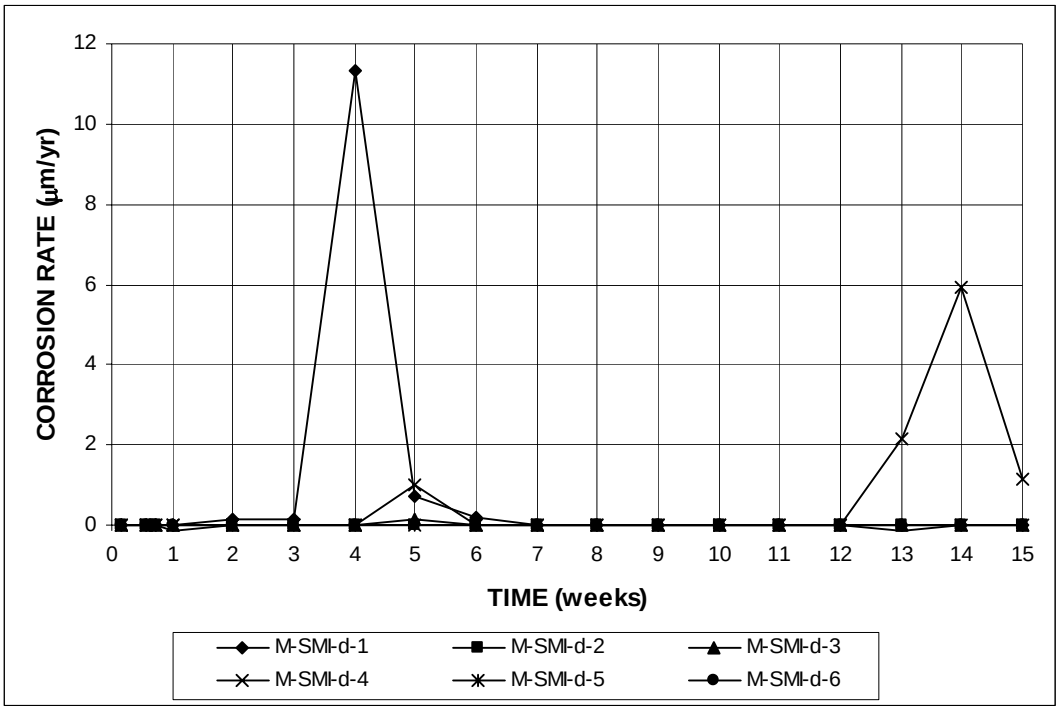

Figure A.17 – Macrocell Test. Corrosion rate (based on total area). Bare SMI steel with four drilled holes in 1.6 m ion NaCl and simulated concrete pore solution

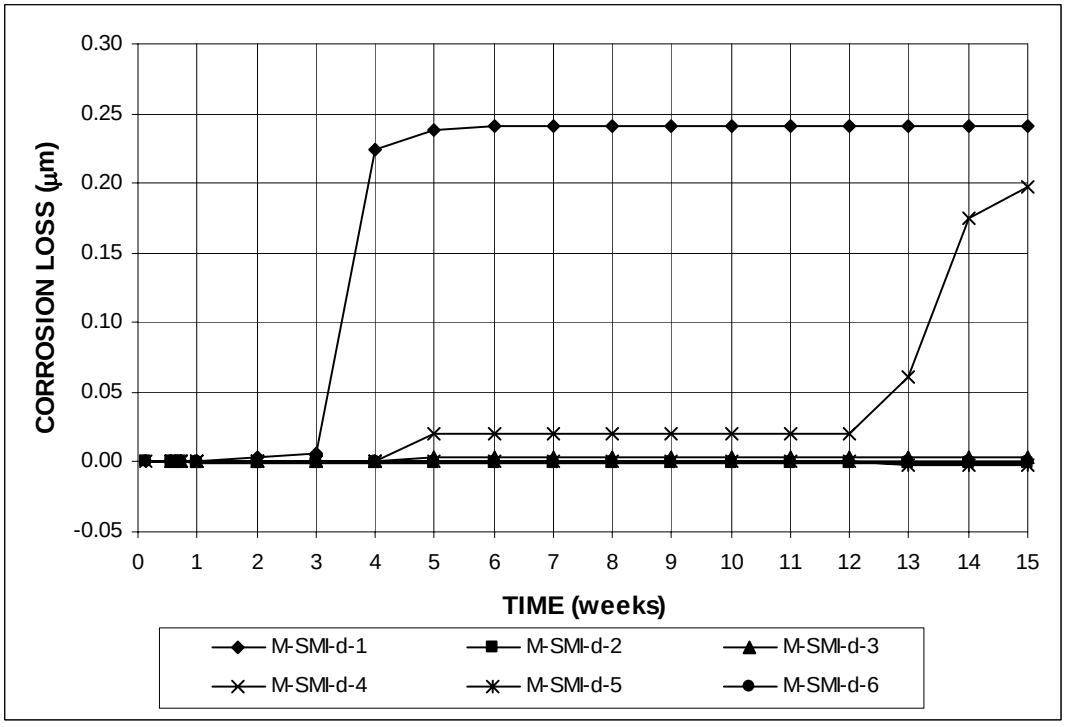

Figure A.18 – Macrocell Test. Corrosion loss (based on total area). Bare SMI steel with four drilled holes in 1.6 m ion NaCl and simulated concrete pore solution

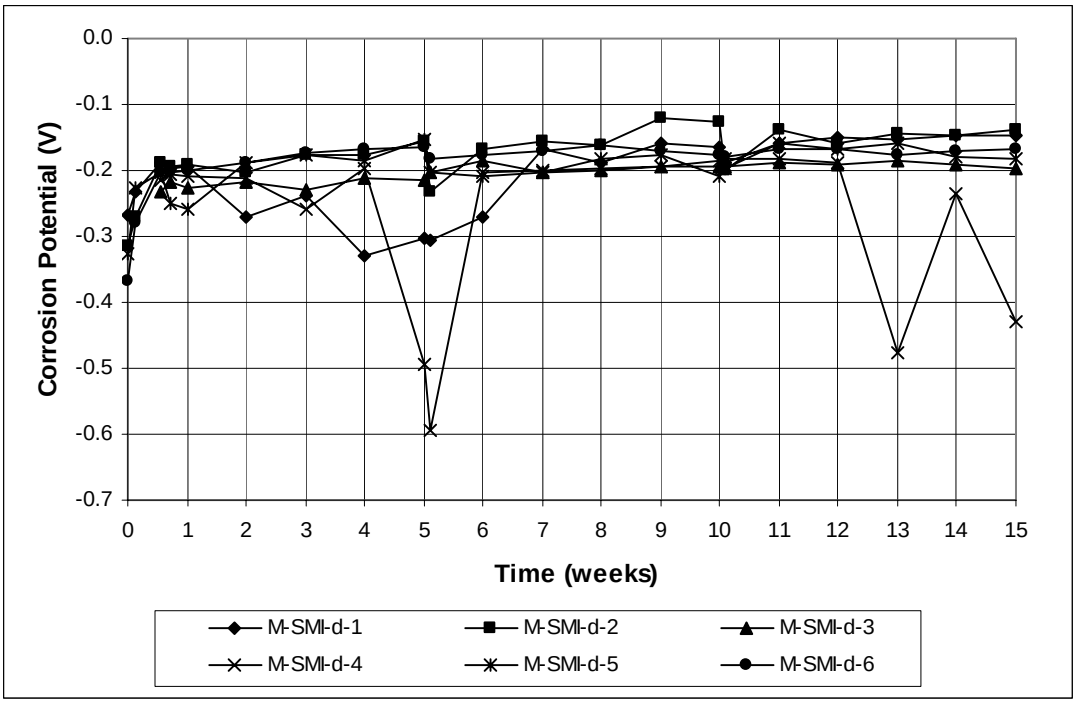

Figure A.19 – Macrocell Test. Anode corrosion potential vs. saturated calomel electrode. Bare SMI steel with four drilled holes in 1.6 m ion NaCl and simulated concrete pore solution

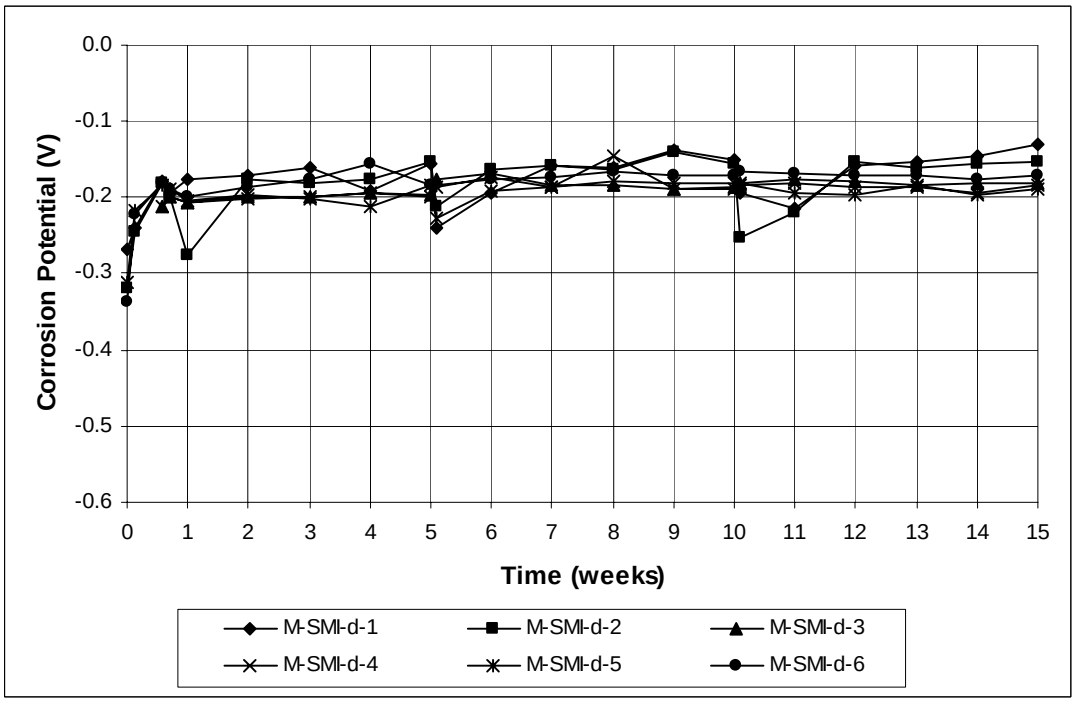

Figure A.20 – Macrocell Test. Cathode corrosion potential vs. saturated calomel electrode. Bare SMI steel with four drilled holes in 1.6 m ion NaCl and simulated concrete pore solution

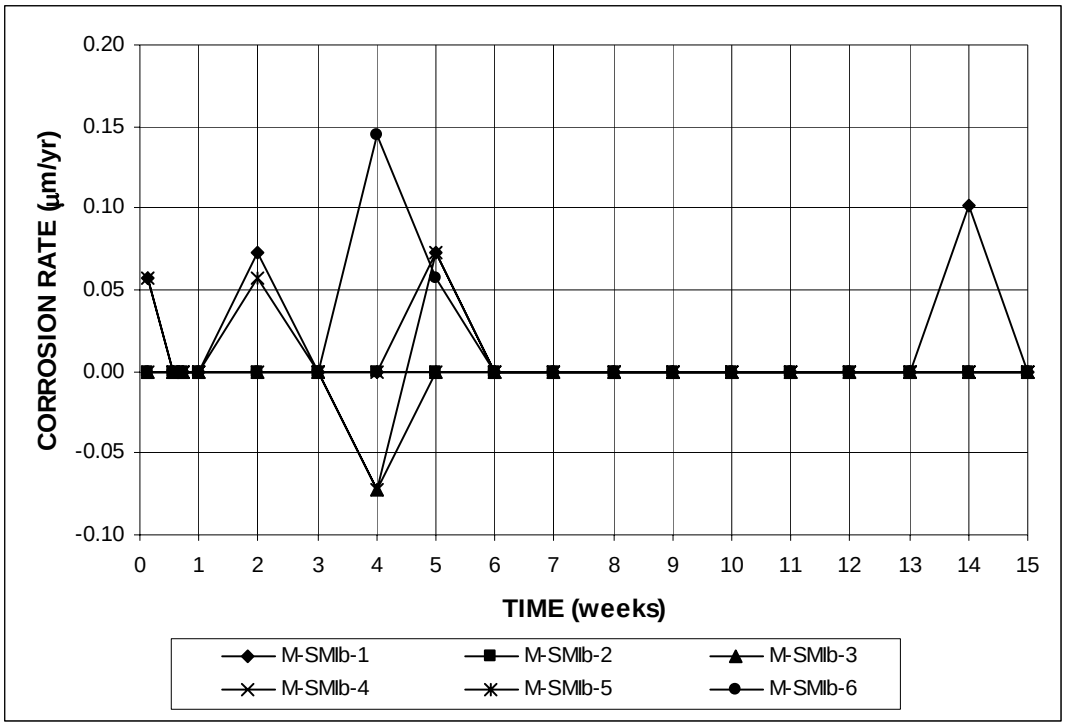

Figure A.21 – Macrocell Test. Corrosion rate (based on total area). Bare SMI steel with 180 degree bend in 1.6 m ion NaCl and simulated concrete pore solution

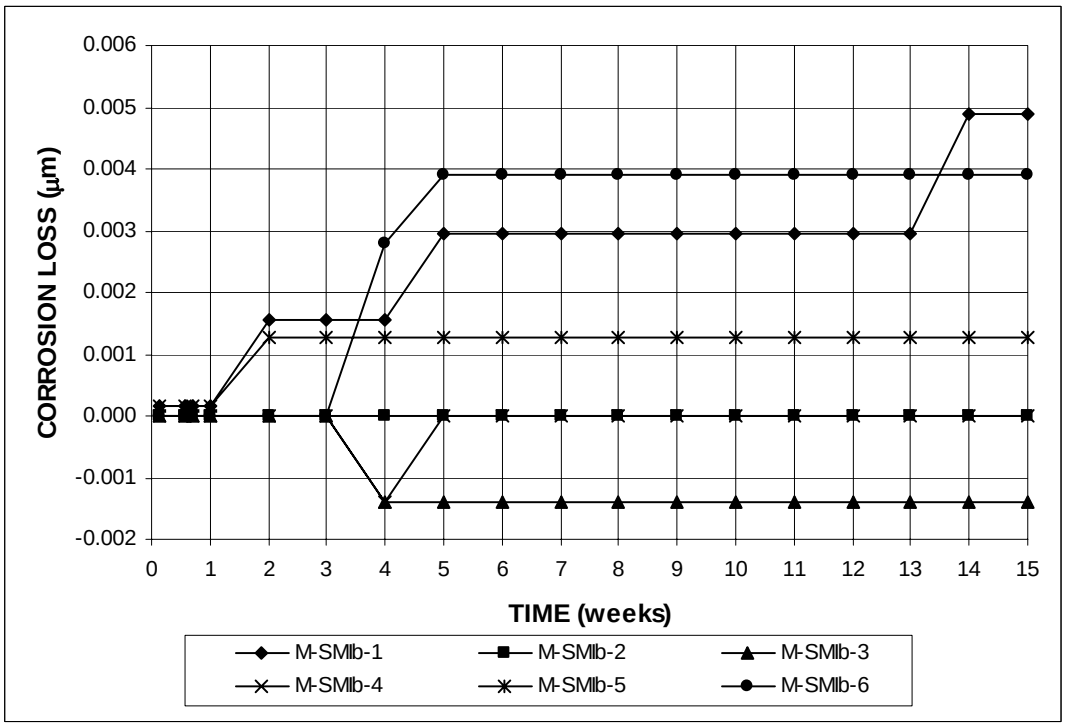

Figure A.22 – Macrocell Test. Corrosion loss (based on total area). Bare SMI steel with 180 degree bend in 1.6 m ion NaCl and simulated concrete pore solution

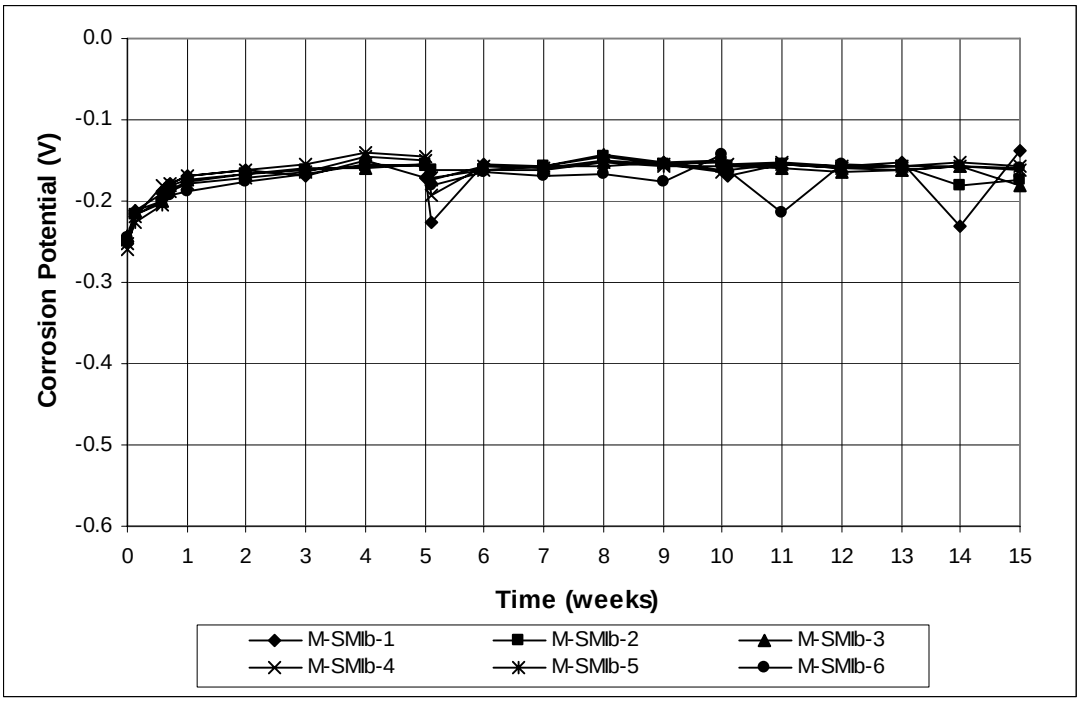

Figure A.23 – Macrocell Test. Anode corrosion potential vs. saturated calomel electrode. Bare SMI steel with 180 degree bend in 1.6 m ion NaCl and simulated concrete pore solution

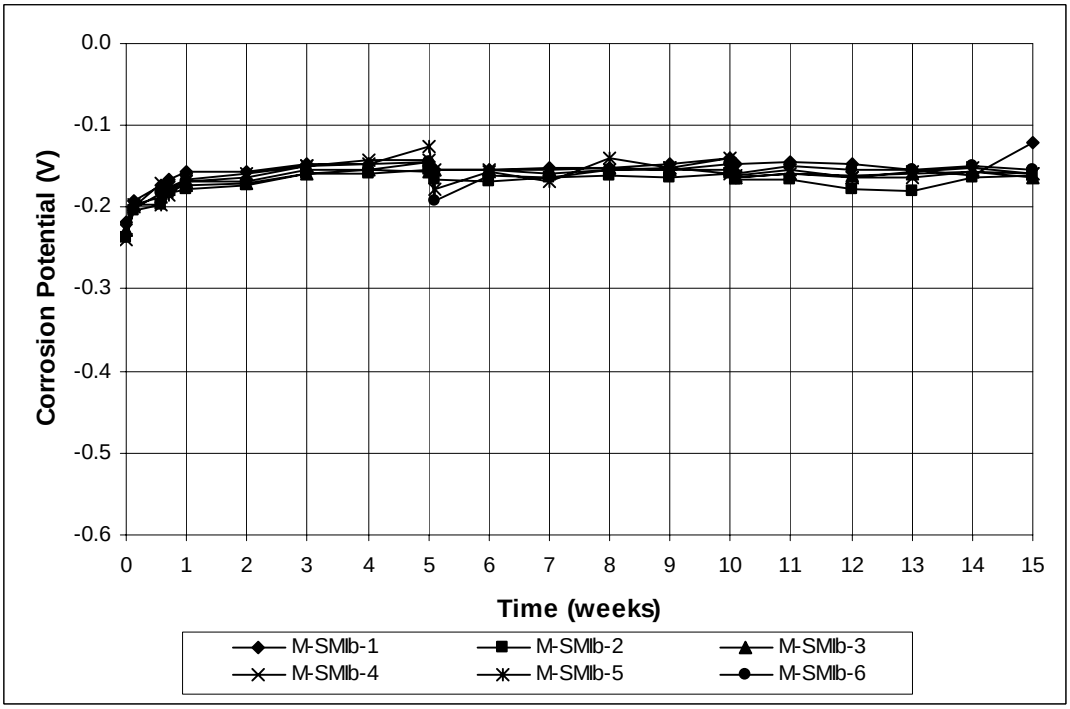

Figure A.24 – Macrocell Test. Cathode corrosion potential vs. saturated calomel electrode. Bare SMI steel with 180 degree bend in 1.6 m ion NaCl and simulated concrete pore solution

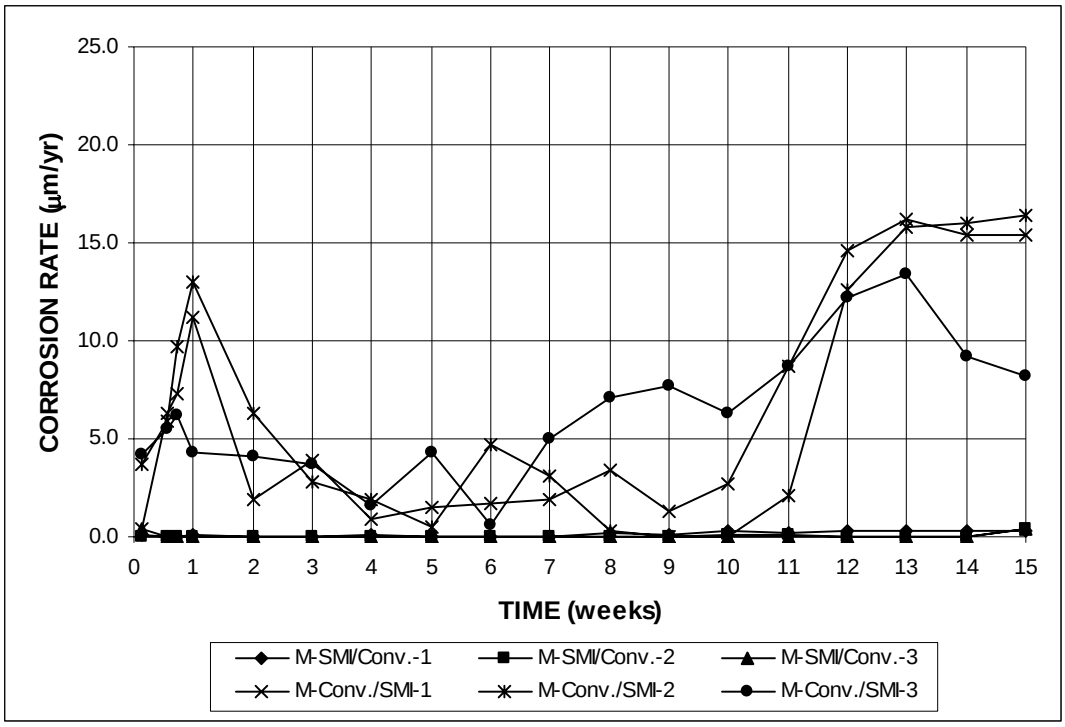

Figure A.25 – Macrocell Test. Corrosion rate (based on total area). Bare SMI steel with conventional steel in 1.6 m ion NaCl and simulated concrete pore solution

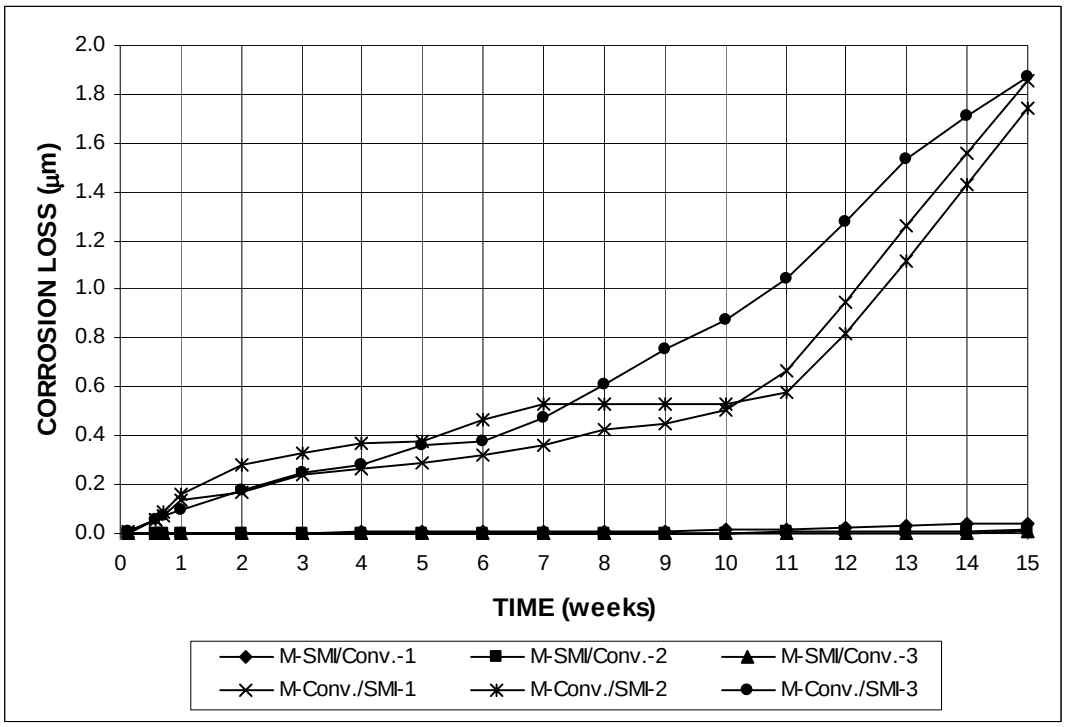

Figure A.26 – Macrocell Test. Corrosion loss (based on total area). Bare SMI steel with conventional steel in 1.6 m ion NaCl and simulated concrete pore solution

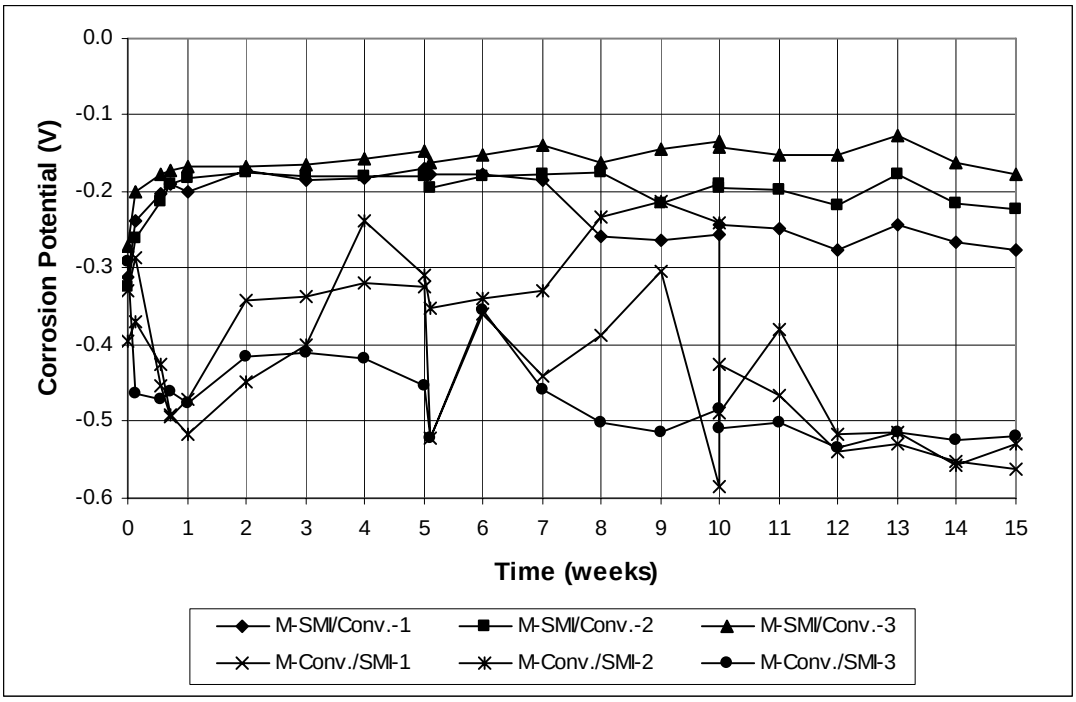

Figure A.27 – Macrocell Test. Anode corrosion potential vs. saturated calomel electrode. Bare SMI steel with conventional steel in 1.6 m ion NaCl and simulated concrete pore solution

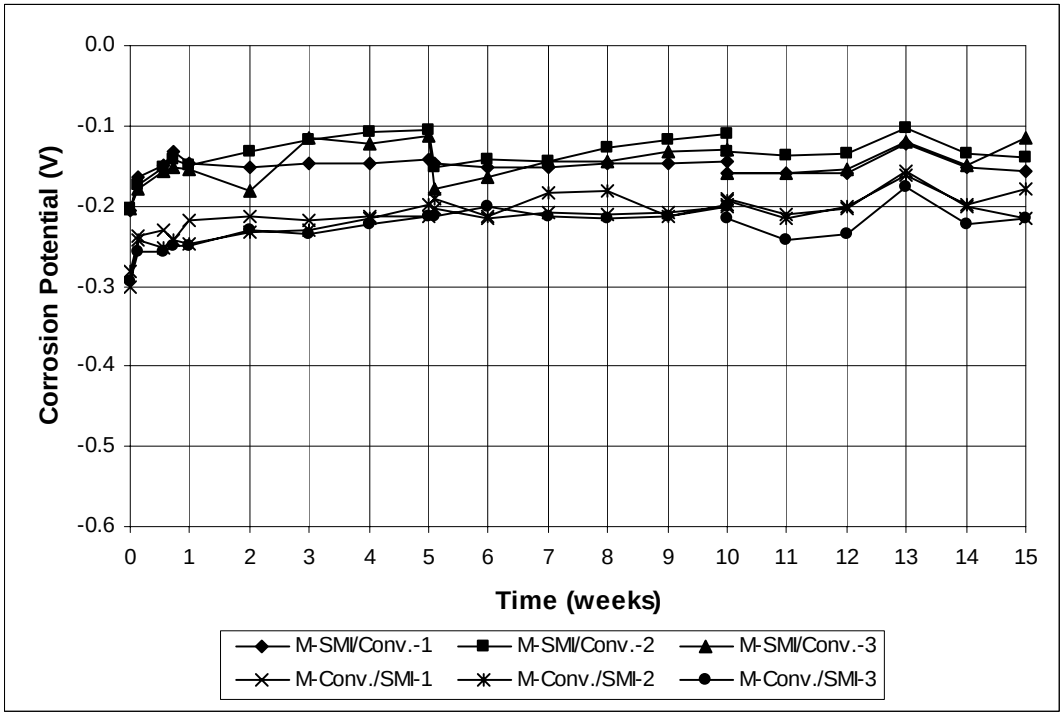

Figure A.28 – Macrocell Test. Cathode corrosion potential vs. saturated calomel electrode. Bare SMI steel with conventional steel in 1.6 m ion NaCl and simulated concrete pore solution

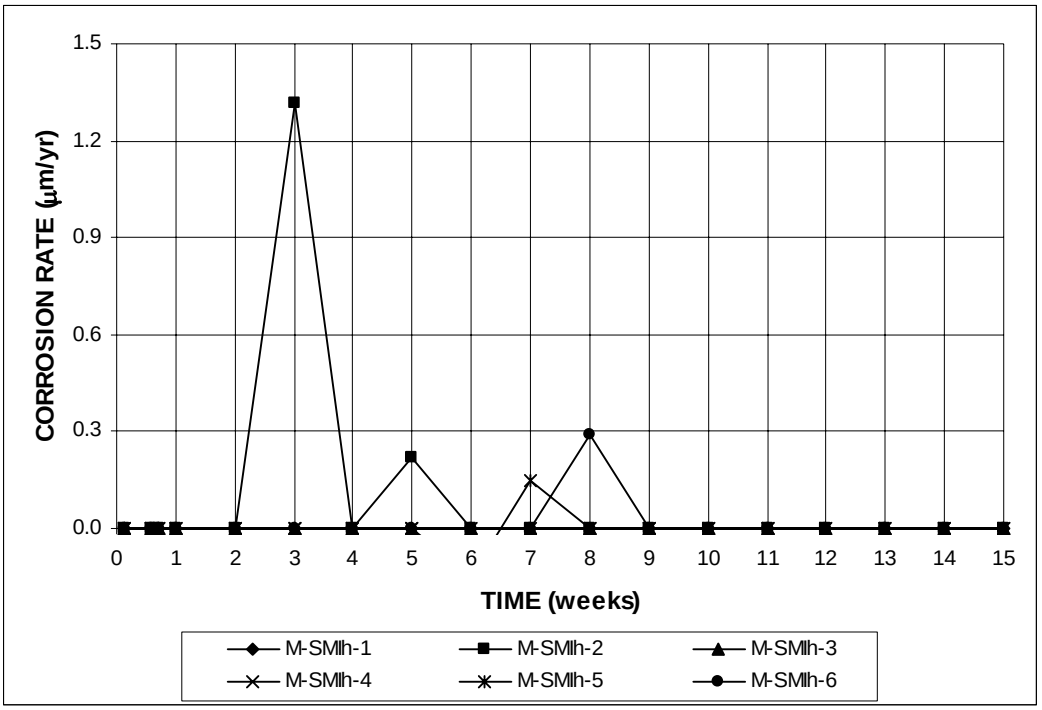

Figure A.29 – Macrocell Test. Corrosion rate (based on total area). Bare SMI steel with cap in 6.04 m ion NaCl and simulated concrete pore solution

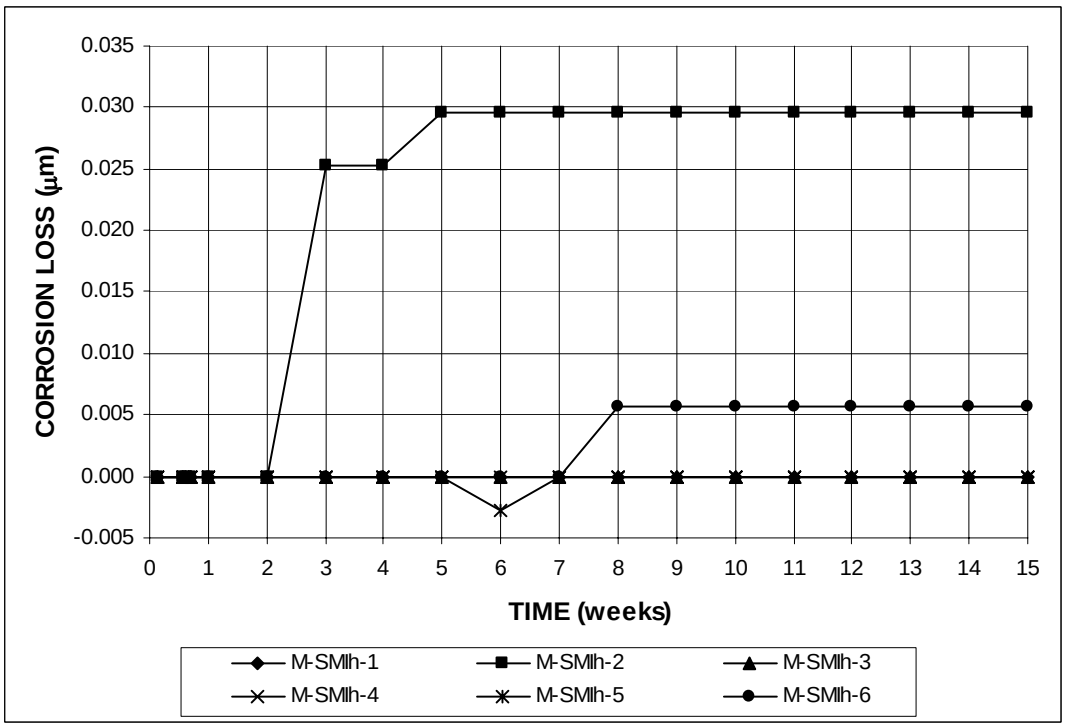

Figure A.30 – Macrocell Test. Corrosion loss (based on total area). Bare SMI steel with cap in 6.04 m ion NaCl and simulated concrete pore solution

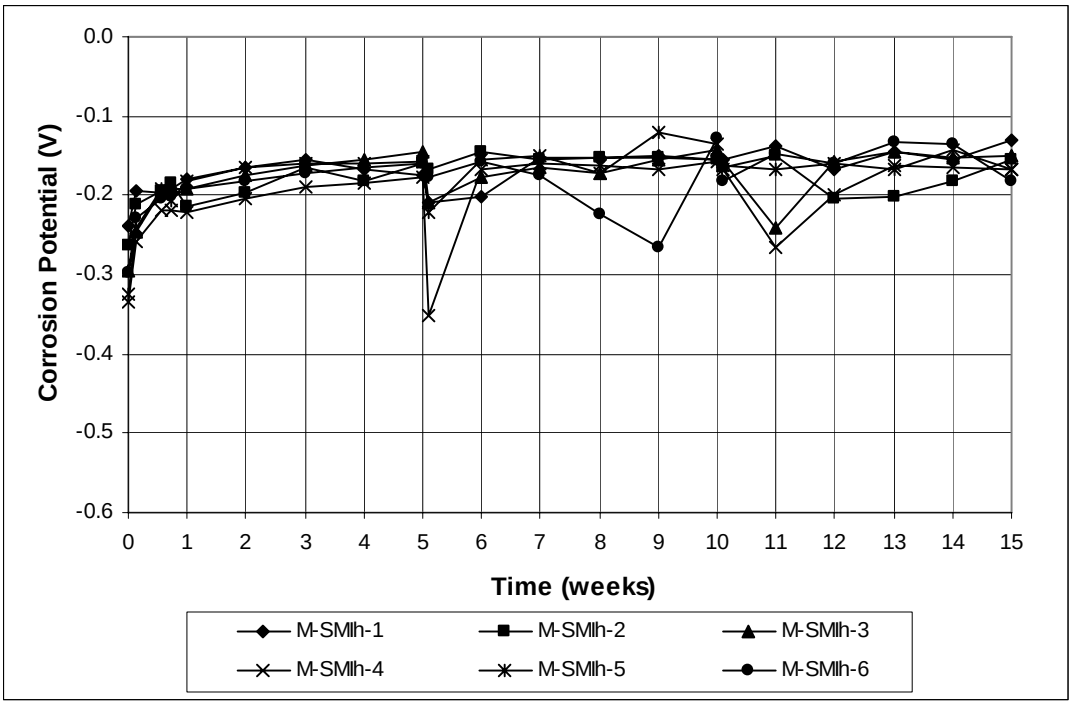

Figure A.31 – Macrocell Test. Anode corrosion potential vs. saturated calomel electrode. Bare SMI steel with cap in 6.04 m ion NaCl and simulated concrete pore solution

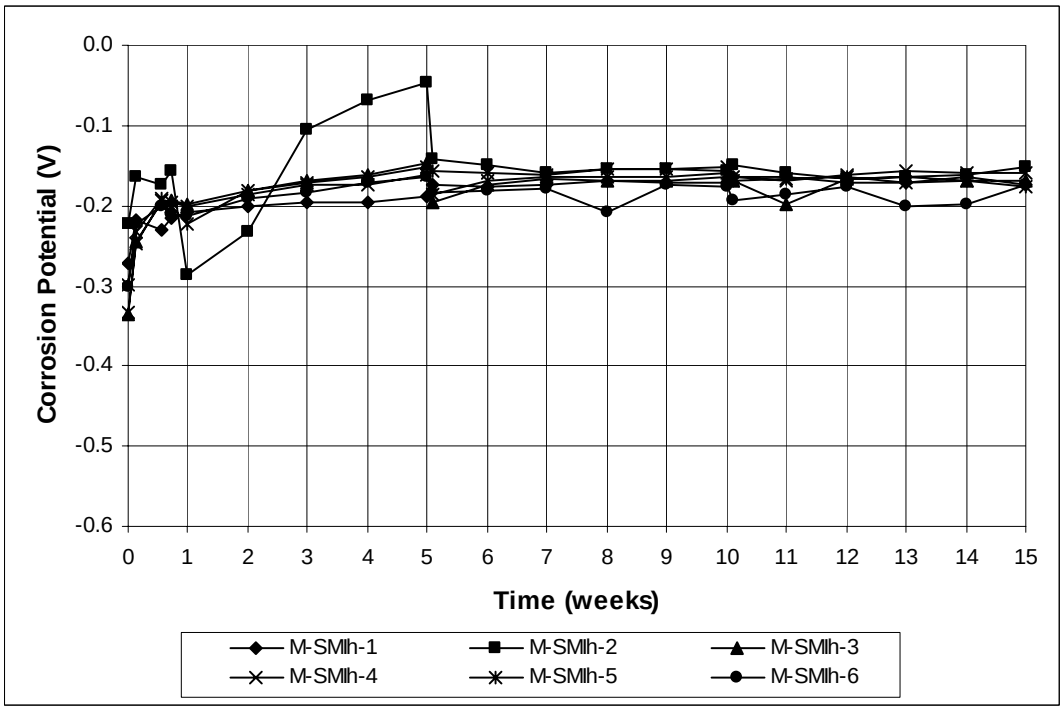

Figure A.32 – Macrocell Test. Cathode corrosion potential vs. saturated calomel electrode. Bare SMI steel with cap in 6.04 m ion NaCl and simulated concrete pore solution

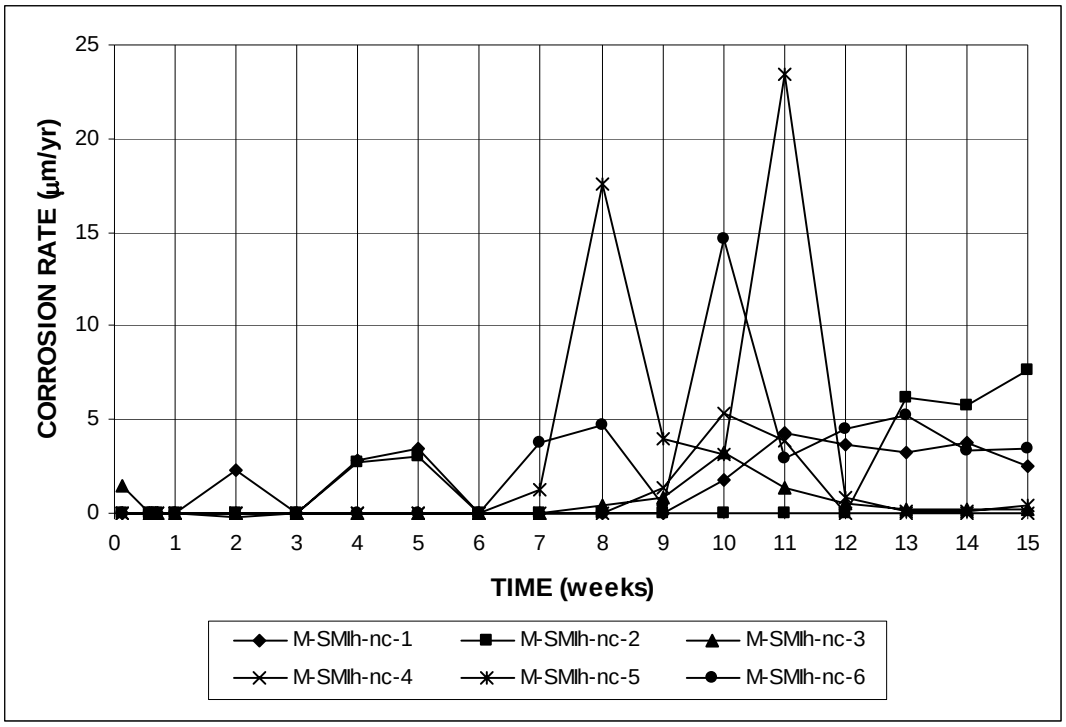

Figure A.33 – Macrocell Test. Corrosion rate (based on total area). Bare SMI steel without cap in 6.04 m ion NaCl and simulated concrete pore solution

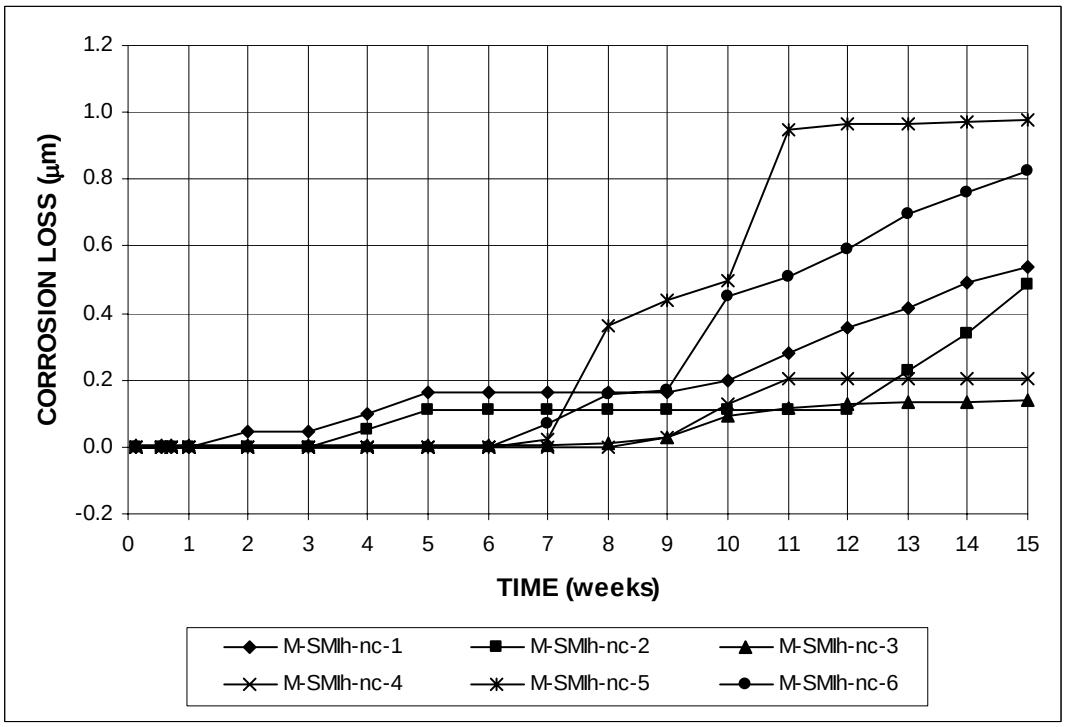

Figure A.34 – Macrocell Test. Corrosion loss (based on total area). Bare SMI steel without cap in 6.04 m ion NaCl and simulated concrete pore solution

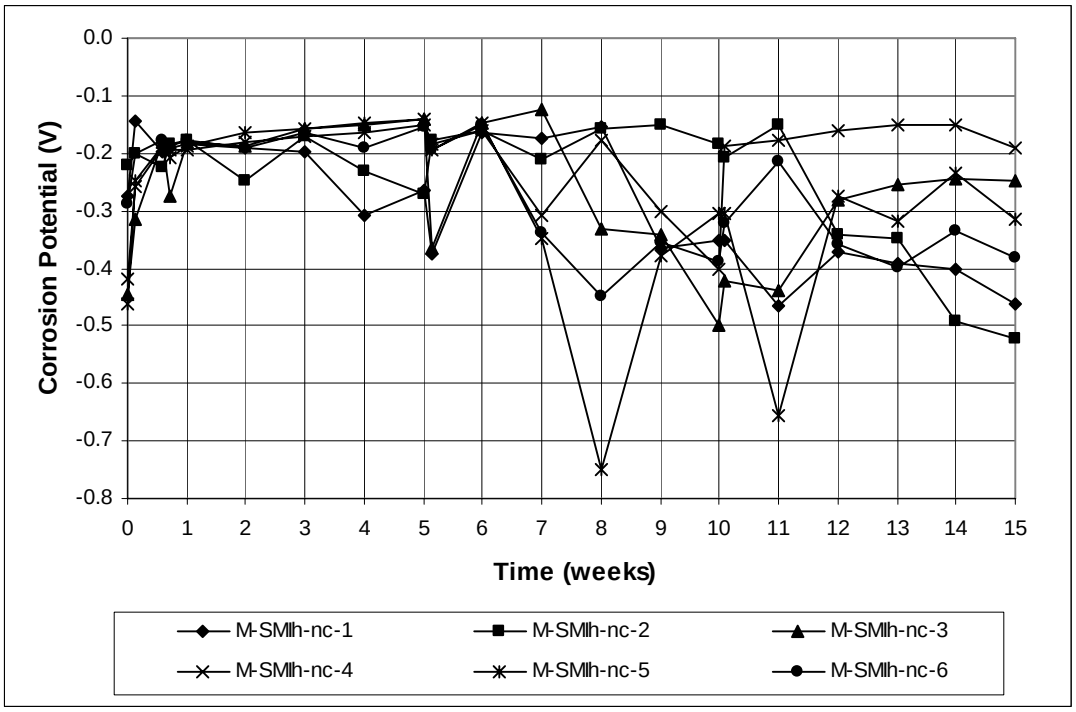

Figure A.35 – Macrocell Test. Anode corrosion potential vs. saturated calomel electrode. Bare SMI steel without cap in 6.04 m ion NaCl and simulated concrete pore solution

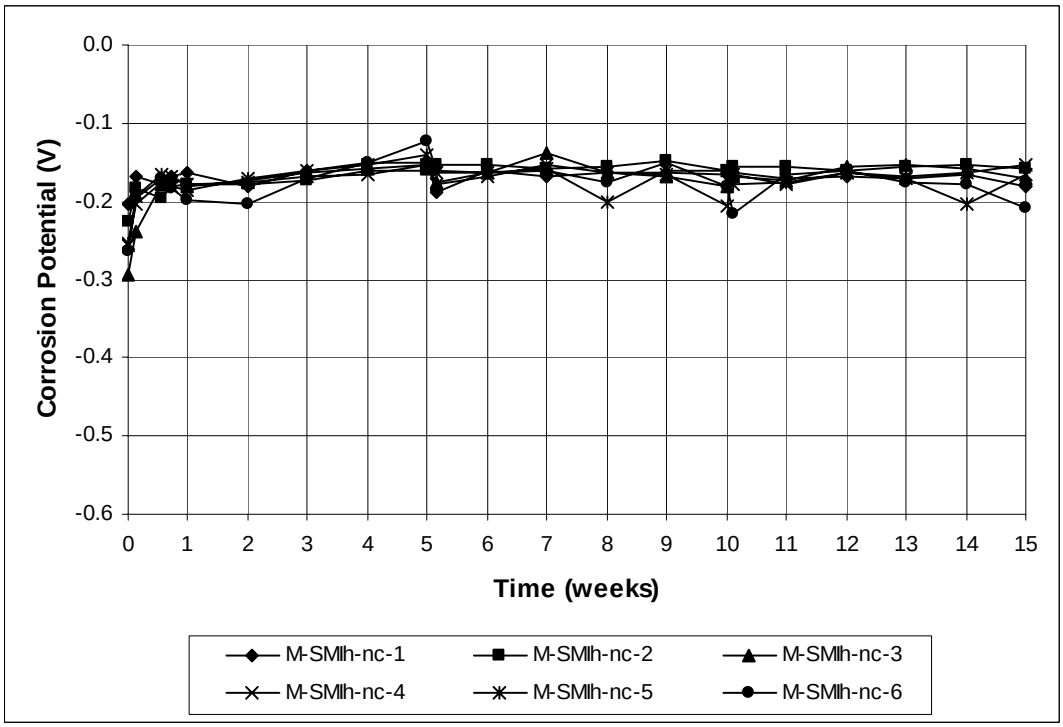

Figure A.36 – Macrocell Test. Cathode corrosion potential vs. saturated calomel electrode. Bare SMI steel without cap in 6.04 m ion NaCl and simulated concrete pore solution

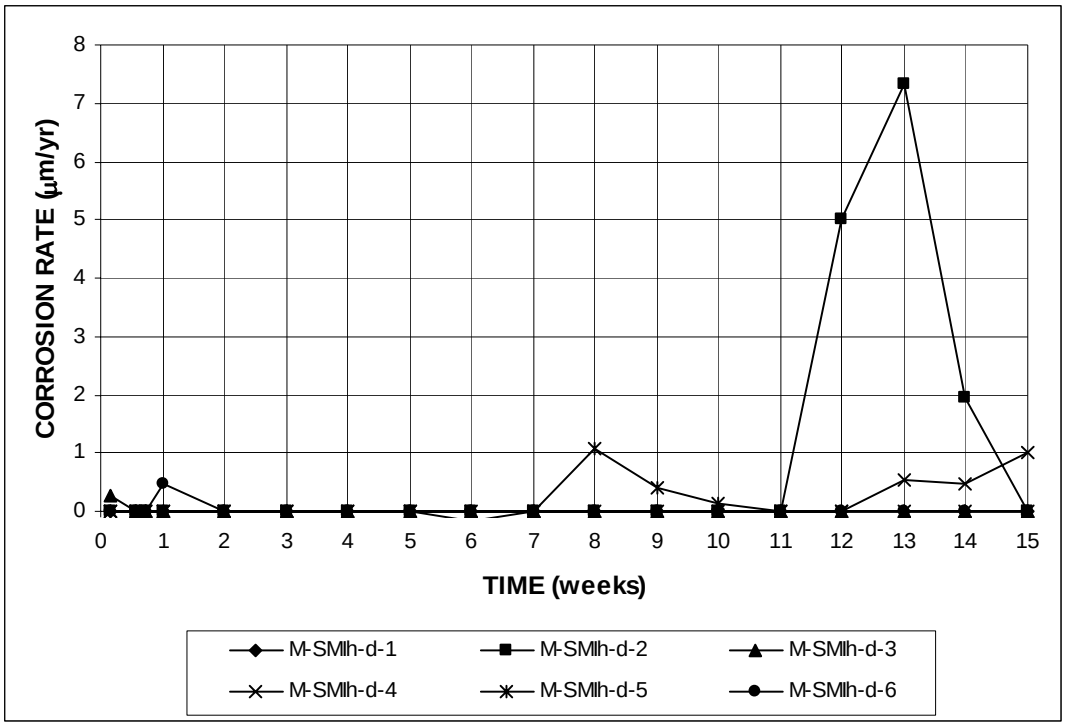

Figure A.37 – Macrocell Test. Corrosion rate (based on total area). Bare SMI steel with four drilled holes in 6.04 m ion NaCl and simulated concrete pore solution

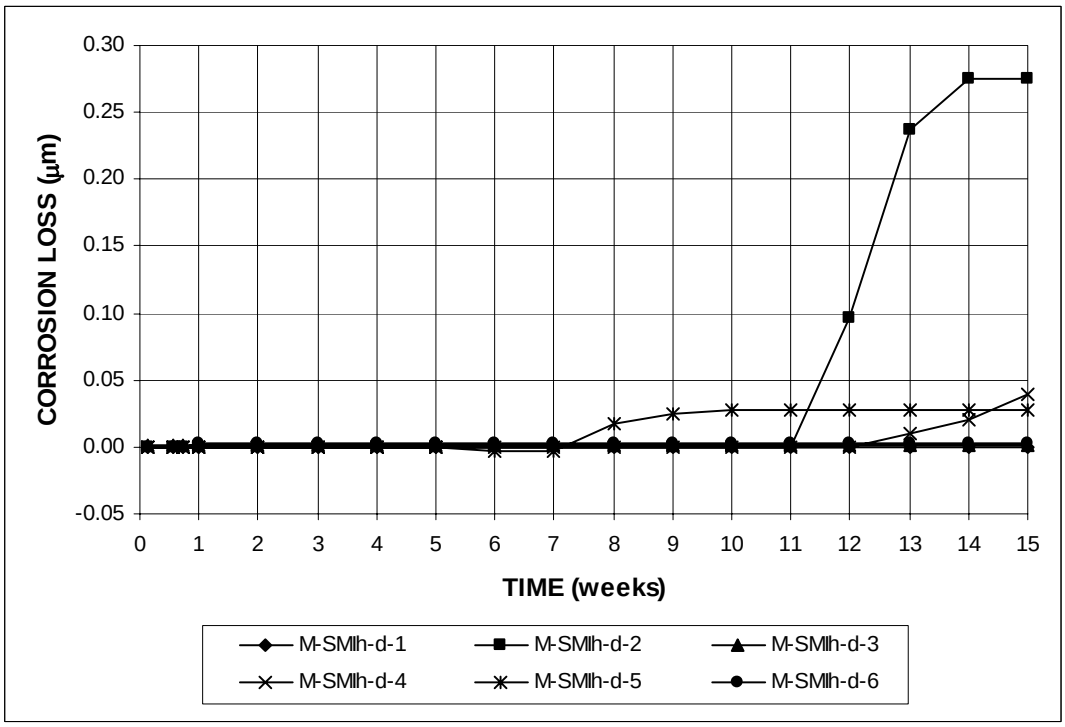

Figure A.38 – Macrocell Test. Corrosion loss (based on total area). Bare SMI steel with four drilled holes in 6.04 m ion NaCl and simulated concrete pore solution

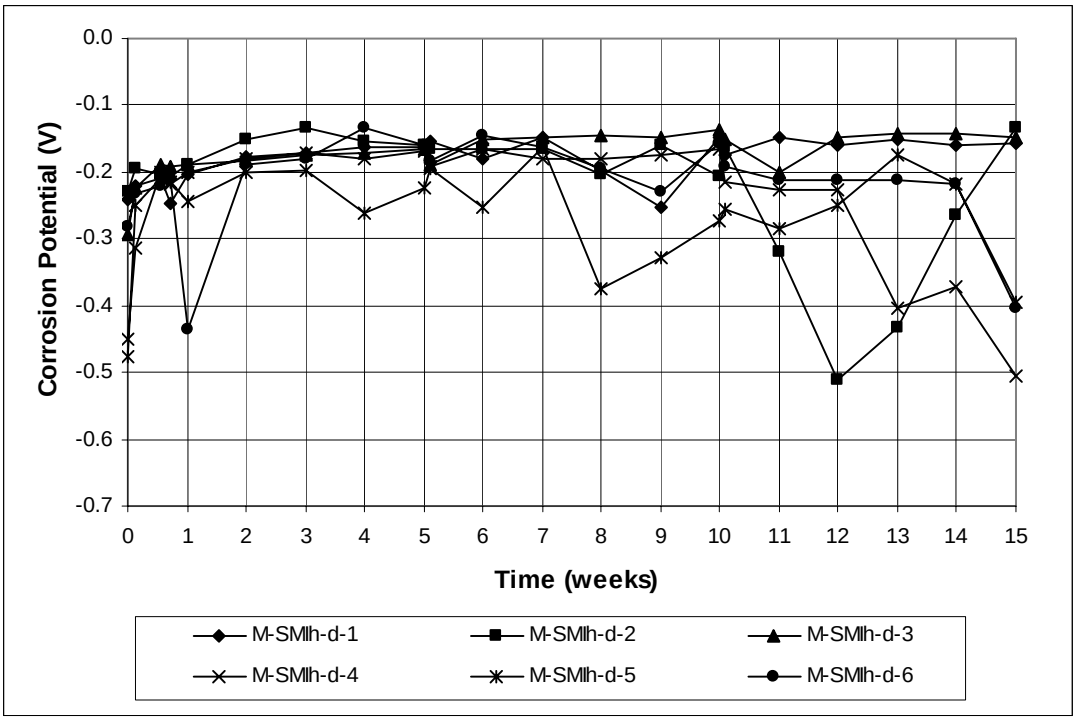

Figure A.39 – Macrocell Test. Anode corrosion potential vs. saturated calomel electrode. Bare SMI steel with four drilled holes in 6.04 m ion NaCl and simulated concrete pore solution

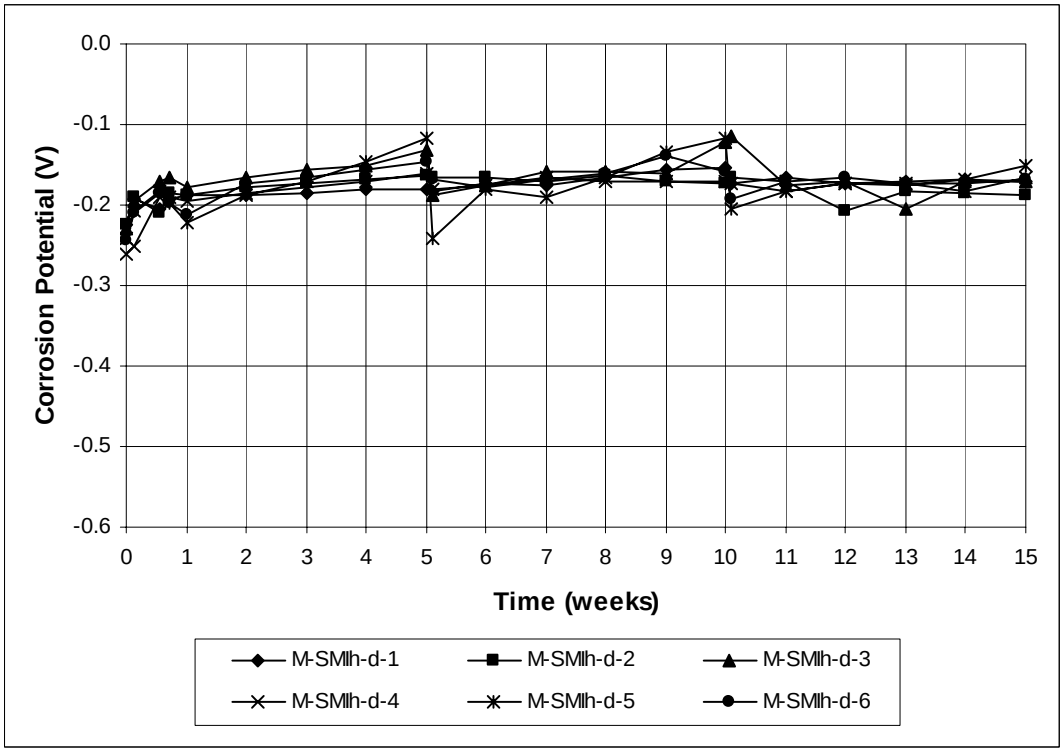

Figure A.40 – Macrocell Test. Cathode corrosion potential vs. saturated calomel electrode. Bare SMI steel with four drilled holes in 6.04 m ion NaCl and simulated concrete pore solution

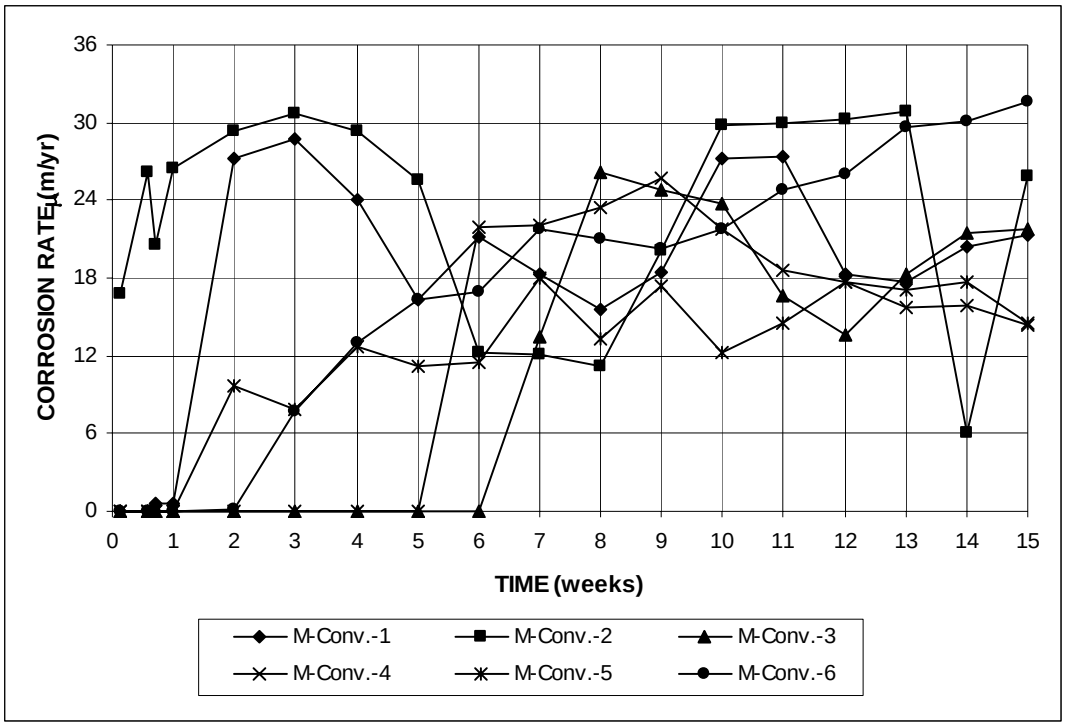

Figure A.41 – Macrocell Test. Corrosion rate (based on total area). Mortar-wrapped conventional steel in 1.6 m ion NaCl and simulated concrete pore solution

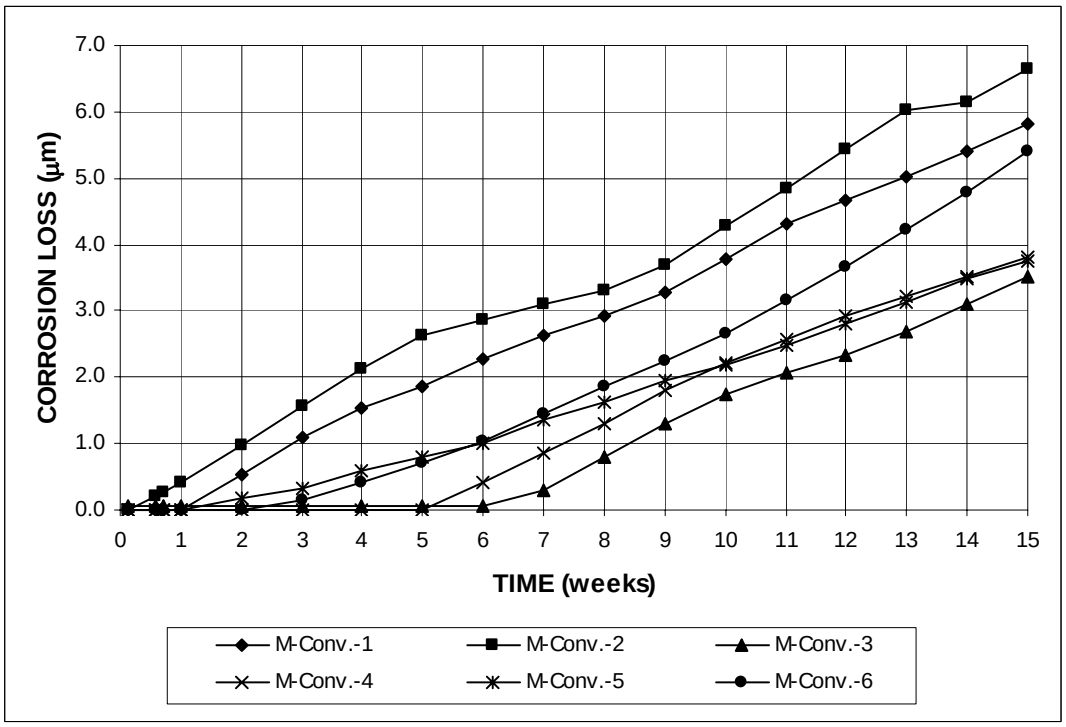

Figure A.42 – Macrocell Test. Corrosion loss (based on total area). Mortar-wrapped conventional steel in 1.6 m ion NaCl and simulated concrete pore solution

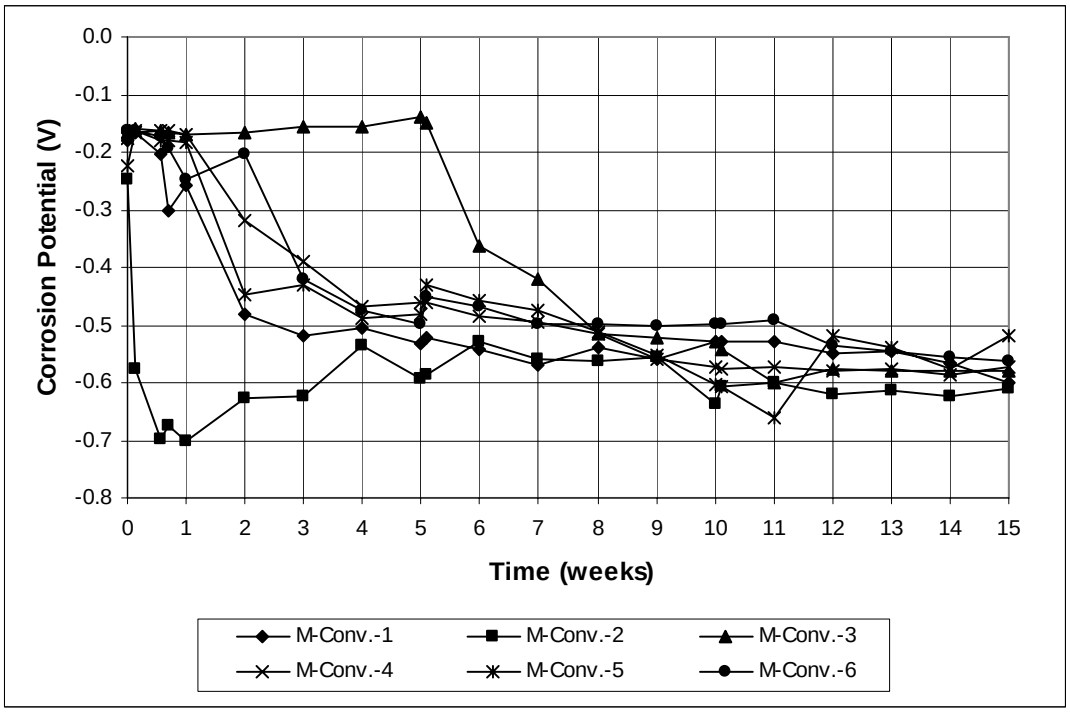

Figure A.43 – Macrocell Test. Anode corrosion potential vs. saturated calomel electrode. Mortar-wrapped conventional steel in 1.6 m ion NaCl and simulated concrete pore solution

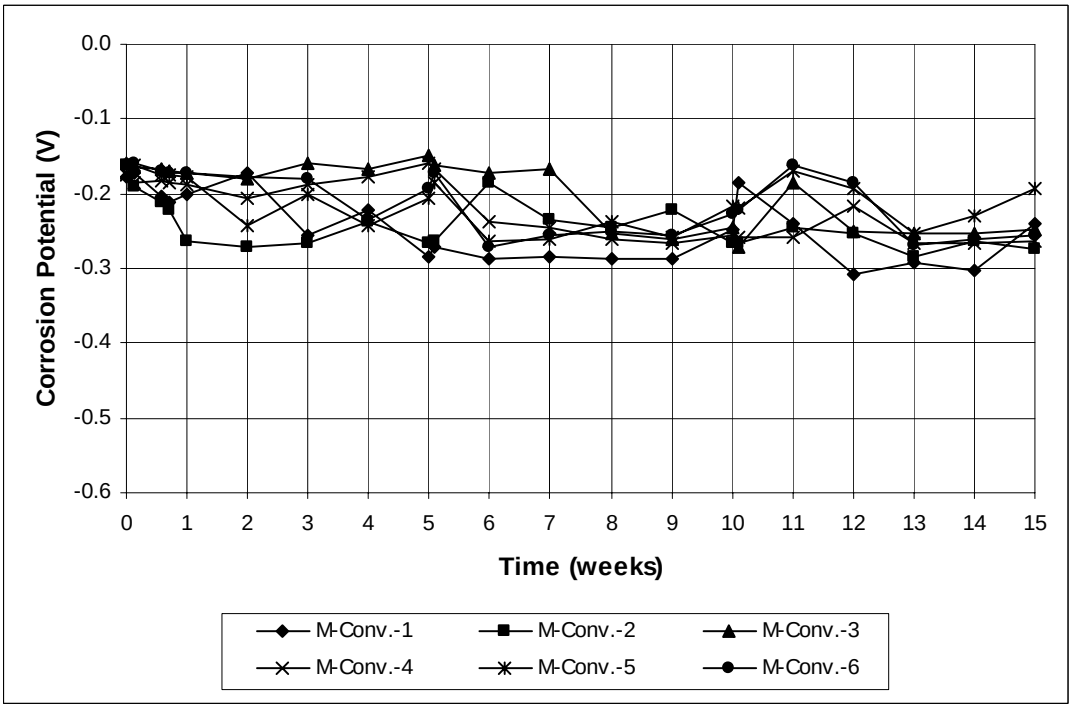

Figure A.44 – Macrocell Test. Cathode corrosion potential vs. saturated calomel electrode. Mortar-wrapped conventional steel in 1.6 m ion NaCl and simulated concrete pore solution

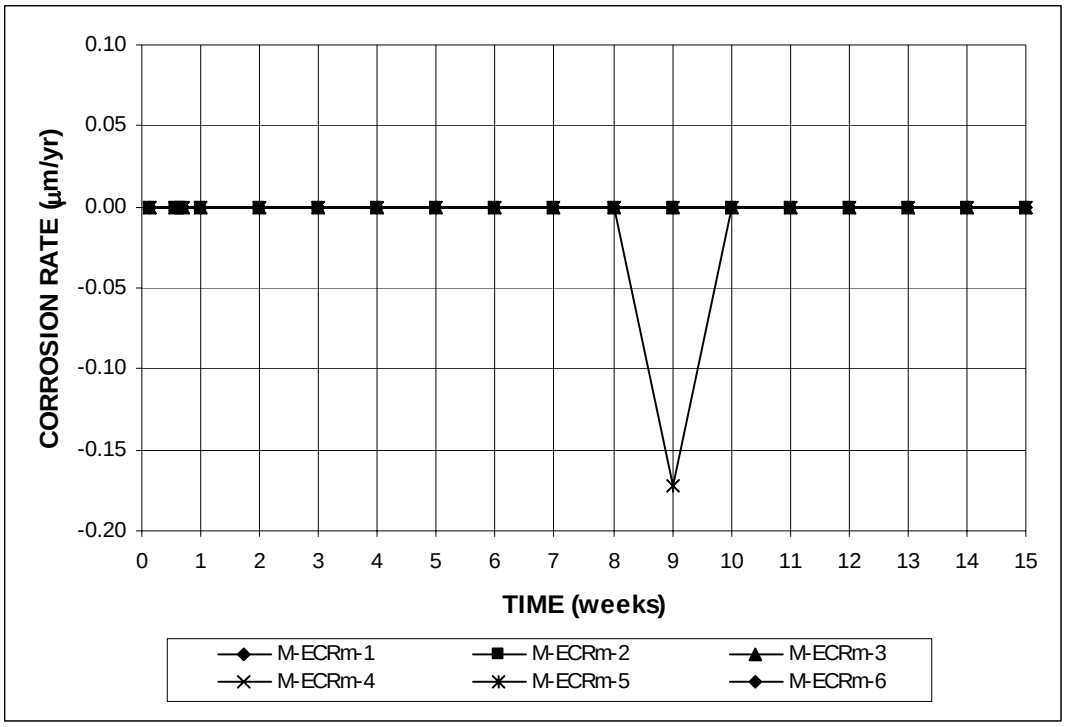

Figure A.45 – Macrocell Test. Corrosion rate (based on total area). Mortar-wrapped epoxy-coated steel with four drilled holes in 1.6 m ion NaCl and simulated concrete pore solution

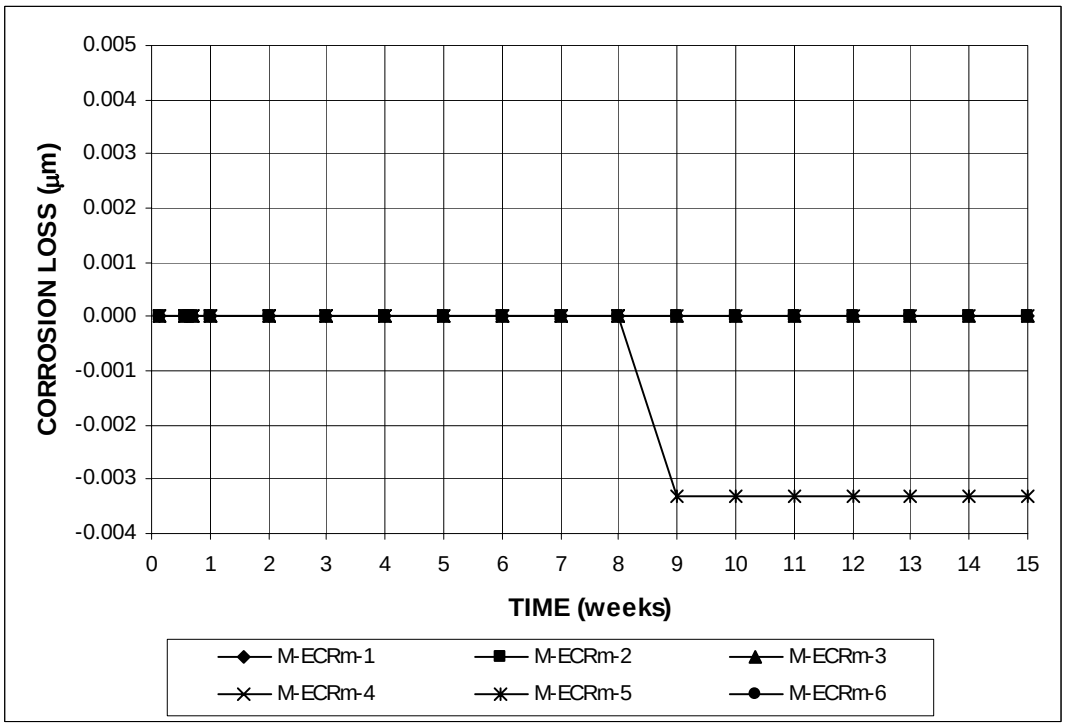

Figure A.46 – Macrocell Test. Corrosion loss (based on total area). Mortar-wrapped epoxy-coated steel with four drilled holes in 1.6 m ion NaCl and simulated concrete pore solution

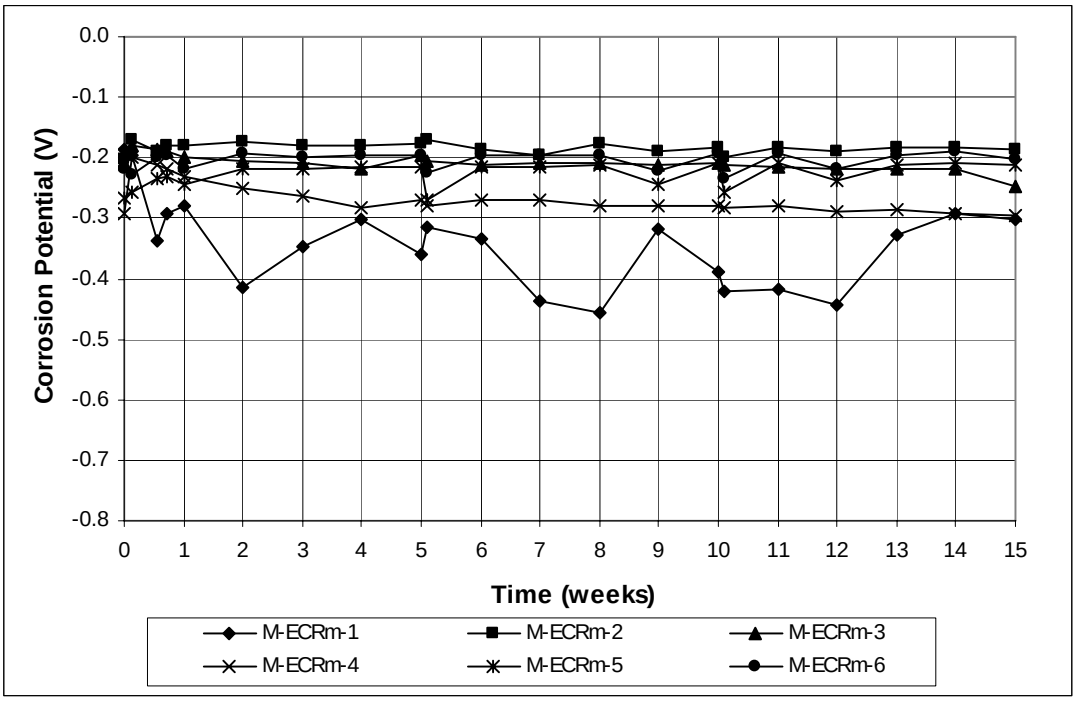

Figure A.47 – Macrocell Test. Anode corrosion potential vs. saturated calomel electrode. Mortar-wrapped epoxy-coated steel with four drilled holes in 1.6 m ion NaCl and simulated concrete pore solution

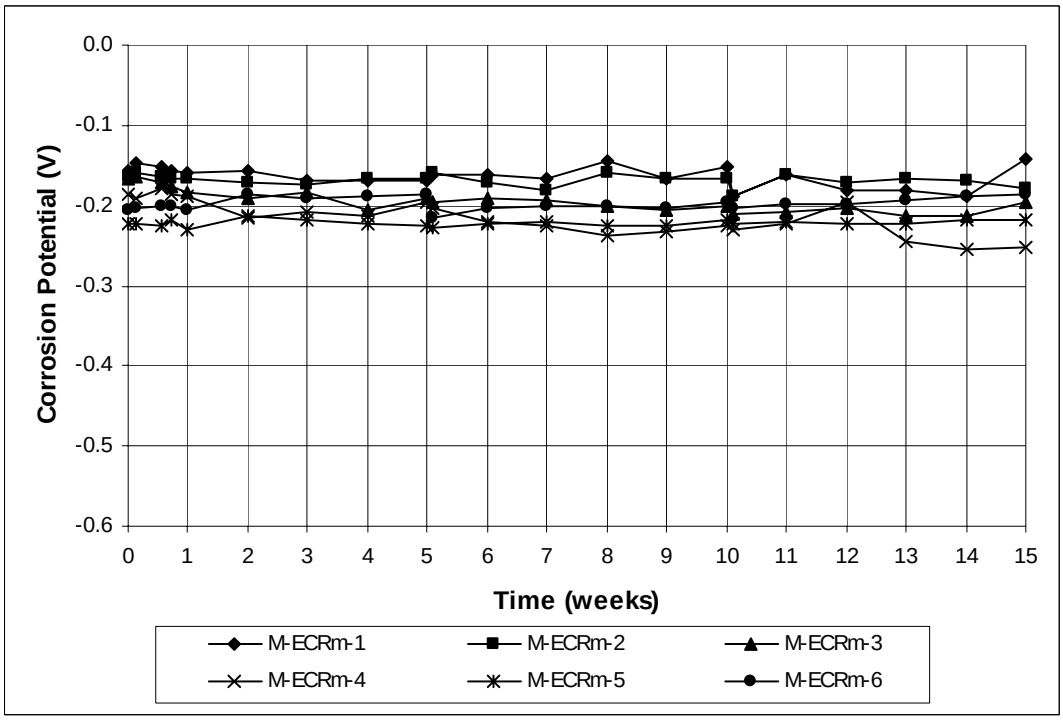

Figure A.48 – Macrocell Test. Cathode corrosion potential vs. saturated calomel electrode. Mortar-wrapped epoxy-coated steel with four drilled holes in 1.6 m ion NaCl and simulated concrete pore solution

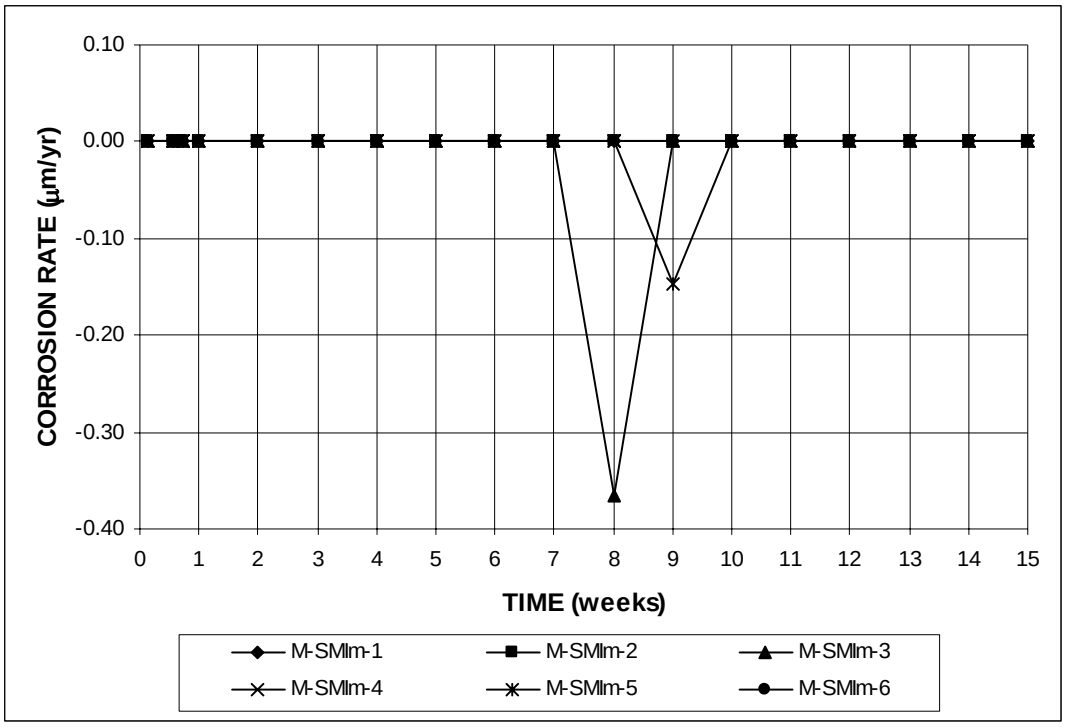

Figure A.49 – Macrocell Test. Corrosion rate (based on total area). Mortar-wrapped SMI steel with cap in 1.6 m ion NaCl and simulated concrete pore solution

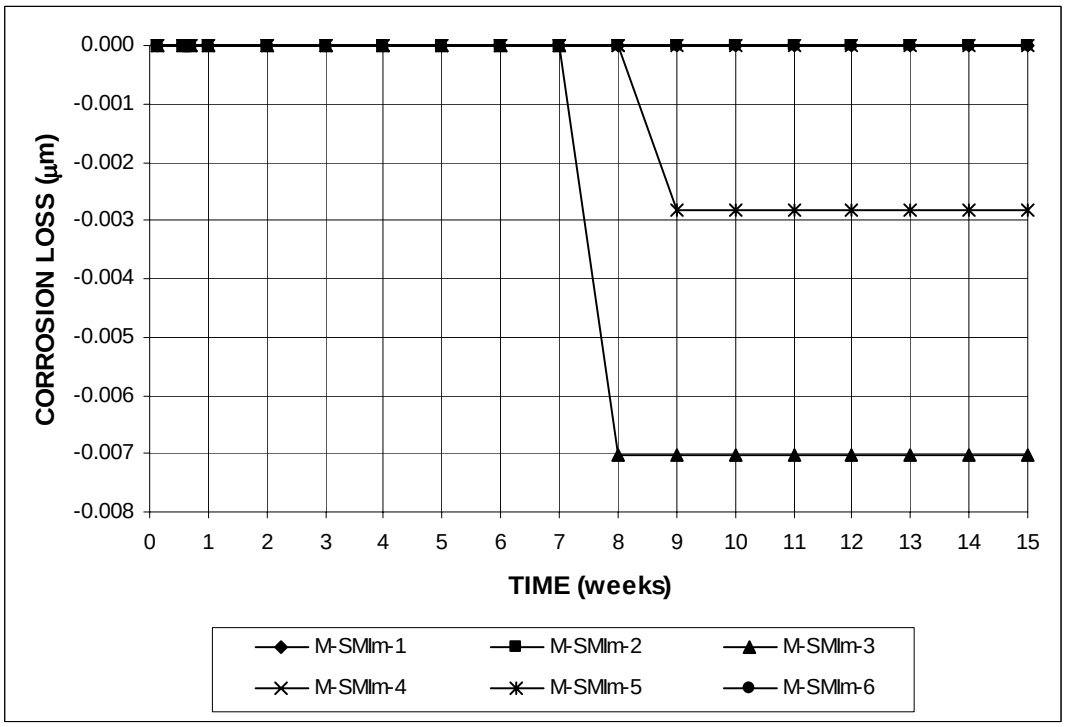

Figure A.50 – Macrocell Test. Corrosion loss (based on total area). Mortar-wrapped SMI steel with cap in 1.6 m ion NaCl and simulated concrete pore solution

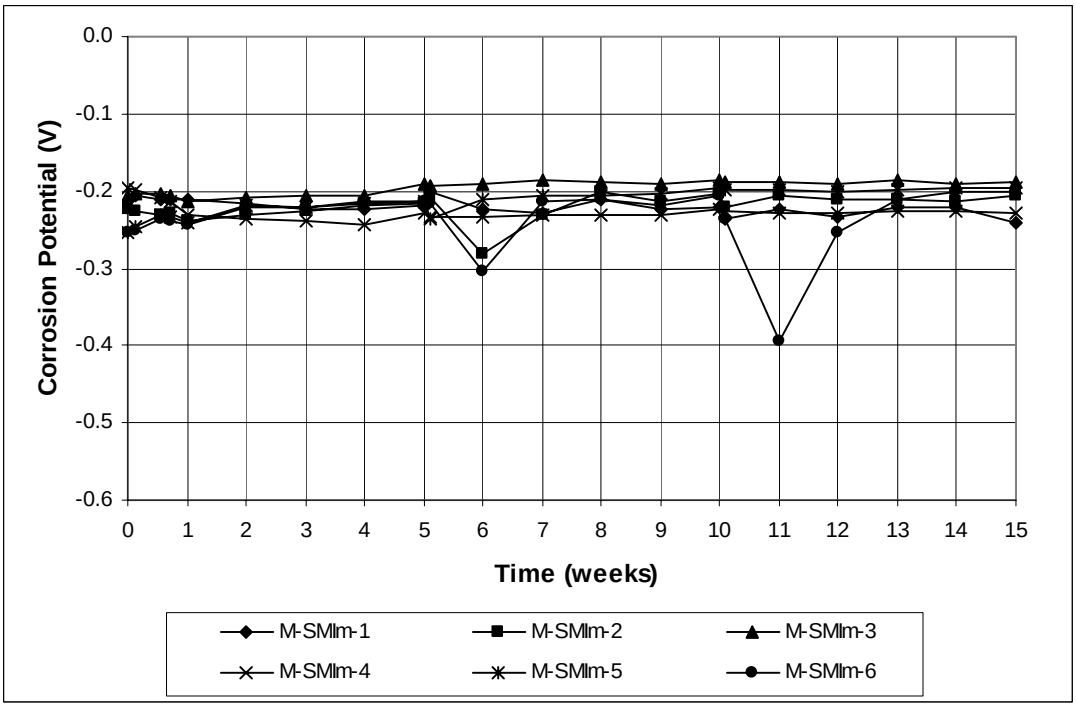

Figure A.51 – Macrocell Test. Anode corrosion potential vs. saturated calomel electrode. Mortar-wrapped SMI steel with cap in 1.6 m ion NaCl and simulated concrete pore solution

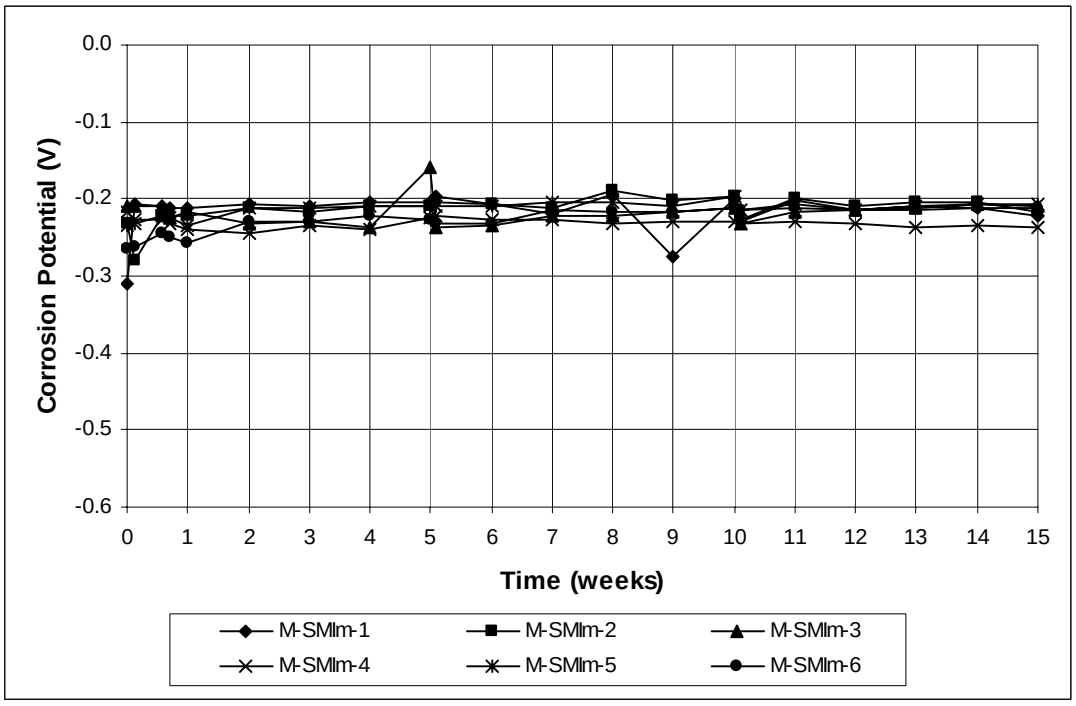

Figure A.52 – Macrocell Test. Cathode corrosion potential vs. saturated calomel electrode. Mortar-wrapped SMI steel with cap in 1.6 m ion NaCl and simulated concrete pore solution

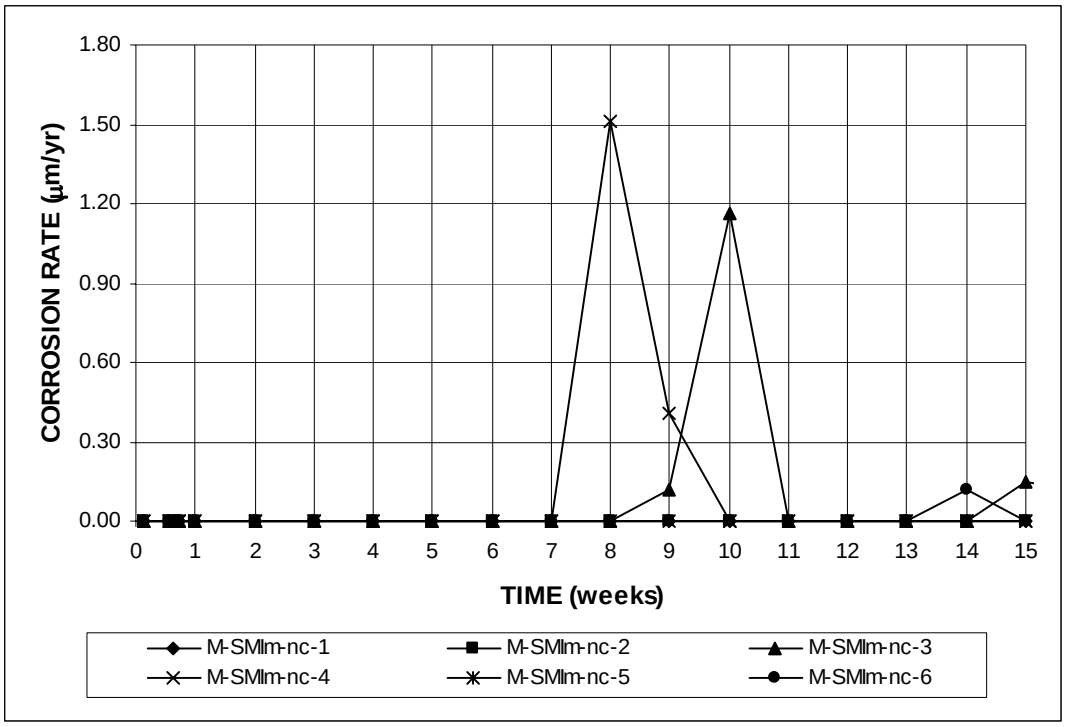

Figure A.53 – Macrocell Test. Corrosion rate (based on total area). Mortar-wrapped SMI steel without cap in 1.6 m ion NaCl and simulated concrete pore solution

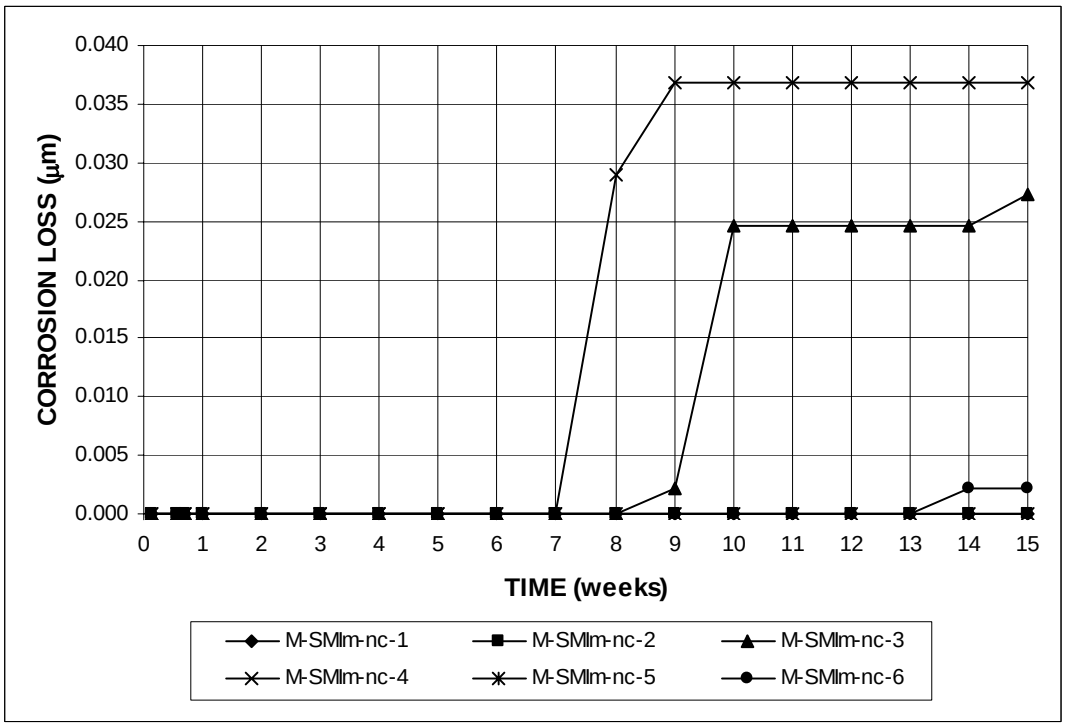

Figure A.54 – Macrocell Test. Corrosion loss (based on total area). Mortar-wrapped SMI steel without cap in 1.6 m ion NaCl and simulated concrete pore solution

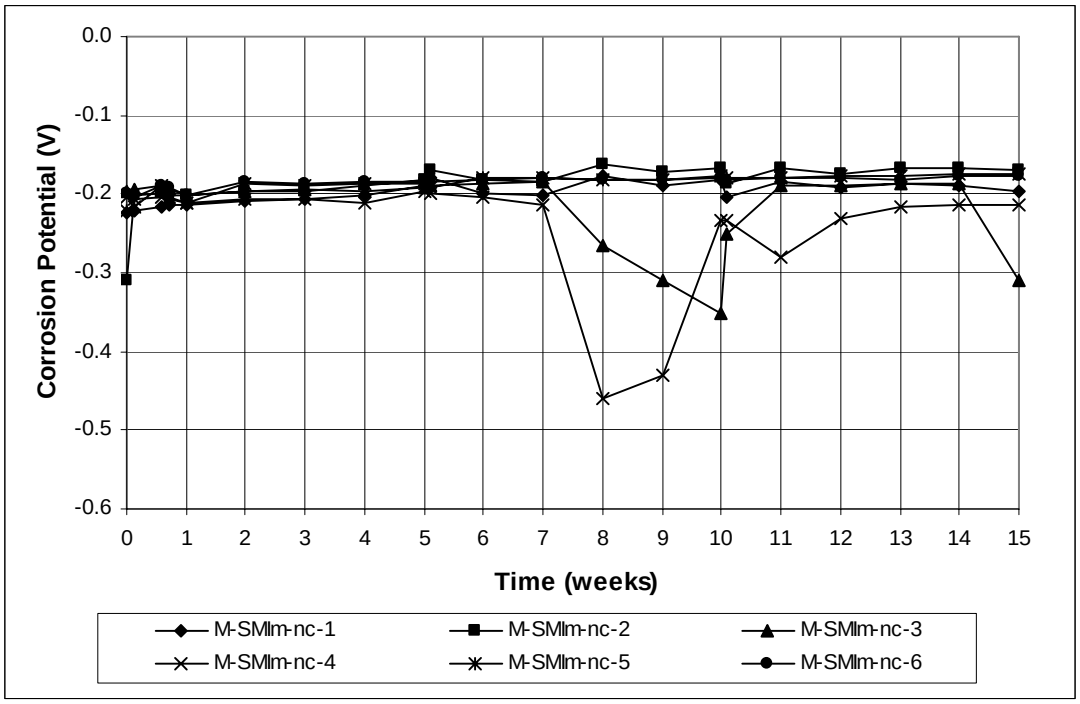

Figure A.55 – Macrocell Test. Anode corrosion potential vs. saturated calomel electrode. Mortar-wrapped SMI steel without cap in 1.6 m ion NaCl and simulated concrete pore solution

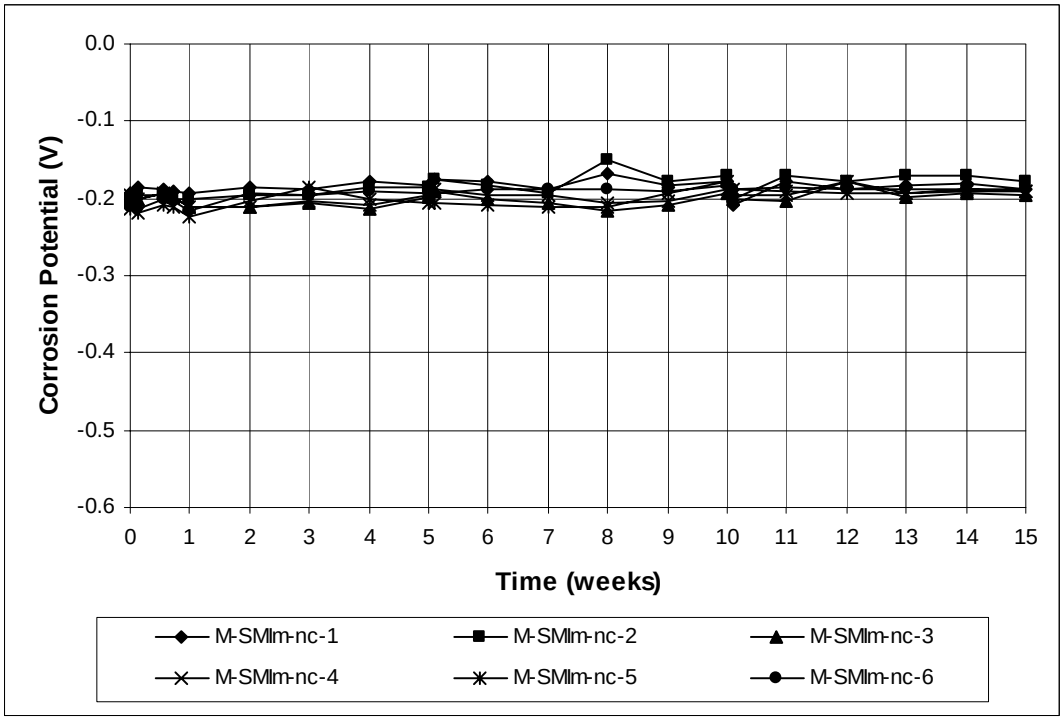

Figure A.56 – Macrocell Test. Cathode corrosion potential vs. saturated calomel electrode. Mortar-wrapped SMI steel without cap in 1.6 m ion NaCl and simulated concrete pore solution

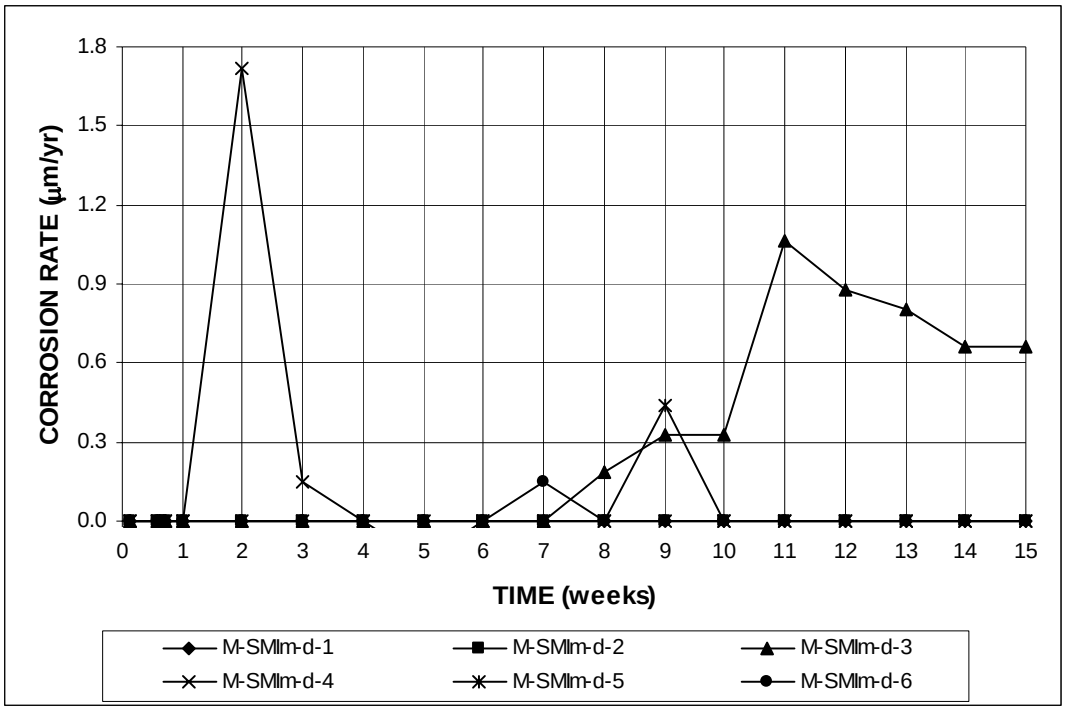

Figure A.57 – Macrocell Test. Corrosion rate (based on total area). Mortar-wrapped SMI steel with four drilled holes in 1.6 m ion NaCl and simulated concrete pore solution

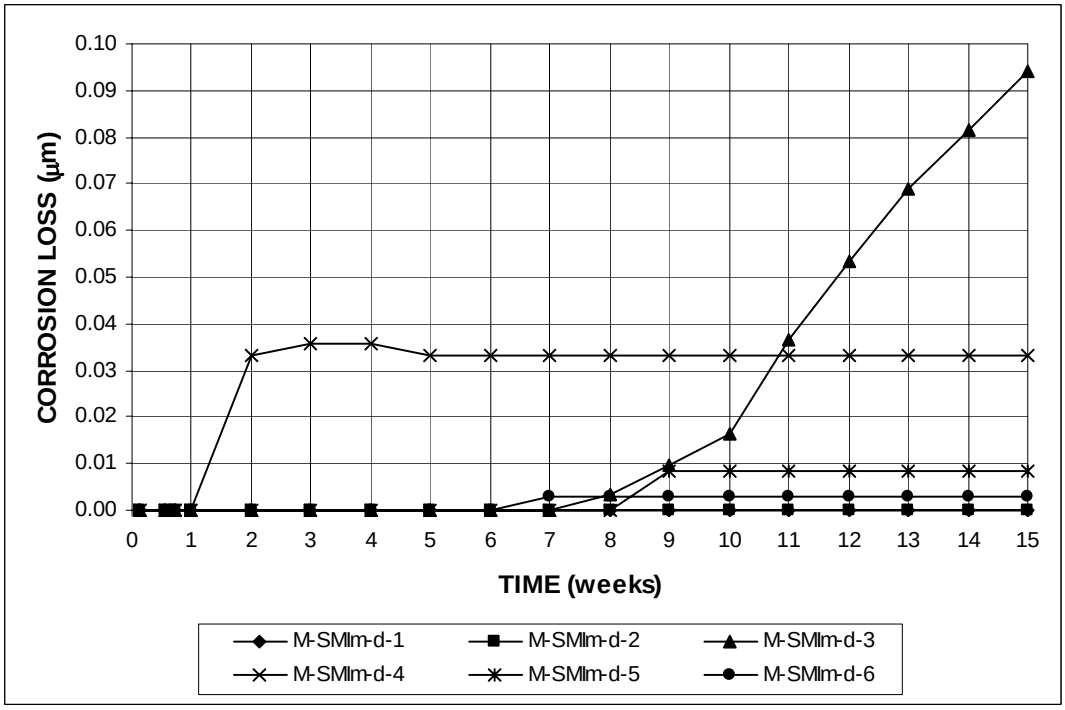

Figure A.58 – Macrocell Test. Corrosion loss (based on total area). Mortar-wrapped SMI steel with four drilled holes in 1.6 m ion NaCl and simulated concrete pore solution

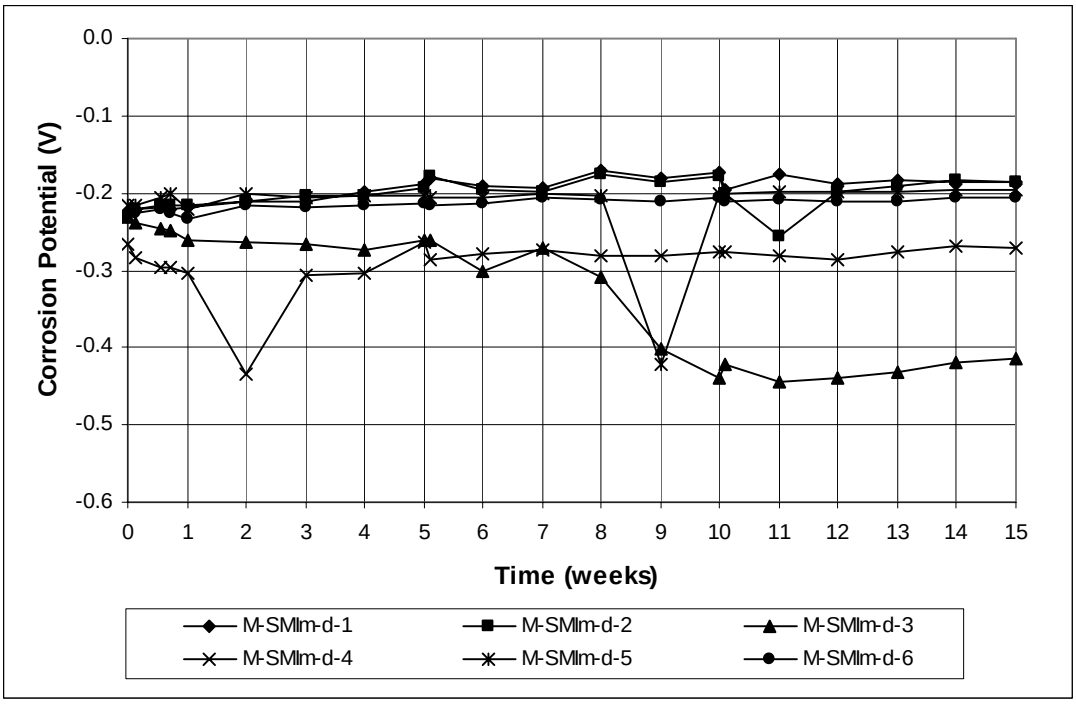

Figure A.59 – Macrocell Test. Anode corrosion potential vs. saturated calomel electrode. Mortar-wrapped SMI steel with four drilled holes in 1.6 m ion NaCl and simulated concrete pore solution

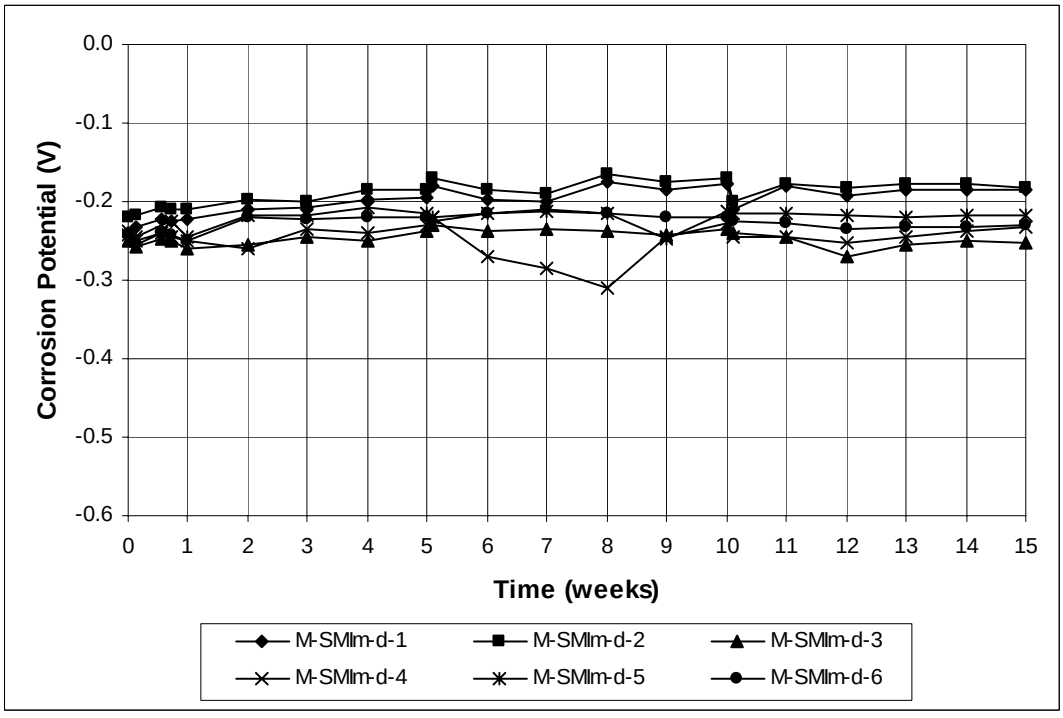

Figure A.60 – Macrocell Test. Cathode corrosion potential vs. saturated calomel electrode. Mortar-wrapped SMI steel with four drilled holes in 1.6 m ion NaCl and simulated concrete pore solution

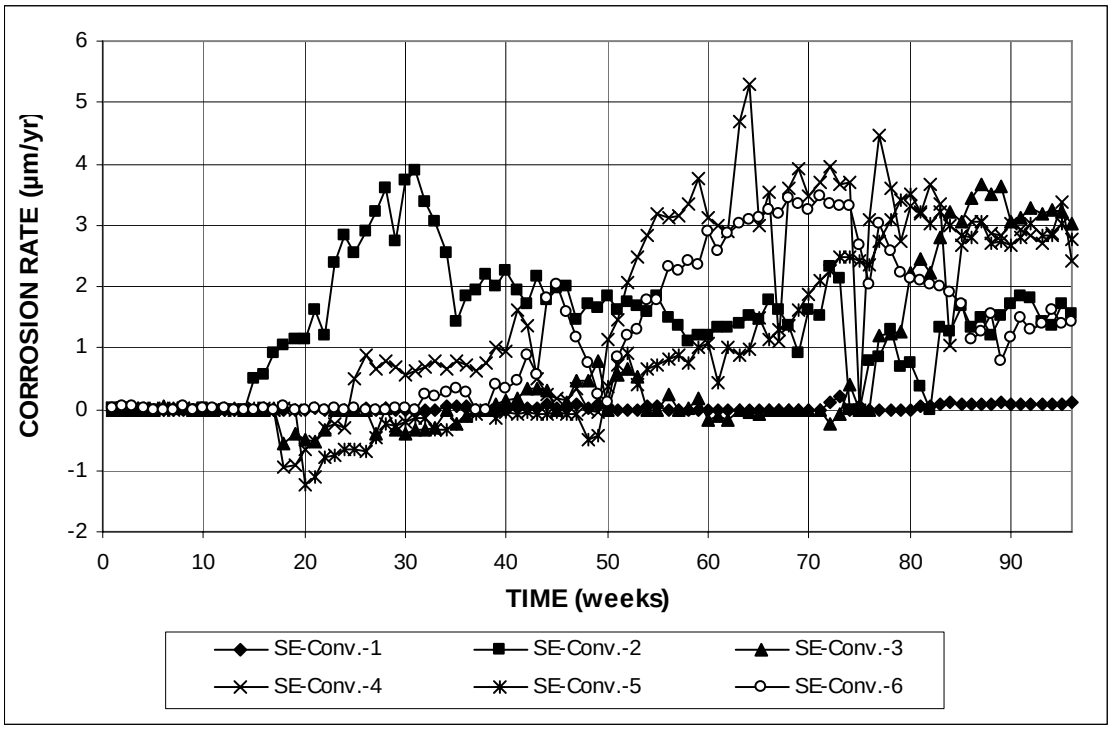

Figure A.61 – Southern Exposure Test. Corrosion rate (based on total area). Conventional steel

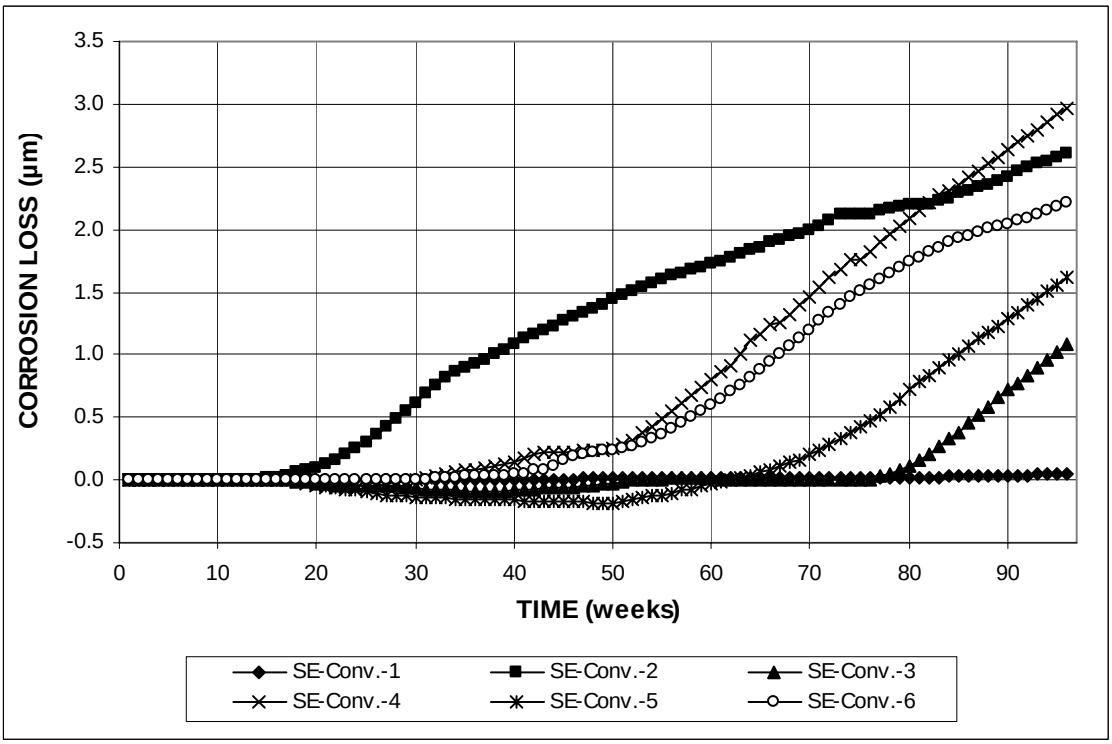

Figure A.62 – Southern Exposure Test. Corrosion loss (based on total area). Conventional steel

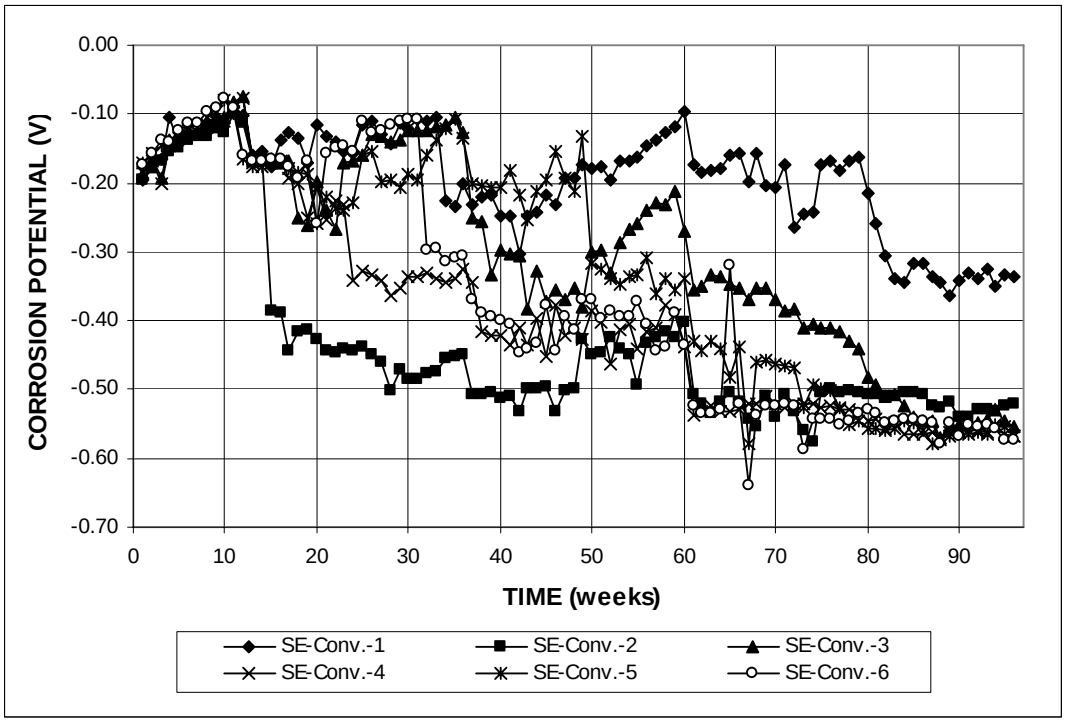

Figure A.63 – Southern Exposure Test. Top mat corrosion potential vs. copper-copper sulfate electrode. Conventional steel

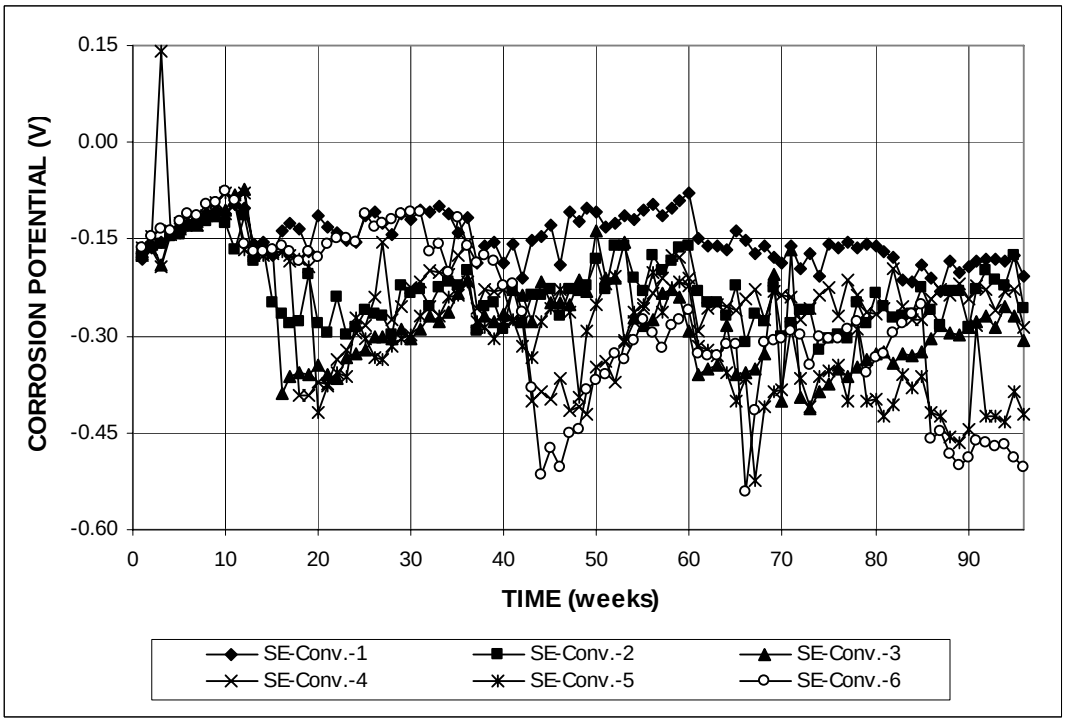

Figure A.64 – Southern Exposure Test. Bottom mat corrosion potential vs. copper-copper sulfate electrode. Conventional steel

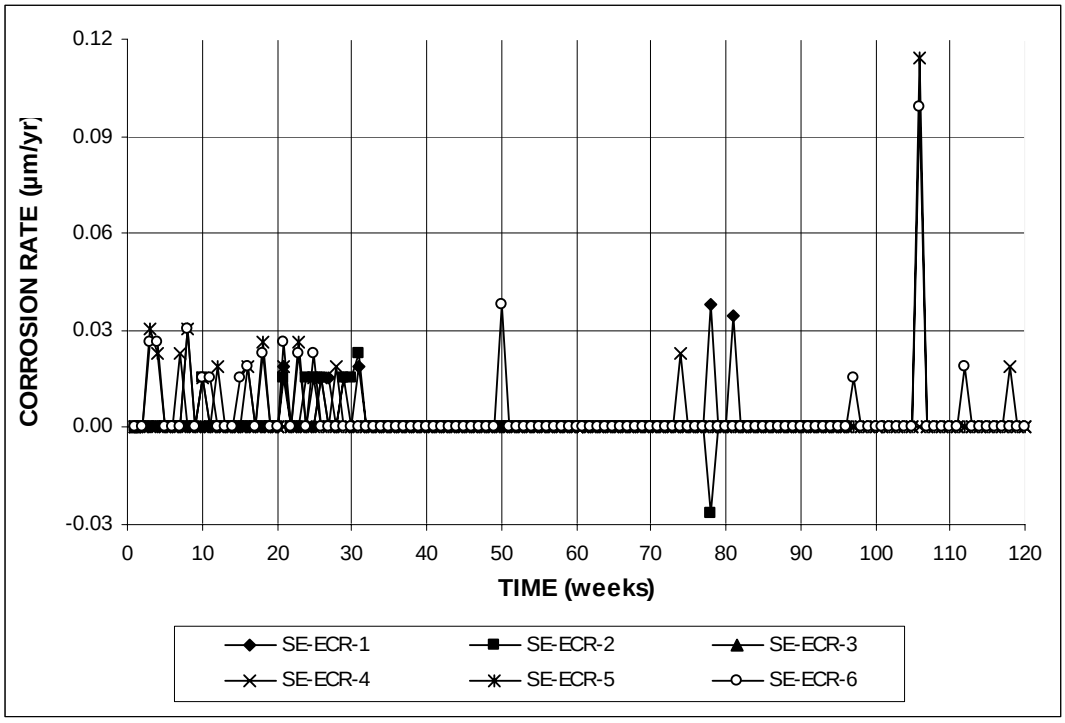

Figure A.65 – Southern Exposure Test. Corrosion rate (based on total area). Epoxy-coated steel with four drilled holes

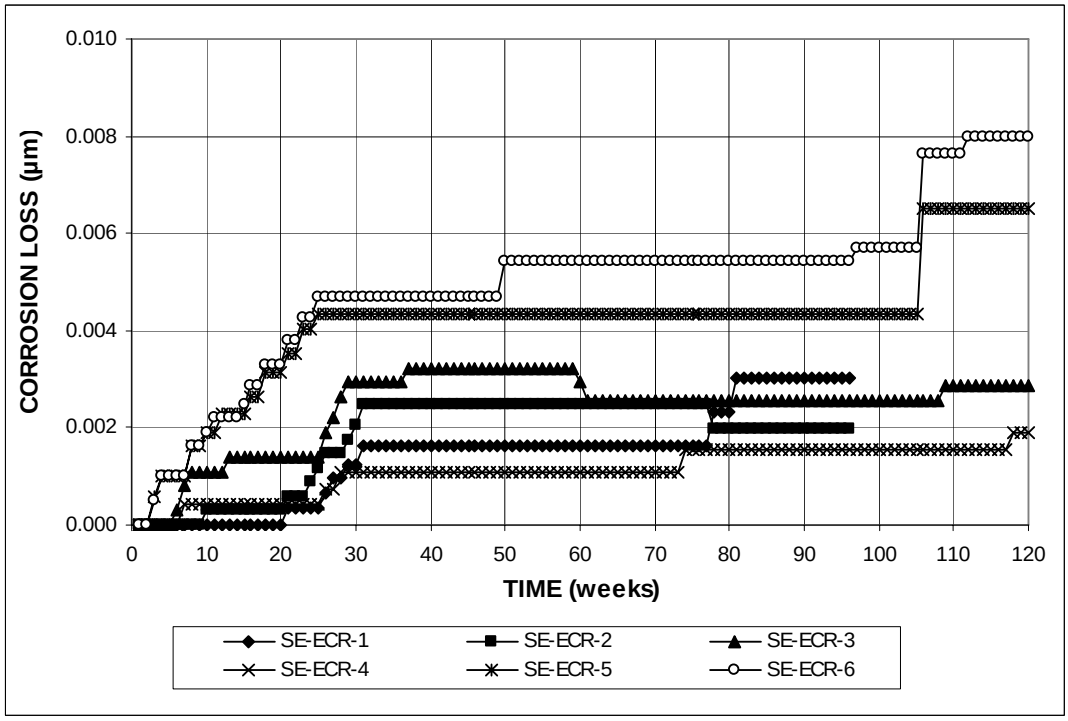

Figure A.66 – Southern Exposure Test. Corrosion loss (based on total area). Epoxy-coated steel with four drilled holes

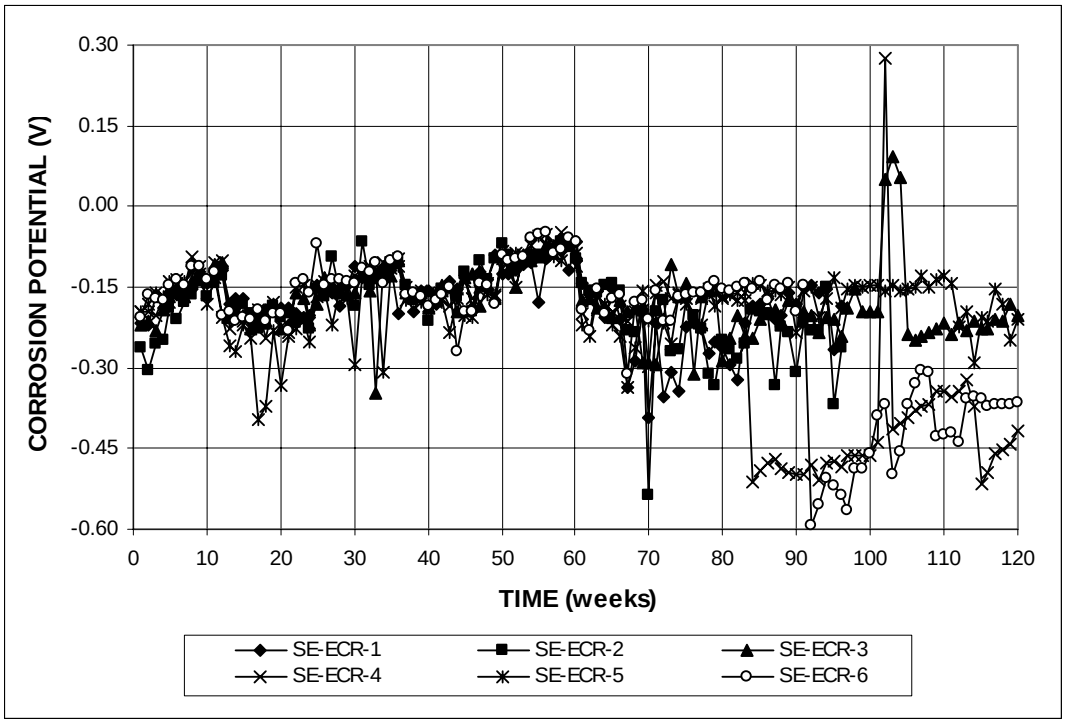

Figure A.67 – Southern Exposure Test. Top mat corrosion potential vs. copper-copper sulfate electrode. Epoxy-coated steel with four drilled holes

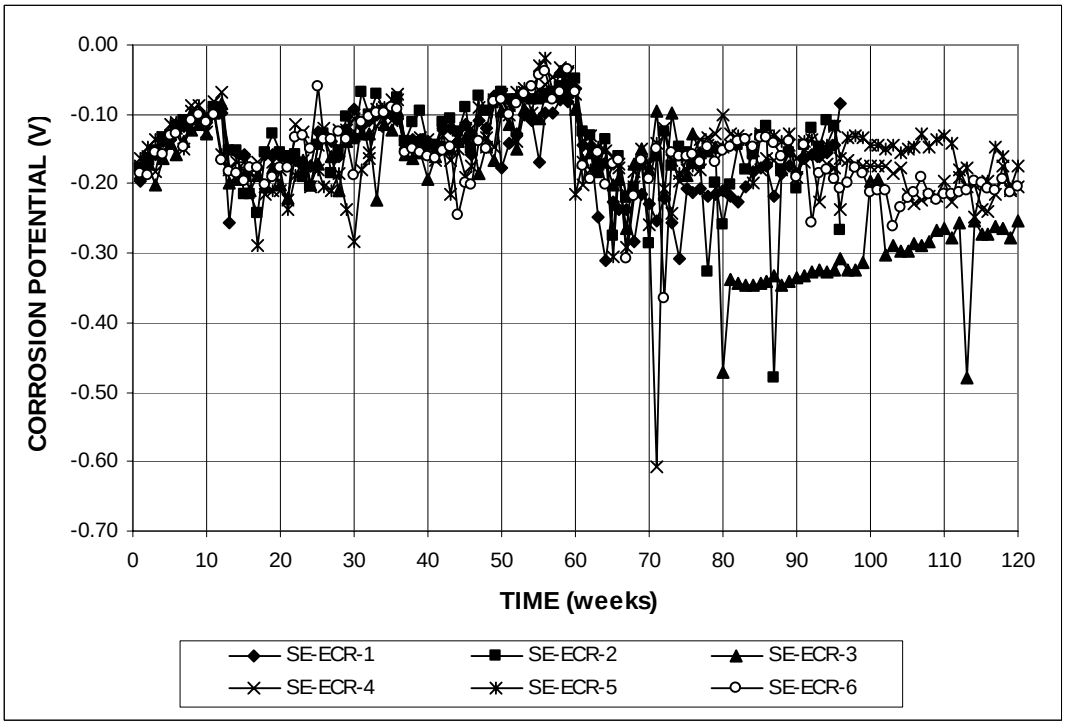

Figure A.68 – Southern Exposure Test. Bottom mat corrosion potential vs. copper-copper sulfate electrode. Epoxy-coated steel with four drilled holes

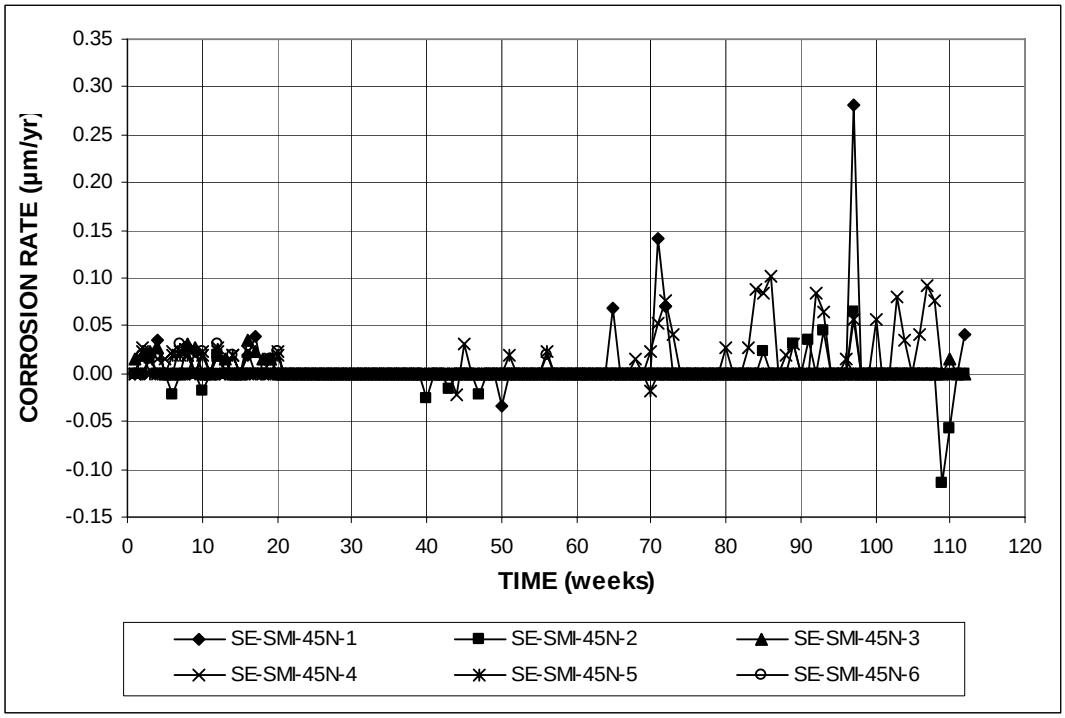

Figure A.69 – Southern Exposure Test. Corrosion rate (based on total area). SMI steel with intact cladding

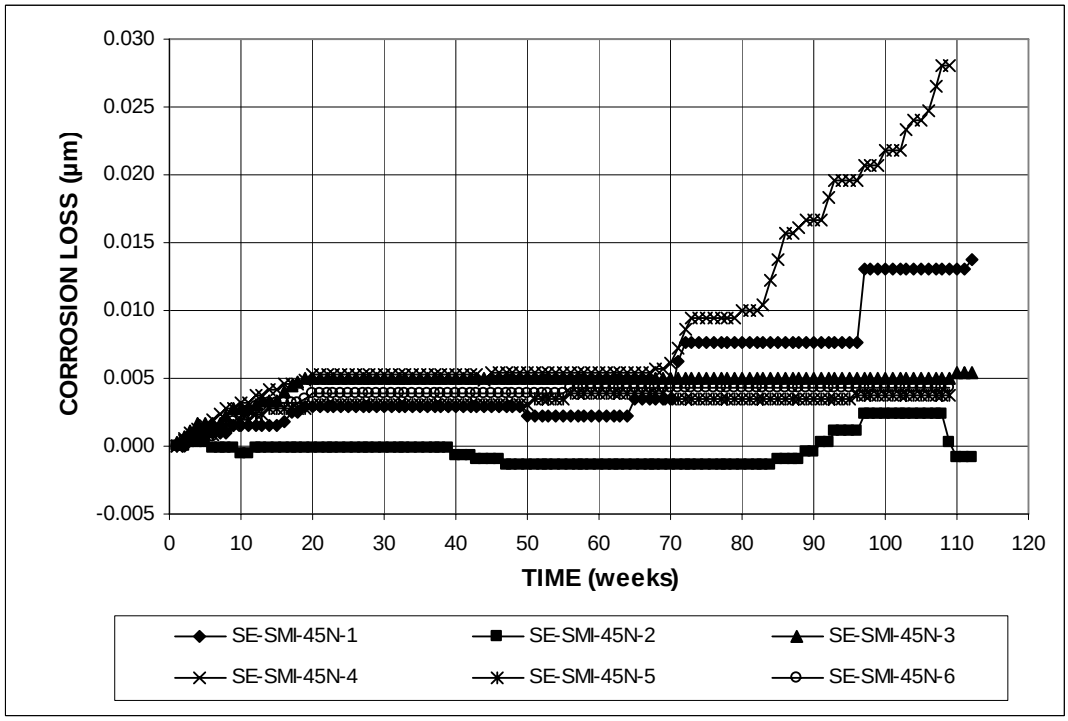

Figure A.70 – Southern Exposure Test. Corrosion loss (based on total area). SMI steel with intact cladding

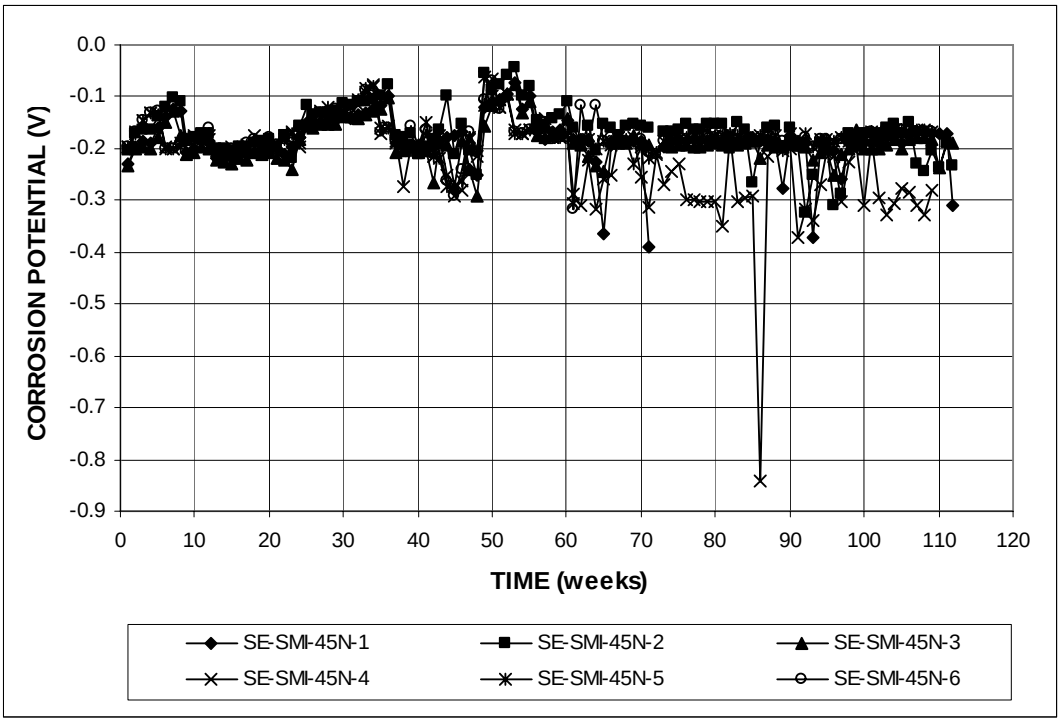

Figure A.71 – Southern Exposure Test. Top mat corrosion potential vs. copper-copper sulfate electrode. SMI steel with intact cladding

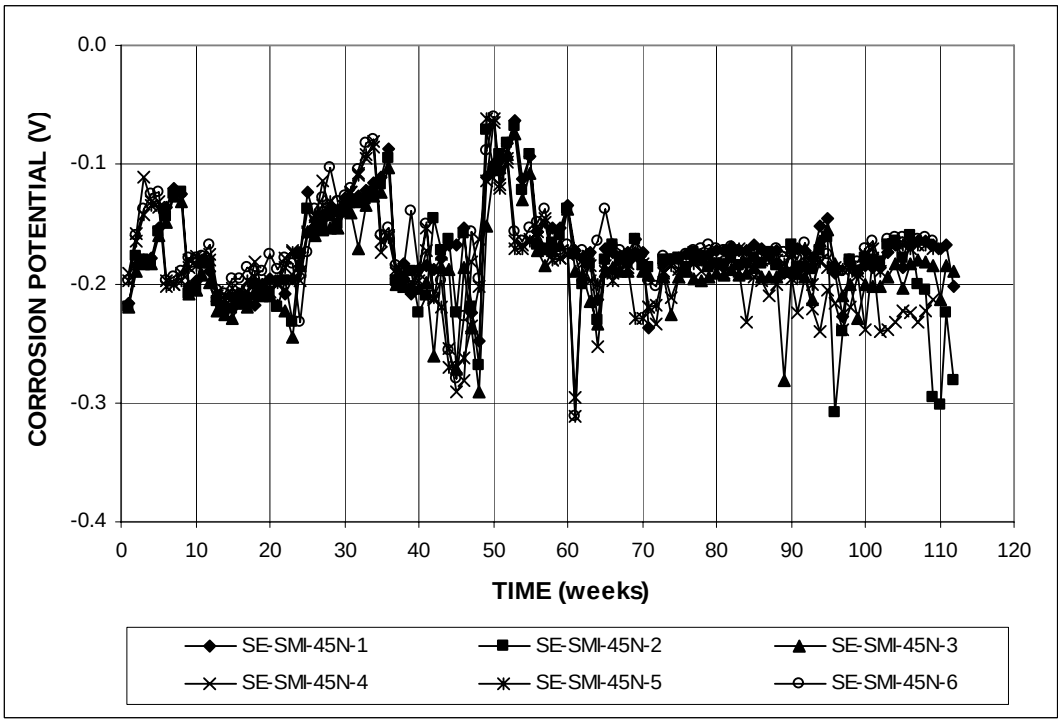

Figure A.72 – Southern Exposure Test. Bottom mat corrosion potential vs. copper-copper sulfate electrode. SMI steel with intact cladding

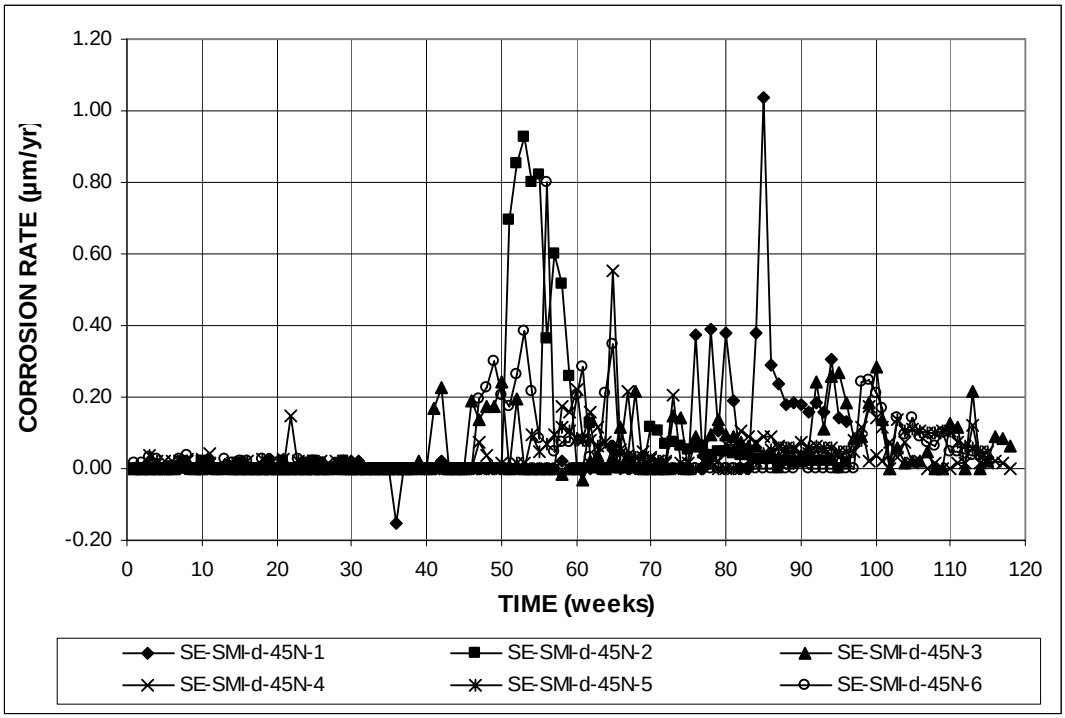

Figure A.73 – Southern Exposure Test. Corrosion rate (based on total area). SMI steel with four drilled holes

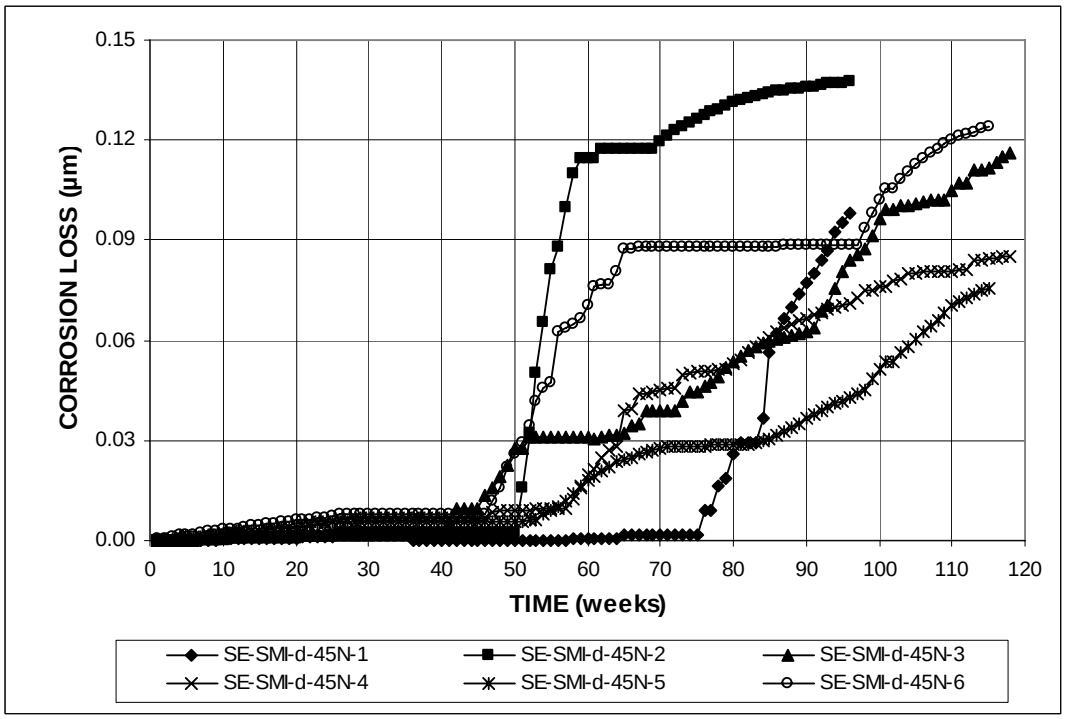

Figure A.74 – Southern Exposure Test. Corrosion loss (based on total area). SMI steel with four drilled holes

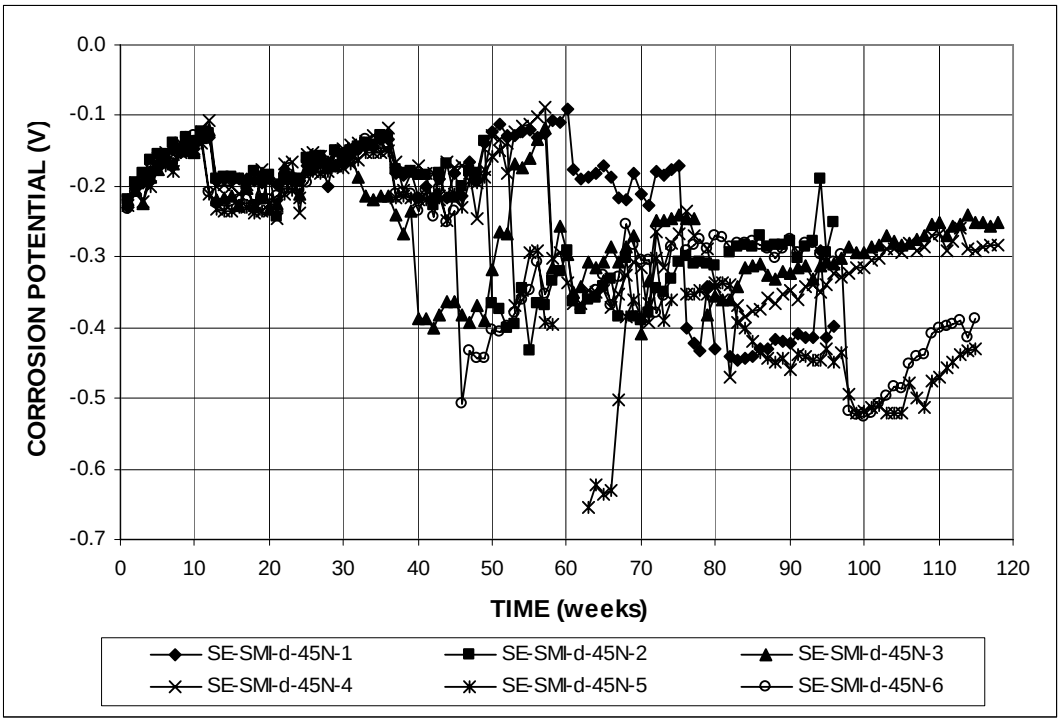

Figure A.75 – Southern Exposure Test. Top mat corrosion potential vs. copper-copper sulfate electrode. SMI steel with four drilled holes

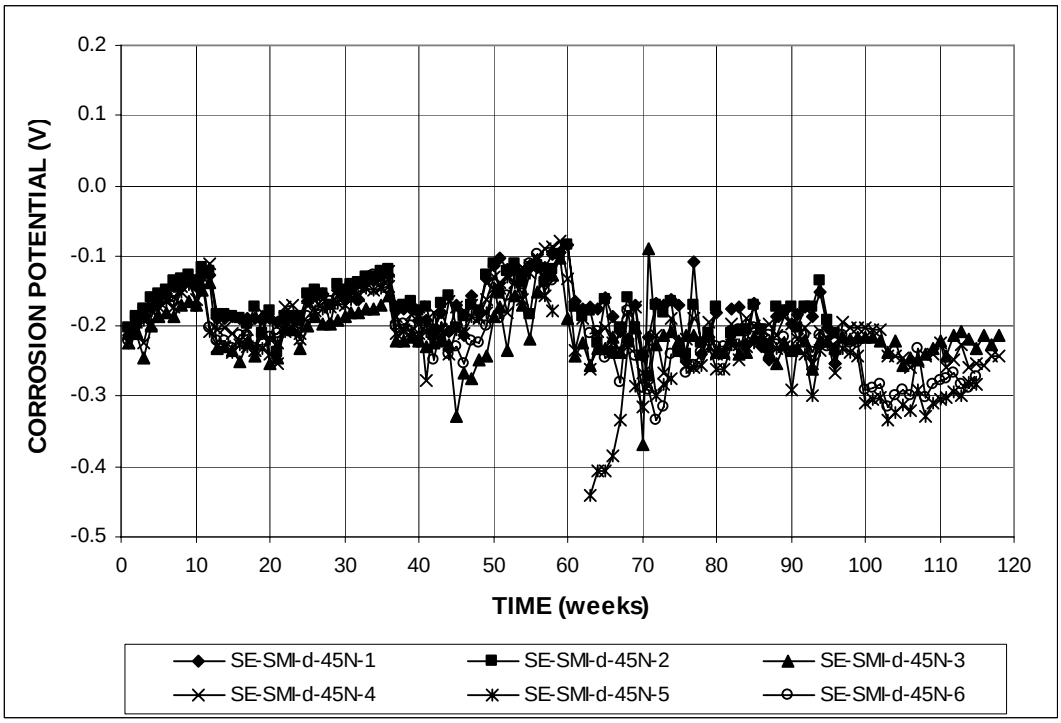

Figure A.76 – Southern Exposure Test. Bottom mat corrosion potential vs. copper-copper sulfate electrode. SMI steel with four drilled holes

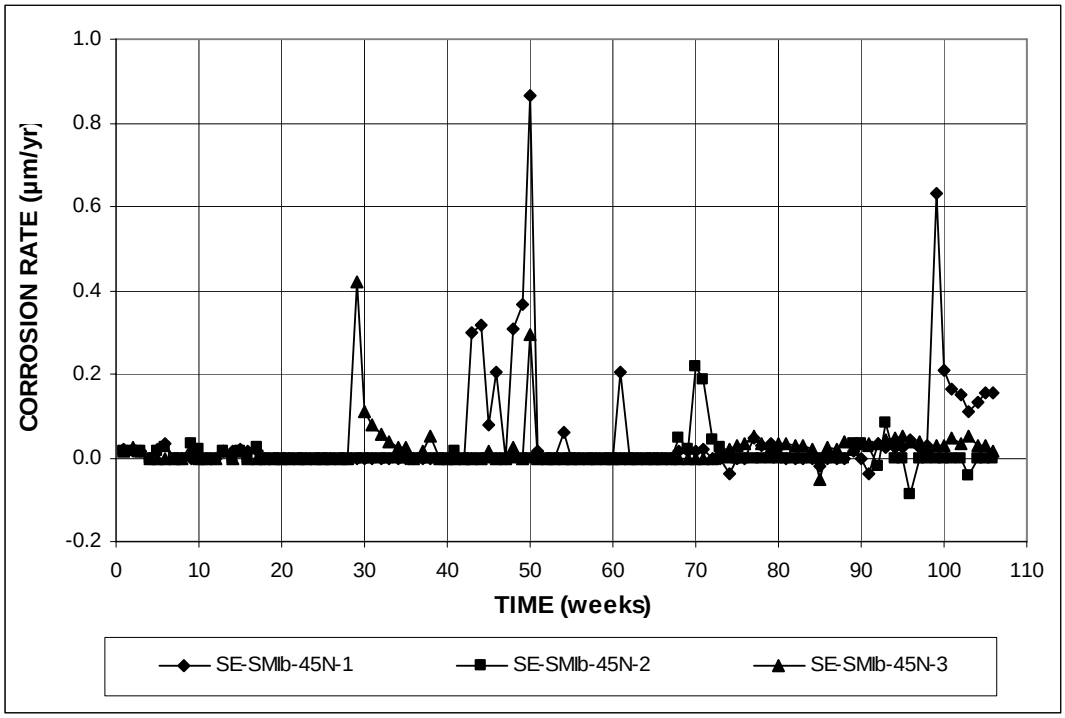

Figure A.77 – Southern Exposure Test. Corrosion rate (based on total area). SMI steel with 180 degree bend

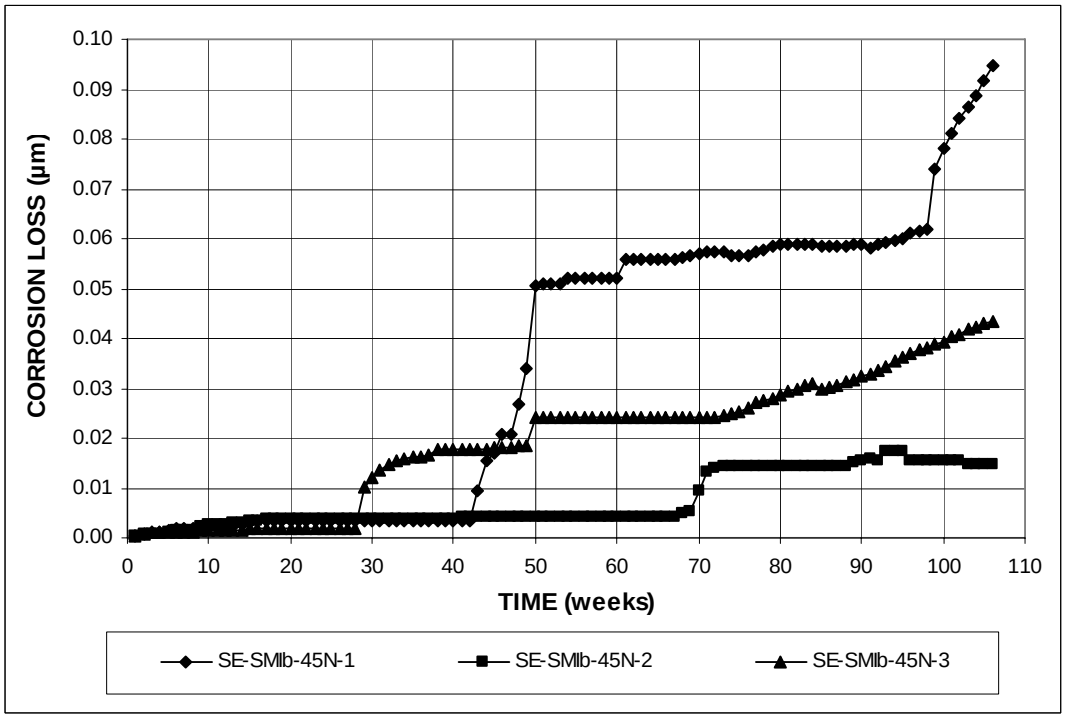

Figure A.78 – Southern Exposure Test. Corrosion loss (based on total area). SMI steel with 180 degree bend

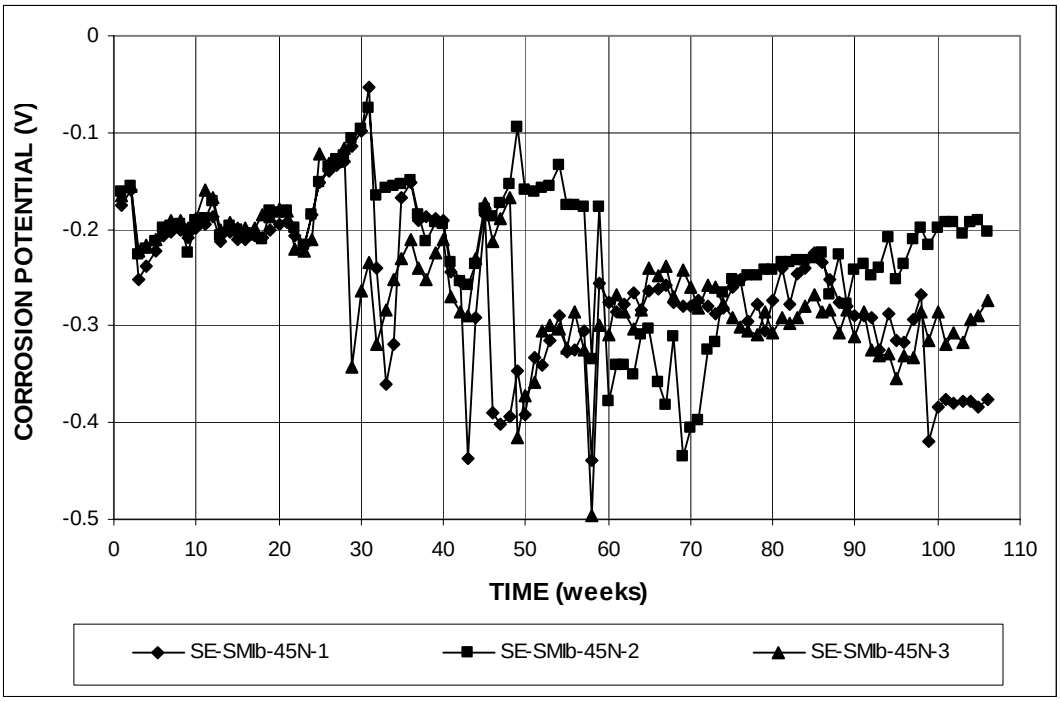

Figure A.79 – Southern Exposure Test. Top mat corrosion potential vs. copper-copper sulfate electrode. SMI steel with 180 degree bend

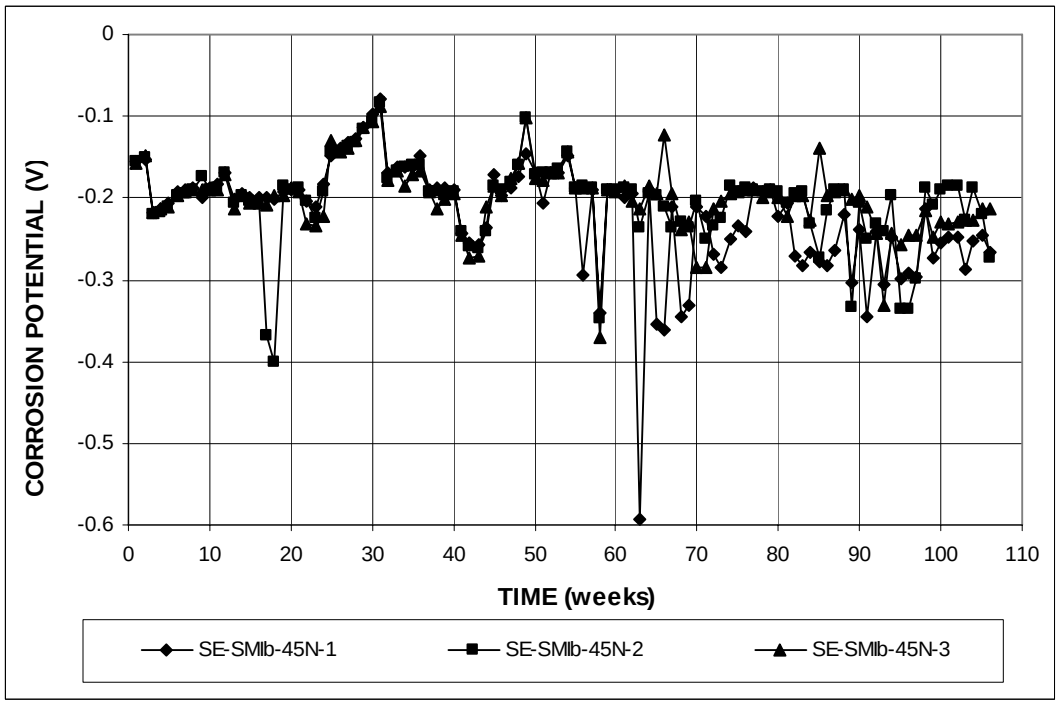

Figure A.80 – Southern Exposure Test. Bottom mat corrosion potential vs. copper-copper sulfate electrode. SMI steel with 180 degree bend

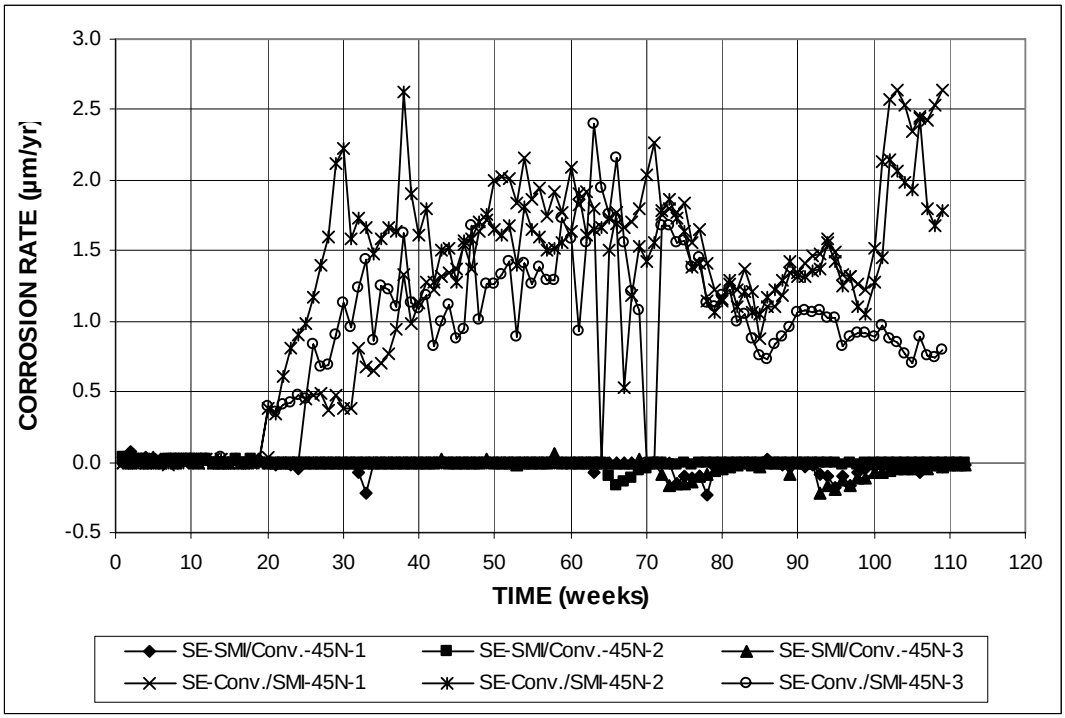

Figure A.81 – Southern Exposure Test. Corrosion rate (based on total area). SMI steel with conventional steel

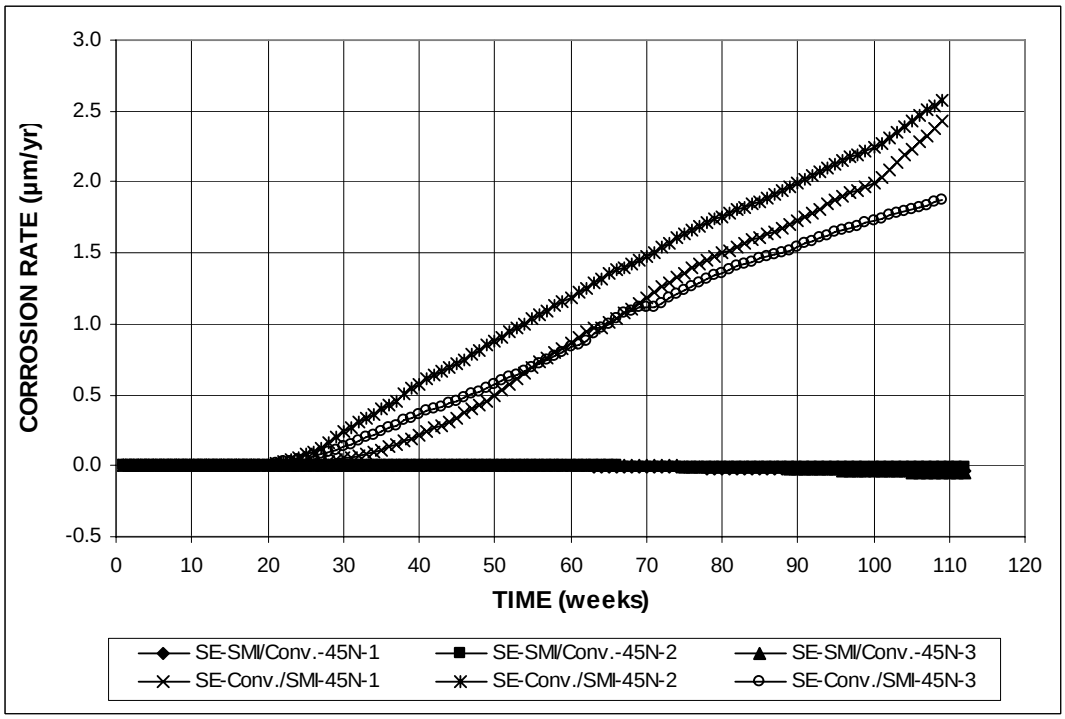

Figure A.82 – Southern Exposure Test. Corrosion loss (based on total area). SMI steel with conventional steel

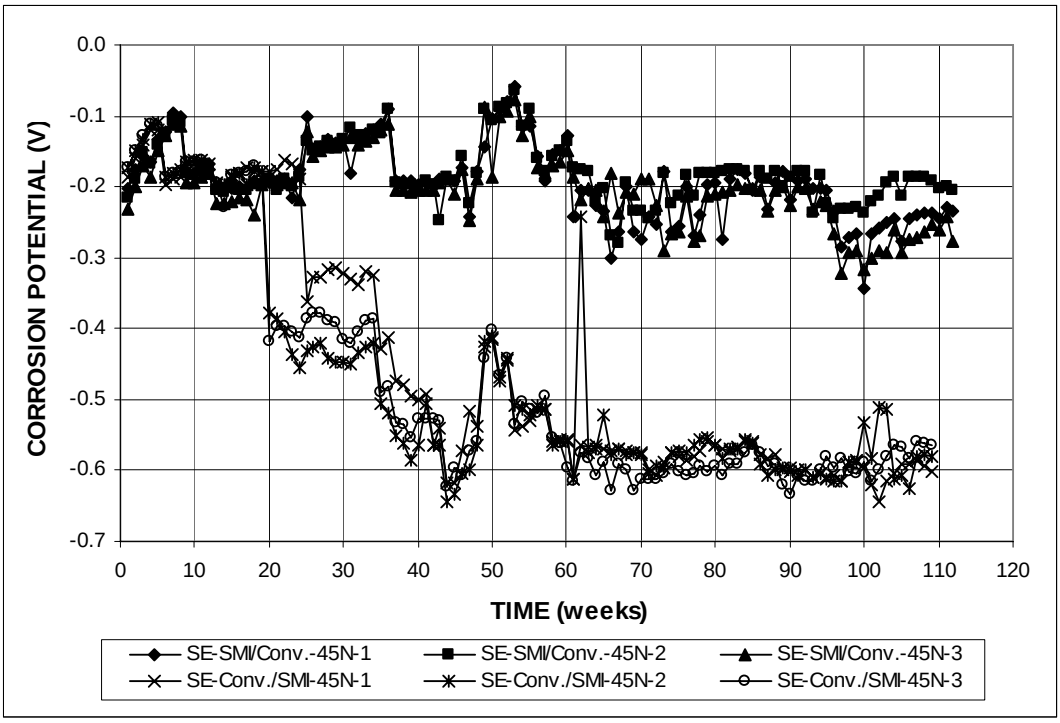

Figure A.83 – Southern Exposure Test. Top mat corrosion potential vs. copper-copper sulfate electrode. SMI steel with conventional steel

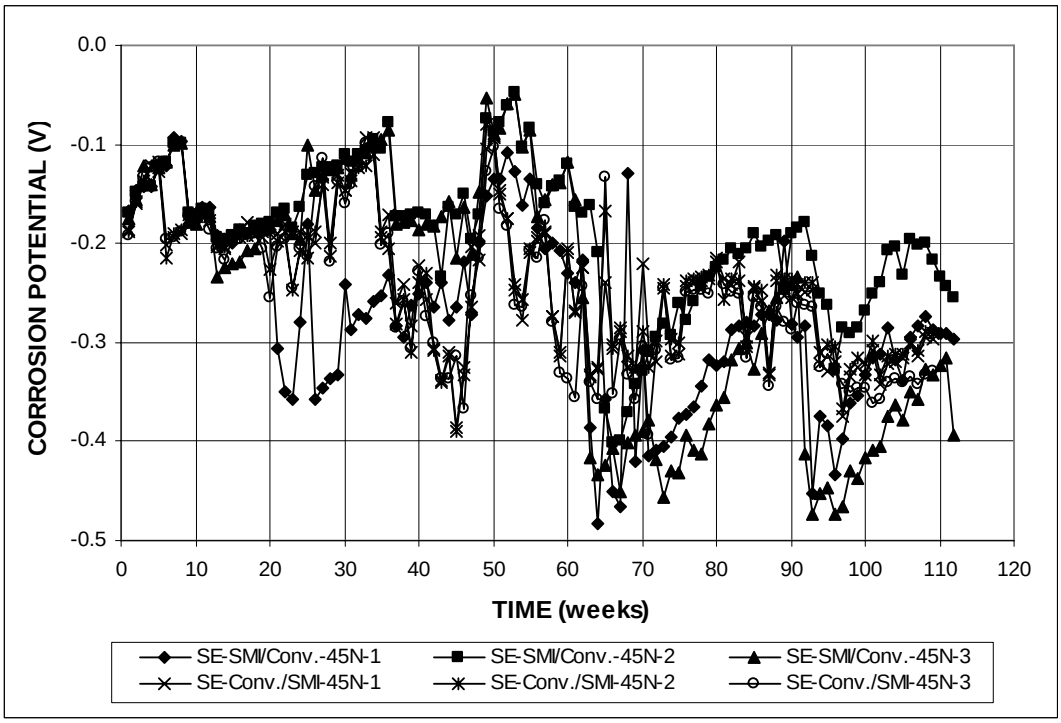

Figure A.84 – Southern Exposure Test. Bottom mat corrosion potential vs. copper-copper sulfate electrode. SMI steel with conventional steel

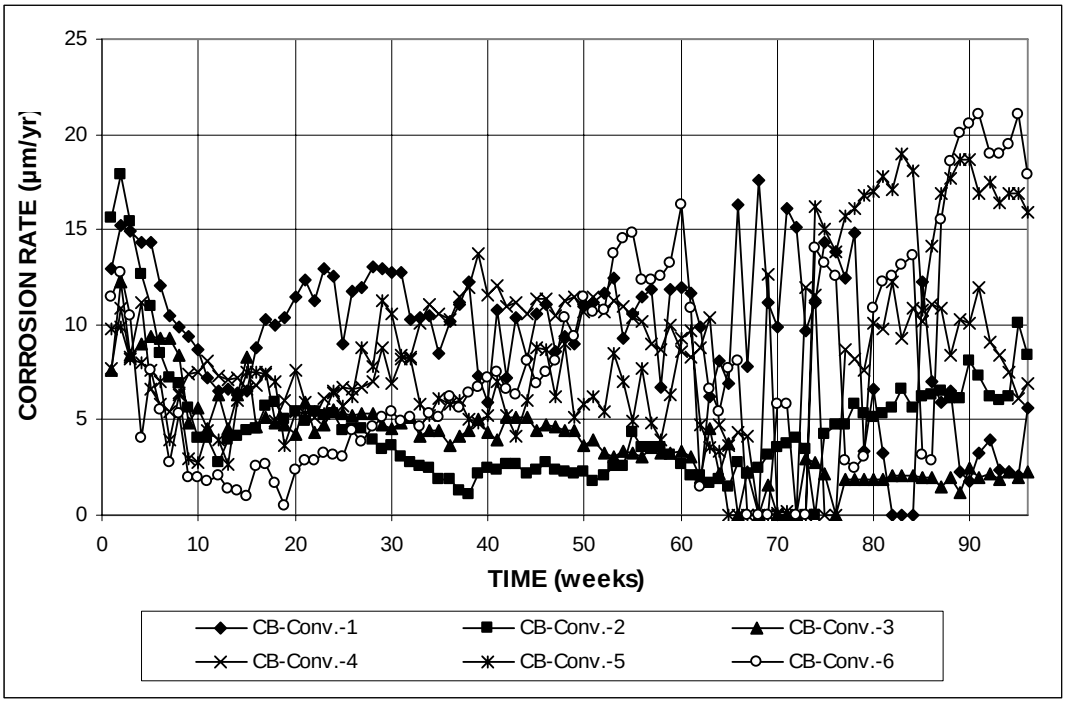

Figure A.85 – Cracked Beam Test. Corrosion rate (based on total area). Conventional steel

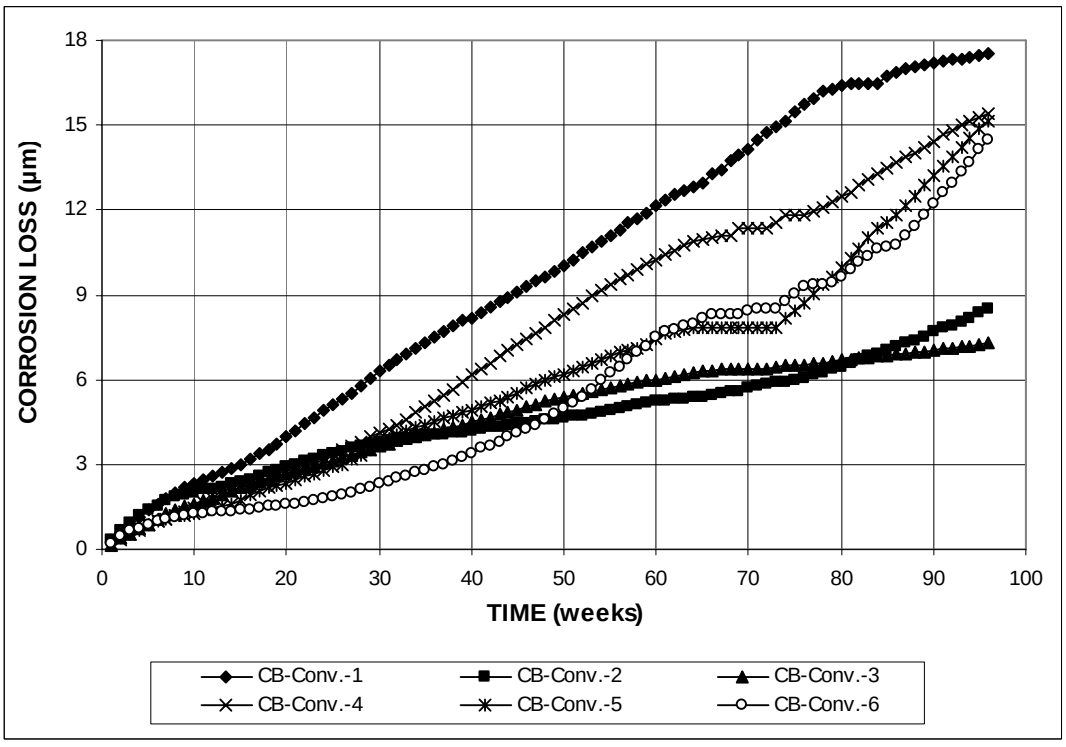

Figure A.86 – Cracked Beam Test. Corrosion loss (based on total area). Conventional steel

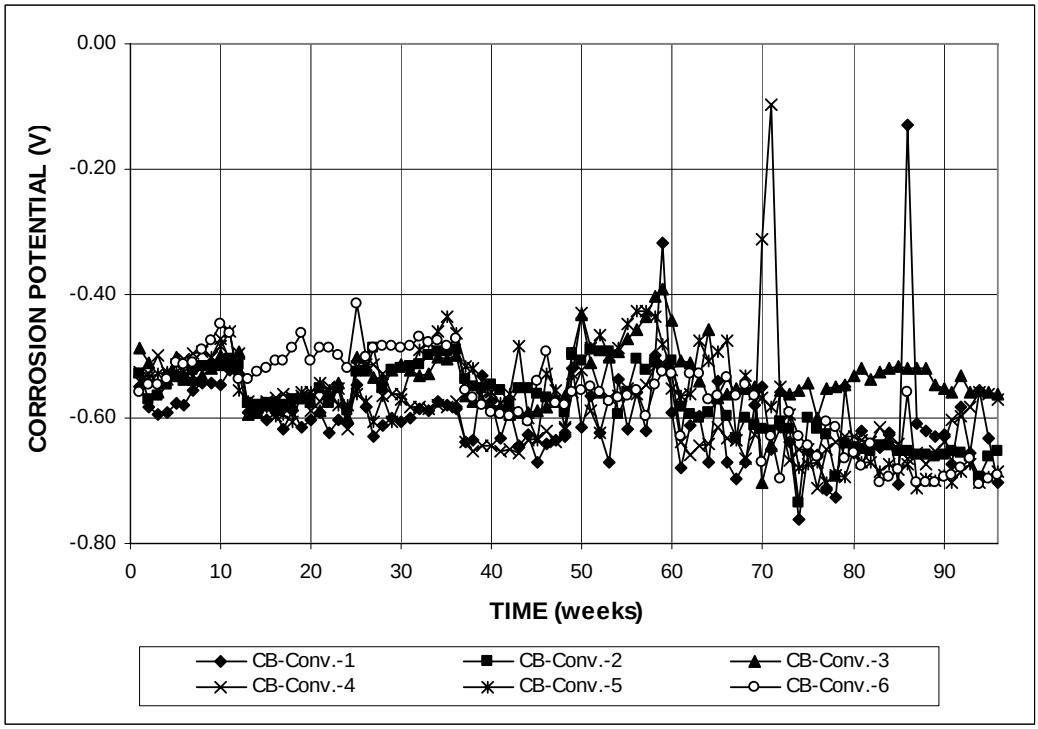

Figure A.87 – Cracked Beam Test. Top mat corrosion potential vs. copper-copper sulfate electrode. Conventional steel

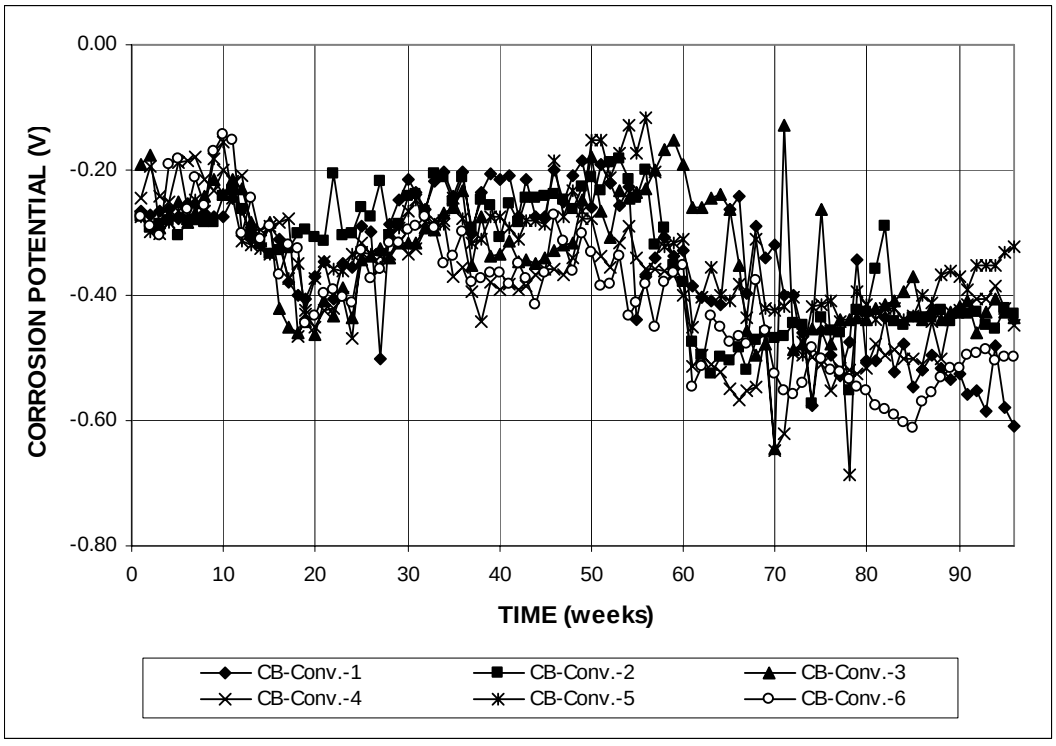

Figure A.88 – Cracked Beam Test. Bottom mat corrosion potential vs. copper-copper sulfate electrode. Conventional steel

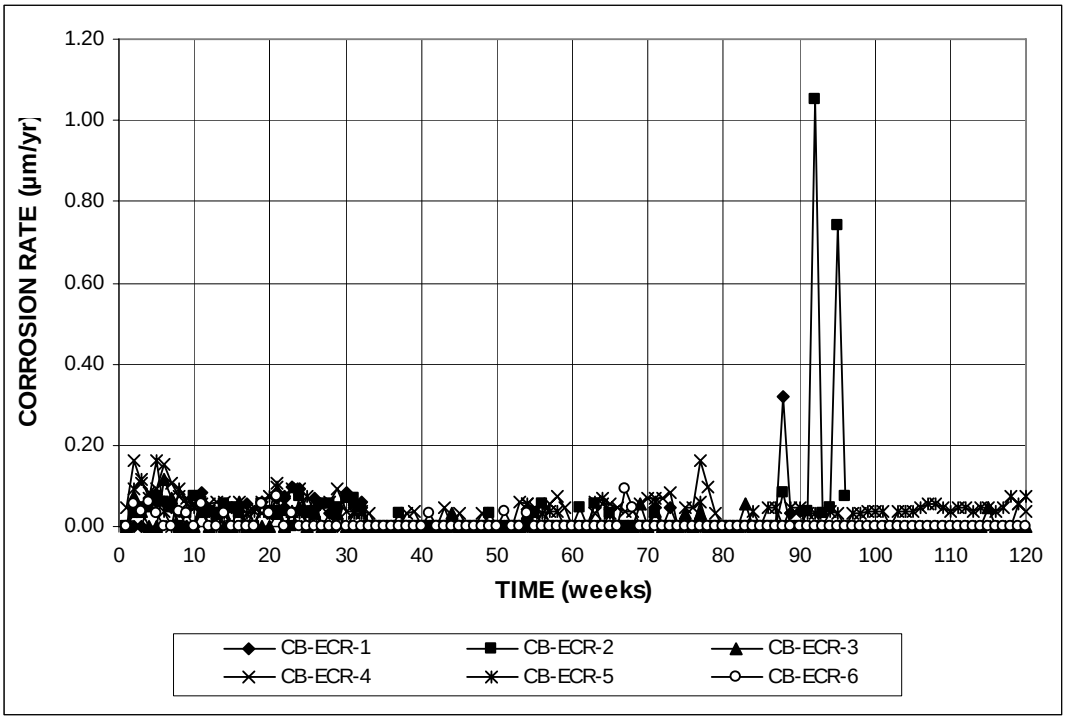

Figure A.89 – Cracked Beam Test. Corrosion rate (based on total area). Epoxy-coated steel with four drilled holes

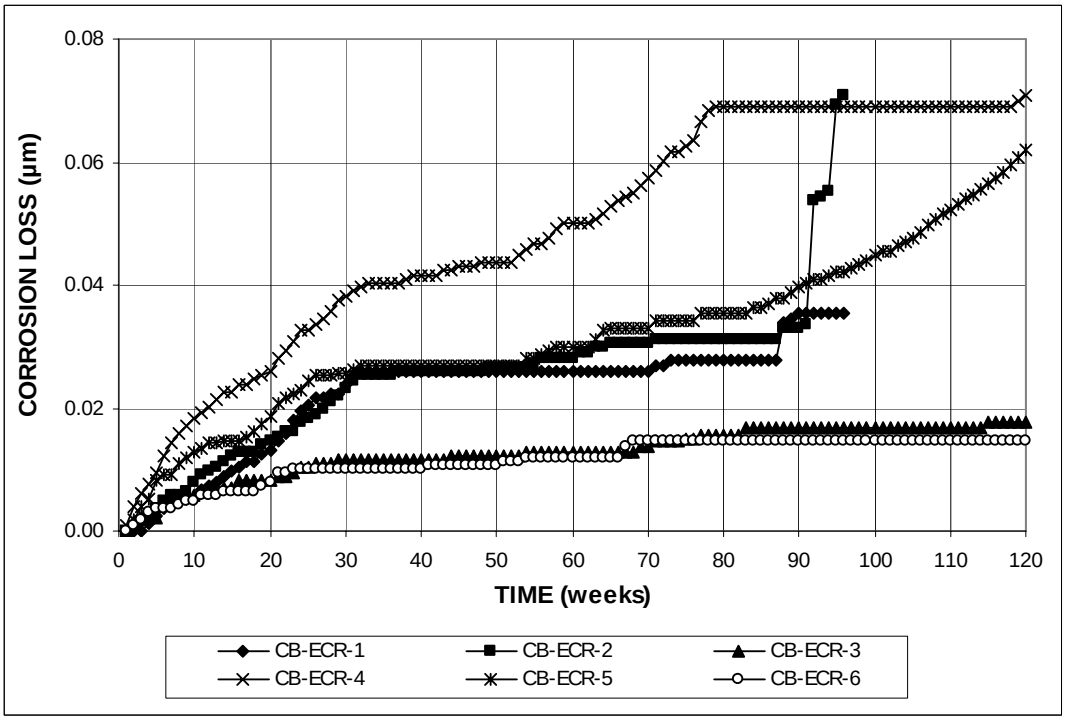

Figure A.90 – Cracked Beam Test. Corrosion loss (based on total area). Epoxy-coated steel with four drilled holes

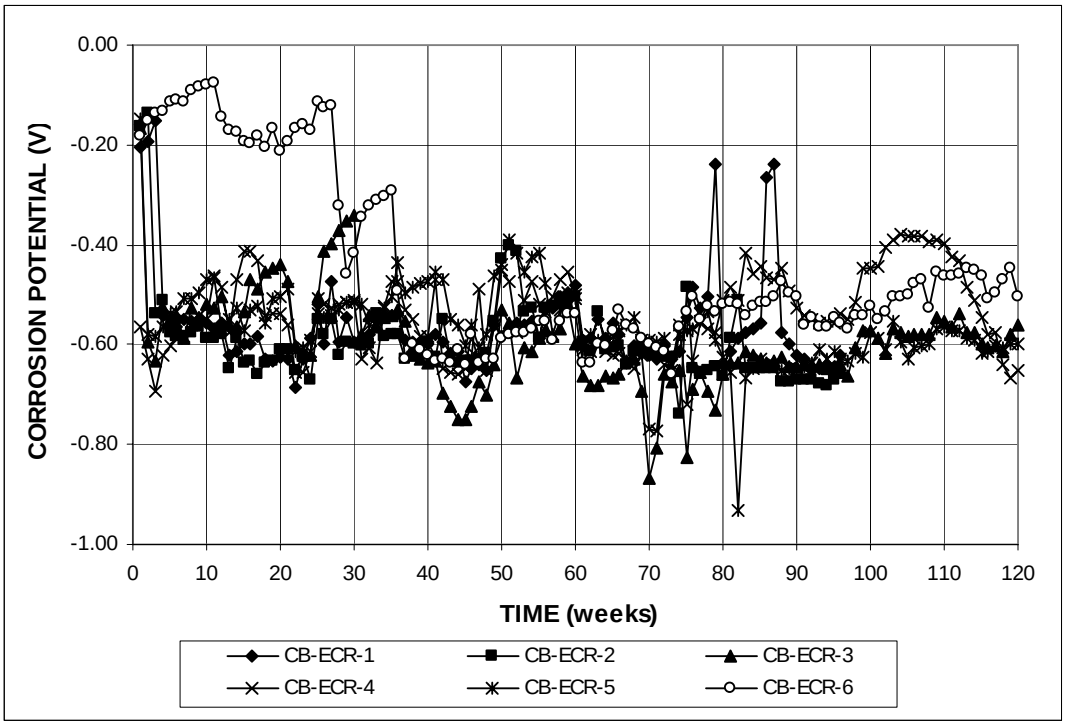

Figure A.91 – Cracked Beam Test. Top mat corrosion potential vs. copper-copper sulfate electrode. Epoxy-coated steel with four drilled holes

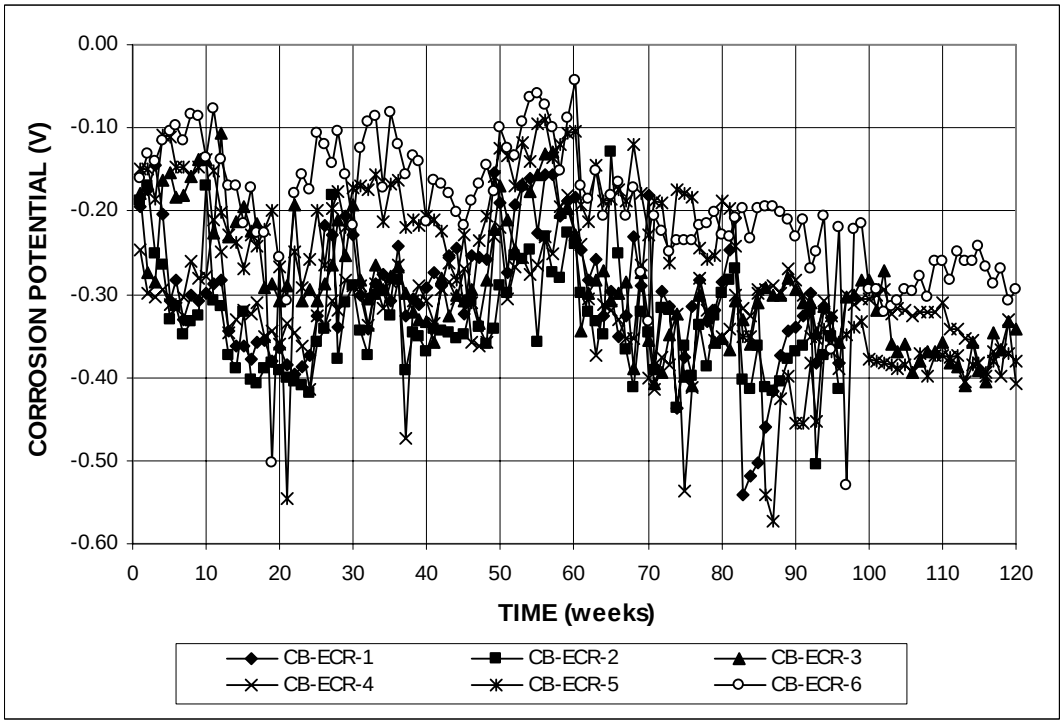

Figure A.92 – Cracked Beam Test. Bottom mat corrosion potential vs. copper-copper sulfate electrode. Epoxy-coated steel with four drilled holes

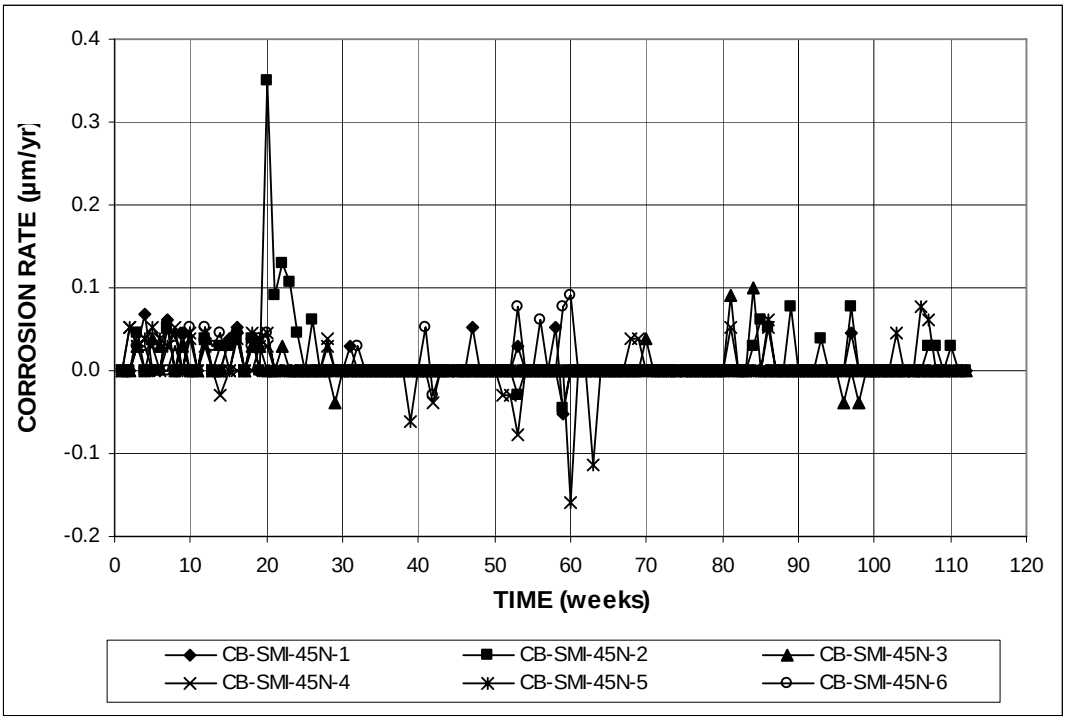

Figure A.93 – Cracked Beam Test. Corrosion rate (based on total area). SMI steel with intact cladding

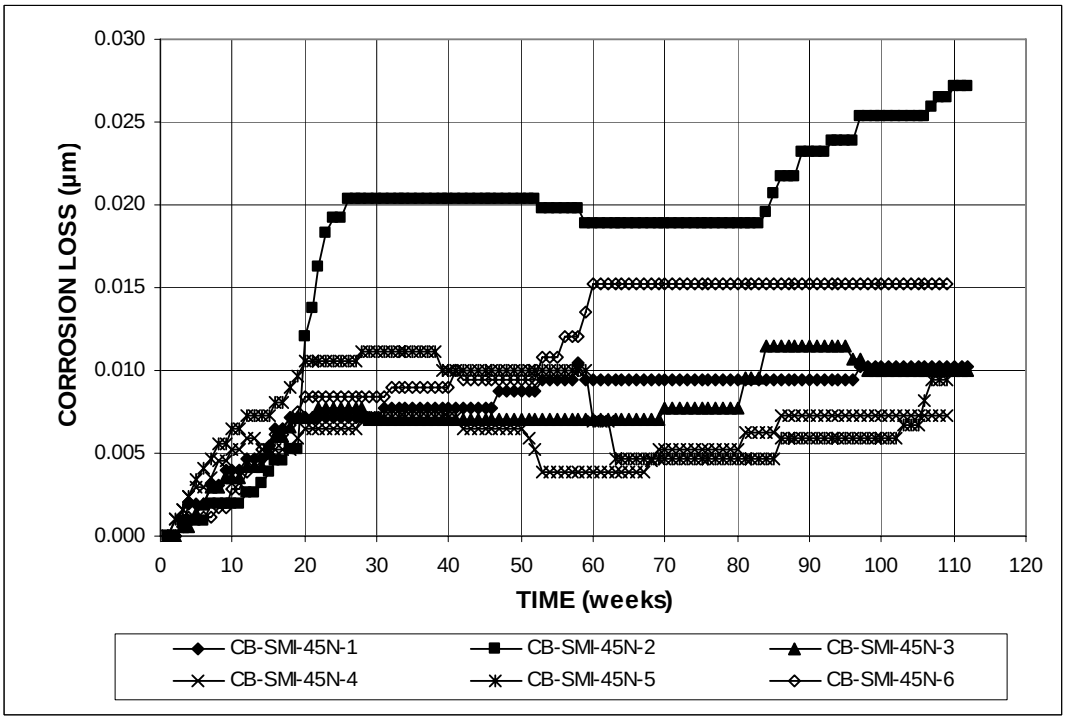

Figure A.94 – Cracked Beam Test. Corrosion loss (based on total area). SMI steel with intact cladding

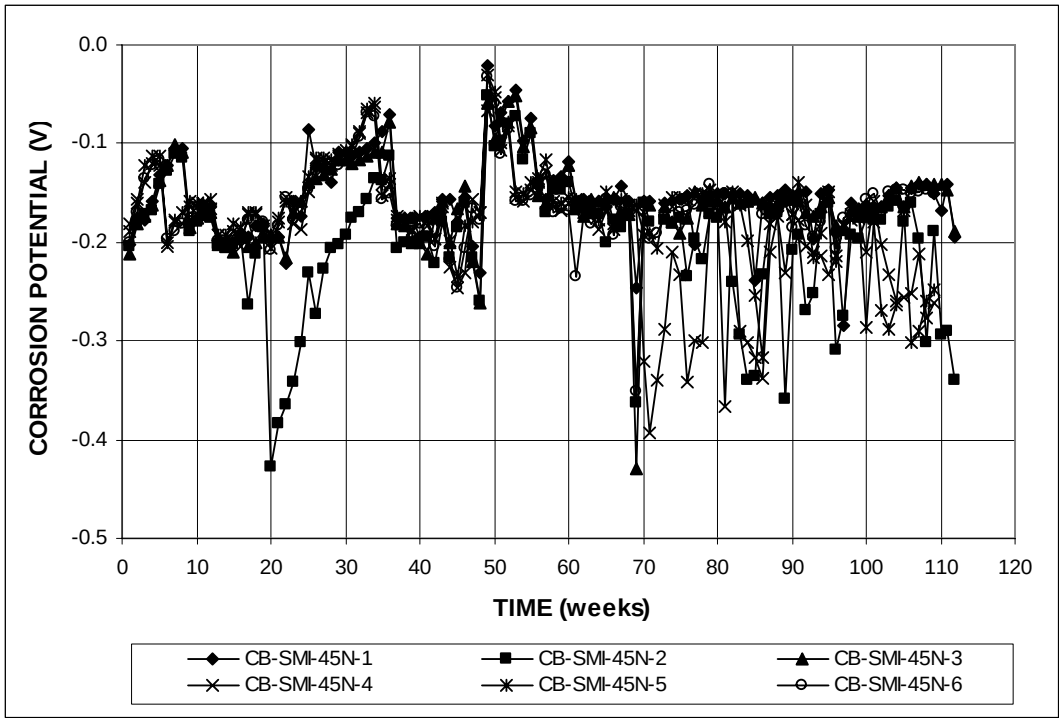

Figure A.95 – Cracked Beam Test. Top mat corrosion potential vs. copper-copper sulfate electrode. SMI steel with intact cladding

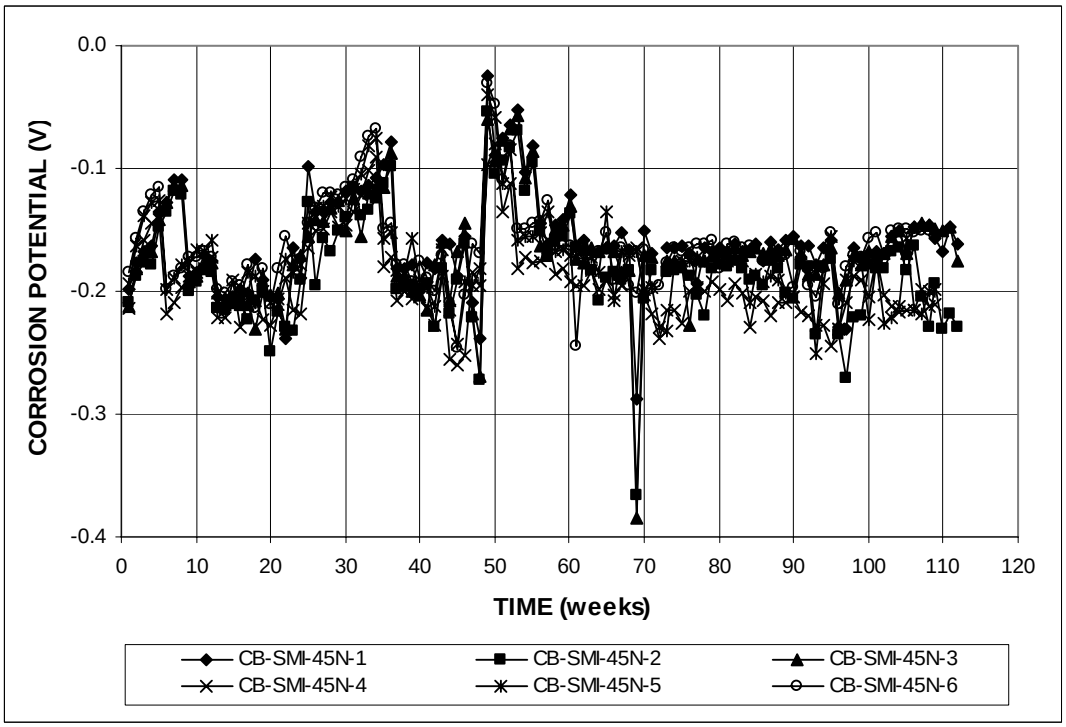

Figure A.96 – Cracked Beam Test. Bottom mat corrosion potential vs. copper-copper sulfate electrode. SMI steel with intact cladding

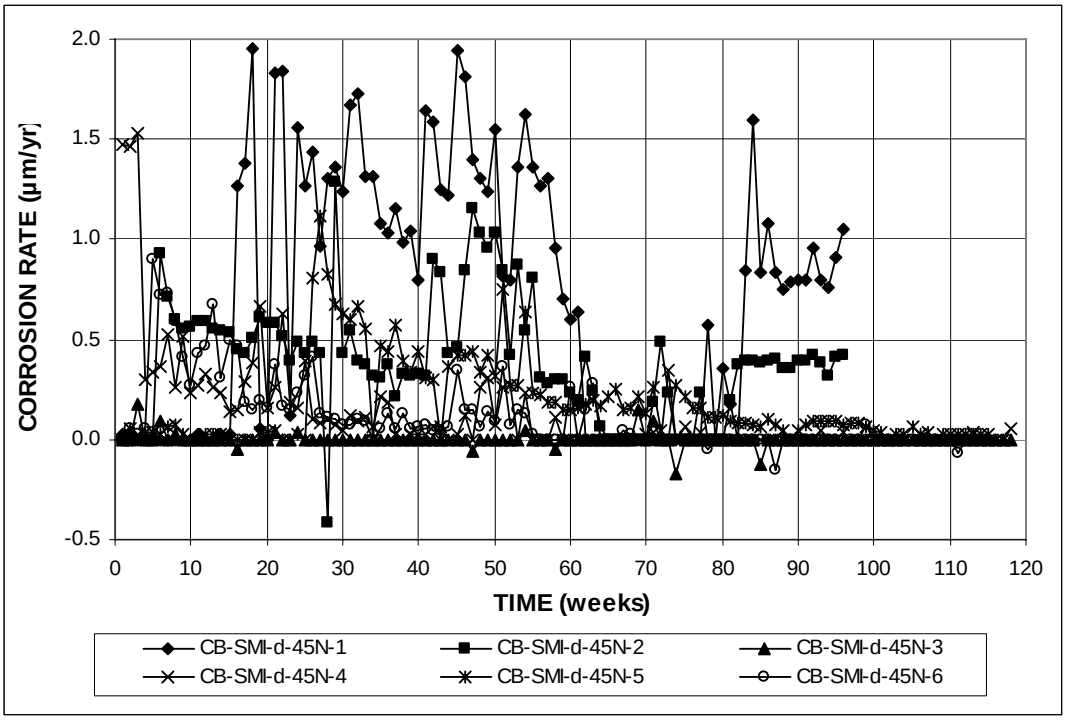

Figure A.97 – Cracked Beam Test. Corrosion rate (based on total area). SMI steel with four drilled holes

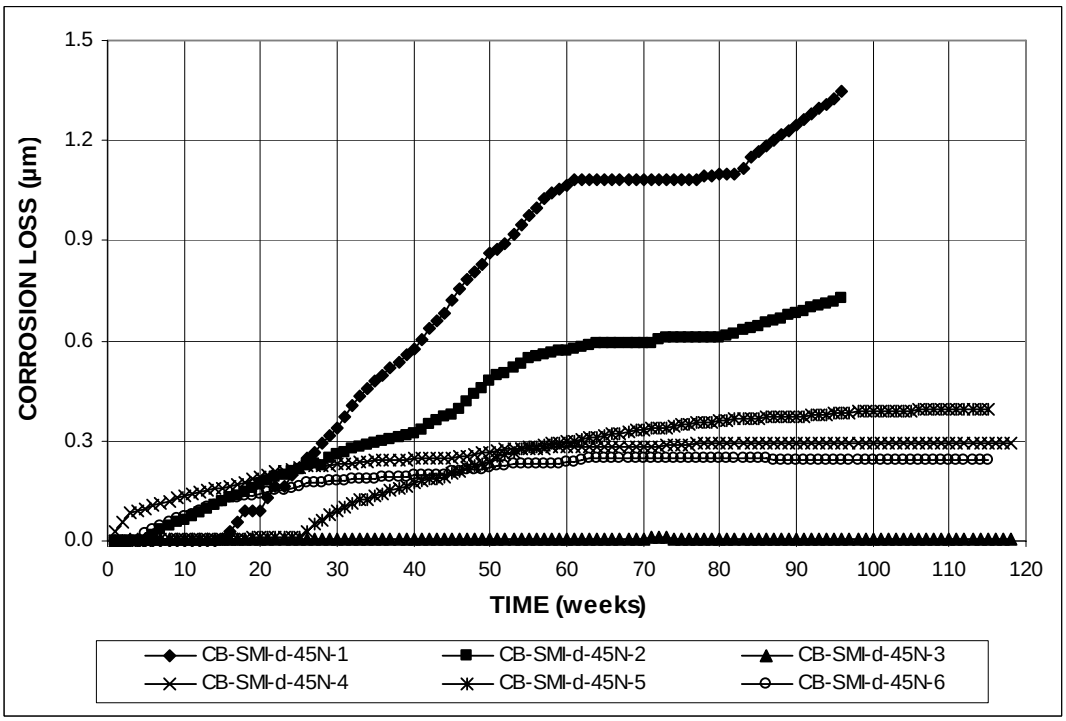

Figure A.98 – Cracked Beam Test. Corrosion loss (based on total area). SMI steel with four drilled holes

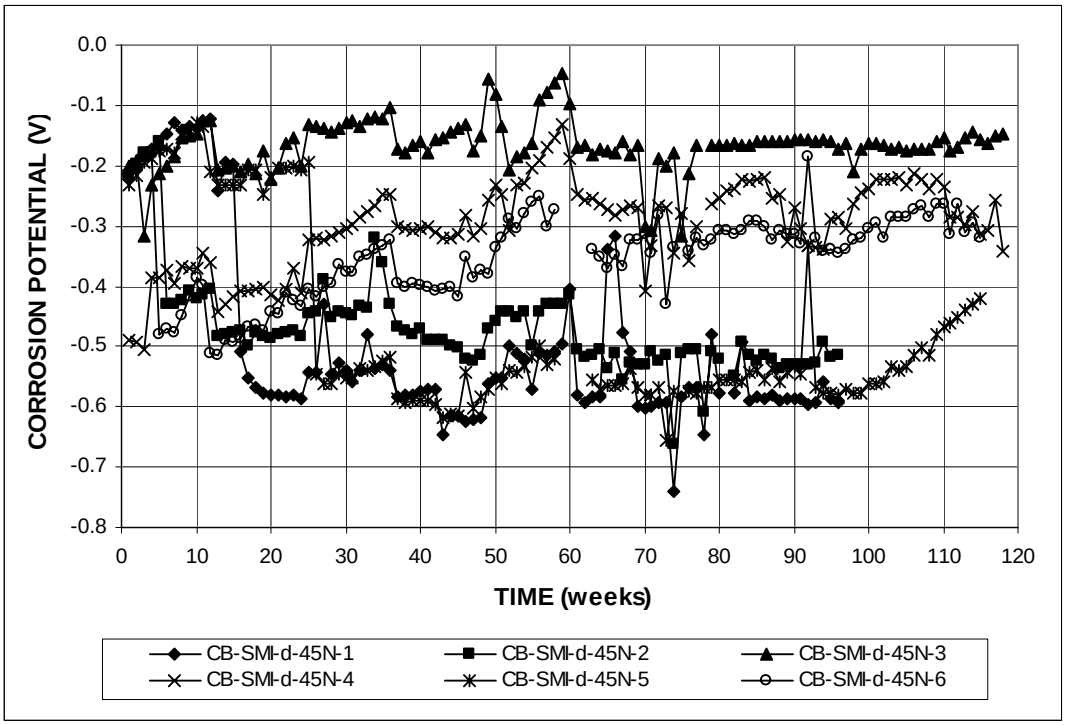

Figure A.99 – Cracked Beam Test. Top mat corrosion potential vs. copper-copper sulfate electrode. SMI steel with four drilled holes

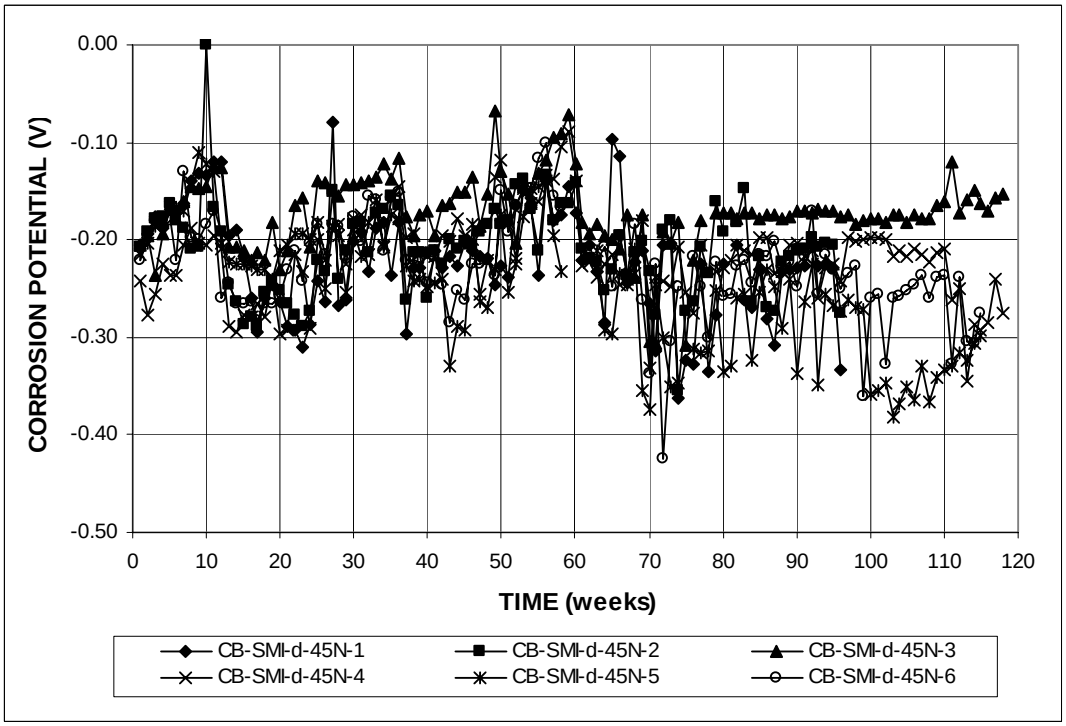

Figure A.100 – Cracked Beam Test. Bottom mat corrosion potential vs. copper-copper sulfate electrode. SMI steel with four drilled holes